

International Atomic Energy Agency

**INDC**

**INTERNATIONAL NUCLEAR DATA COMMITTEE**

CONSOLIDATED PROGRESS REPORT FOR 1974

ON NUCLEAR DATA ACTIVITIES

IN THE NDS SERVICE AREA

Bangladesh

Brazil

Bulgaria

India

Israel

Korea

Pakistan

Poland

Romania

South Africa

December 1974

**IAEA NUCLEAR DATA SECTION, KÄRNTNER RING 11, A-1010 VIENNA**

Cover I  
(I, II, IV - vacant)

*Handwritten signature*

FOREWORD

This consolidated progress report for 1974 has been prepared for the countries in the NDS service area. It is intended to encourage a closer relationship between Member States and provide for a wider circulation of unpublished progress reports from countries within the Nuclear Data Section service area. A second report INDC(SEC)-43/L covers countries outside the NDS service area.}}

The report is arranged alphabetically by country, and reproduces the content of each individual report as it was received by the INDC Secretariat. Also included in the Table of Contents is a list of each laboratory, institute and university referred to in the report, preceded by its internationally used EXFOR code.

As in all progress reports the information included here is partly preliminary and is to be considered as private communication. Consequently, the individual reports are not to be quoted without the permission of the authors.

95%

TABLE OF CONTENTS

	<u>pages</u>
<u>Banladesh</u> .....	1- 16
(3BANRAM) Atomic Energy Center, Ramna, Dacca	
(3BANITD) Institute of Nuclear Technology, Dacca	
<u>Brazil</u> .....	17- 39
(3BZLUSP) Instituto de Física, Universidade de São Paulo, São Paulo	
(3BZLIEA) Instituto de Energia Atomica, São Paulo	
(3BZLRIO) Centro Brasileiro de Pesquisas Físicas, Rio de Janeiro	
(3BZLPUJ) Instituto de Física, Pontificia Universidade Católica, Rio de Janeiro	
(3BZLIEN) Instituto de Engenharia Nuclear, Rio de Janeiro	
(3BZLIPR) Instituto de Pesquisas Radioativas, Belo Horizonte	
(3BZLIDF) Instituto de Física, Universidade Federal do Rio Grande do Sul, Porto Alegre	
(3BZLCOM) Comissão Nacional de Energia Nuclear, Rio de Janeiro	
<u>Bulgaria</u> .....	41- 46
(3BULBLA) Institute of Nuclear Research and Nuclear Energy, Sofia	

<u>India</u> .....	47-123
(3INDTRM) Bhabha Atomic Research Centre, Bombay	
(3INDTAT) Tata Institute of Fundamental Research, Bombay	
(3INDSAH) Saha Institute of Nuclear Physics, Calcutta	
(3INDMJA) Aligarh Muslim University, Aligarh	
(3INDAUW) Andhra University, Visakhapatnam	
(3INDBHU) Banaras Hindu University, Varanasi	
(3INDBIT) Birla Institute of Technology, Pilani and Ranchi	
(3INDBUU) Burdwan University, Burdwan	
(3INDCAU) Calcutta University, Calcutta	
(3INDDIU) Dibrugarh University, Assam	
(3INDIAC) Indian Association for the Cultivation of Science	
(3INDITK) Indian Institute of Technology, Kanpur	
(3INDIMS) Institute of Mathematical Sciences	
(3INDKUK) Kurukshetra University, Kurukshetra	
(3INDMAU) Marathwada University, Aurangabad (M.S.)	
(3INDMEU) Meerut University, Meerut	
(3INDPRA) Physical Research Laboratory, Ahmedabad	
(3INDPUC) Punjab University, Chandigarh	
(3INDPAT) Punjab University, Patiala	
(3INDSAU) Sambelpur University, Orissa	
(3INDDLH) University of Delhi, Delhi	
(3INDUMA) University of Madras, Madras	
(3INDVUU) Vikram University, Ujjain	
<u>Israel</u> .....	125-162
(3ISLWZI) Weizmann Institute	
(3ISLSOR) Soreq Research Centre	
(3ISLNEG) Negev Research Centre	
(3ISLIRC) Israel AEC Research Centres	
(3ISLTEL) Tel Aviv University	
(3ISLUNG) University of the Negev	
(3ISLHEB) Hebrew University	

	<u>pages</u>
<u>Korea</u> .....	163-183
(3KORSEO) Korea Atomic Energy Research Institute, Seoul	
(3KORNSU) Seoul National University	
(3KORUIT) Ulsan Institute of Technology	
(3KOREWU) Ewha Womans University	
(3KORKKU) Sungkyunkwan University	
(3KORKNU) Kyungpook National University, Taegu	
(3KORTU) Inha University	
<u>Pakistan</u> .....	185-187
(3PAKNIL) Pakistan Institute of Nuclear Science and Technology, Rawalpindi	
<u>Poland</u> .....	189-216
(3POLIBJ) Institute of Nuclear Research, Warsaw	
(3POLNWA) University of Warsaw	
<u>Romania</u> .....	217-245
(3RUMBUC) Institute for Atomic Physics, Bucharest	
(3RUMINT) Institute for Nuclear Technology, Bucharest	
<u>Republic of South Africa</u> .....	247-262
(3SAFSUN) Southern Universities Nuclear Institute, Faure	
(3SAFPEL) Physics Division, Atomic Energy Board, Pelindaba	
(3SAFWIT) University of Witwatersrand, Johannesburg	

Progress Report

on

Nuclear Data Activities  
in BANGLADESH

1973

Compiled by

M. Mizanul Islam

ATOMIC ENERGY CENTRE, DACCA

1. Measurement of neutron total cross-section of Mercury and Dysprosium

( M. Hussain, Enayetullah Molla, N. Islam Molla,  
M. Fareeqe, M. Hussain\*, E. Islam\* and M. Hessain\* )

Neutron total cross-section data were measured for Mercury between 16.25 and 18.79 MeV and for Dysprosium between 0.64 and 1.54 MeV, 3.83 and 5.90 MeV, and 16.18 and 19.10 MeV, using transmission method. Neutrons were produced by the  $T(p,n)^3\text{He}$ ,  $D(d,n)^3\text{He}$  and  $T(d,n)^4\text{He}$  reactions. A ZnS Scintillator with pulse shape discrimination was used as neutron detector. Measurements were made in steps of 100 keV and the beam energy spread was of the order of 10 keV. Corrections were made for background neutrons and in-scattering effect. Final analyses of the data are in progress.

---

\* Department of physics, Dacca University.

2. Optical model analysis of fast neutron total cross-section of  $^{165}\text{Ho}$ .

( M.Enayetullah and M.Rahman)

Total neutron cross section of  $^{165}\text{Ho}$  in the energy range of 0.5 to 19 MeV have been analysed in terms of the optical model. Good fit has been obtained in the energy range of 2 MeV to 19 MeV.

In the analysis the interaction potential used was of the type:

$$V(r) = -Uf(r) - iWg(r) + (U_s + iW_s) \frac{1}{r} \frac{d}{dr} f(r)$$

where,

$f(r)$  has a Saxon-Wood form

$f(r) = 1 + \exp \left( \frac{r-R}{a} \right)^{-1}$  and  $g(r)$  either equals  $f(r)$  or has a Gaussian form  $g(r) = \exp \left( -\frac{(r-R)^2}{b^2} \right)$

$U, W, U_s$  and  $W_s$  have their normal meaning and the nuclear radius  $R$  is given by  $R = r_0 A^{1/3}$  and  $a, b$  are the diffuseness parameters.

3. Improvement of Directional Sensitivity of  $\text{BF}_3$  Long counter  
(N. Islam, D. Hussain, M. Hussain\*, E. Islam\* and  
M. Shahjahan\*).

A  $\text{BF}_3$  long counter of the Hanson-Mckibben type has been constructed. To make the counter directionally sensitive a simple detachable collimator has been designed. The angular resolution (half-width at half height) of the long counter is  $32^\circ$  and with the collimator in front of the counter, this becomes  $7.2^\circ$ . This increased resolution makes the counter 'see' only a limited experimental area thus reducing the background counts from scattered neutrons and also from secondary neutrons produced in different parts of an accelerator specially when a deuteron beam is used. The energy responses of the collimated and uncollimated long counter have been compared and it is seen that for source neutrons, the ratio of the counts slowly decreases with energy and the efficiency of the counter remains reasonably constant. Thus a Hanson-Mckibben long counter with the addition of a collimator has the general flatness of response of the basic counter. The absolute efficiency of the long counter has been measured. The calculated absolute efficiency was found to be 5.6%.

---

\* Department of physics, Dacca University.

#### 4. Analogue Resonances in $^{57}\text{Co}$

(M.A.Rahman, S.Khatun, M.A.Awal, M.Rahman and H.M.Sen Gupta\*).

The  $(p, \gamma)$  reaction on  $^{56}\text{Fe}$  target has been investigated to identify the isobaric analogue states in the compound nucleus  $^{57}\text{Co}$  corresponding to the ground and low-lying states of the parent nucleus  $^{57}\text{Fe}$ . In the present experiment the excitation function was measured in the energy range 1.2 to 2.00 MeV and five analogue states at  $E_p = 1.246, 1.261, 1.406, 1.646$  and  $1.965$  MeV corresponding to ground,  $0.014, 0.136, 0.366$  and  $0.707$  MeV states of  $^{57}\text{Fe}$  have been identified. This work will be extended upto 3.0 MeV.

#### 5. Study of $^{27}\text{Al}$ $(p, p_0)$

(M.R.Rahman, M.A.Awal, S.Khatun, M.Rahman & H.M.Sen Gupta\*)

Excitation function for elastically scattered protons from  $^{27}\text{Al}$  have been measured at  $90^\circ, 125^\circ$  and  $140^\circ$ , by using surface barrier detectors. The data have been analysed by using certain predetermined resonance shape. This analysis yields information on resonance widths. The shape analysis of the resonances of excitation functions at various angles gives an estimate of the  $l$  - values of the resonances. Results obtained are shown in the table-I.

---

\* Department of physics, Dacca University.

Table - I

Sl. No.	E <sub>p</sub> resonance (MeV)						Γ (keV) (mean)	Partial width
	Lab			Cms				
	90°	125°	140°	90°	125°	140°		
1.		1.114	1.119		1.075	1.079	1.43	1
2.	1.195	1.202	1.201	1.153	1.159	1.158	4.43	1
3.		1.360	1.363		1.312	1.314	1.43	1
4.	1.452	1.452	1.452	1.401	1.400	1.400	1.71	1
5.		1.496	1.498		1.443	1.440	1.12	1
6.	1.571	1.571	1.575	1.515	1.515	1.519	3.53	
7.	1.700	1.701	1.702	1.640	1.640	1.641	1.12	
8.	1.792		1.794	1.728		1.730	2.28	
9.		2.026	2.029		1.954	1.957	2.83	1
10.	2.473		2.471	2.385		2.383	3.37	
11.	2.661			2.566			4.90	3
12.	2.547		2.547	2.456		2.456	3.37	
13.			2.866			2.764	3.88	1

6.  $T_z$ -dependence of Coulomb displacement energy.

(M.A. Rahman, M.A. Awal, S. Khatun, M. Rahman  
and H.M. Sen Gupta\*)

A least squares analysis has been carried out on all available data on Coulomb displacement energy  $\Delta E_c$  as a function of  $Z/A^{1/3}$ . Anderson et al. (1) made least squares analysis of the experimental data on  $\Delta E_c$  in the mass region  $A=40$  to 165 and obtained

$$\Delta E_c = (1.444 \pm 0.005) Z/A^{1/3} - (1.13 \pm 0.04) \text{ MeV}$$

In the present case with 245 observed values of  $\Delta E_c$  spreading over a mass region  $A=27$  to 238, the result of least squares analysis has been found to be

$$\Delta E_c = (1.437 \pm 0.003) Z/A^{1/3} - (1.081 \pm 0.02) \text{ MeV}$$

This relation may be used with better accuracy.

Attempts have also been made to see the dependence of  $\Delta E_c$  on  $T_z$ , the isobaric spin. To see this the  $\Delta E_c$  values have been arranged into several groups according to  $T_z$  values and least squares analyses have been made. The dependence has been found to be small.

(1) J.T. Anderson, C. Wong and  
J.W. McClure, phys. Rev. 138(1965) B615

---

\* Department of physics, Dacca University.

7. Proton-induced X-ray Fluorescence Analysis of Trace Elements.

(A.H. Khan, M.B. Zaman, M.M. Islam, M.A. Rahman, D. Hossain and M.A. Awal).

Under the programme of Fast Particle Activation Analysis of Trace Elements, at present efforts are being concentrated only on the subject mentioned above. In this regard, a series of experiments were performed on natural copper targets of varying thickness ( $40-70 \mu\text{g}/\text{cm}^2$ ) to identify the 8.4 keV  $\text{CuK}\alpha$  peak. Proton energy was 1.2 MeV and its beam intensity was  $5 \mu\text{A}$ .

Results of these experiments indicated that the signal to noise ratio was so small that it was not possible to separate the 8.4 keV peak for Cu. This was due to the poor detection system in which an uncooled Si(Li) detector was used. Moreover, the Vacuum chamber was too large (18" diameter) for X-ray measurements.

Attempts are now being made to set up a new detection system which will consist of a high resolution gas filled proportional counter and a 6" cubic vacuum chamber. When this system is complete, it is expected that it will improve upon the present level of activities.

8. Separable potential for  $\alpha - \alpha$  interaction

( M. Rahman, S. Ali & D. Hussain\* )

A two term non-local separable potential has been used to study the S,D and G wave  $\alpha - \alpha$  phase shifts. A careful study shows that a separable interaction having a 'long' range attraction and a short range repulsion is capable of reproducing the above mentioned phase shifts within the energy range 0-24 MeV. A paper based on this work has been reported at International Centre for Theoretical Physics, Trieste, Italy and has also been sent for publication in the Physical Review.

So far the interest was to reproduce the phase shifts at energies where the non-elastic contribution to phase shifts could be neglected. As such the strength of the interaction used was assumed to be real. Now attempts are being made to extend the work for higher energies.

9. Non-local separable potential and p-p scattering.

( M. Rahman, S. Ali and D. Hussain\* )

A non-localseparable interaction having the same form as that used in  $\alpha - \alpha$  scattering, has been used to study the S-wave phase shift for the p-p system in the energy range 0-400 MeV. It is observed that a two-term separable potential is capable of reproducing the phase shift within this energy range.

A paper based on this work has been reported at ICTP and has also been accepted for publication in the Physical Review.

---

\* Department of Mathematics, Jahangir Nagar University.

10. Application of the Resonating group formalism

( S.A. Afzal and S. Ali )

Application of the resonating group formalism is done to the case of  $\alpha$ - $\alpha$  phase shifts. The N-N interaction employed here is a soft core nucleon-nucleon potential. As it requires a large computer, preliminary computation work was done at CDC computer of the University of Trieste, Italy; some more calculation is needed.

11. A note on the anatomy of the S-wave  $\alpha$ - $\alpha$  interaction.

( S.A. Afzal, S. Ali and M. Rahman )

The effects of the various terms appearing in the kernel of the S-wave  $\alpha$ - $\alpha$  interaction have been studied. It has been found possible to identify terms which have representability for the kernel.

12. Study of the p- $\alpha$  scattering phase shifts with non-local separable potential

( A.A.Z. Ahmed and S. Ali )

Satisfactory results have been obtained using a non-local potential for the phase shift analysis of the S-wave and p-wave proton/alpha scattering. Analysis of the higher  $\ell$ -wave phase shifts will also be taken up shortly.

13. Photo-disintegration of  ${}^4\text{He}$

(S.A. Afzal, S.M.M.R. Chowdhury and Suhrabuddin\*).

In this study of  ${}^4\text{He} (\gamma, p) {}^3\text{H}$ , investigation is made on the effect of strong short range correlation on the photo-disintegration of  ${}^4\text{He}$ . In both  ${}^4\text{He}$  and triton Jastrow type correlation has been introduced and consequently the calculation requires huge computation. Preliminary part of the work has been completed and the final work is in progress.

14. Calculation of the Energy losses of electrons in thin films with recoil effect.

( S.M.M.R. Chowdhury ).

(a) A quantum mechanical formula for the energy loss function of electrons with recoil effect upto second order in electron-plasmon coupling constant has been derived. It is shown that in this approximation the contribution comes from the change of electron trajectories by successive emission or absorption of plasmons and the result obtained agrees with non-recoil effect.

This work is in progress.

---

\* Department of Mathematics, Dacca University

(b) Energy band of KCl has been calculated by the linear combination of Atomic orbital (LACO) method using Hartree Fock type of exchange potential. The exchange-effects and the influences of admixture of different states to the crystal orbital are extensively studied. These effects are found to change the maximum and minimum of the valence band.

This work is in progress.

INSTITUTE OF NUCLEAR TECHNOLOGY, DACCA

1. A computer code to generate multigroup cross-sections  
( M.A.W. Mondal )

It is well known that multigroup methods in neutron calculations have won wide acceptance in the design of nuclear reactors. Usually all big laboratories engaged in theoretical reactor physics works have their own computer codes to generate multi-group cross-sections. Here at Dacca we do not have any such computer codes. But for our calculations we need to generate multigroup cross-sections. For this reason a computer code has been developed to generate multi-group cross-sections using the IBM 1620 computer. This code can generate group cross-sections needed for  $P_0$  - and  $P_1$  - calculations. Using this code and the analytical expression for the neutron cross-sections of the proton (1) we have generated a set of 33 group cross-sections covering the energy range 10 MeV - 0.614ev for water. The results obtained for slowing down time of neutrons in water using these multi-group cross-sections agree very well with those of experiments. At present attempts are being made to incorporate in this code the effect of up-scattering in the thermal region. The work is in progress.

1. A. Horsley "Neutron cross-sections of the proton in the energy range 0.0001ev - 20 MeV", AWRE - O - 23/65 (July 1965)

## 2. Studies on slowing down length

( M.A.W. Mondal )

The aim of this project is to make a detailed study of the effects of (a) inelastic scattering, (b) anisotropy of the scattering processes, (c) leakage of neutrons, (d) variation of the source neutron energy and (e) finite size of the source on the slowing down length of neutrons. For studying these phenomena the problem of calculating the slowing down length has been formulated with the help of the spatial moments of the slowing down fluxes using the multi-energy group technique.

A computer code to generate the multi-group cross-sections necessary for  $P_1$ -transport calculations has been developed. Using this code, multigroup cross sections for hydrogen have been generated with the help of which some results for the neutron age of fission neutrons for water systems have been obtained. It is seen that diagonal transport approximation yields results which are in good agreement with those obtained from the experiment and other theoretical methods. As for example, the neutron age of Indium resonance (1.46 eV) in water for a fission source obtained from our calculation is  $27.55 \text{ cm}^2$  while those from the experiment <sup>(1)</sup> and the stochastic method of calculation of the Yamamura and Sekiya <sup>(2)</sup> are respectively  $26.48 \pm 0.32$  and  $26.34 \text{ cm}^2$ . Compared to the stochastic method of Yamamura and Sekiya our method is simpler and requires much less computer time.

The slowing down length has also been calculated in an infinite spherical geometry for a spherical neutron source of different radii under the assumption that the source does not absorb or scatter any neutron and becomes a part of the slowing down medium just after emitting the neutrons. Results obtained from this calculation indicate that the slowing down length increases as one increases the finite size of the source. Further works on this project are in progress.

- (1) Pashal, R.K., Nucl. Sci. Engg., 20(1964), 436
- (2) Y. Yamamura and T. Sekiya, J.Nucl. Sci. Technol., 7(1970), 564.

### 3. Thermal Neutron Scattering Kernels in Poly crystalline Solids

( S.A.M.M. Siddiqui )

A computer code is being developed for the thermal neutron scattering kernel in a poly crystalline material. The customary approach, due to Schofield and Hassit<sup>(1)</sup>, is to expand the intermediate scattering function in an infinite series such that the  $\ell$ -th term accounts for the process in which  $\ell$ -phonons are exchanged. The first two terms (i.e. the elastic scattering and the one phonon term) are treated exactly and the remaining terms are approximated by using the central limit theorem of statistics, which is supposed to be a good approximation for terms with large values of  $\ell$ . We therefore expect that an exact treatment

of the  $l=2$  term with the remaining terms approximated by the central limit theorem would improve the results considerably. Our efforts are also directed towards finding suitable representations for the frequency distribution functions, so that some of the integrations can be performed analytically, thus reducing the computation time. Two phonon cross sections for beryllium have been computed by Kothari and Singwi<sup>(2)</sup>, but our work differs from theirs in that we use a more realistic model for the frequency distribution function rather than the Debye spectrum, for energies upto  $2\theta$ ,  $\theta$  being the Debye parameter. For energies  $> 2\theta$ , use of the Einstein model is a gross simplification resulting in an incorrect distribution of final energies. Use of a frequency spectrum which accounts for the spread in energy of the frequency spectrum will give better results. At present, the project is at a computational stage.

1. Scheffield, P. and Hassit, A. Proc. Int. Conf. Geneva 16 (1958) 217
2. Kothari, L.S. and Singwi, K.S.J. Nucl. Energy, 5 (1957) 342

PROGRESS REPORT ON NUCLEAR DATA IN BRAZIL

(June 1973 - May 1974)

1. INTRODUCTION

This Progress Report has been written on the basis of:

a) abstracts which have been sent to the INDC Liaison Officer upon request to individuals who might represent groups doing research in nuclear physics, reactor physics, nuclear chemistry, and nuclear engineering;

b) abstracts of papers published by Brazilian scientists in the "Revista Brasileira de Física", and other international journals;

c) abstracts of papers presented at the Annual Meeting of the Brazilian Society for the Advancement of Science, 1974.

The material has been selected having in mind the eventual interest to nuclear data compilers and evaluators. Although it was tried not to miss any appropriate institution or individual there have been some oversight.

The information herein contained must be considered as private communications, and should not be quoted without author's permission.



S.B. Herdade  
Liaison Officer for Brazil,  
International Nuclear Data Committee

## 2. MAIN EXPERIMENTAL FACILITIES FOR NUCLEAR PHYSICS RESEARCH

### 2.1 - 22 MeV Herb Pelletron Accelerator (Instituto de Física - Universidade de São Paulo)

The Pelletron system consists of a 4 MV injector and a tandem - type accelerator. It is capable of furnishing beams of 22 MeV protons, 27 MeV alphas, and heavy ions of energy 50 MeV for Oxygen to 80 MeV for Sulphur.

Present status: in operation

Utilization: fast neutron physics (time-of-flight spectrometer), heavy ion reactions, nuclear spectroscopy, and charged particle reactions.

### 2.2 - PUC- RJ Van de Graaff Accelerator (Pontificia Universidade Catolica - Rio de Janeiro)

High Voltage Eng. Model KN-4000 machine, with the following characteristics: protons or deuterons: 0.5 to 4.0 MeV, - 3 KeV resolution, 200  $\mu$ A current; electrons: 1.5 to 3.0 MeV 20 KeV resolution, 900  $\mu$ A current.

Present status: in operation

Utilization: atomic and nuclear physics research (nuclear spectroscopy).

### 2.3 - University of São Paulo Electrostatic (Van de Graaff Accelerator (Instituto de Física-Universidade de São Paulo)

Characteristics: 3.5 MeV protons or deuterons; 7 MeV alphas. Beam currents: 10  $\mu$ A for protons or deuterons, and alphas up to 3.5 MeV. Above 3.5 MeV the alpha current is approximately 0.1  $\mu$ A.

Status: presently not in operation

### 2.4 - University of São Paulo Electron LINAC (Instituto de Física - Universidade de São Paulo).

Characteristics: Electron linear accelerator, composed by two SLAC type section, three meter long each. Electron beam is supplied by a 100 kV pulsed electron gun at a repetition rate of 60, 120, 180, 240, 300 and 360 Hz. Maximum nominal energy: 75 MeV. Analysed (0.5% resolution) current, approximately 100 nA at 60 Hz.

Status: in operation in the energy range 8 to 45 MeV, with currents up to 200 nA; the vacuum system will be replaced by one using ion pumps so that the nominal energy could be reached in a near future.

Utilization: electrodesintegration studies, electron and bremsstrahlung induced fission; delayed neutron studies, and nuclear spectroscopy.

2.5 - CBPF Electron LINAC - (Centro Brasileiro de Pesquisas Físicas - Rio de Janeiro).

Characteristics: This machine was designed and built by the CBPF Accelerator Development Group. Energy: 28 MeV; 60  $\mu$ A mean current; pulsed beam with pulses from 500 ns to 3  $\mu$ s.

Status: in operation

Utilization: nuclear spectroscopy and neutron time-of-flight experiments.

2.6 - Variable Energy Cyclotron (Instituto de Engenharia Nuclear - Rio de Janeiro)

Characteristics: Cyclotron Corporation Model CV-28; will deliver over 50  $\mu$ A of external beams of 2 to 24 MeV protons 3 to 14 MeV deuterons, 5 to 38 MeV  $^3\text{He}^{++}$ , and 6 to 28 MeV  $^4\text{He}^{++}$ . Heavier ions can also be accelerated.

Status: the accelerator and chemistry laboratories building will be finished in July 1974; operation of the machine estimated to start in October 1974.

Utilization: production of neutron deficient radionuclides for medical uses; activation analysis; nuclear chemistry; radiation damage; nuclear reactions; neutron cross-section measurements.

2.7 - IEA - RI Swimming Pool Research Reactor (Instituto de Energia Atômica - São Paulo).

Characteristics: Built by Babcock and Wilcox Co. Nominal power: 5Mw. Has been operated during 17 years at 2 Mw. Facilities for experiments and irradiation include: 8 radial beam-holes, 2 tangential beam-holes, 2 pneumatic "rabbit" stations, and 22 irradiation rigs in the core.

Status: shut down for Power upgrade to 10 Mw.

Utilization: radioisotope production; activation analysis; nuclear, neutron, and solid state physics experiments.

2.8 - IPR Triga Reactor (Instituto de Pesquisas Radioativas  
Belo Horizonte)

Characteristics: Designer and builder - General Atomic. Nominal reactor power: 30 Kw (upgraded to 250 Kw).

Status: in operation.

Utilization: radioisotope production; activation analysis; solid state physics; radiation and nuclear chemistry.

2.9 - Brazilian Argonauta Research Reactor ( Instituto de Engenharia Nuclear - Rio de Janeiro)

Characteristics: Designed in ANL, USA, and built by Mecânica CBV Ltda., Rio de Janeiro, Brazil.

Argonauta type ( $H_2O$  - graphite; 20% enriched uranium).

Power: 10 Kw (maximum). Fuel:  $VO_2$ -Al pressed powder mixture with cladding, fabricated by the Metallurgy Division of IEA, São Paulo, Brazil.

Experimental facilities: neutron beams (horizontal-vertical); isotope production (holes, cavities, channels); short time irradiation ("rabbit" system); thermal column (internal and external); shield test removable.

Utilization: neutron and reactor physics, solid state physics, engineering tests, radiochemistry, isotope production, graduate education.

3. NUCLEAR SPECTROSCOPY

3.1 - Spectroscopic Factors of Negative - Parity Multiplet States in Odd Sn Isotopes

S. de Barros<sup>+</sup>, M.J. Bechara<sup>+</sup>, T. Borello-Lewin<sup>+</sup> and V. Paar<sup>++</sup> (International Centre for Theoretical Physics, Trieste, Italy).

The spectroscopic factors of the negative-parity multiplet states  $7/2_1^-$ ,  $9/2_1^-$ ,  $11/2_2^-$ ,  $13/2_1^-$  and  $15/2_1^-$  in odd Sn isotopes are calculated by including leading order scattering and ground-state correlation process. It is shown that ground-state correlations play an important role for the spectroscopic factors of the  $7/2_1^-$  and  $11/2_2^-$  states. The theoretical results are in good agreement with the available experimental data.

(Published in: Physics Letters, 49 B (1974) 113-116).

<sup>+</sup>Permanent address: Instituto de Física, Universidade de São Paulo, São Paulo, Brazil.

<sup>++</sup>Permanent address: Institute "Rudjer Bosković", Zagreb, Yugoslavia.

3.2 - Effective Magnetic Dipole Operators and the Lifetime of the  $3/2^-$  State in  $^{207}\text{Pb}$ .

M. Dost<sup>+</sup> and J. D. Rogers<sup>++</sup>

A lifetime of  $\tau = (0.15 \pm 0.03)$  psec for the 897 KeV  $3/2^-$  state in  $^{207}\text{Pb}$  is determined by the Doppler shift attenuation method in thick target Coulomb excitation by 68 and 61 MeV  $^{16}\text{O}$  ions on  $^{207}\text{Pb}$ . The analysis uses the Monte Carlo method to treat the slowing down of recoiling Pb nuclei in Pb, and takes into account the effects of particle -  $\gamma$  angular correlations, finite detector size, and the slowing down of the projectiles in the target. The derived value of  $B(M1, 3/2^- \rightarrow 1/2^-) = (0.52 \pm 0.10) \left(\frac{e\hbar}{2mc}\right)^2$  can be described with the same effective magnetic moment operator as describes the magnetic dipole moment in nuclei around ...  $^{208}\text{Pb}$ .

(Published in: Revista Brasileira de Física, Vol.3, nº 2, (1973) 217).

+ Rutgers, The State University, New Brunswick, NJ 08903

++ Instituto de Física, Universidade Federal do Rio Grande do Sul, Porto Alegre, Rio Grande do Sul, Brazil.

3.3 - g-Factors of the 264 KeV and 632 KeV States in  $^{77}\text{As}$ .

R.P.Livi, J.Schaf and F.C.Zawislak

(Instituto de Física, UFRGS, Porto Alegre) and

J.M.Gualda and R.N.Saxena

(Instituto de Energia Atomica, São Paulo)

The integral perturbed angular correlation technique has been used to measure g-factors of the 264 KeV and 632 KeV states in  $^{77}\text{As}$ . The measurement of the 264 KeV level was performed in an external magnetic field of  $30 \text{ K O}_e$ . The 632 KeV states, having a shorter lifetime was studied with help of the large hyperfine magnetic field at As nuclei in Fe matrix.

The g-factor of the 264 KeV ( $5/2^-$ ) state was measured using the 367-264 KeV gamma cascade while the 558-417 KeV gamma cascade was used to determine the g-factor of the 632 KeV ( $5/2^+$ ) state. The results are:  $g_{5/2^-} = + 0.33 \pm 0.05$  and  $g_{5/2^+} = + 1.42 \pm 0.32$ . The magnetic moments calculated from

these results are compared with the values obtained from the models available for the nuclei in this mass region.

### 3.4 - Half-Lives of Excited States in $^{77}\text{As}$ and $^{81}\text{Br}$

R.N.Saxena and A.Bairrio Nuevo Jr.

(Instituto de Energia Atomica, São Paulo) and

R.P.Livi and F.C.Zawislak

(Instituto de Física, UFRGS, Porto Alegre)

The odd proton nuclei in the mass region  $71 \leq A \leq 85$  have a very similar low energy level structure. In particular the state with spin of  $5/2^-$  has been identified in most nuclei of this mass region. As a part of our systematic study of nuclear properties in this region, we have measured the half-lives of the excited states in  $^{77}\text{As}$  (264 KeV  $5/2^-$ ) and  $^{81}\text{Br}$  (276 KeV  $5/2^-$ ). The delayed gamma-gamma coincidence technique using Pb loaded plastic scintillators coupled to the RCA-8275 and -8850 photomultiplier tubes and conventional electronics was utilized. For the measurement of the 264 KeV state of  $^{77}\text{As}$  the 367-264 KeV gamma cascade was used while the 276 KeV state of  $^{81}\text{Br}$  was measured through the 290-276 KeV gamma cascade. The half-lives were determined from the slope of the delayed coincidence curves. The results are  $T_{1/2}(264 \text{ KeV}) = 280 \pm 20 \text{ psec}$  and  $T_{1/2}(276 \text{ KeV}) = 236 \pm 15 \text{ psec}$ .

### 3.5 - Directional Correlations of Gamma Transitions in $^{134}\text{Xe}$ .

J.M.Gualda and R.N. Saxena

(Instituto de Energia Atomica, São Paulo) and

F.C.Zawislak

(Instituto de Física, UFRJ, Porto Alegre)

The directional correlation of coincident  $\gamma$ -transitions in  $^{134}\text{Xe}$  have been measured using a Ge(Li)-NaI(Tl) spectrometer. The measurements have been carried out for the 405-884-847, 433-(1072)-847, 540-884-847, 595-(540)-884-847, 621-884-847, 677-884-847, 766-847, 857-884-847, 884-847, 948-(1072)-847, 1072-847, and 1136-884-847 KeV gamma cascades. Spin assignments have been made for the levels at 1920 KeV ( $3^+$ ), 2136 KeV ( $5^+$ ), 2272 KeV ( $4^+$ ), 2352 KeV ( $4^+$ ), 2408 KeV ( $5^+$ ), 2588 KeV ( $4^+$ ) and 2867 KeV ( $4^+$ ). In addition previous spin assignments of levels at 1613 KeV

( $2^+$ ) and 1731 KeV ( $4^+$ ) have also been confirmed. The multipole mixing ratios (E2/M1) obtained from the present data are: (405) =  $0.80 \pm 0.7$ , (433) =  $0.08 \pm 0.06$ , (540) =  $-1.92 \pm 0.10$ , (595) =  $-0.32 \pm 0.20$ , (621) =  $-0.76 \pm 0.05$ , (677) =  $-0.32 \pm 0.02$ , (766) =  $-2.4 \pm 0.2$ , (857) =  $-0.64 \pm 0.1$ , (948) =  $-0.40 \pm 0.1$ , (1072) =  $-0.16 \pm 0.02$ , and (1136) =  $0.48 \pm 0.02$ .

### 3.6 - High Resolution Spectroscopy for the s-d Shell.

J.A. Guillaumon Fo. and I.D. Goldman

(Instituto de Física - Universidade de São Paulo)

The decays of the nuclides  $^{24}\text{Ne}$ ,  $^{25}\text{Na}$ ,  $^{29}\text{Al}$  and  $^{35}\text{P}$ , produced by "bremmstrahlung" irradiation at the University of São Paulo Electron LINAC, are being studied using a Ge(Li) detector with 2.5 KeV resolution at 1332 KeV, and a X-ray detector with 600 V resolution.

In the decay of  $^{29}\text{Al}$ , the transition of 1153 KeV with a measured intensity of  $(0.93 \pm 0.12)\%$  has been detected, besides the higher intensity transitions 1273 (89.3%), 2028 KeV (3.8%), and 2426 KeV (6%).

### 3.7 - Measurement of the Transition $3^+ \rightarrow 1^+$ in the decay of $^{164m}\text{Ho}$ .

V.R. Vanin and I.D. Goldman

(Instituto de Física - Universidade de São Paulo)

The nuclide  $^{164}\text{Ho}$  has been obtained by "bremmstrahlung" irradiation of  $\text{Ho}_2\text{O}_3$  powder at the University of São Paulo Electron LINAC. Thin targets have been utilized due to the high self-absorption coefficient in Ho. A Ge(Li) X-ray detector, associated to a 2048-channel analyser have been used, with a resolution of 0.6 KeV at 80 KeV, sufficient to separate completely the line of 94.0 KeV attributed to the decay of  $^{164m}\text{Ho}$  from the line of 91.4 KeV, produced by the decay of  $^{164g}\text{Ho}$ . The measurement of the ratio of the cross-over intensity  $3^+ \rightarrow 1^+$ , of 94.0 KeV, and the intensity of the transition  $3^+ \rightarrow 2^+$ , of 56.6 KeV, resulted in the value  $0.006 \pm 0.001$ .

## 4. PHOTONUCLEAR REACTIONS

### 4.1 - Cross-section for the Reaction $^{232}\text{Th}(\gamma, n)^{231}\text{Th}$ near threshold.

O.Y. Mafra, M.F. Cesar and C. Renner

(Instituto de Energia Atômica - São Paulo) and

J. Goldemberg

(Instituto de Física - Universidade de São Paulo)

The  $(\gamma, n)$  cross-section of  $^{232}\text{Th}$  has been measured by the activation method, using neutron capture monochromatic gamma-rays from 5.43 to 10.83 MeV, at the IEA-R1 research reactor. The  $^{231}\text{Th}$  activity is measured by the area under the 84 KeV peak measured with a Ge(Li) spectrometer.

Irradiations have been carried out near the gamma-ray sources, with the samples surrounded by cadmium and paraffin to minimize  $(n, f)$  and  $(n, 2n)$  reactions.

The measured cross-section presented the same structure previously observed for the  $(\gamma, f)$  reaction, with agreement with the values obtained through the measurement of the total number of neutrons emitted in the  $(\gamma, n)$  process.

#### 4.2 - Formation of $^{178}\text{Ta}$ Isomeric States.

O.A.M. Helene and I.D. Goldman

(Instituto de Física - Universidade de São Paulo)

The experimentally determined isomeric states formation ratios for  $^{178}\text{Ta}$  have been compared with the calculated ones on the basis of the statistical model. The experimental results have been obtained by irradiating  $^{181}\text{Ta}$  samples with bremsstrahlung produced by the University of São Paulo Electron LINAC. A Ge(Li) detector, with a resolution better than 3 KeV at 1.33 MeV, was utilized to measure the residual activities.

The experimentally determined formation ratio between the states  $1^+$  and  $7^-$ ,  $8^-$ , or  $9^-$  was approximately 1, for electron beams with energies between 30 and 40 MeV. By irradiating  $^{181}\text{Ta}$  near the threshold of the reaction  $(\gamma, 3n)$ , a value significantly greater than 1 has been obtained for the formation ratio between the mentioned states. This result seems to indicate that the  $1^+$  state is the ground state of  $^{178}\text{Ta}$ .

#### 4.3 - Isomeric State Formation by $(\gamma, 3n)$ Reaction in $^{141}\text{Pr}$ .

S.A.S. Vitiello and I.D. Goldman

(Instituto de Física - Universidade de São Paulo)

Sources of  $^{138m}\text{Pr}$  and  $^{138g}\text{Pr}$  were produced by the bremsstrahlung beam of the Linear Accelerator of the Instituto de Física da Universidade de São Paulo, at the energy of 43.5 MeV. The isomeric state  $(7, 8, 9)^-$ ,  $T = 2.02\text{h}$ , and the ground state  $(1^+)$ ,  $T = 1.4\text{min.}$ , were identified by the half lives and the

transition of 788.8 Kev, respectively. In order to obtain sufficient statistics, the analyzed spectra was the result of 10 runs. The obtained experimental branching ratio, was 0.32, and the comparison with the statistical theory is presented in Table I.

$N_{\gamma}$	$\sigma$	Square Well	Parabolic	Exp.
4	2	.038		
4	3	.324	.336	.32
4	4	.755		

4.4 - Isomeric State Formation by  $(\gamma, 3n)$  reaction in  $^{107}\text{Ag}$ .

S.A.S.Vitiello and I.D.Goldman

(Instituto de Física - Universidade de São Paulo)

Natural silver targets were bombarded by the bremsstrahlung beam of the Linear Accelerator of the Instituto de Física da Universidade de São Paulo.

Gamma-ray spectra following the decay were measured, and the isomeric  $(2+)$  and ground state  $(5+)$  are determined by the transition of 555.8 Kev and separation of the half-lives, 33.5 min and 66.5 min, respectively.

The experimental deduced ratio in energies from 33 to 46 MeV, are presented in Table I.

Following Huizenga and Vandenbosch (Phys.Rev. 120(1960)1305 and 1313), a comparison of data was done with statistical theory. The transmission coefficients have been calculated using a square well and a parabolic potential. The gamma-ray cascades with a 10% quadrupole admistures give to the spin cut-off parameter a value greater than 5.

Table I

Energy (MeV)	33	36	38	40	42	44	46
Ratio	.35	.28	.26	.28	.26	.17	.18

4.5 - The  $^{55}\text{Mn} (\gamma, 3n) ^{52}\text{Mn}$  Reaction.

M.Nielsen and I.D.Goldman

(Instituto de Física - Universidade de São Paulo)

We have irradiated powder samples of metallic  $^{55}\text{Mn}$  in the Linear Accelerator of the Instituto de Física da Universidade de São

Paulo. The bremsstrahlung was obtained using a  $2\text{g/cm}^2$  tantalum irradiator.

The measurement was made using a Ge-Li detector and the interference of the 2.6h activity of  $^{56}\text{Mn}$  produced by neutron capture was avoided by waiting the convenient time.

The measurement of the  $^{52g}\text{Mn}$ , 5.7 d activity was made following the transitions 744, 935 and 1434 KeV. The yield was calculated in reference to the  $^{54}\text{Mn}$ , 300 d activity, 835 KeV transition.

The cross section ratio of the  $^{52}\text{Mn}$  to  $^{54}\text{Mn}$ , at energies from 32.5 up to 44 MeV, have been determined and the results presented on Table I.

To determine the  $(\gamma,3n)$  cross section, we shall use the experimental results from  $^{55}\text{Mn}(\gamma,n)^{54}\text{Mn}$  reaction published by P.A.Fournay, R.S.Tickle and W.D.Whitehead, Phys.Rev. 120,1424 (1960) and R. Nathans and J.Halpern, Phys. Rev. 93, 437 (1954) and the thick target bremsstrahlung calculations recently published by M.J.Berger and S.M.Seltzer, Phys.Rev. 62, 621(1970).

Table I

Energy (KeV)	32,5	33,5	35,0	36,5	37,5	38,0	38,2	40	42	42,5	44
Ratio ( $\times 10^{-4}$ )	0,053	0,065	0,30	0,92	1,92	2,22	3,30	5,27	8,21	7,97	12,30

4.6 - Formation Ratio of the  $^{117}\text{In}$  Isomeric States by  $(\gamma,\alpha)$  Reaction.

E.A.Finotti and I.D.Goldman

(Instituto de Física - Universidade de São Paulo)

Measurements of  $^{117g}\text{In}$  and  $^{117m}\text{In}$ , formed in the  $^{121}\text{Sb}(\gamma,\alpha)$  reaction, are very difficult when natural antimony is used as target, due to the formation of  $^{122}\text{Sn}$ . Even though the  $^{122}\text{Sn}$  half-life is 2.8 d, greater than the 40 min and 117 min half-lives for  $^{117g}\text{In}$  and  $^{117m}\text{In}$ , respectively, the measurements of the residual activities are disturbed by the presence of that antimony isotope. In order to measure easily the characteristic lines of 552.9 KeV from  $^{117g}\text{In}$  and 315.3 KeV from  $^{117m}\text{In}$ , a chemical separation of indium from antimony has been carried out. A result  $0.30 \pm 0.15$  has been obtained for the isomeric state formation ratio  $R_m/R_g$  relative to the nuclide  $^{117}\text{In}$ .

#### 4.7 - The $(\gamma, n)$ Reaction in $^{19}\text{F}$ and $^{23}\text{Na}$ in the Energy

Range 0.3 - 1.0 GeV.

F.Salvetti, C.Aurisicchio, V. de Napoli, M.L.Terranova  
(Istituto di Chimica Generale ed Inorganica dell'Uni-  
versità, Roma) and

H.G. de Carvalho and J.B.Martins

(Centro Brasileiro de Pesquisas Físicas, Rio de Janeiro)

Cross-section per equivalent quantum has been measured for the reactions  $^{19}\text{F}(\gamma, n)^{18}\text{F}$  and  $^{23}\text{Na}(\gamma, n)^{22}\text{Na}$  in the energy range 0.3 - 1.0 GeV. The targets were plates of analytical grade sodium oxalate (34%  $^{23}\text{Na}$ ) and lithium fluoride (73%  $^{19}\text{F}$ ) in powder form. The powders were packed uniformly between two lucite discs (5cm diameter and 0.05 cm thickness).

Average absolute cross sections of  $(1.30 \pm 0.10)$  mb and  $(1.60 \pm 0.20)$  mb have been calculated for the two reactions, respectively, over the whole energy range considered, by means of the photon difference method.

#### 4.8 - The Monte Carlo Method for Photonuclear Reactions.

M.Foshina and J.B.Martins

(Centro Brasileiro de Pesquisas Físicas, Rio de Janeiro)

There are many published papers on the utilization of the Monte Carlo method in the study of intranuclear cascades initiated by protons. Nevertheless, in the case of intranuclear cascades initiated by photons there is only the work done by Gabriel and Alssmiller (Phys. Rev. 182 (1969)1035), that allows the determination of important parameters in photonuclear reactions up to 0.4 GeV.

For the estimate of values for the cross-section of photo production of neutrons in the energy range 200 MeV to 1000 MeV we have applied the Monte Carlo method, taking into consideration primary interactions carried out through "quasi-deuteron" or "photo mesonic" processes. 10000 stories have been followed and the probabilities for the photo production of neutrons in the nuclei  $^{12}\text{C}$ ,  $^{19}\text{F}$ ,  $^{23}\text{Na}$ ,  $^{55}\text{Mn}$ ,  $^{103}\text{Rh}$ ,  $^{197}\text{Au}$  and  $^{238}\text{U}$  have been determined.

#### 4.9 - Photoproduction of Neutrons in Complex Nuclei.

H.G. de Carvalho, J.B.Martins, M.Foshina

(Centro Brasileiro de Pesquisas Físicas, Rio de Janeiro)

V. di Napoli and M.L. Terranova  
(Istituto di Chimica Generale ed Inorganica dell'  
Università, Roma)

The estimates of cross-sections for the photoproduction of neutrons using the Monte Carlo method have been compared with previously obtained experimental results, in the energy range 300 MeV to 1000 MeV, using the bremsstrahlung beam of the Frascati accelerator. Estimates of the cross-sections have also been obtained through simple expressions from the nucleons.

The following results have been obtained for the average values of the cross-sections in the energy range 300 MeV to 1000 MeV:  $^{12}\text{C}(\gamma, n)^{11}\text{C} - 0.7 \pm 0.03$ ;  $^{19}\text{F}(\gamma, n)^{18}\text{F} - 1.06 \pm 0.05$ ;  $^{23}\text{Na}(\gamma, n)^{22}\text{Na} - 1.27 \pm 0.06$ ;  $^{55}\text{Mn}(\gamma, n)^{54}\text{Mn} - 2.6 \pm 0.13$ ;  $^{103}\text{Rh}(\gamma, n)^{102}\text{Rh} - 4.36 \pm 0.21$ ;  $^{197}\text{Au}(\gamma, n)^{196}\text{Au} - 8.03 \pm 0.40$  and  $^{238}\text{U}(\gamma, n)^{237}\text{U} - 9.37 \pm 0.45$ , in millibarns.

#### 4.10- A New Method for the Analysis of Electroexcitation Reactions.

I.C.Nascimento and S.B. Herdade  
(Instituto de Física - Universidade de São Paulo)

In the study of photonuclear reactions the nuclei are irradiated with photons produced by an external source and, in this case, they are plane waves where all the angular momenta enter in equal proportion. In electrodisintegration reactions the nuclei are irradiated by photons produced in the electron scattering process in these same nuclei. The virtual photons produced and absorbed are not plane waves. The analysis of these reactions used to be carried out by Plane Wave Born Approximation (PWBA) which, for heavy nuclei may lead to contradictory conclusions as far as the multipolarities of the nuclear transitions are concerned. Gargaro and Onley (Phys. Rev. C4 (1971) 1032) have been calculated the virtual photon spectra using a Distorted Wave Born Approximation (DWBA). This method is being checked in this work by comparing the experimental results for the electrofission of  $^{238}\text{U}$  and for the ratio  $\sigma^-/\sigma^+$ , where  $\sigma^-$  and  $\sigma^+$  are the cross-sections for the reactions  $(e, e'n)$  for electrons and positrons respectively, with the calculated ones. This work is being carried out with the collaboration of Prof. D.S.Onley, Ohio University, Athens, Ohio, USA.

4.11 - E1 Virtual Photon Spectrum for the use in Electrodisintegration Reactions.

E. Wolyneć

(Instituto de Física - Universidade de São Paulo)

The nuclear electroexcitation process is intimately related to the corresponding photoexcitation process. In both cases the nucleus receives the excitation energy through the interaction of an electromagnetic field with the nuclear charges and currents. By relating the two processes it is possible to define a virtual photon spectrum  $N(\lambda, L, E_0, \omega)$  and write the total electron inelastic cross-section  $\sigma_e$ , in a form analogous to the one for the bremsstrahlung yield:

$$\sigma_e(E_0) = \int_0^{E_0 - m_0} \sum_{\lambda, L} \sigma_Y^\lambda(L, \omega) N(\lambda, L, E_0, \omega) \frac{d\omega}{\omega}, \quad \text{where } E_0 =$$

= total energy of the incident electron,  $m_0$  = electron rest energy,  $\omega$  = photon energy,  $\lambda = E$  or  $M$  for electric or magnetic transitions of multipolarity  $2^L$  and  $\sigma_Y^\lambda(L, \omega)$  = cross-section for photoexcitation. Recently,  $N(\lambda, L, E_0, \omega)$  has been calculated using DWBA (Gargaro and Onley, Phys. Rev. C4 (1971) 1032). Nevertheless the calculation results is a non-analytic expression for the virtual photon spectrum. The calculation of a particular virtual photon spectrum using DWBA, which involves the sum of many partial waves, takes a lot of computer time, which makes prohibitive its use for the analysis of electrodisintegration reactions.

Using the computer code VIRFO- 1 developed by Onley for the spectrum calculations, we generated 50 points of the E1 virtual photon spectrum for different values of  $Z$  and  $E_0$  ( $Z$  = atomic number of the target nucleus). From these points an analytical expression has been adjusted to the DWBA calculated spectrum for E1. This expression is :

$$N(E1, E_0, \omega, Z) = NP(E1, E_0, \omega) + \left[ 1.29 \times 10^{-5} \exp(1.245 Z^{1/3} - 0.052\omega) \right] \cdot \left[ (E_f - m_0) / (\omega + m_0) \right] \omega, \quad \text{where : } Z = \text{atomic number of the target nucleus, } NP(E1, E_0, \omega) = \text{expression for the virtual photon spectrum in PWBA, and } E_f = E_0 - \omega.$$

4.12 - An Analysis of Electrodisintegration of Nuclei using  
El Virtual Radiation Spectra Evaluated with Coulomb  
Distorted Waves.

E. Wolyneç, G. Moscati, O.D. Gonçalves and M.N. Martins  
(Instituto de Física - Universidade de São Paulo)

Data on the ratio of photo and electrodisintegration of several nuclei ( $^{12}\text{C}$ ,  $^{64}\text{Cu}$ ,  $^{64}\text{Zn}$ ,  $^{109}\text{Ag}$ ,  $^{181}\text{Ta}$  and  $^{197}\text{Au}$ ) are compared with theoretical ratios predicted by plane and distorted waves calculations. The analysis with distorted waves shows that all data are compatible with photoabsorption through El transitions, as can be explained by the electric dipole sum rule. This outcome does not agree with published conclusions for high Z nuclei using plane wave approximation.

5. NUCLEAR FISSION

5.1 - On the Photofission Cross Sections of  $^{209}\text{Bi}$ ,  $^{232}\text{Th}$   
and  $^{238}\text{U}$  at Intermediate Energies.

H.G. de Carvalho, J.B. Martins and O.A.P. Tavares  
(Centro Brasileiro de Pesquisas Físicas - Rio de Janeiro)

and

V. di Napoli and M.L. Terranova  
(Istituto di Chimica Generale ed Inorganica dell'  
Università - Roma)

Photofission cross sections have been estimated for  $^{209}\text{Bi}$ ,  $^{232}\text{Th}$  and  $^{238}\text{U}$ , in the energy range from 0.15 GeV up to 2 GeV, using fissibility values computed with the Monte Carlo Method. For the calculation of the fissibilities, use has been made of some already known results of proton-induced intranuclear cascade calculations, in order to obtain information about mass number, atomic number and excitation energy distributions of the post-cascade nucleus. The calculation has been carried out as a fission-evaporation competition, using an energy dependence of the ratio of the neutron evaporation width to fission width. The results have been compared with experimental data, showing that the photofission cross sections are consistent with the photomeson mechanism of nuclear excitation.

Published in: Notas de Física, CBPF, Vol. XXI, nº5 (1973)

5.2 - High Energy Photofission Cross Sections of Uranium,  
Thorium and Bismuth.

O.A.P.Tavares

(Centro Brasileiro de Pesquisas Físicas, Rio de Janeiro)

Bremsstrahlung beams produced in a thin tungsten radiator by incident electrons accelerated in the "Deutsches Elektronen Synchrotron" (Hamburg) at energies ranging from 1 GeV to 5.5 GeV, and in an aluminum radiator by electrons accelerated at 16 GeV in the "Two Mile Stanford Linear Accelerator" (SLAC), were used in our experiments. The nuclear emulsion technique has been employed for fission fragment detection. Using a special development process carried out previously in our laboratory, discrimination between fission fragments tracks and alpha particles tracks was possible for nuclear emulsion pellicles loaded with uranium and thorium. The photofission cross sections were obtained from measurements of the cross sections per equivalent quantum by using  $1/k$  bremsstrahlung spectrum approximation ( $k$  is the photon energy) in energy ranges  $L$  GeV - 5.5 GeV and 5.5 GeV - 16 GeV. The results show a decrease in the cross sections with energy, which is in good agreement, within experimental errors, with the results of other authors who used not only this technique but mica and glass detectors as well. For photon energies higher than 1 GeV, the photofission cross sections decrease asymptotically by about fifty times their value at 300 MeV in the case of  $^{238}\text{U}$  and  $^{232}\text{Th}$ , and twelve times in the case of  $^{209}\text{Bi}$ .

5.2 - Photofission Cross Section of  $^{238}\text{U}$  in the Energy Range  
5.43 MeV - 10.83 MeV measured with Polycarbonate Foils  
(Makrofol).

M.F.Cesar, A.M.P.Kuniyoshi and O.Y.Mafra

(Instituto de Energia Atômica, São Paulo)

The cross section for the reaction  $^{238}\text{U}(\gamma, f)$  near threshold has been previously measured in this laboratory by utilizing a fission chamber, as well as by other authors. Although a structure had been always observed in the cross section curve for energies from 5 to 9 MeV, there are certain discrepancies in the data obtained by different research groups. In order to check our results, the photofission cross section of  $^{238}\text{U}$  for neutron-capture gamma-rays in the energy range 5.43 to 10.83

MeV has been measured again by means of a different technique, using polycarbonate (Makrofol) foils as fission fragment detectors. The behaviour of the experimental curve obtained was the same one observed in the previous measurements, using a fission chamber and electronic counting.

#### 5.4 - Angular Distribution of Fragments in the Electron-Induced Fission of $^{232}\text{Th}$ .

J.H. Vuolo, S.B.Herdade and I.C.Nascimento  
(Instituto de Física - Universidade de São Paulo)

Angular distributions of fragments in the electron-induced fission of even-even nuclei can be calculated provided the virtual photon spectrum in the magnetic substates  $M$ , and the rotation matrix  $d_{M,K}^J(\theta)$  are known (Huizenga, Nucl. Tech. 13, April 1972, pg. 20). The distribution for electrofission differs from the one for photofission because it includes also the substate  $M=0$  and a different distribution of multipoles.

The angular distributions of the fragments in the electrofission of  $^{232}\text{Th}$  have been obtained in the energies 8 and 9 MeV. A thorium thin target is irradiated in the electron beam of the University of São Paulo LINAC and the fission fragments are detected by polycarbonate foils (Makrofol)  $10\mu\text{m}$  thick in the angular range from  $-30^\circ$  to  $132^\circ$  with the beam direction. The results of this work are being compared with the theoretically calculated distributions, using a Distorted Wave Born Approximation formalism, as well as with experimental results previously obtained for  $^{238}\text{U}$ . On the basis of these studies, information on the shapes of the fission barriers of  $^{232}\text{Th}$  and  $^{238}\text{U}$  may be obtained. The absolute values of the cross-section for the electrofission of  $^{232}\text{Th}$  will also be obtained in the energy range 8 - 50 MeV.

#### 5.5 - Electron-Induced Fission of $^{209}\text{Bi}$ .

S.B.Herdade, J.H.Vuolo and I.C.Nascimento  
(Instituto de Física - Universidade de São Paulo)

The electron-induced fission of  $^{209}\text{Bi}$  is being studied in the energy range 40 - 60 MeV at the University of São Paulo Electron LINAC. Polycarbonate (Makrofol) sheets  $10\mu\text{m}$  thick are utilized as fission fragment detectors. Preliminary results for the  $^{209}\text{Bi}(e,e'f)$  cross-section have been obtained using a

bismuth target  $2.2 \text{ mg/cm}^2$  thick; for an electron energy of  $(42.0 \pm 0.4) \text{ MeV}$  it was obtained the value  $(1.5 \pm 0.4) \times 10^{-5} \text{ mb}$ . Results with better statistical accuracy will be obtained with a better geometrical efficiency of fission fragment detection. The photofission cross sections will be obtained by an unfolding procedure using a virtual photon spectrum calculated by a DWBA formalism (Gargaro and Onley, Phys. Rev. C4 (1971) 1032). Our experimental results in the energy range 40 - 60 MeV, together with previously obtained results by other authors in different energy ranges (Moretto et al, Phys. Rev. 179 (1969) 1176; Türck et al, Phys. Lett. 49B (1974) 335; Ranjuk et al, Ukrainsky Fizicnyj Zurnal 14 (1969) 408) will be utilized to make a better estimate of the value of the fission barrier for  $^{209}\text{Bi}$ .

#### 5.6 - Yields of Lanthanide Isotopes and Yttrium in the Fission of $^{238}\text{U}$ Induced by 14 MeV Protons.

H.C. Machado

(Instituto de Engenharia Nuclear, Rio de Janeiro)

Radiochemical measurement of fission yields for many mass numbers greater than about 140 has until recently been difficult because the great chemical similarity of the lanthanide elements effectively precludes rapid chemical purification. As a result, mass chain yields have only been determined for those masses where the longest lived member has a half life more than about a few hours.

However in recent years, the advent of high resolution Ge-Li gamma detectors has made possible the identification and measurement of radioisotopes even in very complex mixtures since the accurate gamma energies and the half lives of the peaks usually enable unambiguous assignments to particular radioisotopes to be made. In these work, a lanthanide fraction was separated from the irradiated uranium target within about 15 minutes and 90 minutes of the end of irradiation. This fraction contained isotopes of yttrium, lanthanum and the lanthanides. Half lives as short as 10 mins (eg  $^{95}\text{Y}$ ) could be readily detected and measured.

To calculate the fission yield of each isotope, it is necessary to know the abundance of the gamma ray in the nuclear decay scheme, and the efficiency of the Ge-Li detector at that

energy. The detector was calibrated in the usual way using IAEA standard sources. Abundances of the various gamma rays, however, presented a more difficult problem since literature values often show large discrepancies, particularly for some of the shorter-lived isotopes. To overcome this, abundances were calculated by calibrating with the system  $^{235}\text{U}$  (thermal n, fission), for which the mass yields have been well established.

Preliminary results have been obtained for the relative yields of 10 mass chains (93, 94, 95 Yttrium), 142, 143, 146, 147, 149, 151, 155 La + lanthanides). These have been converted to absolute yields by normalisation with mass yields already published in the literature.

## 6. CHARGED PARTICLE REACTIONS

### 6.1 - Analog Spectroscopy with Proton Inelastic Scattering.

H.Miyake and A.F.R. de Toledo Piza

(Instituto de Física - Universidade de São Paulo)

Proton inelastic scattering through isobaric resonances is analysed in the regions of tin, and of the isotones  $N = 50$  and  $N = 82$ . The scattered wave in the interaction region is decomposed in harmonic oscillator wave functions. The parent states are treated in the BCS + RPA scheme. The single-proton escape amplitudes are calculated with the 2 body coulomb charge exchange force. The partial widths for  $2^+$  and  $3^-$  states in (p,p') reactions are then determined. The results are compared with the ones obtained using the coupled equations method and with calculations utilizing the unified model.

### 6.2 - The Total Width of Isobaric States in $^{123}\text{Sb}$ .

H.Miyake, O.Dietzsch, E.W.Hamburger and A.F.R.de Toledo Piza

(Instituto de Física - Universidade de São Paulo)

Excitation functions for the proton inelastic scattering on  $^{123}\text{Sb}$ , corresponding to excitations of collective  $2^+$  and  $3^-$  states, have been fitted by a formula containing five parameters, representing a resonant amplitude and an energy independent background amplitude. The energy range of the incident protons corresponds to the region where the isobaric analog

resonances of the stated with independent particle configurations  $d_{5/2}$  and  $f_{7/2}$  in  $^{123}\text{Sb}$  are situated. The fact that the non - resonant cross section for inelastic scattering is low, compared with the resonant cross section, resulting in small interference effects, allowed us a better determination of the total widths as compared with previous results from the analysis of the elastic scattering cross section by other authors. An iterative process for the data fit with expressions containing one, two and three resonances, has been utilized. The energies and total widths obtained in the analysis of the  $2^+$  state excitation functions are, respectively:  $d_{5/2}$  ( $E = 8.95$  MeV,  $\Gamma = 52 \pm 3$  KeV),  $d_{5/2}$  ( $E = 9.25$  MeV,  $145 \pm 3$  KeV),  $f_{7/2}$  ( $E = 10.464$  MeV,  $\Gamma = 97$  KeV). The  $3^-$  state presents only one resonance :  $f_{7/2}$  ( $E = 10.426$  MeV,  $\Gamma = 112$  KeV).

### 6.3 - Direct-Compound Contribution to (p,2p) Reactions.

M.S.Hussein

(Instituto de Física - Universidade de São Paulo)

The term corresponding to the formation of a residual compound nucleus (R.C.N.) following the knocking out of a proton would contribute coherently to the direct term in (p,2p) reactions. This, we argue, modifies the angular distribution if one treats the residual compound nucleus statistically (isotropic angular distribution of emitted particles). It is possible to isolate the contribution of this new component of the amplitude using simple Hauser-Feschback analysis on the final nuclear decay. This is a very important program for the better study of hole states in nuclei. Any structure found in the decay amplitude of the R.C.N. would then be understood as intermediate structure in the exit channel. Investigations are in progress to assess the importance of the compound-compound contribution at lower bombarding energies.

### 6.4 - The Excitation of "Gauge Analog States" (GAS) by Heavy Ion Reactions.

M.S.Hussein and H-T. Chen

(Instituto de Física, Universidade de São Paulo)

A new method for the investigation of the transfer of 4 particles in heavy nuclei reactions is proposed. The "Gauge Spin"

concept is introduced to label the different nuclear states reached by the transfer of an even number of neutrons. This leads naturally to consider the possibility of exciting the "Gauge Analogue State (GAS) of the target nucleus by means of stripping or pick-up reactions between heavy nuclei. Reactions with  $^{206}\text{Pb}$  or  $^{210}\text{Pb}$  as projectiles and other lighter or heavier Pb isotopes as targets are suggested. A theory of two coupled equations is constructed to treat these reactions.

6.5 - Measurements of the  $^{27}\text{Al}(p,n)^{27}\text{Si}$  and  $^{12}\text{C}(\alpha,n)^{15}\text{O}$  Reaction Thresholds.

D. Pereira

(Instituto de Física - Universidade de São Paulo)

The "counter ratio" technique of Bonner et al (Phys. Rev. 96 (1954)122) has been utilized in the measurements of the thresholds for the reactions  $^{27}\text{Al}(p,n)^{27}\text{Si}$  ( $E_{\text{th}}=5.7969$  MeV) and  $^{12}\text{C}(\alpha,n)^{15}\text{O}$  ( $E_{\text{th}}=11.3408$  MeV) as part of the program for calibration of the University of São Paulo Pelletron accelerator. The calibration constant of the analysing magnet obtained from these measurements, are in excellent agreement with the one obtained by observing the analog resonance  $T = 3/2$  ( $E_{\text{res}}=14.231$  MeV), through the  $^{12}\text{C}(p,p)^{12}\text{C}$  reaction.

6.6. - Measurement of the  $^{19}\text{F}(p,n)^{19}\text{Ne}$  Reaction Threshold.

V.H. Rotberg

(Instituto de Física - Universidade de São Paulo)

The threshold of the reaction  $^{19}\text{F}(p,n)^{19}\text{Ne}$  at 4.233 MeV has been observed by the use of two  $\text{BF}_3$  counters in an arrangement similar to the "Bonner system" (Rickards et al, Nucl.Phys. 86 (1966) 167), in order to obtain a calibration for the University of São Paulo Pelletron accelerator. The calibration constant obtained for the  $90^\circ$  analysing magnet from this measurement is in excellent agreement with results from other similar experiments carried out in the Pelletron laboratory.

7. NEUTRON PHYSICS

7.1 - A Formula for the Fluctuation Cross-Section of Nuclear Reactions at Low Energies.

M.S.Hussein (+)

(International Centre for Theoretical Physics, Trieste, Italy)

(+) Permanent address: Instituto de Física  
Universidade de São Paulo  
São Paulo, Brazil

An expression is derived for the total fluctuation cross-section valid for the general case of any number of directly coupled open channels. In the limit when this number is very large one recovers the familiar Hauser-Feshbach result for inelastic scattering. A different result emerges for the elastic case. Generally, for many overlapping resonances:

$$\frac{\sigma_{cc'}}{(2\ell+1)\pi\lambda_c} = \left( \frac{N-1}{N+1} \delta_{cc'} + 1 \right) \frac{P_c P_{c'}}{\sum_{c''} P_{c''}}$$

7.2 - Resonance interference in  $^{232}\text{Th} - ^{233}\text{Pa}$  Systems.

M.V.Ballariny

(Comissão Nacional de Energia Nuclear, Rio de Janeiro)

The validity of the hypothesis for the separability of resonances in the solution of the Boltzmann equation for the calculation of neutron slowing-down in an absorbing medium depends upon the importance of the form term due to the resonance interference effect. This effect is related to the Placzek oscillations in the neutron flux and collision density due to the negative source of neutrons represented by an absorption resonance.

By utilizing previous results on the effect of resonance interference in practical homogeneous infinite  $^{232}\text{Th} - ^{233}\text{Pa}$  systems with a carbon moderator (Ballariny and Marable, Trans. Amer. Nucl. Soc. 13 (1970) 714), the interference effect terms have been separated and its relative and absolute variations as a function of the C/Th ratios and of the resonance spacing have been studied, leading to the following conclusions:

The form interference between the  $^{232}\text{Th}$  doublet resonances is always negative (constructive) and its variation with the system degree of moderation presents a maximum. The total form effect term is greater for well thermalized systems.

The total interference of the  $^{232}\text{Th}$  doublet on the  $^{233}\text{Pa}$  resonance of lower energy, in well thermalized systems, oscillates around the value of the asymptotic term, with the increase of the resonance spacing in the two nuclides, so that the form term assumes positive and negative values that can be neglected.

### 7.3 - Neutron Transmission Study of the Rotational Freedom of Methyl Groups in Polydimethylsiloxane.

L.Q.Amaral<sup>+</sup>, L.A.Vinhas and S.B.Herdade<sup>+</sup>  
(Instituto de Energia Atômica, São Paulo)  
I.E.A. - Technical Report nº 320

The total neutron cross section of polydimethylsiloxane has been measured as a function of neutron wavelength in the range 4 Å to 10 Å at room temperature, using a slow-neutron chopper and time-of-flight spectrometer. Scattering cross sections per hydrogen atom were obtained and the slope ( $12.2 \pm 0.2$ ) barns/Å has been derived.

Comparison with calculated neutron cross sections using the Krieger-Nelkin formalism for different dynamical situations as well as comparison with calibration curves relating the slope to the barrier hindering internal rotation indicates the existence of practically free rotation of  $\text{CH}_3$  groups about their  $C_3$  axis.

<sup>+</sup> Presently at the Instituto de Física  
Universidade de São Paulo

7.4 - Molecular dynamics of tert-butanol studied by neutron transmission

L.Q.Amaral<sup>†</sup>, R.Fulfaro and L.A.Vinhas (Instituto -  
de Energia Atômica - São Paulo)

I.E.A. - Technical Report nº 328

Neutron transmission of the globular compound tert-butanol ( $\text{CH}_3)_3\text{COH}$  have been measured in the temperature interval - 0°C to 40°C for 6.13 Å neutrons and in the neutron wave - length range 4 to 7.5 Å in the liquid and solid states. Results show that the cross-section difference at the state transition in 24°C is 13%, while it is only ~1% at the first order phase transition in 14°C. Evidence of existence of a third crystalline phase with the lowest cross section has been found. The barrier to internal methyl rotation in the solid state is estimated as  $(3.8 \pm 0.5)$  kcal/mol and does not change much over the phase and state transitions. The observed dynamical changes must be due to movements of the whole molecule and evidence that tert-butanol is not in the strict sense a plastic crystal; correlation with heat capacity results is discussed.

<sup>†</sup> Presently at the Instituto de Física -  
Universidade de São Paulo.

Progress Report  
on Nuclear Data Activities in Bulgaria  
1973

Compiled by E.Nadjakov

All the activities have taken place at the Institute of Nuclear Research and Nuclear Energy, Bulgarian Academy of Sciences, Sofia 13, some of them in collaboration with the Joint Institute for Nuclear Research (JINR), Dubna.

1. Neutron nuclear data

1. Development and application of the neutron coincidence method for measuring plutonium in fuel elements of water-water power reactors (V.I.Christov, A.I.Trifonov, T.Dragnev)

A device for measuring the quantity of plutonium-240 accumulated in the uranium fuel elements has been worked out by applying the neutron coincidence method. The measurements can be performed directly in the reactor pool.

The device allows determination of about 1g Pu-240 in an 1 hour measurement with a statistical error of 3%. Numerical estimates show that a reliable determination of the quantity of plutonium is possible in this way in reactors of the above mentioned type at a fuel burnup of 10000 MW.day per 1 ton uranium.

2. Programs for reactor physics calculations (T.Apostolov et al)

a) Program "Burnup" for nuclear fuel burnup, reproduction and poisoning by fission products in water-water power reactors.

b) Multigroup two-dimensional program for neutron flux calculations in rectangular lattice reactors.

3. Multilevel analysis of the  $^{239}\text{Pu}$  slow neutron fission cross section (N.Yaneva).

A method of interferential analysis of the resonance neutron fission cross section has been developed on the basis of the Reich-Moore R-matrix formalism.

Programs in FORTRAN 4 for IBM 360/40 computers, in the two-level and few-level approximation have been prepared. The Doppler and resolution broadening are taken into account by numerical calculations. In the unresolved resonance energy region the average cross section for investigating the intermediate structure was analysed by using various theoretical models.

Experimental data from NEUDADA were used. Analysis of the  $^{239}\text{Pu}$  neutron fission cross section in the energy region 0-10 keV was performed. The two-level resonance parameters and the intermediate structure parameters in the energy region up to 2 keV have been obtained (the intermediate structure data see in Table 1).

A multilevel analysis of  $^{239}\text{Pu}$  fission is in progress.

4. Multiplate fission ionization chamber for cooled targets (E.Dermendjiev et al).

A multiplate fission chamber with  $\sim 0.5\text{g}$   $^{235}\text{U}$  depleted on 10 targets with 10 cm diameter and  $\sim 0.5\text{ mg/cm}^2$  layer thickness has been made. The construction permits cooling of U-targets down to liquid nitrogen temperature  $T = 79\text{ K}$ . Geometry and dimensions are suitable for fission and capture gamma-ray measurements.

## 2. Non-neutron nuclear data

1. Photofission cross sections of  $^{232}\text{Th}$ ,  $^{238}\text{U}$ ,  $^{235}\text{U}$  and  $^{239}\text{Pu}$  in the subthreshold region (T.Dragnev, E.Dermendjiev, N.Kalinkova, N.Kashukeev, N.Tchikov, N.Yaneva).

The photofission cross-sections have been measured at gamma-ray energies  $E_\gamma = 6-9\text{ MeV}$ .  $(n,\gamma)$  - reactions on targets of Ca ( $E_\gamma = 6.40\text{ MeV}$ ), Ti (6.76), Be (6.83), Pb (7.38), Fe (7.63), Al (7.72), Cu (7.91) and Ni (8.99) have been used as a source of "monoenergetic" gamma rays. The tangential channel of the IRT-2000 reactor in Sofia with suitable filters and collimators has been used as a source of "monoenergetic" gamma rays. The gamma-ray intensity was high enough, giving the possibility to use thin targets. For the fragments detection a back-to-back

Table 1  
Two-level  $^{239}\text{Pu}$  intermediate structure parameters, neutron energy  
region: 0 - 2000 eV

E	$\Gamma_n$	$\Gamma_f$	$\Gamma_{12 n}$	$\Gamma_{12 f}$ (eV)
215	$0.020 \pm 0.001$	$46 \pm 1$	$0.031 \pm 0.002$	$- 181 \pm 2$
565	$0.048 \pm 0.002$	$45 \pm 1$	$0.053 \pm 0.005$	$- 189 \pm 2$
1020	$0.060 \pm 0.005$	$58 \pm 1$	$0.049 \pm 0.006$	$- 200 \pm 3$
1364	$0.040 \pm 0.003$	$50 \pm 3$	$0.031 \pm 0.003$	$- 136 \pm 4$
1680	$0.025 \pm 0.001$	$30 \pm 2$	$0.034 \pm 0.003$	$- 140 \pm 5$
1920	$0.046 \pm 0.002$	$40 \pm 2$		

Table 2  
Photofission cross-sections  $\sigma_{\gamma f}$  (mb)

(n, $\gamma$ ) source	$E_{\gamma}$ (MeV)	$^{232}\text{Th}$	$^{238}\text{U}$	$^{235}\text{U}$	$^{239}\text{Pu}$
Ca	6.40	$4.46 \pm 0.79$	$2.12 \pm 1.14$	$5.20 \pm 2.16$	$15.70 \pm 2.22$
Ti	6.76	$10.02 \pm 1.42$	$10.04 \pm 1.30$	$12.86 \pm 1.97$	$48.35 \pm 6.72$
Be	6.83	$1.18 \pm 1.28$	$8.06 \pm 3.92$	$8.50 \pm 11.3$	$16.32 \pm 2.35$
Pb	7.38	$3.40 \pm 1.55$	$10.00 \pm 2.54$	$6.00 \pm 6.36$	$17.58 \pm 2.45$
Fe	7.63	$6.28 \pm 1.04$	$10.12 \pm 1.80$	$23.38 \pm 3.82$	$45.59 \pm 5.81$
Al	7.72	$4.02 \pm 0.46$	$10.80 \pm 1.12$	$26.33 \pm 1.79$	$41.86 \pm 6.03$
Cu	7.91	$1.57 \pm 1.33$	$13.62 \pm 2.33$	$35.16 \pm 5.53$	$63.64 \pm 8.92$
Ni	8.99	$3.72 \pm 1.03$	$20.07 \pm 3.78$	$27.16 \pm 2.71$	

ionization chamber with two different targets on the central electrode was used.

The  $\beta\gamma$  results are shown in Table 2. The maxima at  $E = 6.76$  MeV for all the isotopes, and at  $E = 7.63$  for  $^{232}\text{Th}$  must be mentioned.

2. Radioactive decay of neutron deficient isotopes (Zh.Zhelev, I.Adam, B.Amov et al).

The isotopes have been obtained on the 660 MeV proton synchro-cyclotron of JINR - Dubna. Gamma spectra and gamma-gamma coincidences have been measured with Ge (Li) spectrometers, and conversion electron spectra - with a magnetic  $2\pi\sqrt{2}$  beta spectrometer.

a) Levels of  $^{145}\text{Sm}$  excited in the decay of  $^{145}\text{Eu}$  (5.9 days)

$^{145}\text{Eu}$  was obtained by bombarding Ta and Er targets. After chemical separation, the Eu fraction was mass separated. 24 new transitions have been assigned to the decay of  $^{145}\text{Eu}$ : 213.0 , 252.7 , 257.4 , 266.6 , 313.7 , 338.0 , 343.9 , 365.0 , 373.4 , 434.3 , 440.2 , 468.5 , 482.4 , 536.3 , 728.2 , 872.6 , 878.5 , 882.6 , 1003.2 , 1452.6 , 1780.0 , 1847.6 , 1951.9 , 2559.7 keV. By combining several sets of conversion electron and gamma ray intensities, K-shell internal conversion coefficients have been assigned to some of the transitions. From coincidence data levels at 1607.1 , 1843.6 , 2316.9 , 2385.5 , 2340.5 and 2513.5 keV have been established. The levels proposed are compared with those from  $^{144}\text{Sm}(d,p)$  and  $^{145}\text{Sm}(p,p')$  reactions and with a theoretically calculated level scheme known from the literature.

b) Decay scheme of  $^{147}\text{Eu}$

47 transitions have been observed and the relative gamma-ray intensities obtained with high accuracy. New transitions at 278.0 , 368.3 , 471.5 , 750.0 , 846.4 , 1154.0 , 1252.0 , 1454.0 , 1472.1 , 1479.2 , 1600.8 keV have been observed. K-shell internal conversion coefficients have been calculated by combining conversion electron and gamma ray data. Coincidence data gave additional evidence for the existence of 12 excited levels of  $^{147}\text{Sm}$ .  $\log(ft)$  -values have been calculated by using experimental branching ratios, and quantum characteristics of most of the excited levels have been determined. New levels at 1043.8 and 1600.8 keV have been established.

Table 3

Lifetimes and B(E2) values of nuclear rotational states in Yb isotopes

Nucleus	Transition I+2→I	Energy E (keV)	Lifetime $T_{1/2}$ (ps)	Total int. conv. coef. $\alpha_T$	B(E2; I+2→I)		Rigid rotor
					Experiment	( $e^2 b^2$ ) <sup>a</sup>	
$^{166}_{70}\text{Yb}_{96}$	2→0	102.3	1240 ± 200	2.86	1.05 ± 0.17	1.05 <sup>a</sup>	
	4→2	227.8	70 ± 13	0.176	1.12 ± 0.21	1.50	
	6→4	337.5	9.7 ± 1.8	0.052	1.26 ± 0.23	1.65	
	8→6	429.6	3.0 ± 0.7	0.026	1.25 ± 0.29	1.73	
	10→8 <sup>b</sup>	508	1.4 ± 0.6	0.017	1.17 ± 0.50	1.78	
$^{164}_{70}\text{Yb}_{94}$	2→0	123.5	882 ± 88	1.42	0.92 ± 0.09	0.92 <sup>a</sup>	
	4→2	262.8	29.9 ± 3.0	0.110	1.35 ± 0.14	1.32	
	6→4	375.0	5.2 ± 0.7	0.039	1.40 ± 0.19	1.45	
	8→6 <sup>b</sup>	462.8	2.0 ± 0.5	0.022	1.30 ± 0.33	1.52	
$^{162}_{70}\text{Yb}_{92}$	2→0	166.5	401 ± 59	0.50	0.73 ± 0.11	0.73 <sup>a</sup>	
	4→2	320.3	14.1 ± 2.1	0.061	1.12 ± 0.17	1.05	
	6→4	436.2	3.2 ± 0.6	0.026	1.09 ± 0.20	1.15	
	8→6 <sup>b</sup>	521.4	1.4 ± 0.5	0.016	1.03 ± 0.37	1.21	
$^{160}_{70}\text{Yb}_{90}$	2→0	243.3	135 ± 15	0.142	0.428 ± 0.047	0.428 <sup>a</sup>	
	4→2	395.6	8.0 ± 2.0	0.033	0.703 ± 0.175	0.612	
	6→4	508.7	2.0 ± 0.5	0.016	0.813 ± 0.200	0.674	
	8→6 <sup>b</sup>	588.7	0.9 ± 0.3	0.012	0.875 ± 0.290	0.706	

<sup>a</sup> Normalized to experiment. <sup>b</sup> May have additional systematic error due to bad separation from the time between reaction and population

Table 4

Energy parameters (moment of inertia  $J=3/E_2$ , level energy ratio  $E_4/E_2$ ) and transition rate parameters (intrinsic E2 moment Q, deformation  $\beta$ ) in Yb isotopes

Nucleus	$J(\text{MeV}^{-1})$	$E_4/E_2$	Q (barn)	$\beta$
$^{166}_{70}\text{Yb}_{96}$	29.3	3.23	7.25 ± 0.6	0.300 ± 0.025
$^{164}_{70}\text{Yb}_{94}$	24.3	3.13	6.8 ± 0.35	0.285 ± 0.015
$^{162}_{70}\text{Yb}_{92}$	18.0	2.92	6.1 ± 0.45	0.255 ± 0.020
$^{160}_{70}\text{Yb}_{90}$	12.3	2.63	4.64 ± 0.25	0.200 ± 0.010

c) Decay scheme of  $^{148}\text{Eu}$  (50 days)

Sources of  $^{148}\text{Eu}$  were obtained by long irradiations of Er targets. The energies and intensities of 130 gamma transitions have been determined and new gamma lines at 185.7, 253.5, 437.5, 577.5, 662.6, 705.2, 732.6, 810.8, 893.8, 976.4, 1068.5, 1121.6, 1218.0, 1270.4, 1480.9, 1532.8, 1579.1, 1592.8, 1658.3, 1699.1, 1787.1, 1840.1, 1940.0, 2202.3 keV have been observed. Conversion coefficients and multipolarities have been calculated for 52 transitions. New excited levels at 2340.5, 2389.6, 2497.2, 2693.8, 2700.6, 2860.6 keV have been established, and 22 levels have been confirmed from gamma-gamma coincidence data. By using this experimental material and calculated  $\log(ft)$ -values, a level scheme of  $^{148}\text{Sm}$  is constructed.

3. Lifetime measurements of nuclear rotational states (B.Bochev, S.A.Karamian, E.Nadjakov et al)

Lifetimes in the range of  $10^{-12}$  to  $10^{-9}$  s in several ytterbium nuclei obtained in a ( $^{40}\text{Ar}, 4n$ ) reaction at the U-300 heavy ion cyclotron of JINR - Dubna have been measured. The recoil-distance Doppler-shift method has been applied.  $B(E2)$  values have been deduced and compared to the rigid rotor model. The data obtained are presented in Table 3.

Deduced intrinsic E2 moments  $Q$  and deformations  $\beta$  are compared with the energy parameters: moment of inertia  $J=3/E_2$  and  $E_4/E_2$  (10/3 for rigid rotors and 2 for harmonic vibrators) in Table 4. A compatible decrease of all the quantities is observed with decreasing  $A$ , i.e. with penetration into the transitional region.

June 1974

Liaison Officer to the INDC for Bulgaria:

Emil Nadjakov  
Institute of Nuclear Research and Nuclear Energy  
Bulgarian Academy of Sciences  
Sofia 13, Bulgaria

B.A.R.C.-770

GOVERNMENT OF INDIA  
ATOMIC ENERGY COMMISSION

B.A.R.C.-770

PROGRESS REPORT ON NUCLEAR DATA ACTIVITIES  
IN INDIA - X

Compiled by

M. Balakrishnan  
Indian Nuclear Data Group  
Nuclear Physics Division

BHABHA ATOMIC RESEARCH CENTRE  
BOMBAY, INDIA  
1974

## I N T R O D U C T I O N

The tenth progress report on Nuclear Data Activities in India covers the work done during the year 1973. A part of the work given in this report has been presented at the Nuclear Physics and Solid State Physics Symposium held at Bangalore during December 1973.

The total number of CINDA entries sent to the Nuclear Data Section of the International Atomic Energy Agency during the period of the report is 34. The liaison activity with computer programme library (CPL) of the OECD Nuclear Energy Agency was continued.

Progress report on new facilities for research is as follows :

### 1. 224 cm Variable Energy Cyclotron

Construction work on the components of the 224 cm Variable Energy Cyclotron at Calcutta is nearing completion and the assembly work is about to begin. Assembling of the magnet at the Heavy Engineering Corporation, Ranchi has started. The main magnet coils fabricated at the Bharat Heavy Electricals Ltd., Bhopal have been received at the VEC Laboratory, Calcutta. The fabrication of the RF panels, dee and dee-stem has been completed at the Central Workshops, Trombay and these parts are ready for assembling at Calcutta.

Final testing of the power supplies is under progress. The hardware for the magnetic field mapping is ready. Work on the vacuum system, deflector, ion source and other components is nearing completion. The fabrication of the first switching magnet has started. Majority of the staff is now at the VEC Laboratory, Calcutta. Plans for the utilisation of the cyclotron are under way. The cyclotron is expected to go into operation in 1975.

2. 100 MW Thermal Research Reactor

Planning for a 100 MW Thermal Research Reactor for research purpose is under way. The design parameters will be frozen by May, 1975, civil construction will start in January 1975. The Reactor will have a vertical core and will be fuelled with metallic natural uranium. It will be cooled and moderated with heavy water which will also serve as a reflector. Experimental facilities include two engineering loops, hot and cold neutron sources, two horizontal beam tubes through the core, and provision of extending neutron beams into an experimental area outside the containment building. Neutron flux of about  $2 \times 10^{14}/\text{cm}^2/\text{sec}$  is expected. The reactor is expected to be commissioned by the end of 1979.

  
(M.K. Mehta)

Convener,  
Indian Nuclear Data Group.

INDIAN NUCLEAR DATA GROUP

MEMBERS

1. M. Balakrishnan(Secretary): Nuclear Physics Division  
\*BARC
2. B.B. Baliga : Saha Institute of Nuclear  
Physics, 92 Acharya Prafulla  
Chandra Road, Calcutta - 9.
3. V.C. Deniz : Experimental Reactor Research  
Section, BARC.
4. A.S. Divatia : Variable Energy Cyclotron  
Project, Calcutta.
5. S. Gangadharan : Analytical Chemistry Divn.,  
BARC.
6. S.B. Garg (Co-opted) : Reactor Engineering Divn.,  
BARC.
7. M.C. Joshi " : Department of Physics,  
University of Bombay,  
C.S.T. Road, Kalina,  
Bombay 400 029.
8. S.S. Kapoor : Nuclear Physics Division  
BARC
9. M.K. Mehta (Convener) : Nuclear Physics Division  
BARC
10. S.K. Mitra (Co-opted) : Tata Institute of Fundamental  
Research, Homi Bhabha Road,  
Bombay - 400 005.
11. M.P. Navalkar " : Neutron Physics Section,  
BARC.
12. B.P. Rastogi : Theoretical Reactor Physics  
Section, BARC.
13. N.S. Satya Murthy : Nuclear Physics Division,  
BARC.
14. M. Srinivasan : Neutron Physics Section,  
BARC.

---

\* Bhabha Atomic Research Centre,  
Trombay, Bombay 400 085.

<u>I N S T I T U T I O N</u>	<u>PAGE</u>
A. Bhabha Atomic Research Centre, Bombay	1
B. Tata Institute of Fundamental Research, Bombay	16
C. Saha Institute of Nuclear Physics, Calcutta	22
D. Aligarh Muslim University, Aligarh	30
E. Andhra University, Waltair	31
F. Banaras Hindu University, Varanasi	37
G. Birla Institute of Technology, Ranchi	40
H. Birla Institute of Technology, Pilani	41
I. Burdwan University, Burdwan	42
J. Calcutta University	43
K. Dibrugarh University, Assam	44
L. Indian Association for the Cultivation of Science	45
M. Institute of Technology, Kanpur	47
N. Institute of Mathematical Sciences	50
O. Kurukshetra University, Kurukshetra	51
P. Marathwada University, Aurangabad (M.S.)	52
Q. Meerut University, Meerut	53
R. Physical Research Laboratory, Ahmedabad	54
S. Punjab University, Chandigarh	60
T. Punjabi University, Patiala	63
U. Sambalpur University, Orissa	65
V. University of Delhi	66
W. University of Madras	68
X. Vikram University, Ujjain	70

A. BHABHA ATOMIC RESEARCH CENTRE, BOMBAY 400 085

1. The Recoil Ranges and Kinetic Energy Distributions in Reactor Neutron Fission of  $^{232}\text{U}$  and  $^{237}\text{Np}$  and Thermal Neutron Fission of  $^{241}\text{Pu}$  - S.B. Manohar, A. Ramaswami, S.P. Dange, P. Prasanna Venkatesan, Satya Prakash and M.V. Ramaniah - Using direct counting with Ge(Li) detector and radiochemical techniques, the recoil ranges of a number of fission products in reactor neutron fission of  $^{241}\text{Pu}$  have been determined. These recoil ranges were then converted to kinetic energies of fission products with the help of various range-energy equations. These data after correction for neutron evaporation gave the kinetic energy distributions for the two systems. From these distributions, data on kinetic energy deficit and average kinetic energy release were obtained. An interesting correlation between average total kinetic energy released ( $\overline{\text{TKE}}$ ) with fission asymmetry and shell structure has been obtained which shows that  $\overline{\text{TKE}}$  increases linearly as the probability for mass division with doubly magic core of 50P and 82N increases.

2. Fission Fragment Mass versus Angle Correlation in Fast Neutron Fission of Uranium 235 - N.N. Ajitanand, R.K. Choudhary, S.R.S. Murthy, P.N. Rama Rao and S.S. Kapoor - A gridded back to back, argon filled ionisation chamber was used to study the angular distribution of fission fragments in 2.2 MeV neutron induced fission of uranium 235. The neutrons were obtained by

the  $T(p,n)He^3$  reaction with a Van de Graaff accelerator. The uranium source of thickness  $50 \mu\text{gm cm}^{-2}$  electrospayed on a VYNS support film was mounted in the middle of the chamber and subtended an 8 degree half-angle at the proton spot. The grid and collector pulses from each half of the chamber were amplified, digitized by a four parameter recorder and written on magnetic tape. About  $10^5$  fast neutron induced fission events were recorded. Thermal neutron induced fission events were also recorded by thermalizing the fast neutrons with a paraffin block. The data was analyzed by the CDC 3600 computer to obtain the fragment mass and energy distributions from the collector pulses. The grid pulse height distribution for a given mass was analysed to obtain the angular distributions. The angular distributions thus obtained showed a significant variation with fragment mass establishing thereby that the quantum properties of the transition point states which decide the angular distribution of the fission fragments are different for the symmetric and asymmetric saddles.

### 3. Trajectory Calculations in Alpha-particle accompanied

fission and studies of Scission Configuration - R.K. Choudhury

and V.S. Ramamurthy - Trajectory calculations were done for the case of alpha particle accompanied ternary fission with an aim to obtain information on the emission mechanism of the alpha particle. The number of unknown initial parameters were kept

to a minimum by assuming the velocities of the fragments and the alpha particle to be zero at the time of scission. The initial parameters were taken to be the interfragment distance,  $D$ , and the coordinates of the  $\alpha$ -particle,  $x$  and  $y$ . The fragments and the  $\alpha$ -particle were assumed to be point charges and the equations of motion were solved numerically in two dimensions. It was found that reasonable sets of initial parameters could be obtained which reproduced the average experimental values of fragment kinetic energy,  $E_K$ , alpha particle energy,  $E_\alpha$  and alpha particle angle with respect to light fragment,  $\theta_{\alpha L}$  for different mass ratios. The widths of the final distributions were reproduced by assuming Gaussian distributions of the initial parameters around the mean value. It is remarkable to note that with only three parameters one can reproduce all the final distributions within the experimental accuracy. Further implications of the results of our calculation to the various existing models of the emission mechanism are discussed.

4. Possible Influence of the 28 Proton Shell on Fission Mass Distribution - S.G. Marathe, S.M. Sahakundu, V.K. Bhargava, V.K. Rao and R.H. Iyer - Experimental data on the low yield products in the highly asymmetric binary fission of uranium induced by reactor neutrons indicate the presence of 'bumps' or 'shoulders' in the low yield wings ( $A < 70$  and  $A > 160$ ) of the mass distribution curve. A possible explanation of the bumps on the basis of 28 proton core has been suggested.

5. Resonances in the Reaction  $^{32}\text{S}(\alpha, \gamma)^{36}\text{Ar}$  - M.A. Eswaran, N.L. Ragoowansi and H.H. Oza - With a view to study the region in  $^{36}\text{Ar}$  close to 10.9 MeV excitation energy, where the analog state corresponding to the ground state of  $^{36}\text{S}$  is expected, the excitation function for the reaction  $^{32}\text{S}(\alpha, \gamma)^{36}\text{Ar}$  has been measured with a beam of alpha particles from the Van de Graaff accelerator at Trombay. With a target of natural  $\text{Sb}_2\text{S}_3$  which is 7 keV thick for 4 MeV alpha beam and using a large volume NaI scintillation detector excitation function for this reaction was obtained for the bombarding energy range of 4.71 to 4.86 MeV. Two isolated resonances at  $E_\alpha = 4.717 \pm 0.010$  and  $4.740 \pm 0.010$  MeV have been identified in the reaction  $^{32}\text{S}(\alpha, \gamma)^{36}\text{Ar}$  corresponding to the excitation energy of  $10.837 \pm 0.010$  and  $10.857 \pm 0.010$  MeV in  $^{36}\text{Ar}$ . The absolute resonance strengths have also been estimated.

6. Elastic Scattering of Alpha Particles by  $^{26}\text{Mg}$  - L.J. Kanetkar\*, S.K. Gupta, S. Kailas, S.S. Kerekatte and M.K. Mehta - Elastic Scattering of alpha particles by  $^{26}\text{Mg}$  has been studied in the range  $E_\alpha = 4.2$  to 5.2 MeV using MgO target ( $^{26}\text{Mg}$  enrichment 99%) evaporated on a thin carbon film. Surface barrier detectors were placed at  $81^\circ$ ,  $118^\circ$ ,  $135^\circ$  and  $165^\circ$  lab. angles. The first three angles are the zeros of Legendre Polynomials of all odd, second and third order respectively.

The absolute differential cross-sections are measured as a function of energy in 5 keV steps, the experimental resolution being of the same order. The excitation functions exhibit large amount of structure. Strong anomalies are observed around  $E_{\alpha} = 4.25, 4.32, 4.57, 4.70$  and  $4.92$  MeV corresponding to excitation energies  $14.33, 14.39, 14.60, 14.72$  and  $14.91$  MeV respectively in the compound nucleus  $^{30}\text{Si}$ . The first four levels are assigned spin and parity values of  $0^+, 0^+, 0^+$  and  $1^-$  respectively from the shapes observed at the four angles.

\* NSTS Scholar

7. Reaction Mechanism study of the (p,n) Reaction on  $^{51}\text{V}$  and  $^{50}\text{Ti}$  Below 5.0 MeV - S. Kailas, M.K. Mehta and S.K. Gupta - At proton energies below the coulomb barrier but above the neutron threshold, the (p,n) is generally the dominant reaction in the proton target interaction. This being the case, the assumption:  $\sigma_{\text{absorption}} \approx \sigma(p,n)$  is justified and the cross-section may be calculated theoretically through the optical model. In cases where the above assumption is not valid, Hauser Feshbach calculations including Moldauer correction should yield correct fits to the data if the reaction is compound nuclear. These two approaches have been utilised in analysis of the absolute cross-section data measured at our laboratory for the reaction  $^{51}\text{V}(p,n)^{51}\text{Cr}$  and  $^{50}\text{Ti}(p,n)^{50}\text{V}$  upto about 5.0 MeV. The results of this study indicate that

while the optical model yields good fits in case of  $^{51}\text{V}$  target, the non-neutron emitting exit channels (e.g., the compound elastic) dominate over neutron emitting channels in case of the  $^{50}\text{Ti}$  target under proton bombardment at low energies.

8. Study of  $^{50}\text{Ti}(p,n\gamma)^{50}\text{V}$  Reaction - S.K. Gupta, S. Saini, S. Kailas, S.S. Kerekatte and L.J. Kanetkar - The  $^{50}\text{Ti}(p,n\gamma)^{50}\text{V}$  reaction was studied using an enriched  $^{50}\text{TiO}_2$  ( $^{50}\text{Ti}$  enriched to 76.4%) target on tantalum backing employing 30 c.c. Ge(Li) detector. 94 keV and 226 keV gamma rays were observed arising due to the transitions 320 keV  $\rightarrow$  226 keV and 226 keV  $\rightarrow$  g.s. Their yield was found to be significantly higher from  $E_n = 3.420$  MeV which is the threshold of 356 keV level. The excitation functions of 94 keV and 356 keV gamma rays have been measured in 2.5 keV steps. The angular distributions of 94 keV and 226 keV gamma rays have been measured at  $E_p = 3.430$  MeV. Using Litherland-Ferguson method of analysis, the data suggests assignment of  $3^+$ ,  $4^+$  and  $5^+$  to 356, 320 and 226 keV levels respectively.

9. Neutron Resonance Parameters for the states of  $^{33}\text{S}$  -

M. Balakrishnan, M.K. Mehta, S. Kailas and A.S. Divatia - 134 states have been identified in the compound nucleus  $^{33}\text{S}$ , at excitation energies between 9.29 and 11.76 MeV from the observed resonances in the reaction  $^{29}\text{Si}(\alpha,n)^{32}\text{S}$ . Using the principle of detailed balance, cross-sections have been obtained for the inverse (n, $\alpha$ ) reaction for the equivalent neutron bombarding

energies from 640 keV to 3.111 MeV. Neutron resonance parameters for nineteen resonances have been obtained.

Experimentally measured level and width distributions have been analysed in terms of various theoretical expressions of the statistical model. The drop in the number of levels with separation less than 10 keV indicates that the distribution is nearer to the Wigner Category than the exponential one.

10. Are the Nuclei with  $N \sim 43$  Deformed? - B. Lal and S.M.

Bharathi - The low lying negative parity states in  $^{75,77}_{34}\text{Se}$  and  $^{79}_{36}\text{Kr}$  show  $1/2^-$ ,  $3/2^-$  and  $5/2^-$  levels. In the case of  $^{77}\text{Se}$ , the rates of  $E(2)$  transitions between these levels have been found to be 50 times faster than the Weisskopf estimates. These levels have been fitted into a  $K = 1/2^-$  rotational band built on the  $1/2^-$ ,  $[302]$  Nilsson level. Additional support for the deformed nature of nuclei in this region comes from the observation of a  $K = 3/2^-$  band in  $^{75}\text{Se}$  by Protop et al. (Proceedings of International Conference on Nuclear Physics, Munich, August 1973, Vol. 1, p. 216) who excited levels upto  $13/2^-$  of this band by  $(\alpha, xn)$  reaction on Ge isotopes. The character of these bands and Coriolis coupling calculations of the  $K = 1/2^-$  and  $K = 3/2^-$  bands in  $^{75}\text{Se}$  have been completed.

11. Isobaric Analogue States of  $^{73}\text{Ge}$  VIA the  $^{72}\text{Ge}(^3\text{He,d})^{73}\text{As}$

Reaction - C.R. Ramaswamy and N.G. Puttaswamy, and N. Sarma -

The  $^{72}\text{Ge}(^3\text{He,d})^{73}\text{As}$  reaction has been studied at 20 MeV incident  $^3\text{He}$  energy using an MP tandem and a multigap spectrograph. The energy spectrum of deuterons in the region between 9 to 10.5 MeV excitation energy of  $^{73}\text{As}$  shows analogue states corresponding to G.S., 570, 673, 805, 900, 1050 and 1350 keV states of  $^{73}\text{Ge}$ .

Angular distributions for the analogue states and the  $Q$ -values of the transferred protons are extracted. The results are compared with available data on the levels of  $^{73}\text{Ge}$ .

12. High Resolution Measurements of Prompt Gamma Rays in the Fission of Californium 252 accompanied by Light Charged Particles -

N.N. Ajitanand, R.K. Choudhary and S.S. Kapoor - The present work was carried out to investigate the mechanism of light charged particle (LCP) emission in fission through a comparative measurement of the yields of specific primary fission products formed in binary fission and in the fission accompanied by LCP. High resolution measurements of the prompt gamma rays emitted from fission fragments accompanied by LCP and those emitted from normal binary fission fragments in  $^{252}\text{Cf}$  fission were simultaneously carried out using a 30 c.c. Ge(Li) detector. A "sandwich" type arrangement in the source-particle detector assembly was

used to eliminate Doppler broadening of the gamma ray lines in both cases. About 30 lines were assigned to specific isotopes by comparison with published results for binary fission, and the ratio of these gamma ray lines in LCP fission and binary fission were determined. Assuming that the  $2^+$  to  $0^+$  transition intensities of even-even isotopes are a measure of their yields, the yields of several such isotopes in LCP fission relative to binary fission were obtained. The most probable mass and width of the mass distribution for some specified fragment charges in LCP fission were examined in the light of the different proposed mechanisms of LCP emission in fission.

13. On the Entropy Method for obtaining Relative Shell

Correction Energies of Nuclei and the Calculation of Fission Barriers - V.S. Ramamurthy and S.S. Kapoor - It has been shown earlier<sup>1)</sup> that the shell correction energies of nuclei can be obtained from a study of the high temperature behaviour of their thermodynamic properties. We have now formulated a simple method of calculation of the fission barriers which is based on the evaluation of the relative shell correction energies of nuclei as a function of their deformation. It is shown that at temperatures where shell effects have disappeared, the ground state shell correction energy differences,  $\Delta_2 - \Delta_1$  for two adjacent deformations is equal to the excitation energy differences  $(E_1 - E_2)$  plus a weakly entropy dependent term arising from the small differences in the smooth part of the single particle level

densities for the two deformations. The value of  $\Delta_2 - \Delta_1$  can therefore be obtained by extrapolating the values of  $(E_1 - E_2)$  to the zero entropy limit. This method has been applied to the calculation of fission barriers of heavy and superheavy nuclei.

- 1) V.S. Ramamurthy and S.S. Kapoor, Physics Letters  
42 B, 399 (1972).

14. The Effect of Exchange on the Equivalent Sharp Radius  
for Real Proton Optical Potential - D.K. Srivastava and

N.K. Ganguly - Using Green's strong density-dependent nucleon-nucleon force and nuclear matter point-densities, the "equivalent sharp radii"  $R_v$ , as defined by Myres<sup>1</sup> have been calculated for real proton optical potential. The effect of exchange<sup>2</sup> between the incident nucleon and the target nucleons is studied. The value quoted by Myres is  $R_v = 1.16A^{1/3} + 0.45$ , which he obtained phenomenologically, and he shows that it can be computed only if a density dependent force is used. We find that when direct part is used we get a value consistently less than the value obtained by Myres using his force. We also find that  $(R_v - 1.16A^{1/3})$  is dependent on  $A$  and shows minima at doubly closed shell nuclei. Also it is energy independent upto 100 MeV.

When exchange is included, the value increases by about 0.1 fm and shows a very weak energy dependence upto 100 MeV (-0.001 fm/MeV). We feel that the term 0.45 fm is related to the hard core-radius of the nucleon-nucleon force.

Ref. 1. W.D. Myres, Nucl. Phys. A204 (1973) 465

2. B.C. Sinha, D.K. Srivastava and N.K. Ganguly  
Phys. Lett. 43B (1973) 113.

15. Effect of Short Range Correlation on the (p,2p) Reaction -

B.K. Jain - The effect of short range correlation (SRC) in the nucleus on the high energy (p,2p) reaction has been studied using  $^{16}\text{O}$  and  $^{40}\text{Ca}$  as examples. The correlations are introduced using the Jastrow prescription and the (p,2p) cross-section has been calculated using the di-proton model. For the long range part of the bound states we have used the wave function of Elton and Swift. The SRC are found to affect the results at high recoil momentum.

16. Measurement of Multipolarities in a Quadrupole Magnet -

R.C. Sethi, S.K. Das and A.S. Divatia - To know the quality of the quadrupole field the knowledge of the presence of the percentages of various multipolarities other than the quadrupole is essential. By knowing them one can calculate the aberrations produced by them and hence can correct<sup>1)</sup> them in a particular plane. A jig has been made to measure these multipolarities. With the help of the ball bearings and counter weight the jig scans the field in  $(\chi, \theta, z)$  plane without rotating the plane of the field measuring probe. So the plane of the measuring probe can be set independently. The jig has been tested on a small quadrupole magnet. By changing the plane of the probe the field

was measured in both focussing and defocussing plane by using hall probe. The data was smoothened and fourier analysed. The percentages of dipole, sextupole, octupole etc. at a distance of about  $\frac{1}{2}$  mm from the quadrupole centre have been found to be as high as 12, 8, 5 respectively. The variation of multipolarities as a function of current and radius of aperture has been studied.

- 1) Correction of effect of quadrupole magnet multipolarities on beam phase space ellipses: R.C. Sethi et al. Nuclear Physics & Solid State Physics India 15B, 489 (1973).

17. Useful Region of VEC Quadrupole Magnet - R.C. Sethi and A.S. Divatia - Useful region, where the field gradient is constant is affected because of the deviation from the hyperbolic geometry to the circular one. The solution for the vector potential was obtained by solving the POISSON'S equation by Relaxation method for the given geometry of VEC Quadrupole magnet pole pieces, yoke structure and current coils. The magnetic field, field gradient and the value of focal strength were derived from the above vector potentials. The maximum value of the focal strength calculated by the above procedure is 0.744 which is very near to the quoted value 0.75. The field gradient is fairly constant upto a distance of 2.5 cm. from the centre. Hence the useful region of VEC quadrupole magnet is not more than 50% of the total aperture. Therefore, to avoid aberrations the elements of the beam transport system should be placed in such a way that beam divergence

in the quadrupole is not more than 2.5 cm. Also the percentage of duo-decapole and 20th order pole etc. at a distance of 2.5 cms. calculated by assuming 8 fold symmetry are found to be about 6.5 and 1 respectively. The possibilities of improving the useful region by changing R/a ratio (ratio of radius of curvature to the radius of aperture) have been studied.

18. A Method to Design Shims to eliminate  $\theta_0^2$  Aberration in Uniform Field Circular Magnets - R.K. Bhandari and A.S. Divatia-

The effect of second order aberrations in the dipole magnets is to increase the size of the first order image, resulting in a beam with poor energy resolution coming out of the analysing slit. The  $\theta_0^2$  aberration, which is usually the largest, can be eliminated by appropriately curving the entry and exit pole faces of the magnet. Curving the faces amounts to changing the relative bending between the central and off-central rays. A method has been developed to simulate the required curvature at the faces with the help of shims, which are thin ( $\sim 0.5$  mm) foils of the similar magnetic material as the magnet, placed symmetrically on the pole tips. A simple and quick method of calculating the shape of the shims for a uniform field circular magnet has been presented and other design details have been discussed.

The method has been applied to calculate the shape of shims for the switching magnet no. 1 to be used with the 224 cm. Variable Energy Cyclotron at Calcutta. Calculations have shown that shimming this magnet will improve its energy resolution

from 200 keV to 45 keV in 65 MeV for 0.5 mm entry and 1.25 mm analysing slits at the maximum bend of 40°.

19. Orbit Dynamics in the Simulated Field of the VEC -

P. Neogy, N.C. Bhattacharya and S. Chatterjee - The median plane magnetic field of an AVF cyclotron has contributions from the excitation of the main magnet coils (the 'iron field'), and from the selective excitation of the trim coils. The combination is such as to produce a resultant 'isochronous field'.

A model 'iron field' of the VEC, for acceleration of protons to 60 MeV, has been constructed utilizing the geometry of the pole pieces and the magnetization curve for the main magnet. Equilibrium orbits in this model field at various energies have been computed using the usual iterative numerical orbit integration procedure. The equilibrium orbits are, in general, non-isochronous. By a reiterative procedure utilizing the properties of equilibrium orbits in the 'iron field', the model field has been modified to yield isochronous orbits. This model field, which now simulates a combination of the 'iron field' and the 'trim coil field', has been used for studying orbit properties and constructing phase plots.

20. Model Studies on Separated Sector Cyclotrons - A. Jain

and A.S. Divatia - A set of general equations for optimizing the sector shapes in isochronous cyclotrons were presented recently.<sup>1</sup> These equations are also valid for separated sector cyclotrons

in the limit when the valley field tends to zero. These hard edge equations have been evaluated experimentally for the case of separated sectored cyclotrons.

One out of eight periods of a separated sectored electron cyclotron magnet has been built. The magnetic field of the spiral sectored magnet was mapped in the median plane using a polar jig. The equilibrium orbit properties in the measured field were computed using the code ORBIT. These measured orbit properties are compared with those expected with the hard edge equations.

Experimental methods developed for the above studies are described. Some special techniques necessary for orbit analysis in this case are also discussed.

- 1) General Design Equations for Isochronous Cyclotrons  
A. Jain & A.S. Divatia, 1973 Particle Accelerator Conference  
San Francisco IEEE Transactions on Nuclear Science, June 1973,  
p. 902.

B. TATA INSTITUTE OF FUNDAMENTAL RESEARCH, BOMBAY 400 005

1. Dependence of the Binding Energy and the properties of collective states in  $O^{16}$  and  $Ca^{40}$  on the off-shell scattering matrix - Y. Singh <sup>and C.S. Warke</sup> - Phase equivalent potentials have been used to study the sensitivity of reduced transition probabilities  $B(E1)$  for the decay of  $3^-$  and  $1^-$  collective states in  $O^{16}$  and  $Ca^{40}$ . It is observed that the variation of  $B(E3)$  is about 22% both in  $Ca^{40}$  and  $O^{16}$ . However the variation in  $B(E1)$  is less than 2%. As observed in nuclear matter the binding energies of  $Ca^{40}$  and  $O^{16}$  are also sensitive to the off-shell behaviour of the scattering matrix. The observed variation is about 40%.

2. Alpha Decay of Isobaric Analog States - A. Roy, K.V.K. Iyengar and M.L. Jhingan - Alpha decay of isobaric analog states (IAS) is forbidden as the IAS has isospin  $T = T_0 + 1$ ,  $T_0$  being the isospin of the normal compound nuclear state. It is of interest to measure the  $\alpha$  decay of the IAS states as the width of these states give a measure of the isospin impurities in the analog state. We have used  $(p, \alpha)$  reactions on  $^{23}Na$ ,  $^{27}Al$  and  $^{51}V$  to excite isobaric analog states in  $^{24}Mg$ ,  $^{28}Si$  and  $^{52}Cr$ . The source of protons was the TIFR Cascade Generator. States in  $^{24}Mg$  ( $E_x = 11.990$  MeV), in  $^{28}Si$  (11.898, 11.974 MeV) and  $^{52}Cr$  (11.395 MeV) were studied. Since the yield of alphas from these reactions is low owing to the low energies of incident and emitted particles and the forbidden nature of the decay, special techniques are necessary to detect the alphas

in the presence of the intense background of elastically scattered protons. Electronic detection techniques normally fail due to pile up effects. The alphas were therefore detected using cellulose Nitrate. A reagent was used for etching which rendered visible only the etch pits of alphas. This method has the advantage that the reaction products can be detected over a large solid angle thus at least partly compensating for low reaction yields. The strength function for the decay of the 11.395 MeV state in  $^{52}\text{Cr}$ , isobaric analog of the 0.148 keV state in  $^{52}\text{V}$ , is  $(0.18 \pm 0.06)$  eV and this sets a lower limit of 0.02 eV for the  $\alpha$  decay width of this state.

### 3. Distributed Nuclear Magnetism from Internal Conversion -

$^{141}_{59}\text{Pr}_{82}$  - B.N. Subbarao - With 99.7%  $^{140}\text{Ce}$  enriched  $\text{CeO}_2$  targets, 20 cc Ge(Li), double-focussing  $\beta$ -ray spectrometer and intensity standardised NaI(Tl) spectrometers, a new standard for K-shell conversion coefficient, of the 145.441 keV transition in  $^{141}\text{Pr}$ , of 0.35(6) is obtained. The  $L_1$ ,  $L_{11}$ ,  $L_{111}$ , M, (N+0) and total conversion coefficients are obtained to be 0.0444(6), 0.00344(14), 0.00067(14), 0.0114(10), 0.0022(1) and 0.420(6), respectively.  $\lambda$ - $\delta^2$  analyses with a computer require the penetration parameter  $\lambda$  (M1) to be  $+4.4 \pm 0.7$  and the E2/M1 mixing ratio  $\delta^2 \ll 0.2\%$ . These results are discussed and theoretical nuclear model calculations of the M1 penetration matrix element and its relation to distributed nuclear magnetism of  $^{141}\text{Pr}$  are also studied.

4. Electric Monopole Transition in  $^{228}\text{Th}$  - S.H. Devare and

H.G. Devare - We have studied the 184.5 keV transition arising from a 1153.5 keV state in  $^{228}\text{Th}$  excited in the beta decay of 6.1 hr  $^{228}\text{Ac}$ . The gamma spectrum was studied with a 20 cc Ge(Li) detector with a resolution of 2 keV in the energy region of interest. The K,  $L_I$  and  $L_{II}$  conversion lines were measured by  $\Pi\sqrt{2}$  type double focussing spectrometer. From the gamma spectrum and the  $L_I/L_{II}$  subshell ratio the E0 part in the 184.5 keV transition taking place between 1153.5 keV ( $2^+$ ) state and 969.0 keV ( $2^+$ ) state, was found to be  $(93 \pm 2)\%$ . The half-life of the 1153.5 keV state was measured by beta-gamma delayed coincidence technique and obtained as  $T_{1/2} = (0.29 \pm 0.02) \times 10^{-9}$  sec. The value of the monopole matrix element was calculated from the conversion electron transition rate as  $\rho = 0.14$ .

5. Measurement of Lifetimes of States in  $^{77}\text{As}$  and  $^{143}\text{Pr}$  -

R.C. Chopra, P.N. Tandon, S.H. Devare and H.G. Devare - The half-lives of the 632 keV state of  $^{77}\text{As}$  and 350 keV state of  $^{143}\text{Pr}$  excited in the decay of  $^{77}\text{Ge}$  and  $^{143}\text{Ce}$  respectively, have been measured using beta gamma delayed coincidence technique. In the case of  $^{77}\text{Ge}$ , the beta gate was selected at 1100 keV, while the gamma gate was put near the Compton edge of 632 keV gamma ray. The time spectrum gave a slope of  $(77.2 \pm 1.6)$  p sec. The prompt spectrum taken with a  $^{60}\text{Co}$  source and same gates, gave a slope of  $(45.4 \pm 1.6)$  p sec. The half-life of the 632 keV level, deduced from this is  $(62 \pm 6)$  p sec. In case of  $^{143}\text{Ce}$ , the beta gate was fixed at 800 keV and the gamma gate near the Compton edge of 292 keV gamma ray. The time spectrum

had a slope of  $(70 \pm 3)$  p sec and the prompt spectrum taken with  $^{60}\text{Co}$  source using identical gates had a slope of  $(56 \pm 2)$  p sec. We conclude from this that the half-life of 350 keV state of  $^{143}\text{Pr}$  is  $\leq 45$  p sec. The errors quoted in this work include the uncertainty in the time calibration.

6. Electromagnetic Properties of the 264 and 632 keV Levels in  $^{77}\text{As}$  - R.C. Chopra and P.N. Tandon - The g factors of the 264 and 632 keV levels in  $^{77}\text{As}$  have been measured using perturbed angular correlation technique. We have made use of the large hyperfine magnetic field present at arsenic site in iron host for these measurements. Dilute alloys of germanium with iron were made by melting in vacuum, radioactive  $^{77}\text{Ge}$  and iron. An external field of 10 kG was used to polarize the sample. For measurements of the 264 keV level, the 211-264 keV gamma cascade was used. A conventional NaI(Tl)-Ge(Li) detector coincidence system was employed. The mean precession angle obtained was  $\omega\tau = 0.255 \pm 0.025$  rad. This corresponds to  $g = +0.30 \pm 0.03$  and  $\mu = 0.75 \pm 0.08$  n.m. for the 264 keV level. In the case of 632 keV level, the 558-417 keV gamma cascade was used along with a conventional NaI coincidence system. The mean precession angle obtained was  $\omega\tau = 0.12 \pm 0.02$  rad. This corresponds to  $g = +0.79 \pm 0.17$  and  $\mu = 1.98 \pm 0.43$  n.m. for the 632 keV level.

7. Band Structure in  $^{22}\text{Na}$  - M.R. Gunye - The spins and parities of many nuclear states of  $^{22}\text{Na}$  are now well established from the recent experiments. The purpose of this work is to show that the nearly rotational features of the nuclear states of  $^{22}\text{Na}$  can be well explained by microscopic self-consistent calculations in large

configuration space. The validity of the intrinsic band structure in this nucleus is seen from the almost correct prediction of the relative energy separation between the lowest  $3^+$ ,  $1^+$  and  $0^+$  states projected from  $K = 3$ ,  $T = 0$ ,  $K = 0$   $T = 0$  and  $K = 0$   $T = 1$  bands respectively. The nuclear wavefunctions are tested by comparing the computed spectroscopic factors with those extracted from one-nucleon transfer reactions. The present calculations predict the static electromagnetic moments and lifetimes remarkably well. Finally it should be stressed that the high ft value of the allowed  $\beta^+$  transition from the ground state ( $J = 3^+$   $T = 0$ ) of  $^{22}\text{Na}$  to the first excited state ( $J = 2^+$   $T = 1$ ) of  $^{22}\text{Ne}$  is correctly predicted by our calculations. The large ft value due to the K-forbiddenness of the allowed  $\beta$ -transition supports the intrinsic band structure in  $^{22}\text{Na}$ .

8. Total Neutron Emission Cross-sections - E. Kondaiah and A.L. Athougies\* - Weighted averages of experimental (n,2n) cross-sections at 14-15 MeV reported upto October 1973 have been used to obtain the total neutron emission cross-sections ( $\sigma_{n,n} + \sigma_{n,2n} + \sigma_{n,3n}^f$ ) for more than a hundred stable nuclides. When these are divided by the non-elastic cross-sections based on optical model calculations and the resulting ratios are plotted as a function of  $(N-Z)/A$ , it is seen that these lie on a curve of the type,

$$(1-R) = k \exp(-mx)$$

where R is the ratio and  $x = (N-Z)/A$ ; the constants k and m are evaluated by a least squares fit.

---

\*St. Xaviers College, Bombay.

This curve together with the optical model non-elastic cross-sections can be used reliably to predict  $(n,2n)$  cross-section of any nuclide precisely.

C. SAHA INSTITUTE OF NUCLEAR PHYSICS, CALCUTTA - 9

1. Level Density Parameters for Superheavy Nuclei - Sudip Ghosh and Aparesh Chatterjee - Introducing the concept of momentum anisotropy in a free Fermi gas system to account for the nuclear interactions it is possible to obtain an expression for the nuclear level density parameter  $\underline{a}$ . The  $\underline{a}$ -parameters computed from this expression with the help of the renormalised gas model show good agreement with the experimental values. Calculations have been extended to the region of superheavy nuclei in the mass range 250 A 400.

2. Calculation of the Nuclear Deformation Energies from the Renormalised Gas Model - Swapna Mukherjee and Aparesh Chatterjee - By defining the effective single particle occupation factors for a major shell from an effective shell degeneracy, and by estimating the average combinatorial energy corrections for extractore particles in a given shell, we have calculated the nuclear deformation energies from the statistical approach of our renormalised gas model (RGM) using the BELYAEV BES treatment of noninteracting quasi-particles. Our results have been tested and compared in various ways with other realistic calculations and with the available experimental information. The agreements are reasonably satisfactory throughout the region of stable nuclei in the mass range 40 A 208.

3. A Calculation of the Pairing Vibrational State of  $Pb^{208}$  using Two Body Potential - Nandita Rudra and M.K. Pal - The conventional calculations on the pairing vibrational states are done using model

potential. In the present paper, pairing vibrational state in  $\text{Pb}^{208}$ , is calculated using Gillet type two body potential. In a (t,p) reaction on  $\text{Pb}^{208}$ , a pair of neutrons, coupled to  $J^\pi = 0^+$ , is added to  $208\text{Pb}$  core, in  $J^\pi = 0^+$  state, producing the ground state of  $\text{Pb}^{210}$ . Similarly in a (p,t) reaction, a strongly correlated ground state of  $\text{Pb}^{206}$  is obtained. A pair addition, followed by a pair removal, will give pairing vibrational state. The conventional TDA and RPA techniques are used. The results give a good agreement with the B-E of the neutron pair in  $\text{Pb}^{210}$  and  $\text{Pb}^{208}$ . The energy of the first  $0^+$  pairing vibrational level of  $\text{Pb}^{208}$  is, however, poorly reproduced.

4. Magnetic Moment of the 103 KeV  $3/2^+$  State of  $^{153}\text{Eu}$  - B.K. Sinha and R. Bhattacharyya. - The different characteristics of the excited states of the deformed odd-A nucleus  $^{153}\text{Eu}$  have been the subject of a large number of experimental studies. The magnetic moment of the level has been found out both by Mossbauer effect studies as well as by IPAC studies of the 69-103 keV cascade. The two values differ substantially. Moreover, the  $A_2$  coefficients as found from angular correlation measurements indicate values of the mixing ratios which are not in agreement with the values found from high resolution ICC measurements. We have studied the angular correlation of the above cascade by using sum coincidence technique and our results indicate a somewhat larger  $G_2A_2$  - coefficient than that found by other authors. With the value of  $G_2A_2 = 0.028 \pm 0.006$  thus obtained and with our value of the rotation of the angular correlation pattern

we find  $\mu = 2.13 \pm 0.60$  which is nearer to the value as found by Mossbauer spectroscopy. The significance of this value is discussed.

5. Decay of 42-min  $^{123m}\text{Sn}$ . - V.K. Tikku, H. Singh, and B. Sethi - The  $\gamma$ -transitions associated with the 42-min  $^{123m}\text{Sn}$  were investigated with large volume Ge(Li) detectors. The  $^{123m}\text{Sn}$  sources were produced by irradiating enriched  $^{124}\text{Sn}$  and  $^{122}\text{Sn}$  targets with 14.7 MeV and thermal neutrons, respectively. Besides the well known 160 keV  $\gamma$ -transition three new  $\gamma$ -transitions have been identified and established as belonging to  $^{123}\text{Sb}$ . The accurate energy (intensity) values from the present measurements are  $160.0 \pm 0.3$  (100),  $381.1 \pm 0.7$  ( $0.05 \pm 0.006$ ),  $541.4 \pm 0.7$  ( $0.02 \pm 0.004$ ) and  $552.8 \pm 1.0$  ( $0.01 \pm 0.003$ ) keV. Based on the measurements a revised decay scheme of  $^{123m}\text{Sn}$  is proposed with energy levels at  $160.0^{5/2}$ ,  $541.1^{3/2}$ ,  $712.8^{1/2}$  keV. A preliminary study of the singles  $\gamma$ -X spectra recorded with the Ge(Li) X-ray detector gives  $\alpha_K = 0.15 \pm 0.015$  for the 160.0 keV transition. A comparison of the experimental value of  $\alpha_K$  with the corresponding theoretical value yields the 160 keV transition to be almost M1. The measurements for  $\alpha_L$  and  $\alpha_K$  for the transition are continuing using a  $30 \text{ mm}^2 \times 3 \text{ mm}$  Si(Li) detector.

6. Decay of 6.2-min Isomer of  $^{130}\text{Sb}$  - V.K. Tikku, H. Singh, and B. Sethi - The decay of the 6.2-min isomer of  $^{130}\text{Sb}$  was investigated with Ge(Li) and scintillation spectrometers. The  $^{130}\text{Sb}$  activity was obtained from the fast neutron irradiation of enriched  $^{130}\text{Te}$  target. The electron decay of the irradiated  $^{130}\text{Te}$  target in G.M. tube gave two half-life values of  $6.2 \pm 0.3$  min and  $41.7 \pm 1.7$  min. The end-point energy of the highest  $\beta$  group in the decay of the 6.2 min isomer is found to be  $2.7 \pm 0.3$  MeV. In all 18  $\gamma$ -rays have been assigned to the short lived isomer. The  $\beta$ - $\gamma$  and  $\gamma$ - $\gamma$  coincidence studies are in progress. The results of the  $\beta$ ,  $\gamma$  and the coincidence measurements are incorporated into a hitherto unknown decay scheme of the 6.2 min isomer of  $^{130}\text{Sb}$ .

7. Effect of the Coulomb Interaction on Proton Optical

Potential - S.K. Samaddar\* and Subrata Ray - In the local approximation the Coulomb interaction makes the real part of the proton optical potential deeper compared to that of the neutron. In the phenomenological analysis this is taken as Woods-Saxon of depth  $0.4Z/A^{1/3}$ . It is observed that the Z-dependence part due to use of an equivalent local potential (ELP) falls faster than Woods-Saxon. We have estimated the contribution due to Coulomb excitation which may be called the intrinsic Z-dependence. If this intrinsic Z-dependence is added to the ELP, the total Z-dependence agrees with the phenomenological value.

\* Department of Physics, Chandernagore College, Hooghly.

77

8. On the Validity of Glauber Theory - H. Banerjee, B. Dutta-Roy and S.K. Sharma - Many attempts have been made to explain the remarkable success of Glauber theory. Among these, the first important attempt was made by Harrington. He proposed that the success of the Glauber theory is due to cancellations in the multiple scattering series. Later Pauli and Tobocmann, refuting Harrington, suggested that the success of Glauber theory is due to the damping of the terms neglected in Glauber series. This damping is brought about by 'Adiabatic approximation'. In this report we show that the cancellations proposed by Harrington do not take place while one considers exact amplitudes. We then show that in general 'Adiabatic approximation' is not responsible for the success of Glauber theory. We propose that the validity of Glauber theory is dependent on the binding energy of the nucleus. We show that for loosely bound nuclei (such as deuteron) Glauber theory should be very good approximation. We also discuss its validity in the resonance region.

9. p-He<sup>4</sup> and p-O<sup>16</sup> Elastic Scattering at 1 GeV Energy - Shibani Devi and Dipti Pal - Using the Glauber's theory of high-energy multiple scattering, we attempt to get a theoretical interpretation to 1 GeV proton elastic scattering data of the Brookhaven Group for He<sup>4</sup> and O<sup>16</sup> nuclei. The generator co-ordinate method has been adopted to construct the nuclear ground state wave-functions with the shell-model description of single particle wave-functions, treating the oscillator constants as the generator co-ordinates. The variational problem is then solved with the Brink-Bosker force. The theoretical results, we get, for the

10. Inelastic Pion - Scattering to the Low Lying  $T = 1$  States of  $^{12}\text{C}$  - J. Mahalanabis and A. Choudhury - We have studied the inelastic scattering of pions leading to the excitation of the low-lying  $T = 1$  states ( $J = 1^+, 2^+, 1^-, 2^-$ ) of  $^{12}\text{C}$ , for incident energy of pion from 120-280 MeV. The results obtained with a simple nuclear model and impulse approximation are in good agreement with experiments. The inelastic spin-flip scattering is discussed to give information on nuclear structure.

11. Centrifugal Stretching Effect on the Anomalous Behaviour of High Spin Rotational States - S.C.K. Nair and A. Ansari - A variational calculation after an approximate angular momentum projection for  $^{158}\text{Er}$  has been carried out which indicates that the anomalous behaviour of the energy spacings of high spin states may be due to centrifugal stretching - an increase in deformation accompanied by a decrease in pairing correlations.

In many other theoretical attempts to understand the origin of this anomalous feature, often Coriolis-anti-pairing effect is considered to be the main source. But this is not yet a finally settled problem. We are trying to elucidate more on this by doing also a constrained Hartree-Bogoliubov calculation taking the expectation value of the  $X$ -component of the total angular momentum, i.e.,  $\langle J_x \rangle$  as the constraint.

12. Excited Band Spectra of  $^{18}\text{O}$  in Small-Amplitude

Approximation Scheme - J.N. De - The excited band spectra of  $^{18}\text{O}$  nucleus and the B(E2) values among various members of the bands are thoroughly investigated in the small-amplitude approximation (SAA) scheme in a multishell harmonic oscillator basis. The results are quite encouraging. The SAA scheme reduces the projection algebra to simple decoupling and coupling of angular momenta and thus bypasses the enormous computational labour involved in multishell projection.

13. Odd Mass Tellurium Isotopes in a Unifield Vibrational

Model - S. Sen - The odd-A Te isotopes,  $^{125}\text{Te}$ ,  $^{127}\text{Te}$  and  $^{129}\text{Te}$  are studied in a version of the unifield vibrational model which incorporates both pairing effects and anharmonicity in the core vibrations. The neutron quasi particle states in the N = 50-82 shell are coupled to anharmonic vibrations of the corresponding Te cores. Essentially, the only adjustable parameter in the calculation is the coupling strength. The calculated energy spectra and the spectroscopic factors are in good agreement with the corresponding experimental values. The static and dynamic electromagnetic properties are calculated for some of the levels and the results are analysed in the light of the recent experimental findings.

14. Single Hole-Core Coupling in the N = 50 Region. - S.K. Basu and S. Sen - The low-energy nuclear properties of  $^{85}\text{Kr}$ ,  $^{85}\text{Sr}$ ,  $^{87}\text{Sr}$  and  $^{89}\text{Zr}$  nuclei have been calculated in a semi-microscopic model in which the neutron hole motion in the  $1g_{9/2}$ ,  $2p_{1/2}$ ,  $2p_{3/2}$

and  $1f_{5/2}$  orbitals in the  $N = 28-50$  shell is coupled to the quadrupole and octupole vibrations of the corresponding even core. Calculated energy spectra, spectroscopic factors, electromagnetic moments and transition rates are compared with the recent experimental findings.

D. ALIGARH MUSLIM UNIVERSITY, ALIGARH

1. On the Faddeev-Yacubovsky Model of four particle scattering

problem - V.K. Sharma - The Faddeev-Yacubovsky model of four identical spinless particles with the resonating group approximation is considered. The integral equations of 4-particle scattering problem are formulated in the case of two-body channel (i.e., one particle + bound three particle type, and bound pair + bound pair type). It is shown that with resonating group approximation the four-particle scattering problem can be reduced to solve a set of one-dimensional coupled integral equations. Further, it is noticed that the Faddeev-Yacubovsky approach can be reduced to much more simple form with the nonlocal separable potential, and we believe this might bring the 4-particle problem within the range of modern computers.

2. Study of (n, $\alpha$ ) Reactions at Thermal Energy - J. Alam and M.L.

Sehgal - Using the activation technique, cross-section ratios  $\sigma(n,\alpha)/\sigma(n,\gamma)$  at thermal neutron energy for the target nuclei  $^{180}\text{Hf}$ ,  $^{203}\text{Tl}$ ,  $^{208}\text{Pb}$  and  $^{209}\text{Bi}$  have been measured to be  $(38.5 \pm 1.1) \times 10^{-3}$ ,  $\leq 2.5 \times 10^{-3}$ ,  $(15.4 \pm 1.7) \times 10^{-3}$  and  $(4.4 \pm 0.4) \times 10^{-3}$  respectively. The reaction  $^{181}\text{Ta}(n,\alpha)^{178}\text{mLu}$ ,  $^{178}\text{Lu}$  has also been studied and the ratio  $\sigma_{25 \text{ min}}(n,\alpha)/\sigma_{5 \text{ min}}(n,\alpha)$  for the production of 25 min and 5 min half-lives have been assigned to the respective isomeric states of  $^{178}\text{Lu}$ , the energy difference between the isomeric states has been estimated, and the spin assignment to these isomeric states have also been made.

E. ANDHRA UNIVERSITY, WALTAIR, VISAKHAPATNAM - 3 (AP)

1. Relative Intensities of Gamma Rays in Re-187 - K. Subba Rao, P. Ila, K. Sudhakar, K.L. Narasimham and V. Lakshminarayana - Gamma ray spectra resulting from the decay of W-187 are recorded with a 35 cc Ge(Li) detector and a 512 channel analyser. The energies and intensities of the different gamma rays are obtained from a computer program of the recorded spectrum. Twenty six gamma rays are identified of which four gamma rays are new. The relative intensities are compared with those of two recent investigations. Considerable discrepancies are noticed in the intensities of gamma rays at low energies. The data will be presented and discussed in the light of relative efficiency calibrations.

2. Bremsstrahlung from  $^{32}\text{P}$  Betas - R. Prasada Babu, V.A. Narasimha Murty and K. Narasimha Murty - The spectral distributions of the Internal Bremsstrahlung of  $^{32}\text{P}$  is measured from 30 keV to 1200 keV using a NaI(Tl) scintillation spectrometer with a standard geometrical arrangement, similar to that of K. Narasimha Murty et al. (Proc. Phy. Soc., 1967, 90, 109-123). Special care is taken to avoid spurious effects and corrections were made for several factors such as background, energy resolution, back-scattering, Compton and escape electrons, geometrical and gamma detection efficiency of the crystal. The experimental results are compared with the allowed theory of Kripp and Uhlenbeck and Bloch (KUB theory) and also with the Coulomb corrected theory due to Lewis and Ford.

Using the same experimental arrangement, the external bremsstrahlung emitted when the  $^{32}\text{P}$  beta rays are completely stopped in carbon, aluminium, tin and lead is also measured and the experimental results are compared with theoretical results of Bethe and Heitler and also of Elwert.

3. Beta Gamma Directional Correlation Measurements in the Decay of

Lu-177 - B. Verma Reddy, M.L.N. Raju and D.L. Sastry - The energy dependence of the  $384 \text{ keV } \beta - 113 \text{ keV } \gamma$  directional correlation is measured with a conventional slow-fast coincidence scintillation spectrometer. The correlation is isotropic within the limits of experimental error, disagreeing with the earlier results reporting a non-zero anisotropy. An attempt is made to extract the nuclear matrix element parameters consistent with the Nilson model and available experimental data.

4. Internal Conversion Measurements of Transitions in  $^{143}\text{Pr}$  -

K. Venkata Ramaniah, T. Seshi Reddy and K. Venkata Reddy - The internal conversion studies in the decay of 33 hour  $^{148}\text{Ce}$  employing the Siegbahn-Slatis beta ray spectrometer of the intermediate image type have been studied. The 231, 293, 351, 492, 665, 723 and 810 keV transitions have been examined in the internal conversion spectrum. The relative gamma ray intensities for the above transitions have been taken from the Ge(Li) data of P.R. Gregory et al. (Can. J. Phy. 46, 2797, 1963). Using the well determined k-conversion coefficient of the 298 keV transition, the following conversion coefficients have been obtained:

232(0.108±0.02), 351(0.026±0.003), 490(0.018±0.004), 668  
(0.005±0.0005), 722(0.005±0.0006) and 810(0.003±0.0004).

Some spin and parity assignments like  $5/2^+$  for the 492 keV level  $3/2^+$  for the 351 keV level,  $3/2^+$  for the 725 keV level and  $5/2^+$  for the 938 keV level have been established in the light of the present conversion coefficient data and gamma-gamma angular correlation data of S. Venkata Ratnam (Ph.D. Thesis, Andhra University, Waltair, 1972).

5. Beta Spectrum of  $^{143}\text{Pr}$  - C. Narasimha Rao, B. Mallikarjuna Rao, P. Mallikharjuna Rao and K. Venkata Reddy - The spectrum shape of  $^{143}\text{Pr}$  beta transition has been carefully measured in a magnetic Intermediate-Image spectrometer. The beta spectrum was analysed using exact ERWFs of Bhalla and Rose. A detailed analysis of the shape factor yields the end point energy as  $934 \pm 2$  keV. The coefficient 'a' in the shape factor  $C'(w) = 1+a'(w)$  is  $A' = -0.19 \pm 0.005$  which is in striking disagreement with earlier works.

6. On the Beta Hindered Allowed Transitions in  $^{110\text{m}}\text{Ag}$  and  $^{134}\text{Cs}$  - M. Ravindranath, B. Mallikarjuna Rao, C. Narasimha Rao, P. Mallikharjuna Rao and K. Venkata Reddy - The Beta spectra of  $^{110\text{m}}\text{Ag}$  and  $^{134}\text{Cs}$  were thoroughly investigated with a Siegbahn-Slatis Intermediate Image Spectrometer. Four betas with end point energies 529, 1462, 2175 and 2880 keV of  $^{110\text{m}}\text{Ag}$  were observed. The shapes of the  $6^+ - 6^+$  transition with  $E_0 = 529$  keV in  $^{110\text{m}}\text{Ag}$

and the  $4^+ - 4^+$  transition with  $E_0 = 656$  keV in  $^{134}\text{Cs}$  were found to be statistical in nature. An attempt is made to explain the high  $\log ft$  values associated with the transitions.

7. Comparative Study of Various Theories of Rotational Levels for Selected Light Nuclei - N. Krishna Rao, U. Satyanarayana and S. Ramamurty - Various theories of rotational levels have been tried for the rotational bands in O-16, Sc-43 and Ti-45 indicating the parameters for the models, the model which gives the best fit and additional levels predicted on that model. Some preliminary calculations are also reported for Ne-20, Ne-22, Mg-24, Si-28 and Ti-48. The models used are the Rigid Rotator model, the Sood model, the Holmberg-Lipas model, the Variable moment of Inertia model, the Harris model and the Diamond Stephens-Swiatecki model.

8. Comparative Study of Various Theories of Rotational Levels in the Rare Earth Region - S. Ramamurty, U. Satyanarayana, N. Krishna Rao and V.V.V. Subramanyam - There have been developed various models of rotational levels. We have taken six such models namely the Rigid Rotator model, the Sood model, the Holmberg-Lipas model, the variable moment of Inertia model, the Harris model and the Diamond-Stephens-Swiatecki model and made a comparative study of how good they are for Sn-152, Sn-154, Gd-158, Dy-160, Dy-162, Ho-163, Ho-166, Er-166, Yb-168, Yb-172, Yb-174, Hf-178, W-182 and Os-188. The following information is given: the parameters for the various models, the model which gives the best fit for each nucleus and two levels predicted on the model for best fit in addition to those already known. It is believed that

such information should form part of the basis for our views on the rotational levels of atomic nuclei.

9. Negative Parity States in Au-195 - P. Ila and V. Lakshminarayana -

The nuclear structure and the properties of the low lying levels of negative parity in Au-195 are investigated in the frame work of the intermediate coupling approach of the unified model. It is assumed that the last odd proton has available the  $h\ 11/2$  state and is coupled to the collective surface vibrations of the doubly even core. The Hamiltonian of the coupled system including all the states upto two phonons of quadrupole vibrations is diagonalized. The coupling parameter is varied from 3 to 8. The levels obtained are compared with the experimental energy levels of spin  $7/2^-$ ,  $9/2^-$ ,  $15/2^-$  and  $11/2^-$ . The negative parity states are reproduced satisfactorily by the model. The wave functions derived from the best fit are used to calculate the transition probabilities. From the available experimental conversion coefficients of several transitions occurring among the negative parity states, mixing ratios are deduced. Using the theoretical  $T(E2)$  and  $T(M1)$  and mixing ratios, branching ratios are calculated and compared with the experimental values.

10. Spin of the 1251 Kev Level in Nb-97 - D.K. Priyadarsini,

B. Vema Reddy, B.R. Sastry and D.L. Sastry - The spin of the 1251 KeV level of Nb-97 populated in the decay of Zr-97 is inferred from a measurement of beta-gamma angular correlation. For the 1410 KeV beta and 508 KeV gamma cascade in the decay of Zr-97, the observed

angular correlation is  $A_2(\beta) = 0.5559 \pm 0.1599$  at  $E_\beta = 1375$  KeV. This result is consistent with a  $5/2^-$  spin-parity assignment to the intermediate 1251 KeV level of Nb-97 nucleus thus indicating the unique first forbidden nature of 1410 KeV beta transition. The present result excludes the  $1/2^-$  and  $3/2^-$  assignments to this level.

11. Strong Absorption Model Calculations for the Principal

Fissile and Fertile Nuclei - U. Satyanarayana and S. Ramamurty -

Strong absorption model calculations have been conducted for Th-232, U-235, U-238 and Pu-239 on the additional assumptions that the transparency coefficient and the imaginary part of the reflection coefficient are negligible, as was also assumed by Bassichis and Dar. The energy range is 1-20 MeV at intervals of 1 MeV. The principle findings are that the theoretical cross section is consistently lower than the experimental cross section and that, in the range 2-4 Mev, for all the nuclei investigated, the calculated cross section exhibits single fluctuation which is superimposed upon an otherwise consistently downward trend of cross section with energy.

F. BANARAS HINDU UNIVERSITY, VARANASI - 5.

1. Three Body UPA Calculations with Hamada Johnston and Yale

Potentials - V.S. Mathur, A.V. Lagu and C. Maheshwari - The use of realistic potentials like Hamada Johnston and Yale in Faddeev formalism for three nucleon systems presents formidable problems of analytical and computational nature. To simplify the problem computationally, we have used the Unitary Pole Approximation (UPA) which has been found to be successful in the case of potentials with hard core (Mathur et al.). In this method the information regarding the potential enters the t-matrix only through the two-body bound state wavefunction in the triplet channel and the virtually bound state wavefunction in the singlet channel. In the case of triplet channel, these functions are available in numerical as well as analytical form (Humberston & Wallace, Kottler & Kowalski). The  $^1S$  wavefunction is determined by the method of Mathur et al. after fitting the singlet potential to an exponential shape. Adapting Fuda's method suitably, coupled one dimensional equations for the three nucleon bound system have been set up and solved by the usual method of reducing them to a matrix eigenvalue equation.

2. Variation of Nuclear Potential and Charge Distribution Radii

in Isotopic Sequences - D.C. Agrawal and P.C. Sood - In the shell model and optical model studies the radius of nuclear potential is generally adopted to vary as  $A^{1/3}$  in correspondence with the assumption that the radius of the density distribution in nuclei follows

$A^{1/3}$  dependence. However, from various experiments e.g. electron scattering, atomic spectra studies, it has been recently concluded that, atleast in isotopic sequences, the proton distribution radius increases less rapidly than  $A^{1/3}$ . Thus the validity of the assumption of  $A^{1/3}$  dependence of nuclear potential radius in such case also needs confirmation. We have examined the variation of nuclear potential radii for nuclei in isotopic sequences and its correlation with variation in radii of the corresponding charge distributions. The nuclear potential radius is obtained by fitting the last particle binding energy. The possible physical explanation for the observed correlation between neutron potential radius and the charge distribution radius is discussed.

3. Rotation Particle Coupling in the [523 $\uparrow$ + 521 $\downarrow$ ] - Based Bands in  $^{166}\text{Ho}$ . - D.K. Gupta and P.C. Sood - The coupling of  $7/2^-$  [523 $\uparrow$ ] proton and  $1/2^-$  [521 $\downarrow$ ] neutron Nilsson orbitals gives rise to  $3^+$  and  $4^+$  intrinsic states in certain doubly odd deformed nuclei in the rare earth region. In the nucleus  $^{166}\text{Ho}$  the rotational bands built on these states are likely to be highly admixed due to rotation particle coupling term in the Hamiltonian. The indication for such an effect is provided by the following observations: (a) The same spin levels of these two bands are observed to have energy separation in the range 110 - 135 keV; (b) The known interband transitions do not obey Alaga rules; (c) The inertial parameters calculated assuming no admixture are found to be quite different for the two bands. In this work we report on the analysis of the relevant spectrum to find the unmixed and mixed level energies and the admixture coefficients in the respective wave functions. The implication of these results

is discussed.

#### 4. Evaluation of Band Mixture Coefficient for $^{183}\text{W}$ . -

P.C. Joshi and P.C. Sood - The low lying energy levels of the highly deformed nucleus  $^{183}\text{W}$  mainly consist of the rotational levels associated with two bands with  $K^\pi = 1/2^-$  and  $K^\pi = 3/2^-$ ; these levels deviate strongly from the predictions of the adiabatic model and interpreted as arising from the admixture of the two bands. However the admixture coefficient has so far been determined only empirically to obtain the admixed wavefunctions for investigation of other properties. No attempt at theoretical evaluation of this coefficient has been reported so far. We calculate this coefficient using the Coriolis interaction  $H_c$  in a perturbation approach with modified Nilsson potential. The effect of deforming the spin-orbit coupling term is also investigated. Coupling of the  $3/2^-$  band levels with all the possible  $1/2^-$  states in the same oscillator shell is considered. The results are used to analyse the characterisation of the non-adiabatic corrections for this nucleus.

G. BIRLA INSTITUTE OF TECHNOLOGY, RANCHI

1. Single Particle Potential and Rearrangement Energy of Nuclear Matter - K.M. Khanna and P.K. Barhai - The single particle potential, effective mass ratio ( $m^*/m$ ) and rearrangement energy,  $R$  of nuclear matter have been calculated using two density dependent effective interactions, one with equal exchange mixtures and the other with unequal exchange mixtures, determined in our earlier work.<sup>1</sup> The values of the effective mass ratio obtained from these interactions are quite comparable to those obtained by Brueckner and Gammel<sup>2</sup> (BG) and others. The value of the rearrangement energy,  $R = 12.37$  MeV for the interaction with equal exchange mixtures and  $R = 7.44$  MeV for the interaction with unequal exchange mixtures. The former value of  $R$  is in excellent agreement with the 12 MeV rearrangement energy obtained by Brueckner and Gammel, while the latter is considerably lower compared to the BG value.

References:

1. K.M. Khanna and P.K. Barhai, Nucl. Phys. A 250 (1973)
2. K.A. Brueckner and J.C. Gammel, Phys. Rev. 109 (1958), 1023.

H. BIRLA INSTITUTE OF TECHNOLOGY, PILANI, RAJASTHAN

1. Energy Levels of Zirconium Isotopes using Modified Surface Delta Interaction - G. Ramachandra Rao and K.S. Subudhi - Following the suggestion made by Moszkowski we have chosen to study surface delta interaction in modified form (MSDI) for zirconium isotopes ( $N = 51$  to  $56$ ). In MSDI the radial integrals are not assumed to be the same. Therefore the two particle matrix elements of the interaction depend upon two parameters, the strength of MSDI and the oscillator constant of the harmonic oscillator well. We consider the space to contain pure configurations  $2d_{5/2}^n$  and those with one particle raised to  $3S_{1/2}$  and  $2d_{3/2}$ .

There are 29 experimental energy levels to be determined by diagonalizing the energy matrices, which depend upon the two parameters mentioned earlier, and single particle binding energy of  $2d_{5/2}$  level. The binding energies of  $3S_{1/2}$  and  $2d_{3/2}$  are respectively fixed at 1.57 MeV and 2.32 MeV above that of  $2d_{5/2}$  level.

The three parameters are varied to fit experimental values of 29 energy levels and B.E. of  $2d_{5/2}$  level.

I. BURDWAN UNIVERSITY, BURDWAN

1. Asymmetric Rotor Model with Angular-Momentum Dependent Moments of Inertia - B.C. Samanta and P.K. Banerjee - The centrifugal stretching model of Sood and the variable moment of inertia (VMI) model of Mariscotti et al. have been particularly successful in explaining the rotational spectra of deformed even-even nuclei. The essential similarity of these models has been demonstrated by Wold. For symmetric deformed even-even nuclei, Sood has given a formula for the variation of moment of inertia with angular momentum of the rotational state. We have assumed the formula to be true even in the case of asymmetric even-even nuclei. The rotational energies of the different positive parity states of the latter type of nuclei have been calculated on the basis of the Davydov-Filippov model using the above formula for the variation of moments of inertia with angular momentum. The results have been compared with experiment. Good agreement has been obtained and a comparison with other works has also been made.

J. CALCUTTA UNIVERSITY

1. On the Bound States of Spin  $\frac{1}{2}$  Particles for Certain Central Potentials - B.G. Sidharth - Bound state solutions of the Dirac equation for spin  $\frac{1}{2}$  particles are investigated by the polynomial method for potentials  $U(r)$  where,  $rU(r) =$

This includes the Yukawa, Gaussian, and other potentials of interest in nuclear theory.

It is deduced that except for a special class of potentials satisfying restrictive conditions, bound states do not exist.

2. Effect of Deuteron Break-Up Channel on Single Particle Transfer Reactions - Soumen Kumar Roy\*, Subrata Ray\*, Suproakash Mukherjee\*, and S.K. Samaddar - The reaction cross-sections for (d,p) and (p,d) processes have been formulated in such a fashion that we can directly estimate the contribution of break-up channel of the deuteron over DWBA integrals using an average energy denominator. Calculations of  $Ca^{40}(d,p)$  and  $Pb^{208}(p,d)$  exhibit significant contribution of the break-up channel. It is further observed that the angular distributions are somewhat sensitive on the value of average energy denominator which questions the validity of adiabatic approximation of Johnson et al<sup>1)</sup>. Ambiguity in the choice of effective interaction for the inclusion of break-up channel has also been discussed.

1) R.C. Johnson and P.J.R. Soper, Phys. Rev. C1 976(1970)

J.D. Harvey and R.C. Johnson, *ibid* C3 636(1971)

\* Saha Institute of Nuclear Physics, Calcutta-700009.

K. DIBRUGARH UNIVERSITY, ASSAM

1. Shell Model Study of  $O^{18}$  and  $F^{18}$  Using Realistic N-N

Potential.- A.K. Deka and P. Mahanta - Shell model calculations of energy levels of  $O^{18}$  and  $F^{18}$  are made using two realistic soft core N-N potentials proposed recently<sup>1</sup>. These potentials obtained by fitting the low energy N-N phase shift use respectively Gaussian and Yukawa potentials and are used here for the simplicity in evaluating the corresponding Talmi integrals. The potential matrix elements are mostly repulsive and the energy levels given by the latter potential are very similar to those obtained by OBEP models. None of the potentials reproduces the observed energy levels, thus showing the necessity of using the G-matrix formalism and probably the inadequacy of soft core potentials.

1) H. Eikemeier and H.H. Hackenbroich, Nucl. Phys

A 169(1971)407

I. Uehla et al., Rutherford Laboratory preprint RPP/C/41  
(March 1972).

L. INDIAN ASSOCIATION FOR THE  
CULTIVATION OF SCIENCE

1. Triton Binding Energy for Local Square Well Potential with Faddeev approach - G. Purkayastha and N.C. Sil - The triton bound state has been studied by Faddeev approach using local two body short range nuclear square well potential. The separable representation of the two body t-matrix, corresponding to the above mentioned potential, is obtained utilizing a separable approximation of the integral representation of the interaction potential in momentum space, which is achieved by a summation over a suitable and finite number of quadrature points. Then this t-matrix, separable in momentum space, has been used in the homogeneous integral Faddeev equation to compute the triton binding energy. Using a two term and three term expansion for the integral transform of the square well potential, the binding energy values of the triton have been evaluated considering the triplet plus singlet states of the target deuteron of the neutron deuteron system for two sets of parameters of potential. We have compared our result with the convergent theoretical result obtained by Kharchenko and Storozhenko for the same potential. It is observed that the binding energy value in the first case is higher than the convergent value of Kharchenko and Storozhenko while in the second case, our result is very close to their result.

2. Scattering of High Energy Electron by Oriented  $^{165}\text{Ho}$  Nucleus in Eikonal Approximation - S. Sarkar and Sofia Khaton - We have adopted eikonal approximation due to Yennic and Petrov's

analytic method to treat the interaction of electron with a nucleus having Fermi type charge distribution (which has poles in a complex plane) to study the scattering of electron by oriented  $^{165}\text{Ho}$  nucleus having quadrupole moment. We have also considered the effect of low lying rotational levels of Holmium in order to compare our calculation done for 200 MeV electron energy with the experimental findings of Safrata. It may be noted that Wright and Onley have treated the above mentioned problem considering phase shifted distorted waves for the electron. Our expression for the scattering by the quadrupole moment of the nucleus differs from that of Petkov because we have considered Wright's form for quadrupole charge distribution which is somewhat different from that assumed by Petkov. This expression is compared with that of Petkov by numerical computation. We have been able to obtain a closed analytical expression for the Born amplitude for elastic and inelastic electron scattering by quadrupole moment of a nucleus. We have pointed out that if we include a certain term (which is very small for very large momentum transfer and perhaps so neglected by Petkov) in Petkov's expression for inelastic scattering of electron by nucleus, we can get the expression for Born amplitude in Born approximation limit.

M. INDIAN INSTITUTE OF TECHNOLOGY KANPUR

1. Trajectory Calculations on Long Range Alpha Fission -

B. Krishnarajulu, A.J. Gadgil and G.K. Mehta - There is a major disagreement between the results of various trajectory calculations as far as the initial kinetic energies of the  $\alpha$ -particle and the fission fragments are concerned. One of the important arguments in favour of high initial energies is based on the observed anticorrelation between the final  $\alpha$ -particle energy ( $E_\alpha$ ) and the final total fragment kinetic energy ( $E_F$ ). Boneh et al. concluded that the observed anticorrelation cannot be explained unless one assumes that the fragments are moving with about 20% of their final kinetic energy, at the moment of scission. The authors would like to emphasize that most trajectory calculations are made by fixing all but one initial variable and could thus lead to misleading conclusions. It has been shown that an acceptable anticorrelation curve can be obtained with low initial energies by including appropriate variation in the initial fragment separation ( $D$ ). Inclusion of this variation also explains the experimental results on the variation of  $\bar{E}_\alpha$  with the angle of emission of the  $\alpha$ -particle ( $\theta_L$ ), and the results on the variation of  $\bar{Q}_L$  as a function of fragment mass ratio.

2. A Phenomenological Estimation of Renormalisation Corrections to Free Nucleon-Nucleon Interaction - I. Mehrotra, -M. Prakash and

Y.R. Waghmare - Effect of central, spin-orbit and tensor components of Sussex matrix elements on low energy spectra of  ${}^6\text{Li}$ ,  ${}^{18}\text{F}$ ,  ${}^{18}\text{O}$ ,  ${}^{42}\text{Sc}$ ,  ${}^{42}\text{Ca}$ ,  ${}^{58}\text{Ni}$  and  ${}^{92}\text{Zr}$  nuclei has been studied. As expected,

the level energies receive maximum contribution from the central component, while the spin-orbit and the tensor components provide the finer details of the spectra. The two-body spin-orbit force is found to be least important. Calculated spectra do not compare favourably with experiment. We assume that, for  $T = 0$  states, all renormalization corrections can be dumped into matrix elements of the  $3S_1$  relative state. It is found that if the  $3S_1$ -Sussex matrix elements are multiplied by a factor  $\gamma$ , low lying levels can be satisfactorily reproduced by an appropriate choice of  $\gamma$ . Some of the  $T = 1$  low-lying excited states can be obtained if the realistic interaction, as represented by the Sussex matrix elements, is supplemented by a  $\delta$ -function force of appropriate strength.

3. Rotational Flow Model and its Significance - V.R. Prakash and V.K. Deshpande - Some important features of the Rotational Flow Model (RFM)<sup>1,2</sup> with a constant vorticity flow in three dimensions are discussed here. The velocity field obtained on the basis of a constant vorticity flow in an incompressible drop of ellipsoidal shape is shown to be unique. Further, it is shown that to obtain the rotational Hamiltonian in the form  $H = \sum (I_j^2 / 2I_{j\text{eff}})$ , it is essential to assume the frequency ( $\Omega_j$ ) of intrinsic particle motion to be directly coupled to the rotational frequency ( $\omega_j$ ) of the ellipsoidal drop through the vorticity constant ( $k_j$ ) thus, giving adiabatic motion only for values of  $k_j$  much larger than unity.

From a study of variation of the ratio of effective moment of inertia ( $I_{j\text{eff}}$ ) to the rigid body moment of inertia ( $I_{jR}$ ) as a function of  $k_j$  for a given deformation and vice-versa, the values

of  $k_j$ 's are shown to lie between 0.8 to 1.0 for the nuclei in the rare-earth region. Further, it is shown that small but finite values of  $I_{j\text{eff}}/I_{jR}$  could be obtained for very small deformations with  $k_j$  slightly less than unity in the case of RFM, and for very large deformations with  $k_j = 1$  in the case of irrotational flow model.

REFERENCES:

1. V.R. Prakash, B.M. Bahal and V.K. Deshpande, Can.J.Phys. **50** 2957(1972)
2. V.R. Prakash and V.K. Deshpande, ibid., **51**, 1752 (1973).

N. INSTITUTE OF MATHEMATICAL SCIENCES

1. Cluster Model Wave Functions of  ${}^6\text{Li}$  and  ${}^7\text{Li}$  - K. Srinivasa Rao - Cluster model wave functions of  ${}^6\text{Li}$  and  ${}^7\text{Li}$  are constructed by considering alpha-deuteron and alpha-triton configuration, respectively, for the light nuclei. The wave functions are antisymmetrized and each wave function involves two parameters. The effect of the antisymmetrization of the wave functions on the root mean square radii of  ${}^6\text{Li}$  and  ${}^7\text{Li}$  is studied. Results of the study, on comparison with available experimental data, yield the allowed range of the parameters in the wave functions.

0. KURUKSHETRA UNIVERSITY, KURUKSHETRA

1. Comparison of Various Level Density Formulae - B.S. Wadhwa, K.K. Menocha\* and R.K. Mohindra - The level density formulae based on the Fermi gas model: (i) Lang-LeCouteur (ii) Constant nuclear temperature (iii) Weisskopf and shell dependent formulae due to (iv) Newton and (v) Baba<sup>1</sup> have been compared using recently compiled data<sup>1</sup> for about 200 nuclides (neutron resonance capture cases). The Newton's shell dependent level density formula gives better results. The effects of closed shells, pairing energy, odd-even effects and spin dependence have been studied. The best value of the spin out off parameter has been found.

1. H. Baba, Nucl. Phys. A 159 (1970) 625.

\* Present Address: Medical College, Rohtak (Haryana)

P. MARATHWADA UNIVERSITY, AURANGABAD(M.S.)

1. Electromagnetic Properties of  $^{55}\text{Mn}$  - P.N. Patarwale, R.G. Kanitkar and R.G. Kulkarni - The magnetic dipole  $T(M_1)$  and electric quadrupole  $T(E2)$  transition probabilities have been obtained from the Coulomb excitation reaction on  $^{55}\text{Mn}$  with alpha-particles. The electric quadrupole transition probabilities  $T(E2)$  and the corresponding life times have been found for the four excited states of  $^{55}\text{Mn}$  with alpha-particles. The electric quadrupole transition probabilities  $T(E2)$  and the corresponding life times have been found for the four excited states of  $^{55}\text{Mn}$ . With the aid of measured branching ratios, the magnetic dipole transition probabilities  $T(M_1)$ , the reduced  $M_1$  transition probabilities  $B(M_1)$  and mixing ratios  $\int^2 = \frac{E_2}{M_1}$  for 126 and 986 keV states in  $^{55}\text{Mn}$  have been determined. These electromagnetic properties of 126 and 986 KeV states in  $^{55}\text{Mn}$  have been found for the first time. These properties will be discussed in the light of theory of life-times of nuclear states by D. Kurath<sup>(1)</sup>.

Ref. (1) D. Kurath, Invited Paper, Bull. Am. Phys. Soc. 13, 1400 (Nov. 1968).

Q. MEERUT UNIVERSITY, MEERUT

1. Study of the 20.3-MeV State in  ${}^4\text{He}$  by the Cluster Model -  
V.K. Jain and B.B. Srivastava - The first excited state of  ${}^4\text{He}$  at about 20.3 MeV has been observed in many nuclear reactions during the past several years. However, the various measurements of its excitation energy and width are not consistent. A recent investigation by Gross et al.<sup>1</sup>, yields a value of  $20.28 \pm 0.05$  MeV for the excitation energy and  $0.41 \pm 0.05$  MeV for the width of this state. On the basis of an analysis of their data these authors observe that the state is consistent with a  $0^+$  assignment and corresponds to a pure  ${}^1\text{S}$ -wave resonance in the  $p\text{-}{}^3\text{H}$  system. In the present study, therefore, a variational procedure has been used to calculate the energy of this state described as a triton cluster plus a proton. Properly antisymmetrized wave function and a nucleon-nucleon potential yielding good fit to the low energy scattering data have been used. The calculation yields a value of 20.54 MeV for the excitation energy of this state relative to the ground state which is in quite good agreement with the experimental value obtained by Gross et al.

1. E.E. Gross et al., Phys. Rev. 178(1969)1584.

R. PHYSICAL RESEARCH LABORATORY, AHMEDABAD

1. The Generator-Coordinate Calculations for the Electric Quadrupole-Moments and Transition Rates - S.B. Khadkikar and

D.R. Kulkarni - The electric quadrupole moments and the transition probabilities are calculated for all the even-even ( $N = Z$ ) nuclei in the d-s shell using the generator-coordinate formalism. These quantities being quite sensitive to the structure of the eigenfunctions, offer a measure of the goodness of the calculated wave functions. It was found that the calculated quadrupole moments of the first  $2^+$  states are within the error of the experimental values for the nuclei  $^{28}\text{Si}$ ,  $^{32}\text{Si}$ , and  $^{36}\text{Ar}$  whereas they are slightly lower than the experimental values for the nuclei  $^{20}\text{Ne}$  and  $^{24}\text{Mg}$ . The calculated transition rates are consistently smaller than the experimentally observed values for all the nuclei.

2. Energy Vs Deformation Curve for Nuclei in the ds-Shell -

R. Haq and J.C. Parikh - We report here calculations, using the spectral distribution method, for the Elliott  $\text{SU}(3)$  group, which describe the average deformation ( $\langle Q_{20} \rangle$ ) of a nucleus in the ds-shell as a function of excitation energy.

3. Minimization of Energy Variance for Determinants - V. Satyan

and J.C. Parikh - We describe in this note a general method to minimize the energy variance

$$\sigma^2 = \langle H^2 \rangle - \langle H \rangle^2$$

for single determinantal states. Calculations for light spherical nuclei have been done and compared with the Hartree-Fock results.

4. An Improved Estimate of SU(4) Symmetry Mixing in Light

Nuclei - R. Haq, J.C. Parikh and K.H. Bhatt - The spectral distribution method of French has been very successful in determining ground state energies and mixing intensities of various irreps of a group near the ground state. For the SU(4) group these methods have been extensively used. The method incorporated actually estimates an upper limit for the mixing and lower amounts of mixing cannot be ruled out. This is because the total variance  $\sigma^2$  which is composed of  $\sigma_{\text{external}}^2$  and  $\sigma_{\text{internal}}^2$  is used for estimating the amount of mixing. Whereas  $\sigma_{\text{int}}^2$  gives rise to spreading of various irreps, it is only  $\sigma_{\text{ext}}^2$  which leads to symmetry mixing. Better methods of estimating the mixing shall be discussed.

5. On Intra-Shell Quartet Excited States - A.K. Dhar,

D.R. Kulkarni and K.H. Bhatt - Possible existence of intrashell quartet excited states for the nuclei  $^{20}\text{Ne}$ ,  $^{24}\text{Mg}$  and  $^{28}\text{Si}$  in the ds and  $^{44}\text{Ti}$ ,  $^{48}\text{Cr}$  and  $^{52}\text{Fe}$  in the fp shells has been examined. Quartet excited intrinsic states are obtained by exciting two protons and two neutrons from the highest occupied to the lowest unoccupied orbitals of the lowest energy axially deformed Hartree-Fock(HF) solutions. Good-J states are projected from the prolate and the oblate HF and the quarter excited intrinsic states. Due to nonorthogonality of these states it is found that the relative separation of the projected states is drastically changed by orthogonalization. For  $^{20}\text{Ne}$  the low-lying states do not have pronounced quartet structure whereas the excited states of  $^{24}\text{Mg}$

and  $^{28}\text{Si}$  which do have dominant quartet structure lie very high in energy. For the fp shell nuclei, none of the excited states are likely to have a well defined quartet structure.

6. Shell Model Calculation for Odd Ti Isotopes - D.R. Kulkarni, A.K. Dhar and K.H. Bhatt - The band mixing calculations for odd Ti isotopes  $^{45}\text{Ti}, ^{47}\text{Ti}, ^{49}\text{Ti}, ^{51}\text{Ti}$  are performed in the frame work of Projected Hartree-Mock (PHF) formalism using the Kuo Brown effective interaction with  $T = 1$  part replaced by the interaction obtained by McGrory et al(1). Different intrinsic states are obtained by  $1p-1h$  excitations over the lowest prolate and oblate HF solution adopting a suitable energy criterion for truncating the Hilbert space. The energy spectra of the nuclei are obtained by diagonalizing the Hamiltonian in the basis of projected and orthogonalized states. For the nucleus  $^{47}\text{Ti}$  the calculated spectrum is in good agreement with the observed spectrum upto  $\sim 3$  MeV. Certain high spin states are predicted in the energy range of 3 to 5 MeV. For all other isotopes the energy sequence is well reproduced within 400 kev. In order to reproduce better relative separation between the various states, modifications in the interaction are suggested.

1) McGrory J.H., Wildenthal B.H., and Halbert E.C., Phys. Rev. C2, (1970), 186.

7. Band-Mixing Calculations for Na Isotopes - D.R. Kulkarni and S.P. Pandya - The spectra of odd sodium isotopes viz.  $^{21}\text{Na}$ ,  $^{23}\text{Na}$  and  $^{25}\text{Na}$  are obtained by performing the band-mixing calculations in the framework of projected Hartree-Fock formalism. Different bands are obtained by various particle-hole excitations

over the lowest HF solutions. The two-body matrix elements of Freedom et al<sup>1)</sup> are used along with the experimental  $17_0$  single particle energies. The calculated spectra of nuclei  $^{21}_{Na}$  and  $^{23}_{Na}$  are in fairly good agreement with the experimental spectra. However the spectrum of  $^{25}_{Na}$  is not so well reproduced. It appears that the interaction producing less deformation might give better experimental agreement in this nucleus. Some modifications in the interaction to this effect would be suggested.

- 1) Freedom B.M. and Wildenthal B.H. Phys. Rev. C6 (1972) 1633.

8. Generator Coordinate Spectra of the Nuclei  $^{24}_{Mg}$ ,  $^{32}_{S}$  and  $^{36}_{Ar}$  - S.B. Khadkikar and D.R. Kulkarni - The generator coordinate spectra<sup>1)</sup> for the nuclei  $^{24}_{Mg}$ ,  $^{32}_{S}$  and  $^{36}_{Ar}$  are obtained by solving the Hill-Wheeler integral equation approximately. The energy and the overlap kernels required in the equations are obtained in the projected and constrained Hartree-Fock formalism. The two-body matrix elements of Freedom et al<sup>2)</sup> are used along with the experimental  $17_0$  single particle energies. Despite the fact that for  $^{24}_{Mg}$  the triaxial solution is lowest in energy, the first  $0^+$ ,  $2^+$ ,  $4^+$ ,  $6^+$  and  $8^+$  states are in good agreement with the experimental and the shell model states. The first excited  $0^+$  level also agrees well with the corresponding state in the shell model spectrum. The results for the nuclei  $^{32}_{S}$  and  $^{36}_{Ar}$  indicate that the two body interaction needs some modifications.

1. Khadkikar S.B. and Kulkarni D.R. Phys. Rev. C6 (1972) 866.
2. Freedom B.M. and Wildenthal B.H. Phys. Rev. C6 (1972) 1633.

9. Double Humped Barriers in Medium Weight Nuclei - K.H. Bhatt, A.K. Dhar and D.R. Kulkarni - The low lying highly collective intershell 'Core' excited states in the nuclei in neighbourhood of  $O^{16}$  and  $Ca^{40}$  are known. In this note we propose the possible existence of low lying highly deformed, intrashell excited states for some of the fp shell nuclei. The proposition is borne out by Projected Hartree-Fock(PHF) calculations for the nuclei  $Cr^{50}$  and  $Fe^{52}$ . We have employed the two body effective interaction which gives rise to deformations of the fp shell nuclei consistent with the experimental E2 transition systematics. The interaction gives two distinct Hartree-Fock states, having very different deformation. The state with smaller deformation lies lower in energy. Despite the large differences in the deformation the other solution lies very close to the ground state. It is interesting to note that the states projected from the more deformed state are orthogonal to the states projected from both the lowest prolate and oblate HF states. The existence of such states in fp shell nuclei would be analogous to the fission isomers in heavy nuclei. The experimental identification of such states would be interesting and would help to improve the effective interaction.

10. Intermediate Coupling Model Description of  $^{57}Fe$  - J.J. Dikshit and B.P. Singh,- The properties of the negative parity states of  $^{57}Fe$  are investigated in the framework of the intermediate coupling in the unified vibrational model. In the model, a quasineutron is coupled to an anharmonically vibrating core. Observed properties of the  $^{56}Fe$  nucleus are used to describe anharmonicities of the

core. The model is applied to this nucleus for the first time. Energy levels, electromagnetic transition rates, branching ratios, lifetimes and spectroscopic factors have been calculated. The theoretical results have been compared with experimental results. The ground state spin is correctly predicted for reasonable values of parameters. Comparison with rotational model calculations shows that both models have limitations in describing the  $^{57}\text{Fe}$  nucleus. It is concluded that a model in which three quasineutrons are coupled would give better results.

S. PUNJAB UNIVERSITY, CHANDIGARH

1. Gyromagnetic Ratio of the 656 KeV State in  $^{110}\text{Cd}$  - Bhupender Singh, S.C. Bedi, V.R.K. Murty and H.S. Hans - As there is considerable disagreement in the measurements of the gyromagnetic ratio of the 656 keV state in  $^{110}\text{Cd}$ , IPAC method has been used to remeasure the gyromagnetic ratio of the 656 keV state. The internal hyperfine field acting at Cd nuclei in iron has been used. 1504-656 keV and 1384-885-656 keV caseades were used simultaneously for measuring the rotation of the angular correlation pattern. The measured value of the gyromagnetic ratio i.e.  $g = 0.34 \pm 0.07$  is in good agreement with the value reported by K. Johansson et. al<sup>1)</sup> making use of the internal field in gadolinium. A couple of earlier measurements made through PAC radioactivity and IMPACT methods give a low value with the recent accurate value of the hyperfine field. Our measured value agrees well with the value estimated on the basis of Greiner model for the gyromagnetic ratio of vibrational nuclei.

1. K. Johansson, E. Karlsson, L.O. Norlin, R.A. Windahl and M.R. Ahmed. Nucl. Phys. A188 (1972) 600.

2. Core Excitation Effects and Nuclear Spectra - S. Shelly and R.K. Bansal - Fragmentation of spectroscopic strength observed in the spectra of nuclei which consist of a closed neutron shell plus a proton in one of the empty shells indicates that additional degrees of freedom associated with the core after the proton has been added are to be properly taken into account. The formalism

for calculating the effects of isospin excitation as well as two particles-two holes excitation of the core, for nuclei falling in this category, has been developed. Particular cases involving addition of a proton to  $^{48}\text{Ca}$  and  $^{60}\text{Ni}$  targets have been discussed.

The single particle strength which is expected to be concentrated in one level in the absence of core excitations is fragmented into  $3/2(2j_2+1)+2$  pieces where  $j_2$  is the angular momentum of the orbit to which the proton is added, thus giving rise to a fine structure of the spectrum.

Systematics of calculated spectroscopic strength distribution and energy eigen values show a fairly good agreement with the experimental results.

3. Level Structure Studies in  $^{192}\text{Pt}$  and  $^{192}\text{Os}$  and Experimental Test of Pairing-Plus Quadrupole Model - Nirmal Singh, S.S. Bhati, P.C. Mangal and P.N. Trehan - Gamma ray intensity measurements have been done with great precision in  $^{192}\text{Pt}$  and  $^{192}\text{Os}$  in the decay of  $^{192}\text{Ir}$  using 8 c.c. Ge(Li) detector. In addition gamma-gamma directional correlation measurements have been done for 296-316, 308-296, 308-612, 308-(296)-316, 589-296, 589-(296)-316, 604-316, 468-316, 589-612, 885-316, 1062-316 keV cascades in  $^{192}\text{Pt}$  and 486-206 keV cascade in  $^{192}\text{Os}$  using NaI(Tl)-Ge(Li) and NaI(Tl) - NaI(Tl) detectors. From the data spin assignments have been confirmed for 1379(3) and 1200 (4<sup>+</sup>) keV levels of .

$^{192}\text{Pt}$  and  $691(3^+)$  keV level of  $^{192}\text{Os}$ . Multipole admixtures in 296, 308, 589, 604, 885, 1062 and 486 keV gamma rays have been found out to be  $M1+(97\pm 1)\%E2$ ,  $M1+(96.5\pm 5)\%E2$ ,  $E2+(4\pm 2)\%M3$ ,  $M1+(79\pm 7)\%E2$ ,  $E2+ .04\%M3$ ,  $E1+.04\%M2$  and  $M1+(94\pm 2)\%E2$  respectively. The values of multipole mixing in 296, 308, 604 and 436 keV gamma transitions are compared to those predicted by pairing-plus quadrupole model of Kumer and Barangar and the agreement is found to be fairly good.

T. PUNJABI UNIVERSITY, PATIALA

1. A New Good Quantum Number in Collective Model - S.D. Sharma -

A nuclear spin quantum number of restricted goodness is seen to show up in perturbed rotational bands of odd-A and odd-odd nuclei due to the physical quantum constraints effective on the systems. A new type of state-labelling is discussed, which can furnish information about the nucleonic and corral contributions in separate for all such nuclei in deformed regions. Theoretically expected systematics of nuclear dynamics below and above this good spin are supported by the available experimental reports for many nuclei.

2. Magnetic Dipole and Electric Quadrupole Moments of Deformed Odd-A and Odd-Odd Nuclei - Jagdev Gargi and S.D. Sharma -

Ascuitto and Davidson calculated the Magnetic Dipole and Electric Quadrupole moments diagonalising the state matrices for a set of parameters giving the best fit for nuclear spectra using symmetric core collective model for deformed nuclei. Here instead of diagonalising we have simplified the expressions for Magnetic Dipole and Electric Quadrupole moments for single nucleonic state without configuration mixing. The results are computed and compared with experimental reports wherever available and also with other theoretical predictions.

3. The Spectra and Static Moments of Re<sup>186</sup> - V.P. Garg and S.D. Sharma - Lowlying spectrum and static magnetic and quadrupole moments of Re<sup>186</sup> are computed using symmetric and asymmetric core

collective models of odd-odd deformed nuclei. The spectral computations are compared with the experimental reports on this nucleus by R.K. Sheline et. al. The model predictions are found quite satisfactory.

U. SAMBALPUR UNIVERSITY, ORISSA

1. A Method for Fast Convergence of the Reaction Matrix(II) -

R.K. Satpathy and N.M. Guru. - The reaction matrix of Brueckner  $t$  is expanded in terms of short-range part  $t_s$  and terms involving  $(V_1 - V_2)$  and  $V_2$  only. Here  $V_1$  is the long-range part of the actual two-body potential and  $V_2$  is an auxiliary potential, nonlocal and separable in nature. This expansion is an improvement over our earlier work (Nucl. Phys. 185, 284 (1972)). The merits of the method are analysed.

2. Regge-Type Representations of the Partial Wave Amplitude

for Spin-One case - R.K. Satpathy and A.P. Mishra - Regge-type representation of the partial wave amplitude in the complex angular momentum plane are derived for elastic scattering of spin-one particles from nuclei. These representations are found to be similar in form to those for spin-zero and spin-half particles. The importance of the method is discussed.

V. UNIVERSITY OF DELHI

1. Velocity-Dependent Nucleon-Nucleon Potential and Short-Range

Correlations - R.S. Kaushal - A velocity-dependent potential is constructed by performing a unitary transformation, based on Jastrow type correlation function, on the Hamiltonian of single particle model. Though this potential has structure similar to that used earlier by several authors, however, it ensures, to some extent, the inclusion of the effects of short-range repulsive forces between nucleons. The parameters of this potential are known from the experiments.

2. Decay of  $^{127m,g}\text{Te}$  To Levels of  $^{127}\text{I}$  - S.K. Soni, Ashok Kumar, D. Ghosh, S.L. Gupta and S.C. Pancholi - The Gamma spectrum of  $^{127m}\text{Te}$  in equilibrium with  $^{127g}\text{Te}$  has been studied in singles using a 88 cc Ge (Li) detector. The gamma-ray energies in keV (relative intensities in parantheses) were found to be  $57.86 \pm 0.04 (58.0 \pm 0.7)$ ,  $88.25 \pm 0.04 (7.9 \pm 0.2)$ ,  $115.6 \pm 0.1 (1.0 \pm 0.6)$ ,  $145.34 \pm 0.07 (0.3 \pm 0.1)$ ,  $172.11 \pm 0.06 (0.02)$ ,  $202.69 \pm 0.04 (5.2 \pm 0.2)$ ,  $214.90 \pm 0.05 (3.6)$ ,  $360.23 \pm 0.05 (13.3 \pm 0.3)$ ,  $374.9 \pm 0.1 (0.06)$ ,  $417.87 \pm 0.05 (100)$ ,  $593.1 \pm 0.1 (0.29 \pm 0.1)$ ,  $619.9 \pm 0.3 (0.03)$ ,  $629.9 \pm 0.3 (0.006)$ ,  $651.9 \pm 0.3 (0.01)$ ,  $658.1 \pm 0.1$  and  $687.40 \pm 0.09$ .

Gamma-Gamma directional correlation measurements have also been performed on (57-360) and (57-658) keV cascades using an aqueous solution of  $^{127m}\text{Te}$  and a NaI(Tl)-Ge(Li) detector coincidence system.

3. Half-Life Measurement of the 57.6 keV Level in  $^{127}\text{I}$  -

Suvva Sanyal, R.K. Gupta, S.L. Gupta and S.C. Pancholi - The half-life of the 57.6 keV level in  $^{127}\text{I}$  has been measured by recording  $\beta\gamma$ -coincidences in  $^{127\text{m}}\text{Te}$  decay using leading-edge timing technique. The time delay curve was analysed by the slope method. A half-life value of  $T_{1/2}$ (57.6 keV level in  $^{127}\text{I}$ ) =  $1.98 \pm 0.01$  ns is obtained. The electromagnetic transition rates from the low lying states in odd-mass I isotopes are discussed and compared with available theoretical results.

4. High Resolution Study of Low Energy Gamma-Rays in the Decay of  $^{237}\text{Np}$  and  $^{241}\text{Am}$  - S.D. Chauhan, Suvva Sanyal, R.K. Garg,

S.C. Pancholi, and S.L. Gupta - High resolution low energy ( $E_\gamma \lesssim 122$  keV)  $\gamma$ -ray spectra in singles have been studied in the decay of  $^{237}\text{Np}$  and  $^{241}\text{Am}$  using a  $0.4 \text{ cm}^2$  Ge(Li) Low Energy Photon detector (resolution 300 eV at 6.40 keV and 600 eV at 121.94 keV). The measured  $\gamma$ -ray energies in keV (relative intensities in parentheses) are as follows:  $^{237}\text{Np}$ :  $8.10 \pm 0.04$  ( $0.48 \pm 0.07$ ),  $29.375$  ( $12.0 \pm 0.3$ ),  $32.05 \pm 0.03$  ( $0.16 \pm 0.02$ ),  $36.28 \pm 0.05$  ( $0.048 \pm 0.017$ ),  $46. \dots \pm 0.03$  ( $0.094 \pm 0.016$ ),  $57.09 \pm 0.01$  ( $0.35 \pm 0.02$ ),  $86.41 \pm 0.02$  ( $12.1 \pm 0.3$ ),  $87.9 \pm 0.1$  ( $0.095 \pm 0.024$ ),  $106.2 \pm 0.1$  ( $0.02 \pm 0.01$ ),  $115.47 \pm 0.07$  ( $0.41 \pm 0.03$ ) and  $117.83 \pm 0.03$  ( $0.17 \pm 0.02$ ).

$^{241}\text{Am}$ :  $3.43 \pm 0.03$ ,  $8.6 \pm 0.1$ ,  $9.60 \pm 0.02$  ( $0.28$ ),  $26.345$  ( $2.06 \pm 0.03$ ),  $33.17 \pm 0.02$  ( $0.13 \pm 0.01$ ),  $43.37 \pm 0.03$  ( $0.07 \pm 0.01$ ),  $55.40 \pm 0.10$  ( $0.108 \pm 0.004$ ),  $59.537$  ( $35.3$ ),  $98.89 \pm 0.05$  ( $0.025 \pm 0.001$ ) and  $102.86 \pm 0.05$  ( $0.023 \pm 0.001$ ). Component L- and  $K_\alpha$  x ray intensities are also measured.

W. UNIVERSITY OF MADRAS

1. Trace Techniques for Angular Momentum Operators -

P.R. Subramanian and V. Devanathan - Traces of angular momentum matrices for systems of arbitrary spin are derived using their well - established properties. The nature and the general form of the trace of a product of an arbitrary number of matrices is given. The trace techniques developed herein are supplied to the problems of spin orientation. For the purpose of illustration we have obtained the explicit forms for the spin tensors and evaluated their reduced matrix elements. Also the elastic scattering of particles of arbitrary spin by a target nucleus of zero spin is investigated.

2. Photoproduction of Charged Pions From  $^{41}\text{K}$ ,  $^{60}\text{Ni}$  and  $^{65}\text{Cu}$  -

G.N.S. Prasad and V. Devanathan - Numerical results for the reactions  $^{41}\text{K}(\gamma, \pi^+)^{41}\text{A}$ ,  $^{60}\text{Ni}(\gamma, \pi^-)^{60}\text{Cu}$ ,  $^{65}\text{Cu}(\gamma, \pi^+)^{65}\text{Ni}$  and  $^{65}\text{Cu}(\gamma, \pi^-)^{65}\text{Zn}$  are reported and compared with the available experimental results. Independent Particle model for the nuclei and the volume and surface production mechanisms are used in the present study. The Reactions of the type  $\text{A}(\gamma, \pi^\pm)\text{B}$  can be used to extract information regarding the low-lying states of the nucleus B which are stable against nucleon emission.

3. On D-State Admixture in  $\pi^0$  Photoproduction from the Deuteron -

K. Srinivasa Rao, (Matscience) and S. Srinivasa Raghavan - In the earlier studies<sup>1)</sup> on neutral pion photoproduction cross-sections,

the effect of the D-state admixture was taken into account through the normalization and scale of the S-state wave function only. In this article, we include the D-state admixture explicitly (through the radial integrals  $F_{SD}$  and  $F_{DD}$ ) and study the differential cross section for  $\gamma d \rightarrow d \pi^0$ , near the first pion-nucleon resonance region, at fixed momentum transfers. A comparison with available experimental data shows that, the cross sections are slightly more enhanced than the earlier theoretical results. Our results with deuteron wave functions obtained with (i) the soft core OBEP of Ueda and Green<sup>2)</sup> and (ii) the Modified Hamada-Johnston hard core potential<sup>3)</sup>, are comparable. The energy dependence of the total cross section is also studied.

- 
- 1) K. Ananthanarayanan & K. Srinivasa Rao, Nuo. Cim. 44(1966) 31; K. Srinivasa Rao, R. Parthasarathy and V. Devanathan, J. Physique 34(1973)683.
  - 2) T. Ueda & A.E.S. Green, Phys. Rev. 174(1968)1304.
  - 3) J.W. Humberston & J.B.G. Wallace, Nucl. Phys. A. 141(1970)362.

X. VIKRAM UNIVERSITY, UJJAIN

1. Realistic Interactions and Effective Nuclear Force -

Gopal K. Upadhyay and K.P. Joshi - We examine the realistic Yale, Sussex and Tabakin interactions through their equivalents. The equivalent potentials are of the form central and tensor forces and are determined by best fitting the relative matrix elements of the respective realistic interactions. The equivalent potentials are compared with one another and with other phenomenological potentials in widespread use. This leads one to draw some conclusion about the general nature of the effective nuclear force.

2. T = 1 Effective Interaction in sd Shell and Configuration

Space - S.C. Gupta and K.P. Joshi - The T = 1 interactions in sd shell are examined in terms of the equivalent potentials. The interactions studied are Kuo's interaction derived from Hamada-Johnston potential and other phenomenological effective interactions. The nature of the effective nuclear force is discussed and its dependence on configuration space chosen is examined. The short-range part of the equivalent potentials is found to be very sensitive to the choice of configuration space.

3. Single-Particle Energies Near  $^{16}\text{O}$  and Effective Nuclear

Force - S.C. Gupta and K.P. Joshi - The single particle energies near  $^{16}\text{O}$  are calculated using various effective interactions.

interactions used successfully to study sd shell spectra. Many of the interactions fail to reproduce the single-particle energies near  $^{16}\text{O}$  and binding energies. We calculate the effective two-body l.s. force which will reproduce the spin-orbit splittings observed. This is compared with the l.s. force components of the widely used realistic interactions.

Previous reports published by the Indian Nuclear  
Data Group (INDG) :-

1.	A.E.E.T./NP/10	Progress report on Nuclear data activities in India-I	1964
2.	A.E.E.T. - 227	Nuclear Data measuring facilities in India	1965
3.	A.E.E.T. - 228	Progress report on nuclear data activities in India-II	1965
4.	A.E.E.T. - 227	Progress report on nuclear data activities in India-III	1966
5.	B.A.R.C. - 305	Progress report on Nuclear data activities in India-IV	1967
6.	B.A.R.C. - 401	Progress report on Nuclear data activities in India-V	1969
7.	B.A.R.C. - 474	Progress report on Nuclear data activities in India-VI	1970
8.	B.A.R.C. - 553	Progress report on Nuclear data activities in India-VII	1971
9.	B.A.R.C. - 614	Progress report on Nuclear data activities in India-VIII	1972
10.	B.A.R.C. - 695	Progress report on Nuclear data activities in India IX	1973



PROGRESS REPORT

NUCLEAR DATA PROGRAM AND LOW ENERGY NUCLEAR RESEARCH IN ISRAEL

JUNE 1974

### SUMMARY

The contribution to nuclear data research in Israel consists mainly of research into the evaluation and calculation of neutron cross sections carried out at the Soreq Research Centre and the Haifa Technion. There is also a substantial research program in low energy physics carried out at most of the country's research establishments and universities. The experimental programs are centered around three major facilities, the Tandem Laboratory at the Weizmann Institute of Science and the two research reactors at the Negav Research Center and the Soreq Research Centre.

## NUCLEAR EXPERIMENTATION FACILITIES

### Facilities at the Weizmann Institute

A 6 MV Tandem accelerator, type EN, manufactured by HVEC. This machine is the primary installation of the Dannie N. Heineman Accelerator Laboratory, a nuclear structure laboratory owned and operated jointly by the Weizmann Institute, the Hebrew University in Jerusalem, the Technion in Haifa and the Ben Gurion University in Beer Sheva.

A 3 MV Van-de-Graaf accelerator, manufactured by the High Voltage Engineering Corp. of Burlington, Mass., type K. This instrument was the backbone of the nuclear structure research at the Weizmann Institute in the period 1957-1965 and with modern auxiliary equipment it has recently again come into intensified use.

The construction of a new accelerator was started recently. This will be a 14 MV Tandem-Pelletron accelerator, type 14 UD, manufactured by the National Electrostatic Corp. of Middleton, Wisc. This new accelerator and the adjoining laboratory will also be jointly owned and operated by several institutions of research and higher learning in Israel.

### Facilities at the Neq Research Centre

IRR-1 Research Reactor 5MW Light Water Pool Type Reactor, 90% enriched  $^{235}\text{U}$  fuel. This reactor is used for isotope production, activation analysis, neutron radiography, neutron irradiations, and

for low energy nuclear research.

Facilities at the Negev Research Center

IRR-2 Research Reactor 26 MW Heavy Water Tank Type Reactor, Natural U Fuel. Used for studies in fuel irradiation, isotope production, nuclear research, and neutron diffraction studies.

## RESEARCH PROGRAMS

### Weizmann Institute

In the Department of Nuclear Physics work is being carried out both in theoretical and experimental research in the fields of nuclear structure and particle physics. The theoretical work deals with problems in nuclear structure and various nuclear reactions, but most of the effort is in the field of subnuclear or elementary particle physics. The experimental work in nuclear physics is concentrated around the rather old 6 million volt EN tandem accelerator. The experimental research in high energy physics (particle physics) is in the analysis of bubble chamber photographs taken at the giant particle accelerators in the U.S.A.

In nuclear structure theory work continued in studying the effective interactions between protons and neutrons in nuclei. These were studied both by starting from the interaction between free nucleons using the many body theory and from the actual energy levels using the shell model. Nuclear reactions were investigated extensively, in particular those which involve high energy nucleons and pions as projectiles.

#### *Experimental nuclear structure physics*

The need for a new accelerator has been felt for a long time. The present machine is rather limited in energy. Therefore, many experiments originated here had to be carried out in other laboratories. The situation will be greatly improved with the planned installation of the most modern and high energy 14 UD Pelletron accelerator. This machine is now being constructed by the National Electrostatic Corporation in Madison, Wisconsin. Building will begin in summer 1973 and it is hoped that the accelerator will become operational late in 1974. The only other accelerator of this advanced kind is being installed now at the National Australian University in Canberra. Preliminary tests which have been carried out so far indicate that its performance is far above what was promised.

## Experimental Nuclear Structure Physics

### HYPERFINE INTERACTIONS OF THE FIRST EXCITED $2^+$ STATE OF $^{16}\text{O}$ IN $7^-$ AND $6^-$ IONS

G. Goldring, D. A. Hutcheon, W. L. Randolph, D. F. H. Start, B. Goldberg and M. Popp

Perturbed angular correlations were measured between 1.98-MeV  $\gamma$  rays de-exciting the 3.3-psec  $2^+$  state of  $^{16}\text{O}$  and the  $^{16}\text{O}^*$  particles following the reaction  $^{12}\text{C}(^{16}\text{O}, ^{16}\text{O}^*)^{12}\text{C}$  at 33 MeV. A magnetic spectrometer was used to resolve the  $^{16}\text{O}^*$  ions into the component  $8^-$ ,  $7^-$ , and  $6^-$  charge states, and the correlations were determined separately for each. The measurements yield information on hyperfine interactions in the  $7^-$  and  $6^-$  charge states. Limits are obtained on the ionic ground-state occupancies and on the value of the nuclear  $g$  factor.

### THE MAGNETIC MOMENT $3^-$ 5.83 MeV LEVEL IN $^{14}\text{N}$ AND THE BLUME-SCHERER MODEL OF PAC IN GAS WITH AN ARBITRARY CORRELATION TIME

Z. Berant, G. Goldring, M. Hass and Y. Horowitz

Perturbed angular correlation of an ionic ensemble recoiling into gas is discussed in the frame-work of the Blume-Scherer model. The magnetic moment of the  $3^-$  5.83 MeV level of  $^{14}\text{N}$  is deduced.

Reported also by University of the Negev.

### MAGNETIC MOMENT OF THE FIRST EXCITED STATE OF $^{10}\text{B}$

R. Avida, I. Ben-Zvi, G. Goldring, S. S. Hanna, P. N. Tandon and Y. Wolfson

The magnetic moment of the  $1^+$  first excited state of  $^{10}\text{B}$  at 0.72 MeV has been determined by an integral perturbed angular correlation measurement in an external magnetic field. The value obtained for the  $g$ -factor,  $+0.63 \pm 0.12$ , is compared with calculations based on the effective-force treatment of  $^{10}\text{B}$ . A measurement of the perturbation produced in  $^{10}\text{B}$  nuclei implanted in iron showed that the internal field  $H_{\text{int}}$  at the boron nuclei was less than 4 kG.

### THE REORIENTATION EFFECT IN $^{110}\text{Cd}$ AND $^{114}\text{Cd}$

Z. Berant, R. A. Eisenstein, Y. Horowitz, U. Smilansky, P. N. Tandon, I. S. Greenberg, A. M. Kleinfeld and H. G. Magg

New detailed measurements of the reorientation effect in the first  $2^+$  state of  $^{110}\text{Cd}$  and  $^{114}\text{Cd}$  were carried out using back scattered  $^4\text{He}$  and  $^{16}\text{O}$  ions. They yield  $Q_2^+ = (-0.28 \pm 0.09)$  eb with  $B(E2; 0 \rightarrow 2) = (0.513 \pm 0.005)e^2b^2$ , or  $Q_2^+ = (-0.03 \pm 0.09)$  eb with  $B(E2; 0 \rightarrow 2) = (.512 \pm 0.005)e^2b^2$  for  $^{114}\text{Cd}$  depending on the sign of the interference term. The results for  $^{110}\text{Cd}$  are  $Q_2^+ = (-(0.42 \text{ or } 0.21) \pm 0.10)$  eb with  $B(E2; 0 \rightarrow 2) = (0.432 \pm 0.006)e^2b^2$ . The deduced  $Q_2^+$  for  $^{114}\text{Cd}$  is approximately half of the rotational model value.

Reported also by University of the Negev.

### THE ROLE OF THE $\alpha+t$ CHANNELS IN THE COULOMB EXCITATION OF THE $\frac{1}{2}^-$ STATE IN $^7\text{Li}$

U. Smilansky, B. Povh and K. Traxel

The role of the virtual excitation of the  $\alpha+t$  channel in exciting the  $\frac{1}{2}^-$  state in  $^7\text{Li}$  is discussed in terms of the known properties of the  $\alpha+t$  channel. It is shown that this effect is larger than the reorientation caused by the ground state quadrupole moment. Existing data on the Coulomb excitation of the  $\frac{1}{2}^-$  state are analysed in terms of both the virtual breakup and the reorientation effects. The resulting  $Q_{3/2}$  and  $B(E2; 3/2 \rightarrow 1/2)$  are consistent with values obtained in former measurements.

### ELASTIC SCATTERING OF $^{16}\text{O}$ AND $^{18}\text{O}$ BY EVEN Ca ISOTOPES, $^{52}\text{Cr}$ AND $^{62}\text{Ni}$ AT INCIDENT ENERGIES NEAR THE COULOMB BARRIER

Y. Eisen, R. A. Eisenstein, U. Smilansky and Z. Vager

Elastic scattering of  $^{16}\text{O}$  and  $^{18}\text{O}$  by even Ca isotopes,  $^{52}\text{Cr}$  and  $^{62}\text{Ni}$  was studied at incident energies near the Coulomb barrier. The excitation functions measured in this experiment show marked differences between  $^{16}\text{O}$  and  $^{18}\text{O}$ . The experimental data are analyzed and discussed by means of an incoming wave boundary condition method (IWB).

### SEARCH FOR A POSSIBLE $J^\pi = 0^+, T = 2$ RESONANCE

IN  ${}^9\text{Be}(\tau, \gamma\gamma){}^{12}\text{C}$

S. S. Hanna, M. Haas, Z. Shkedi and Y. Horowitz

A 50 cm<sup>3</sup> Ge(Li) detector has been used to reexamine the reaction  ${}^9\text{Be}(\tau, \gamma\gamma){}^{12}\text{C}$  over a previously reported resonance at  $E(\tau) = 1.739 \pm 0.007$  MeV which was suggested as the lowest  $T = 2$  state in  ${}^{12}\text{C}$ . This state is expected to  $\gamma$  decay via the  $1^+, T = 1$  state at 15.11 MeV. However a search with  $\tau$  bombarding energies ranging two standard deviations above and below the reported resonance energy revealed no resonance in high energy gamma rays. An upper limit of  $\Gamma_\tau \Gamma_\gamma / \Gamma < 2.0$  MeV is established for the  $T = 2$  resonance strength which is one-fourth of the previously reported strength and which strongly corroborates an additional negative result reported as  $\Gamma_\tau \Gamma_\gamma / \Gamma < 1.5$  MeV. In the course of the experiment a new value of  $\Gamma_{\text{lab}} = 2.94 \pm 0.20$  keV was obtained for the resonance at  $E_p = 1.083$  MeV in  ${}^9\text{Be}(p, \gamma){}^{10}\text{B}$ .

Reported also by University of the Negev.

### MEASUREMENT OF THE NUCLEAR RAMAN EFFECT

M. Haas and D. Salzmann

The parameters of the giant dipole resonance of  $\text{U}^{238}$  are calculated from the experimental cross-sections of the nuclear Raman effect. It is shown that there is no need to include direct mechanisms to explain the interaction of the  $\gamma$  with the nucleus.

### DEPENDENCE OF THE DOPPLER SHIFT LIFETIME METHOD ON SLOWING ENVIRONMENT

C. Broude, P. Engelstein, M. Popp and P. N. Tandon

To check for systematic analysis errors in the Doppler shift attenuation method for nuclear lifetimes, a mean life in  ${}^{22}\text{Ne}$  has been measured in 39 different solid elemental slowing materials. A range of lifetimes of 1.9 strongly correlated with atomic number is observed.

**A COMPARISON OF SPECTROSCOPIC FACTORS FROM  
 $^{95}\text{Mo}(d,t)^{94}\text{Mo}$  AND  $^{94}\text{Mo}(p,p'\gamma)^{94}\text{Mo}$  EXPERIMENTS**

E. Abramson, G. Engler, Z. Vager, N. Cue, I. Plesser and G. F. Wheeler

Spectroscopic factors from the  $^{95}\text{Mo}(d,t)^{94}\text{Mo}$  reaction have been compared with partial decay strengths obtained from the  $^{94}\text{Mo}(p,p'\gamma)^{94}\text{Mo}$  reaction proceeding through the  $5/2^+$  g.s. analogue resonance. The results of the comparison support the treatment of the compound enhancement applied in the analysis of the  $^{94}\text{Mo}(p,p'\gamma)^{94}\text{Mo}$  reaction.

**EMISSION OF THE  $^3\text{He}$  IN THE SPONTANEOUS FISSION OF  $^{252}\text{Cf}$**

E. Cheifetz, B. Eylon, Z. Fraenkel and A. Gavron

The emission of  $^3\text{He}$  ( $T_{1/2} = 8 \times 10^{-22}$  sec for decay into  $\alpha + n$ ) in spontaneous fission of  $^{252}\text{Cf}$  is established from a correlation measurement involving the direction and the kinetic energies of the neutrons and the long-range  $\alpha$  particles. Approximately 11% of these  $\alpha$ 's are products of  $^3\text{He}$  breakup. The initial energy of the fragments and of the  $^3\text{He}$  at scission are calculated from the properties of the  $^3\text{He}$  decay. They are  $31 \pm 11$  and  $3.2 \pm 0.9$  MeV, respectively.

**Theoretical Physics**

**THEORY OF EFFECTIVE INTERACTIONS**

M. W. Kirson

The paper concentrates on the many-body perturbation theory approach to the theory of effective interactions. The emphasis is on the relative importance of various effects rather than on agreement with experiment.

**FORCE DEPENDENCE OF  $0^+$  STATES IN  $^{208}\text{Bi}$**

J. Rajewski and M. W. Kirson

The  $0^+$  energy levels of  $^{208}\text{Bi}$  are calculated with the reaction matrix deduced from the Sussex and Tabakin potentials. Special attention is paid to the isobaric analogue of the ground state of  $^{208}\text{Pb}$  which comes 4-5 MeV below the experimental value, and is particularly sensitive to the potential.

### SHELL MODEL HAMILTONIANS WITH GENERALIZED SENIORITY EIGENSTATES

S. Shlomo and I. Talmi

The conditions on shell-model Hamiltonians which have eigenstates with generalized seniority  $\nu = 0$  and  $\nu = 2$  are stated and investigated in detail. For even semi-magic nuclei the conditions for  $\nu = 0$  eigenstates give rise to a simple binding energy formula with terms linear and quadratic in nucleon number. If also the  $\nu = 2$  conditions are satisfied, constant spacings, independent of nucleon number, are obtained between ground states and the low lying  $J = 2, 4, \dots$ , levels. This feature is clearly demonstrated by the existence of a single particle operator which transforms the  $\nu = 0$  state into one with  $\nu = 2$  and which obeys a *linear equation of motion* when acting on the  $\nu = 0$  state. The constant spacings are obtained in the general case for *one* state with a given  $J$ , unlike the situation in the quasi-spin scheme in which there are *n*-independent separations between *all* levels. Examples are given of cases in which these conditions are actually fulfilled and yet in which the eigenstates are not those of the quasi-spin formalism.

### COULOMB ENERGIES AND CHARGE ASYMMETRY OF NUCLEAR FORCES

S. Shlomo

Charge-symmetry-breaking potentials suggested in the literature to resolve the discrepancy between calculated Coulomb energy differences of analog states and the experimental values are considered in detail. We calculate the contributions of these potentials to the ground state energy differences of the mirror nuclei  $\text{He}^3\text{-H}^3$ ,  $\text{O}^{15}\text{-N}^{15}$ ,  $\text{F}^{17}\text{-O}^{17}$ ,  $\text{Ca}^{39}\text{-K}^{39}$  and  $\text{Sc}^{41}\text{-Ca}^{41}$ . It turns out, due to the short range character of these symmetry-breaking potentials, that their inclusion may resolve the  $\text{He}^3\text{-H}^3$  difficulty but not the  $\text{Sc}^{41}\text{-Ca}^{41}$  discrepancy.

### VERTEX PARAMETERS AND COUPLING CONSTANTS FOR THE VIRTUAL DECAY OF LIGHT NUCLEI

A. S. Rinat (Reiner), L. P. Kok and M. Stingl

Various sources of information on vertex functions are compared. Explicit wave functions, scattering and reaction data, and dispersion relations are used to extract range parameters and spectroscopic factors of parametrized vertex functions describing the virtual decay of nuclei with  $A \leq 6$ . Mutual agreement is found in general, with the exception of the  ${}^6\text{Li}\text{-}{}^4\text{He}\text{-d}$  vertex parameters.

## THE CASE FOR DI-NUCLEAR MOLECULES

A. S. Rinat (Reiner)

A survey is given of the evidence for di-nuclear molecules drawn from elastic and inelastic scattering as well as from rearrangement collisions between  $\alpha$ -particles clusters. Some tests for additional confirmation of the intermediate doorway resonance picture are suggested. Several semi-microscopic descriptions are compared and found to possibly coexist.

## SCATTERING FROM NON-OVERLAPPING POTENTIALS.

### I. GENERAL FORMULATION

D. Agassi and A. Gal

The problem of scattering from an assembly of non-overlapping spherical potentials is solved in partial-wave basis for each of the constituent potentials. The resulting scattering operator is a quotient of two infinite matrices and depends on "on-shell" partial wave amplitudes of the individual potentials. It suggests in general a truncation scheme which essentially considers only those partial waves effective for each collision at the given energy. The multiple-scattering series is recovered and limiting cases of low energy and high energy are considered. Applications to high energy scattering of elementary particles on nuclei are briefly discussed.

## STRIPPING TO ISOBARIC ANALOG RESONANCES

D. Agassi, N. Auerbach and A. Moalem

The form factor for the stripping distorted-wave Born-approximation amplitude to isobaric analog resonances is derived using a fine-structure theory of these resonances. It is found that the corrections due to compound-nucleus mixing are small. Using the derived form factor, the spectroscopic factors are calculated for the reaction  $\text{Mo}^{92}(\text{He}^3, d)\text{Te}^{93}$ .

## RESEARCH PROGRAMS

### Israel AEC Research Centres

#### RESONANCE SCATTERING MEASUREMENTS WITH Se AND Hg CAPTURE SOURCES

E. Arad, G. Ben-David and H. Szichman

New experiments on the resonance scattering of photons from Bi, Zr, Mn, Cu and Cd natural targets using a Se(n, $\gamma$ ) source are now in progress. Resonances at energies of 7418.7 and 500.9 keV were found in  $^{204}\text{Bi}$  and  $^{90}\text{Zr}$  with respective spin assignments of  $9/2^{(-)}$  and  $1^{(-)}$ . Further experiments on these nuclei are planned using a Compton polarimeter and a cryostat for temperature variation of the intensity of the scattered radiation.

In preliminary experiments, large resonances were found in the natural scatterers Hg, Zr, Mo and Ti using a Hg(n, $\gamma$ ) source.

#### STUDIES ON THE LEVEL SCHEMES OF $^{66}\text{Zn}$ , $^{144}\text{Sm}$ , $^{120}\text{Sn}$ AND $^{80}\text{Se}$ USING THE ( $\gamma$ $\gamma'$ ) REACTION

G. Ben-David, H. Szichman and B. Arad

The decay schemes of highly excited levels in  $^{66}\text{Zn}$ ,  $^{144}\text{Sm}$ ,  $^{120}\text{Sn}$  and  $^{80}\text{Se}$ , reached via the ( $\gamma$   $\gamma'$ ) reaction, were investigated using a nickel capture source, and the respective level schemes were deduced. Measurements of the angular distributions of the scattered radiation permitted determination of the spins of the low-lying levels in these nuclei. The reduced strength of the transitions shows that they are predominantly E1. The total radiation width of the 3995 keV resonant level in  $^{144}\text{Sm}$  was re-evaluated and found to be  $73 \pm 15$  neV.

#### STUDY OF THE ENERGY LEVELS OF $^{69}\text{Ga}$ USING NUCLEAR PHOTOEXCITATION \*

R. Moreh, O. Shahal, J. Tenenbaum, A. Wolf and A. Nof

Elastic and inelastic scattering of monochromatic photons were used for studying nuclear energy levels in  $^{69}\text{Ga}$ . The photons were produced by thermal neutron capture in copper and vanadium. The decay of one resonance at 7306 keV excited by the copper  $\gamma$ -source and another resonance at 6874 keV

excited by the vanadium  $\gamma$ -source were studied in detail and 30 low lying levels were observed from the ground state up to 3.4 MeV, 17 of which are believed to be new levels in  $^{69}\text{Ga}$ . The angular distribution of some elastic and inelastic lines were measured and the following spin determinations were made (keV,  $J^\pi$ ): 326,  $1/2^-$ , ( $3/2^-$ ); 574,  $5/2^-$ ; 872,  $3/2^-$ ; 1488,  $3/2^-$ , ( $7/2^-$ ); 1525 ( $1/2$ ,  $3/2$ ); 1891,  $3/2^-$ ; 1978, ( $1/2$ ,  $3/2$ ); 2457,  $3/2$ ; 2484,  $5/2$ ; (2565), ( $1/2$ ,  $3/2$ ); 2660,  $3/2$ ; 3051, ( $3/2$ ,  $7/2$ ); 3076,  $5/2$ ; 3318, ( $7/2$ ); 6874,  $1/2$ ; and 7306,  $5/2^+$ , where parentheses denote uncertainties. The parity of the 7306 keV level was directly determined using a Compton polarimeter. The total radiative width of the 7306 keV level was measured and found to be  $\Gamma = 0.105 \pm 0.020$  eV. For the 6874 keV level, a positive correlation coefficient was obtained,  $\rho = 0.69$ , between the ( $\gamma, \gamma'$ ) and (d,n) transition strengths leading to the same final states in  $^{69}\text{Ga}$ . The levels of  $^{69}\text{Ga}$  were compared with recent theoretical calculations.

#### STUDY OF THE ENERGY LEVELS OF $^{100}\text{Mo}$ USING PHOTON INELASTIC SCATTERING \*

R. Moreh, O. Shaha, J. Tenenbaum, A. Wolf and A. Nof

Elastic and inelastic scattering of monochromatic photons were used to study nuclear energy levels in  $^{100}\text{Mo}$ . The photons were produced by thermal neutron capture in titanium, copper and vanadium. The decay of the resonances at 7637, 6517, and 6418 keV were studied in detail. The angular distributions of some elastic and inelastic lines were measured and the following spin determinations were made: (keV,  $J^\pi$ ): 535,  $2^+$ ; 695,  $0^+$ ; 1063,  $2^+$ ; 1461,  $2^+$ ; 2033,  $0^+$ ; 2040,  $2^+$ ; 5186,  $1^-$ ; 6418,  $1^-$ ; 6517,  $1^-$ ; and 7637,  $1^-$ . The parities of the last three levels were directly determined using a Compton polarimeter. Total radiative widths were measured and the following results were obtained:  $\Gamma(6418) = 50 \pm 35$  meV,  $\Gamma(6517) = 110 \pm 30$  meV and  $\Gamma(7637) = 98 \pm 15$  meV. The M2/E1 mixing ratios for two primary transitions were found to be about 3 orders of magnitude higher than that predicted by the simple theory.

#### LARGE E1 AND M1 RADIATIVE WIDTHS IN NUCLEI NEAR CLOSED SHELLS \*

A. Wolf, R. Moreh, A. Nof, O. Shaha and J. Tenenbaum

The radiative widths, spins and parities of ten levels photoexcited by the ( $\gamma, \gamma'$ ) reaction at excitation around 7 MeV in  $^{139}\text{La}$ ,  $^{140}\text{Ce}$ ,  $^{141}\text{Pr}$ ,  $^{142}\text{Nd}$ ,  $^{144}\text{Nd}$ ,  $^{205}\text{Tl}$  and  $^{209}\text{Bi}$ , were measured. The  $\gamma$  beam was produced by thermal neutron capture in titanium, iron, cobalt and copper. The spins of the resonance levels were obtained by angular distribution measurements and the parities were determined by using a Compton polarimeter. These levels together with other resonance levels in  $N \sim 82$  and  $N \sim 126$  were considered with regard to a possible connection to a giant M1 resonance.

\* Reported also by University of the Negev.

EXCITATION FUNCTIONS AND PHOTON EMISSION IN COMPOUND NUCLEUS REACTIONS WITH HIGH ANGULAR MOMENTUM

J. Gilat, E.R. Jones, III and J.M. Alexander

Measured excitation functions were compared with detailed evaporation calculations for the reaction  $^{140}\text{Ce}(^{16}\text{O},xn)^{156-x}\text{Dy}$ ,  $^{144}\text{Nd}(^{12}\text{C},xn)^{156-x}\text{Dy}$ ,  $^{136}\text{Ba}(^{20}\text{Ne},xn)^{156-x}\text{Dy}$  ( $x = 5,6,7$ ),  $^{154}\text{Gd}(^4\text{He},xn)^{158-x}\text{Dy}$  ( $x = 7,8,9$ ) and  $^{181}\text{Ta}(^4\text{He},xn)^{185-x}\text{Re}$  ( $x = 2,3,4$ ). The agreement between theory and experiment was found to depend critically on the rate of photon emission within about 10 MeV of the Yrast levels. For the first 4 systems above, good fits were obtained only when the gamma-emission rate is strongly enhanced with respect to the rate indicated by the gamma width of neutron resonances. A gamma emission rate proportional to  $(2J+1)$  or a constant (independent of  $J$ ) enhancement factor of about 100 led to reasonably good fits with experiment. For the system  $^{181}\text{Ta} + ^4\text{He}$  such pronounced enhancement does not seem to be required. These results were interpreted in terms of the structure of the gamma cascade band. At sufficiently high angular momenta, the gamma cascade band is predicted to give way to an alpha band. Possibilities for experimental verification of some of the theoretical predictions were considered.

AN  $\alpha$  PARTICLE MONITOR FOR THE NEUTRON GENERATOR

M. Etzion, H.M. Loebenstein and Y. Gazit

A monitor was built for our Texas Nuclear neutron generator. In fast neutron activation measurements the knowledge of the integrated neutron flux on the sample is crucial. Measurement of the deuteron current on the target is not sufficient for monitoring the neutron production rate because the target tends to deteriorate with the continuation of the bombardment and also because the beam composition of  $\text{D}^+$  and  $\text{D}_2^+$  particles may vary. Fast neutron detectors are bulky, sensitive to scattered low energy neutrons and often need recalibration because of drift problems. Neutron production by the  $d(t,n)\alpha$  reaction can also be monitored by counting the  $\alpha$ -particles produced. Because of the high Q-value of the reaction and the almost complete absence of competitive reactions, the  $\alpha$ -particles can be counted easily.

A monitor consisting of two silicon surface barrier detectors set at  $175^\circ$  to the beam was built. The monitor is easily mounted on the existing beam tube and because of the backward geometry of the counters does not interfere with experiments.

A SIMPLE BEAM CHARGE MONITOR FOR NEUTRON GENERATORS

H.M. Loebenstein and Y. Gazit

The  $\text{D}^+$  beam in neutron generators is accompanied by a  $\text{D}_2^+$  beam. The current ratio of the two beams is not fixed and therefore can be troublesome in some experiments. A solid state counter set at a backward angle, monitoring the  $\alpha$ -particles for the  $d(t,n)\alpha$  reaction, can differentiate between the contributions of the two beams and thus monitor the beam charge composition.

## UNFOLDING OF NEUTRON SPECTRA

U. Feldman and R. Divon

A procedure being developed for unfolding fast neutron spectra requires as an input the detector response function to monoenergetic neutrons. The functions used are based on Monte Carlo computations.

A computer code for smoothing and correcting the computed responses of organic scintillation detectors to monoenergetic neutrons was written. The code uses the interactive graphics of a CDC computer to smooth the computed response in cases of insufficient statistics, and corrects the response for broadening caused by statistical photon emission.

The response of a NE102A plastic scintillator to 14.8 MeV neutrons was measured, and was found to be in good agreement with the computations, which took into account the contribution of  $\gamma$ 's from neutron inelastic scattering from carbon nuclei in the detector.

## APPLICATION OF A He-JET FOR THE RAPID TRANSFER OF FISSION PRODUCTS

H. Feldstein and S. Amiel

Rapid transfer at minimum loss of fission products from a target irradiated in a high neutron flux to the ion source of a mass separator, is vital for the study of short-lived nuclei with low fission yield. Considerable amounts of carrier gas, in excess of the pumping capacity of the mass separator, are required to stop fission fragment recoils and for rapid transfer. Selective removal of the carrier gas with minimal loss of the fission products is, therefore, required for efficient operation of the system.

The helium-jet technique, applied successfully in the case of  $^{252}\text{Cf}$  fission products and cyclotron-produced heavy ions has been studied. A  $^{252}\text{Cf}$  fission source with an intensity of  $2.4 \times 10^5$  fissions/sec was used. The source, coated with  $100 \mu\text{g}/\text{cm}^2$  gold and covered with  $1.4 \text{ mg}/\text{cm}^2$  Al-Mylar foil, was mounted on a 400 cc chamber in which the fission products were stopped by water vapor saturated helium. The chamber was irradiated with uv light from a 2 kW carbon arc and evacuated at a maximum rate of 5 cc STP/sec through a 0.5 mm diameter, 5 m long capillary tube,

At the evacuated end of the capillary tube, where a pressure of  $\sim 0.5$  torr was maintained, a well-defined jet of heavy particles with an angle of dispersion of  $\sim 4^\circ$  was obtained. Autoradiography showed that the diameter of the radioactive spot was  $\sim 1$  mm at the end of the capillary tube and  $\sim 3$  mm at a distance of 34 mm. No elemental fractionation (within the accuracy of the experiment) was disclosed when the X-ray spectrum of the heavy-ion jet, stopped in a thin graphite filter, was compared with the spectrum obtained by placing the same filter directly in front of the  $^{252}\text{Cf}$  source

The overall transfer efficiencies of the jet as compared with direct recoil collection was found to be 30-50% and the minimum transfer time about 12 sec.

## A. HIGH INTENSITY EMANATION SOURCE

### II. Bcazi

The preparation of a novel, highly efficient, emanation source of fission-product krypton and xenon has been reported. The emanating power of this source was further investigated for long-lived fission product noble gases. The gamma spectrum of a sealed ampoule containing the irradiated emanation source and the spectrum of the same ampoule after it was opened and its contents ventilated were measured.  $^{99m}\text{Tc}$ ,  $^{139}\text{Ba}$  and  $^{132}\text{Te}$ , which are present in the irradiated source and are not volatile, served as internal standards.

## NEUTRON RADIOGRAPHY

Neutron radiography has in recent years become a very important method of nondestructive testing in industry and research. This application requires a change in the physics and construction of part of the reactor. We have fitted one of the IRR-I reactor beam tubes for neutron radiography by adapting the following newly developed methods for appropriately adjusting the neutron beam.

### 1. A METHOD FOR OBTAINING A HOMOGENEOUS FLUX IN A REACTOR BEAM TUBE (D. Kedem, M. Mahlav and I. Pelah)

To overcome the small diameter of the beam tube in our reactor, a homogeneous high neutron flux over a large area was required. Such a neutron beam was obtained using a plain tube collimator and a shaped absorber, especially designed and built for this purpose. Aluminum was chosen for the absorber material because its low absorption and scattering cross sections permit rounding off of small changes in the flux at adjacent points with gross variations in the thickness of the absorber. Other advantages of aluminum are ease with which it can be cut to shape, ability to withstand high radiation fields and resulting high temperatures, and short half-life.

### 2. A METHOD FOR OBTAINING A LARGE-AREA BEAM FROM A REACTOR BEAM TUBE (D. Kedem)

The resolution of neutron radiographs is an important parameter and is determined by several factors: (a) beam divergence; (b) converter thickness; (c) distance between the object and the converter; (d) distance between the converter and the film; (e) grain size of the film. Gadolinium deposited on aluminum foil is the most frequently used converter. Enrichment with  $^{157}\text{Gd}$  allows a thinner coating and influences the resolution. The beam divergence is measured by the parameter  $D/L$  (inverse of the collimation ratio  $L/D$ ) and about  $10^9 \text{ n/cm}^2$  are needed for a radiograph.

We redesigned the set-up so that the entrance slit for thermal neutrons was not placed close to the core, but set at 80 cm from the object to provide a larger radiograph area, while keeping the resolution constant. The collimation system was improved and is described in detail in Ref. 2.

AN APPROXIMATE ANALYTIC REPRESENTATION OF THE NEUTRON ENERGY SPECTRUM IN THE RANGE OF UNRESOLVED RESONANCES

M. Segev

The neutron energy spectrum in fast reactors in the range of unresolved resonances has been described. The description is analytic, approximate in nature and based on the statistical properties of the resonance population.

The neutron collision density is given by:

$$F(u) = \frac{1}{X(u)} \exp [-v(u)u]$$

$\chi(u)$  and  $v(u)$  are parameters which change slowly with lethargy  $u$ .  $\chi(u)$  is directly related to the statistical averages of the scattering probability (scattering, element/total, mixture).  $v(u)$  is related to these averages via a transcendental equation. A series solution of the transcendental equation was developed and proved effective.

AN IMPROVED CALCULATION OF THE ELASTIC SCATTERING MATRIX

Y. Gur, M. Segev and S. Yiftah

The YOM and ABN methods of treating the elastic scattering in a multigroup cross section set by an "elastic removal" cross section from a group to its immediate neighbor was modified to include a full elastic scattering matrix.

An algorithm which determines the integration limits,  $E_{hi}$ ,  $E_{li}$ ,  $E_{hk}$ ,  $E_{lk}$  from the scattering kinematics and the group structure was built into the code NANICK (1).

Preliminary results of elastic out-of-group scattering for carbon and oxygen were obtained and compared with results obtained by the previous ABN method (Table 1). The weighting flux used presently is the SNEAK flux and the source for this run is ENDF/B-1.

As could be expected the improved method does modify the elastic scattering matrix (note, especially, group 6 of oxygen). The significance of the modification will be considered after representative nuclear systems are calculated by the two methods and compared.

TABLE I  
Elastic out-of-group cross sections for carbon and oxygen

Scattering to the next group, of Group No.	CARBON		OXYGEN	
	ABN	PRESENT	ABN	PRESENT
1	0.4497	0.3670	0.4589 <sup>a</sup>	0.3783 <sup>a</sup>
2	0.5679	0.7135	0.3960	0.5091
3	0.9277	0.7156	0.5480	0.3494
4	0.5297	0.5791	0.4691	0.3602
5	0.8940	0.9598	1.1120	0.9106
6	0.7980	0.8896	0.8254	1.9710
7	0.9056	0.9773	0.7407	0.5952
8	0.8806	0.9513	0.5551	0.5604
9	0.8625	0.9074	0.5166	0.5237
10	0.7961	0.8469	0.4647	0.4828
11	0.8208	0.8465	0.4732	0.4831
12	0.8488	0.8955	0.4855	0.5072
13	0.7673	0.8218	0.4375	0.4631
14	0.8035	0.8569	0.4582	0.4842
15	0.7600	0.8205	0.4343	0.4631
16	0.7610	0.8110	0.4363	0.4607
17	0.6880	0.7606	0.3953	0.4290
18	0.6740	0.7478	0.3885	0.4227
19	0.6500	0.7262	0.3760	0.4110
20	0.6600	0.7355	0.3830	0.4178
21	1.0130	0.8363	0.5887	0.4963
22	0.7650	0.8271	0.4462	0.4765
23	0.6937	0.7695	0.4057	0.4419
24	0.5540	0.6520	0.3246	0.3685

<sup>a</sup>This includes contribution of inelastic scattering.

NUCLEAR DATA EVALUATION FOR PLUTONIUM-240 PLUTONIUM-241 AND PLUTONIUM-242

H. Caner and S. Yiftah

The following <sup>240</sup>Pu, <sup>241</sup>Pu and <sup>242</sup>Pu neutron cross sections were evaluated in the range 10<sup>-3</sup> eV to 15×10<sup>6</sup> eV: total, elastic, radiative capture, fission, total inelastic, partial inelastic, (n,3n), and differential elastic. Also the number of neutrons per neutron-induced fission and the average elastic scattering cosine in the lab system were evaluated.

The following derived quantities were also tabulated: nonelastic, absorption and transport cross sections, alpha and eta.

The experimental data were supplemented by optical model and statistical theory code calculations and by systematics.

The present work constitutes an updating of a previous evaluation<sup>(1)</sup>.

PRELIMINARY COMPARATIVE ANALYSIS OF AMERICAN AND GERMAN NUCLEAR DATA FILES FOR THE CALCULATION OF FAST FISSION REACTORS

S. Yiftah, Y. Gur, H. Segev and L. Gitter

The American ENDF/B III, the German Kodak, the British UKNDL and the Russian evaluated nuclear data files serve today as the main sources of nuclear data for the calculation of fission reactors. Specifically, the files serve as the major sources of nuclear input for the calculations for the various large fast reactor programs. Every country, naturally, uses its evaluated file and the questions arise as to whether the parameters calculated are a function of the specific evaluated data file that is used, and would these parameters remain the same were the calculations based on input of a different data file. Therefore a comparative analysis of the evaluated files was performed on the following levels: the basic microscopic data level, the multigroup cross section set level and the physical parameters of specific systems level.

Typical 1000-1200 MWe fast reactor systems with a core of about 4000 liters, modelling the fast reactors being designed today, were calculated<sup>(1)</sup> using the evaluated nuclear data files ENDF/B III and KODAK as nuclear input. Significant differences in  $k_{eff}$  and the Na void coefficient were found. Identical techniques were used to obtain multigroup sets from the files. Also the reactor physics codes used were the same.

The differences in results, therefore, were attributed directly to the nuclear data input.

COMPARISON OF ENDF/B-III DATA WITH RECENT OBNINSK ABSOLUTE MEASUREMENTS FOR ALPHA OF PU-239 AND U-235

S. Yiftah and Y. Gur

An IAEA translation of a Russian Obninsk report by Kononov et al. on absolute measurements of  $\alpha$  for U-235 and Pu-239 in the 10 keV - 1 MeV neutron energy range as well as a copy of the third evaluated American file ENDF-B/III were recently received. The crucial importance of  $\alpha$ , (the ratio of capture-to-fission cross sections) mainly plutonium- $\alpha$ , for fast breeders, combined with the memory of many past discrepancies, led us to compare the  $\alpha$ 's from the recent Obninsk measurements with those deduced from the recent ENDF-B/III file.

While the Russian  $\alpha$ 's were taken directly from the report, two codes had to be prepared to extract the data from ENDF-B/III. The first code, for the tabulated presentation above 25 keV, finds, for fission and capture, the two energy points just above and just below the desired energy point, interpolates between them using the mode of interpolation as given in the file to obtain the cross sections at the desired energy point and divides capture to fission to obtain alpha. The second code, for the energy range in which unresolved resonance parameters are given, sums up the contributions of all (l,j) series at the desired energy points both for capture and fission and then takes the ratio to obtain alpha.

A careful look at the comparative results reveals the following:  
U-235: In the unresolved resonances energy range below 25 keV, there is a marked resonance-like structure or large fluctuations in the value of  $\alpha$  in the Russian measurements, while it remains almost constant in ENDF-B/III.

In the range 25 keV to 60 keV the agreement is poor. The Russian data are consistently lower than the ENDF-B/III data.

In the range 60 keV to 1.1 MeV the agreement is quite good.

Pu-239: In the unresolved resonances energy range below 25 keV there is again a marked resonance-like structure or large fluctuations in the Russian data, while the American data shows a smooth decrease with increasing energy. The fluctuations in the Russian data continue up to about 40 keV. From 40 to 450 keV the agreement is good, the Russian  $\alpha$  being consistently lower. From 450 keV to 1 MeV there is poor agreement, the Russian data being higher by a factor of about 2.

#### COMPARISON OF FOUR AVAILABLE CODES FOR THE CALCULATION OF THE DOPPLER-BROADENED LINE SHAPE FUNCTIONS OF BREIT-WIGNER RESONANCES

Y. Gur

Within the Breit-Wigner formalism, the contribution of single resonance to the capture, fission and elastic cross sections is given by:

$$\sigma_c(E) = \sigma_0 \frac{\Gamma_c}{\Gamma} \sqrt{\frac{E}{E_0}} \psi(x, E)$$

$$\sigma_f(E) = \sigma_0 \frac{\Gamma_f}{\Gamma} \sqrt{\frac{E}{E_0}} \chi(x, E)$$

$$\sigma_n(E) = \sigma_0 \frac{\Gamma_{no}}{\Gamma} \psi(x, E) + \sqrt{\sigma_0 \sigma_p} \frac{\Gamma_n}{\Gamma} \chi(x, E) + \sigma_p$$

where  $\psi$  and  $\chi$  are the line-shape functions and the rest of the symbols denote resonance parameters. Four existing routines for the numerical calculation of  $\psi$  and  $\chi$  were compared on the IBM 370/165:

PSIXI	(X, T, U, V)	(by Karlsruhe)
PSICHI	(X, XR, PSI, CHI)	(by Karlsruhe)
WANL	(REZ, AIMZ, REW, AIMW)	(by Argonne)
W	(REZ, AIMZ, REW, AIMW)	(in the MC <sup>2</sup> code)

The WANL routine was found to be the most efficient, namely the most economic in computer time, and is now incorporated in the NANICK code system which generates group cross sections from ENDF/B-III tapes.

NANICK - A FULLY AUTOMATIC CODE FOR THE GENERATION OF INFINITE DILUTION  
MULTIGROUP CROSS SECTIONS FROM ENDF/B-II AND ENDF/B-III NUCLEAR DATA TAPES

Y. Gur

This code is an extension of the older NANICK code. It uses essentially the same algorithms, but accomodates itself to ENDF/B-II and ENDF/B-III nuclear data tapes.

Major differences between these codes are in the sections on resonance treatment and inelastic scattering which had to be rewritten in order to take care of ENDF/B-III tapes, and some changes in the treatment of tabulated cross section files.

This code was recently used to prepare 26-group cross section sets for application in transport and diffusion calculations.

NASIF - A FULLY AUTOMATIC CODE FOR CALCULATING THE GENERATION OF TEMPERATURE  
DEPENDENT MULTIGROUP SHIELDING FACTORS USING ENDF/B-III DATA LIBRARY TAPES

Y. Gur

The shielding factor  $f(\sigma_0, T)$  is the ratio of the temperature-dependent flux, averaged at temperature  $T$  and background cross section  $\sigma_0$ , to the same cross section at  $T \rightarrow 0^\circ\text{K}$  and  $\sigma_0 \rightarrow \infty$  (the infinite-dilution cross section). For a given element in a given energy group,  $f(\sigma_0, T)$  is the ratio of the cross section at temperature  $T$  of the medium and background cross section  $\sigma_0$  for the element considered. The effect of temperature and background cross section on the shielding factor is the result of resonant cross sections.

Special routines for an efficient evaluation of shielding factors were written, taking advantage of the fact that the resonance lineshape functions are not dependent on reaction type or on  $\sigma_0$ . As a result a very efficient code for the shielding factors calculations both in the resolved and in the unresolved resonance region is now available.

NASIF is now being converted to handle Kodak tapes.

FAST REACTOR KINETICS

A.D. Kruinbein

The Hansen exponential transformation method for solving the space-time dependent diffusion equation was combined with certain advantageous features of the SHOVAV<sup>(2)</sup> program\*. The resulting code, called HASHOV, is capable of calculating cross section mixing and shielding factors, as in SHOVAV, and in addition retains the temperature feedback and reactivity insertion formulations of SHOVAV. HASHOV, however, makes use of the matrix factorization method of Hansen's GARD<sup>(3)</sup> code. It also assumes that the neutron and precursor densities behave exponentially over the time interval used. This latter premise justifies the use of the exponential transformation

As soon as the HASHOV program has been entirely "debugged" we will endeavor to determine how the speed and accuracy of the method compares with SHOVAV as well as to experiment with different transformation techniques<sup>(4)</sup>. Thereafter, the program and the calculations will be extended to 2 dimensions.

## A FAST REACTOR DYNAMIC ANALYSIS CODE SET

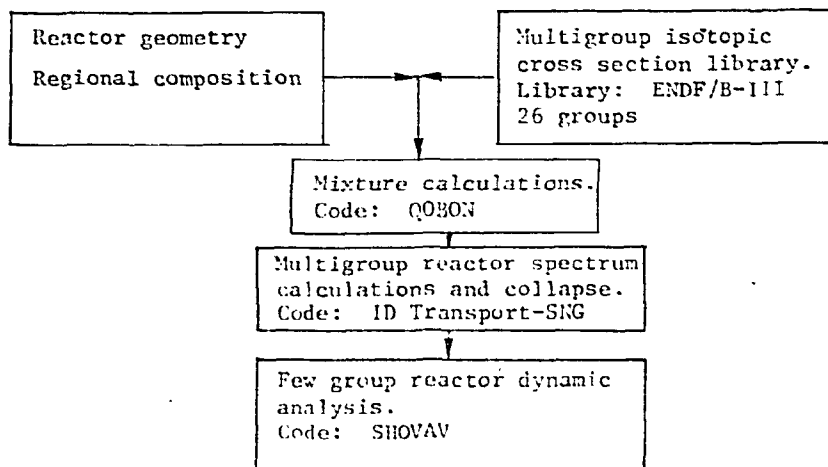
D. Ilberg, D. Saphier and S. Yiftah

The few group space-time-dependent solution of the diffusion equation for a fast reactor requires several steps:

- a) preparation of a multigroup cross section set from a standard cross section file;
- b) preparation of multigroup mixture cross sections;
- c) static calculations to obtain the reactor spectra and to collapse the multigroup set to a few group cross section set;
- d) few group reactor dynamic analysis.

Step (a) need be performed only once for several reactor calculations. However, steps (b) and (c) must be repeated for every change in the reactor data or geometry.

To facilitate parametric study of fast reactors the following computing scheme was built by using existing codes and preparing convenient interfaces. The flowchart shows the codes used and their interconnection.



By using the above scheme, which was implemented on the IBM 370/165 computer, it is now possible to use ENDF/B-III data for the dynamic analysis of fast reactor systems.

SOURCE PROJECTION METHODS TO ACCELERATE REACTOR DYNAMIC CALCULATIONS

D. Saphier

The implicit relaxation method used in solving the multigroup space-time dependent diffusion equation, while being unconditionally stable, requires very long computer times. The source iteration method followed requires many iterations until convergence is obtained for a single time step. A new method was developed whereby it is possible to "predict correctly" the magnitude of the fission source at time  $t^{j+1} = t^1 + \Delta t$  by a simple, inexpensive method. As a result a single iteration in the majority of time steps is sufficient to obtain convergence and much bigger time steps may be chosen.

The new source at  $t^{j+1}$  is predicted by projecting the existing fission sources at times  $t^j, t^{j-1}, t^{j-2}$ , etc. Three projection algorithms were tested, namely, linear projection, exponential projection and parabolic projection. The exact formulas are given in Ref. 1, and the results are shown in Table 2.

TABLE 2

Comparison of computer times required for various methods of source projection for solving the multigroup space-time-dependent diffusion equation

Test Case	Method of Solution	Physical Time	Total Power (%)	Time Steps Required	$\epsilon$	Machine Time (sec)
I. Bare Homogeneous Slab Reactor	Relaxation	2 msec	265.2	2000	$10^{-6}$	180
	Exponential	2 msec	265.3	513	$10^{-6}$	33
	Linear	2 msec	265.3	469	$10^{-6}$	28
	Parabolic	2 msec	265.2	139	$10^{-6}$	10
II. Four Regions, Fast, Plutonium-Oxide-Fueled Reactor	Relaxation	20 sec	301.1	13.778	$5.10^{-5}$	1460
	Exponential	20 sec	307.4	426	$5.10^{-5}$	25
	Linear	20 sec	302.5	417	$5.10^{-5}$	24
	Relaxation	20 sec			$10^{-6}$	$10^4$
	Exponential	20 sec	305.2	757	$10^{-6}$	44.5
	Linear	20 sec	304.1	675	$10^{-6}$	39.2

<sup>a</sup> estimated value

RESEARCH PROGRAMS

Tel Aviv University

EXPERIMENTAL NUCLEAR PHYSICS

A.I. Yavin, J. Alster, D. Asheri, M.A. Moinester, S. Cohavi

Students: A. Moalem, G. Finkel, Y. Shamaï, M. Zaider, N. Haik

The experimental nuclear physics group is currently engaged in the following research projects:

- 1) The measurement of the charge exchange reaction of pions on nuclei. A first result has been obtained at one energy and the project is now being extended at different energies in order to clarify the large differences in theoretical predictions of this reaction process as a function of energy.
- 2) Good results have been obtained from the measurement of stripping to unbound isobaric analog states. This work is now being extended to more nuclei in order to test spectroscopic predictions in some selected nuclei.
- 3) Detailed spectroscopic information has been obtained in a series of neighbouring nuclei by direct one- and two- nucleon transfer reactions. This work continues for a larger sample of nuclei where the spectroscopy is less known.
- 4) Shortly the first experiment will be performed on elastic- and inelastic electron scattering from deformed nuclei. These measurements yield detailed information on the shape of the charge distributions.

All these experiments are being performed at the Centre d'Etudes Nucleaires, at Saclay, France

DETECTION OF PION SINGLE CHARGE EXCHANGE IN ZIRCONIUM

J. Alster, D. Ashery, A.I. Yavin, J. Duclos, J. Miller and M.A. Moinester

The reaction  ${}^{91}\text{Zr}(\pi^+, \pi^0){}^{91}\text{Nb}^*$  was observed by detecting the decay proton from the isobaric analog state  ${}^{91}\text{Nb}^*$  in the sequential process  ${}^{91}\text{Zr}(\pi^+, \pi^0 p){}^{90}\text{Zr}$ . The observed cross section for an incident pion energy of 30 MeV is  $1.1 \pm 0.8$  mb, and is in reasonable agreement with theoretical calculations.

### $(^3\text{He},d)$ STRIPPING TO UNBOUND ANALOG STATES IN Tc ISOTOPES

D. Ashery, S. Alper, A. Moalem

Y. Shamaï, A.I.Yavin, G. Bruge, A. Chameaux and M.A. Moinester

A systematic study of 14 unbound isobaric analog states in Tc isotopes was performed using the  $(^3\text{He},d)$  reaction. It is shown that if a proton form factor based on a simple single particle resonance model is used, the DWBA deduced spectroscopic factors agree very well with existing  $(d,p)$  data for the parent states.

### AN EXPERIMENTAL STUDY OF THE $^{92}\text{Mo}(\tau,dp)^{92}\text{Mo}$ REACTION

D. Ashery, S. Alper, A.I.Yavin,

J.P. Longequeue, D. Kong-A-Siou and A. Giorni

Levels in  $^{93}\text{Tc}$  up to a few MeV above the proton-decay threshold were investigated via the  $^{92}\text{Mo}(\tau,d)^{93}\text{Tc}$  reaction. The subsequent proton decay of six analogs of low-lying states in  $^{93}\text{Mo}$  were also investigated

via the  $^{92}\text{Mo}(\tau,dp)^{92}\text{Mo}$  reaction. On the basis of  $(\tau,d)$ ,  $(\tau,dp)$ ,  $(p,p)$  and  $(p,p')$  reactions it is concluded that the analogs of the first  $5/2^+$ ,  $1/2^+$ ,  $7/2^+$  and  $3/2^+$  states decay mainly to the ground state of  $^{92}\text{Mo}$ , while the second  $7/2^+$  and  $3/2^+$  states decay mainly to the  $2^+$  first excited state of  $^{92}\text{Mo}$ .

### THEORETICAL NUCLEAR PHYSICS

The main areas of interest are:

- isobaric analog states, the theory of the shell model, Coulomb energies, Hartree-Fock theory, nuclear fission, generalized approximative procedures in the many body problem.

In addition, close contacts are maintained with the experimental nuclear physics group, with interest focussing on the interaction of pions with complex nuclei.

## ISOVECTOR MONOPOLE STRENGTH IN NUCLEI

N. Auerbach

In the present work we deal with the isovector monopole strength in nuclei. In the first part we calculate the energy positions and eigenfunctions of the isovector monopole state in several  $N = Z$  nuclei. We discuss some of the properties of the resulting wave functions. In the second part of the work we treat the isovector monopole strength with an excess of neutrons. Expressions for transition probabilities to states with definite isospin  $T + 1$ ,  $T$  and  $T - 1$  are derived and estimates of these transitions are given. The importance of the isovector monopole strength in various Coulomb mixing effects is discussed. Using the estimates of the transition matrix elements we calculate some of the effects. These include: isospin mixing in ground states, Coulomb energy shifts and widths of isobaric analog resonances.

### THE THEORY OF ISOBARIC ANALOG RESONANCES

N. Auerbach, J. Hufner, A.K. Kerman and C.M. Shakin

A theory of analog resonances is reviewed which makes use of projection operators. The Hilbert space is divided into three parts: a continuum or open channel space, an analog state space and a **compound space**. The phenomena are discussed in terms of the dynamical coupling of these spaces. The parameterization of the  $T$  matrix is discussed in detail, and equations are presented for various cross sections. The commutator  $[H, T_-]$ , where  $T_-$  is the isospin lowering operator plays an important role in the theory, and the various terms which contribute to this commutator are discussed. The energy splitting of the isospin multiplet, i.e. the Coulomb displacement energy, is discussed in detail. The importance of the analog resonance phenomena for the extraction of spectroscopic information is stressed, and it is shown how such information may be obtained. Various processes which contribute to the escape amplitude of the analog state are classified, and some numerical estimates are given. For several regions of the Periodic Table, graphs are presented for the various theoretical escape amplitudes, continuum energy shifts, **asymmetry** phases, and optical phase shifts, etc. Spectroscopic factors are calculated and compared with those obtained in other experiments.

## DEFORMATION IN THE UPPER s-d SHELL

I. Kelson

A simple approximation procedure for perturbing the self-consistent Hartree-Fock equations in an enlarged single-particle space is given. Using phenomenological interactions and observed single particle splittings, the second half of the s-d shell is shown to require pear-shaped intrinsic states, involving excitations from the s-d to the p-f shell.

## LOWERING OF CALCULATED FISSION BARRIERS OF SUPERHEAVY NUCLEI

I. Kelson and Y. Shoshani

The effect of angular momentum explicit conservation is evaluated in the framework of models which utilize single-particle wavefunctions to calculate fission barriers. Using simple assumptions, and extrapolating from known data, the calculated superheavy barriers are lowered by 2-2.5 MeV. Fission barriers for the actinides are unaffected.

## RESEARCH PROGRAMS

### University of the Negev

#### EXPERIMENTAL ACCELERATOR NUCLEAR PHYSICS

##### Optical Model Analysis of the Elastic Scattering of 100 MeV Protons from $^{24}\text{Mg}$ and $^{28}\text{Si}$

Y.S. Horowitz

Elastic scattering differential cross sections for the interaction of 100 MeV protons with  $^{24}\text{Mg}$  and  $^{28}\text{Si}$  have been measured using a high resolution Ge(li) spectrometer to resolve the inelastic scattering contribution from the elastic peak. The results have been analyzed using the conventional optical model, and the experimental differential cross sections and total reaction cross section are excellently reproduced. The results agree with previous analyses of the elastic scattering of 100 MeV protons on lp shell nuclei in that no set of geometric parameters can provide a quantitative fit to both nuclei. It is observed, however, that the fluctuations of the optical model parameters for optimum fits is decreased over the fluctuations observed for the lp shell nuclei. The present results combined with previous optical model analyses on  $^{24}\text{Mg}$  and  $^{28}\text{Si}$  at 50 MeV and 40 MeV respectively are found to be consistent with an energy dependence of  $dV/dE = -0.3$  for the depth of the real central potential in agreement with other, more extensive, investigations of the energy dependence for protons elastically scattered from  $^{16}\text{O}$  and  $^{40}\text{Ca}$ .

##### The Reorientation Effect in $^{110}\text{Cd}$ and $^{114}\text{Cd}$

Z. Berant, R.A. Eisenstein, Y.S. Horowitz, U. Smilansky,  
P.N. Tandon, J.S. Greenberg, A.M. Kleinfeld and H.G. Maggi

New detailed measurements of the reorientation effect in the first  $2_+$  state of  $^{110}\text{Cd}$  and  $^{114}\text{Cd}$  were carried out using back scattered  $^4\text{He}$  and  $^{16}\text{O}$  ions.  $Q_{2_+} = (-0.28 \pm 0.09)eb$  with  $B(E2, 0-2) = (0.513 \pm 0.005)e^2b^2$ , or  $Q_{2_+} = (-0.03 \pm 0.09)eb$  with  $B(E2, 0-2) = (0.512 \pm 0.005)e^2b^2$  for  $^{114}\text{Cd}$  depending on the sign of the interference term. The results for  $^{110}\text{Cd}$  are  $Q_{2_+} = \{-(0.42 \text{ or } 0.21) \pm 0.10\}eb$  with  $B(E2, 0-2) = (0.432 \pm 0.006)e^2b^2$ . The deduced  $Q_{2_+}$  for  $^{114}\text{Cd}$  is approximately half of the rotational model value.

Reported also by Weizmann Institute.

Search for a Possible  $J^\pi = 0^+, T = 2$  Resonance in  ${}^9\text{Be}(\tau, \gamma){}^{12}\text{C}$

S.S. Hanna , M. Hass , Y.S. Horowitz and Z. Shkedi

A 50 cm<sup>3</sup> Ge(li) detector has been used to reexamine the reaction  ${}^9\text{Be}(\tau, \gamma){}^{12}\text{C}$  over a previously reported resonance at  $E(\tau) = 1.739 \pm 0.007$  Me which was suggested as the lowest  $T=2$  state in  ${}^{12}\text{C}$ . This state is expected to gamma decay via the  $1^+, T = 1$  state at 15.11 MeV. However, a search with bombarding energies ranging two standard deviations above and below the reported resonance energy revealed no resonance in high energy gamma rays. An upper limit of  $\Gamma_{\tau\gamma}^{\text{ex}}/\Gamma < 2.0$  meV is established for the  $T=2$  resonance strength which is one fourth of the previously reported strength and which strongly corroborates an additional negative result reported as  $\Gamma_{\tau\gamma}^{\text{ex}}/\Gamma < 1.5$  meV. In the course of the experiment, a new value of  $\Gamma_{\text{lab}} = 2.94 \pm 0.20$  keV was obtained for the resonance at  $E_p = 1.083$  MeV in  ${}^9\text{Be}(p, \gamma){}^{10}\text{B}$ .

Reported also by Weizmann Institute.

The Magnetic Moment of the 3-, 5.83 MeV Level in  ${}^{14}\text{N}$  and the Blume-Scherer Model of PAC in Gas with an Arbitrary Correlation Time

Z. Berant , M. Hass , Y.S. Horowitz and G. Goldring

The  ${}^{12}\text{C}({}^3\text{He}, \gamma){}^{14}\text{N}$  reaction was used to populate the 3-, 5.83 MeV level in  ${}^{14}\text{N}$ . The 730 keV gamma rays from the  ${}^{14}\text{N}$  ions recoiling at  $v/c = 3\%$  into vacuum and He at gas pressures up to 600 torr were detected in coincidence with back-scattered protons. The results are interpreted in the framework of the Blume Scherer model and enable a simultaneous determination of the correlation time and the g-factor of the excited nuclear level. A 1s static field perturbs the 3-, 18 psec. level of  ${}^{14}\text{N}$  down to hard core. At low gas pressures charge exchange collisions tend to distribute the perturbation amongst the whole ionic ensemble, thus reducing the anisotropy below that measured in vacuum. Assuming 1s fields dominate the interaction one obtains a correlation time at 50 torr of  $0.8 \pm 0.2$  ps which with the calculated field  $H_{1s} = 57.3$  MG implies  $0.5 < |g| < 0.85$ . The calculated g factor assuming wave functions from Glendenning is  $g = 0.55$ .

Reported also by Weizmann Institute.

Width of the 6.20 MeV,  $J^\pi = 1^-$ , Level of  ${}^{18}\text{O}$

M. Hass , Z. Shkedi , D.F.H. Start , Y. Wolfson and Y.S. Horowitz

The width of the 6.20 MeV,  $J^\pi = 1^-$  state of  ${}^{18}\text{O}$  has been measured using a resonance fluorescence self-absorption technique. For a ground state branching ratio,  $\Gamma_0/\Gamma = 0.38$ , one finds  $\Gamma_0 = 180 \pm 30$  eV. The energy of this state was determined to be  $6202.7 \pm 0.8$  keV.

Y.S. Horowitz, J.O. Allan\*, J.W. Jury\*,  
J.G. Woodworth, R.G. Johnson and K.G. McNeill

Using the neutron time-of-flight facility of the U. of Toronto Electron-Linac Lab. the energy spectra of photoneutrons from  $^{18}\text{O}$  were investigated. An  $^{18}\text{O}$  target in the form of 200 grams of  $\text{D}_2\text{O}$  enriched 98.7% in  $^{18}\text{O}$  was irradiated with 10 ns bursts of bremsstrahlung from a thick tungsten target at endpoints of 18.8, 22.6 and 24.8 MeV. The resulting photoneutrons were timed over a 50 m. flight path at  $98^\circ$  to the beam direction. Distinct peaks in the photoneutron energy spectrum were observed at 2.53, 3.11, 3.48, 4.09, 5.00, 5.87, 6.60 and 7.69 MeV. Also possible peaks could exist at 2.3, 2.8 and 3.8 MeV. These peaks correspond favourably with structure in  $^{18}\text{O}(\gamma, p)^{17}\text{N}$  measurements. Angular distributions were also measured and will be discussed.

The Angular Distribution of Gamma Rays  
Following the (p,n) Reaction on  $^{74}\text{Ge}$

S. Mordechai, A.A. Jaffe, D. Nir and M. Paul

The angular distribution of gamma rays excited by the (p,n) reaction on  $^{74}\text{Ge}$  leading to the final nucleus  $^{74}\text{As}$  have been measured. The results have been compared with the compound nucleus statistical model. Possible spin values are extracted for the  $^{74}\text{As}$  low lying states at 172, 197, 200, 206, 267 and 273 keV excitation energy. It was found also that the variation of the gamma ray angular distribution with incident energy, following the (p,n) reaction, is correctly predicted by the model.

Study of  $^{74}\text{As}$  by the  $^{73}\text{Ge}(^3\text{He}, d)^{74}\text{As}$  Reaction

B. Rosner, S. Mordechai and D.J. Pullen

The energy levels of  $^{74}\text{As}$  have been studied by the  $^{73}\text{Ge}(^3\text{He}, d)^{74}\text{As}$  reaction, with an overall energy resolution of 20 keV (FWHM). 25 levels in  $^{74}\text{As}$  were identified up to 2.2 MeV excitation energy. Angular distributions were measured in the angular interval  $3\frac{3}{4}^\circ$  to  $86^\circ$ . Spectroscopic information has been extracted for most of the transitions by means of a distorted wave analysis of the differential cross sections. The results are consistent with those previously obtained by  $(^3\text{He}, d)$  reaction on the even Ge isotopes. A comparison between the  $^{73}\text{Ge}(^3\text{He}, d)$  and  $^{75}\text{As}(p, d)$  reactions established a very interesting doublet structure in  $^{74}\text{As}$ .

EXPERIMENTAL REACTOR NUCLEAR PHYSICS\*

Utilization of 11.4 MeV Photons from the  
 $\text{Ni}^{59}(n,\gamma)\text{Ni}^{60}$  Reaction for Scattering Experiments

R. Moreh and T. Bar-Noy

A new reaction,  $\text{Ni}^{59}(n,\gamma)\text{Ni}^{60}$ , producing the highest energy of all known useful capture  $\gamma$  rays is utilized for photon scattering experiments in the energy region of the giant dipole resonance. The  $\gamma$  line energies of the ground state transitions of the  $\text{Ni}^{59}(n,\gamma)$ ,  $\text{Ni}^{61}(n,\gamma)$  and  $\text{Ni}^{63}(n,\gamma)$  reactions were measured and found to be  $11387.5 \pm 1.7$  keV,  $10596.2 \pm 3.7$  keV and  $9657.4 \pm 2.8$  keV respectively. A comparison is made of the intensity of the 11387.5 keV  $\gamma$  line with that obtained from other  $(n,\gamma)$  sources.

Large E1 and M1 Radiative Widths in Nuclei Near Closed Shells

A. Wolf, R. Moreh, A. Nof, O. Shahal and J. Tenenbaum

The radiative widths, spins and parities of ten levels photoexcited by the  $(\gamma,\gamma')$  reaction at excitation around 7 MeV in  $^{159}\text{La}$ ,  $^{140}\text{Ce}$ ,  $^{141}\text{Pr}$ ,  $^{142}\text{Nd}$ ,  $^{144}\text{Nd}$ ,  $^{205}\text{Tl}$  and  $^{209}\text{Bi}$ , were measured. The  $\gamma$  beam was produced by thermal neutron capture in titanium, iron, cobalt and copper. The spins of the resonance levels were obtained by angular distribution measurements and the parities were determined by using a Compton polarimeter. These levels together with other resonance levels in  $N \sim 82$  and  $N \sim 126$  nuclei are discussed with regard to a possible connection to a giant M1 resonance.

Reported also by Israel AEC.

Study of the Energy Levels of  $\text{Ga}^{69}$  Using Nuclear Photoexcitation

R. Moreh, O. Shahal, J. Tenenbaum, A. Wolf and A. Nof

Elastic and inelastic scattering of monochromatic photons were used for studying nuclear levels in  $\text{Ga}^{69}$ ; the photons were produced by thermal neutron capture in copper and vanadium. The decay of one resonance at 7306 keV excited by the copper  $\gamma$  source and another resonance at 6874 keV excited by the vanadium  $\gamma$  source were studied in detail and 30 low lying levels were observed from the ground state up to 3.4 MeV, 17 of which are believed to be new levels in  $\text{Ga}^{69}$ . The angular distribution of some elastic and inelastic lines were measured and the following spin determinations were made (keV,  $J^\pi$ ): 320,  $1/2^-$ , ( $3/2^-$ ); 574,  $5/2^-$ ; 872,  $3/2^-$ ; 1488,  $3/2^-$ , ( $7/2^-$ ); 1525, ( $1/2, 3/2$ ); 1891,  $3/2^-$ ; 1978, ( $1/2, 3/2$ ); 2457,  $3/2$ ; 2484,  $5/2$ ; (2565), ( $1/2, 3/2$ ); 2660,  $3/2$ ; 3051, ( $3/2, 7/2$ ); 3076,  $5/2$ ; 3318, ( $7/2$ ); 6874,  $1/2$ ; and 7306,  $5/2^+$ , where parentheses denote uncertainties. The parity of the 7306 keV level was directly determined using a Compton polarimeter. The total radiative width of the 7306 keV level was measured and found to be  $\Gamma = 0.105 \pm 0.020$  eV. For the 6874 keV level, a positive correlation coefficient was obtained,  $\rho = 0.69$ , between the  $(\gamma,\gamma')$  and  $(d,n)$  transition.

Reported also by Israel AEC.

### Comment on M2/E1 Mixing Observed in ( $\gamma, \gamma'$ ) Reactions

R. Moreh, A. Wolf and O. Shahal

It is shown that the effect of overlapping resonances in the photo-excitation process of a ( $\gamma, \gamma'$ ) reaction is very small. The influence of this effect on the angular distributions of the inelastic transitions and hence on the M2/E1 mixing ratios is shown to be negligible.

### Delbrück Scattering of 7.9 MeV Photons

R. Moreh and S. Kahane

The elastic scattering cross section of 7.9 MeV photons by U and Th was measured in the angular range  $25^\circ$ - $140^\circ$ . It is shown that at this energy the forward elastic scattering is due almost entirely to Delbrück scattering. The results are systematically lower by  $> 50\%$  than the calculated values. A good agreement with theory was obtained only after excluding the contribution of the real part of the Delbrück scattering amplitude.

### Elastic and Raman Scattering of Photons from $^{238}\text{U}$

T. Bar-Noy and R. Moreh

The results of measuring the elastic and Raman scattering cross sections for 7 discrete photo energies between 7.9 and 11.4 MeV are presented. It is shown that by making slight changes in the parameters of the dipole resonance of  $^{238}\text{U}$ , the measured scattering cross sections are found to be in fair agreement with predictions of the simple rotator model.

### E1, M1, E2 and M2 Widths of Transitions from Bound Levels Excited by the ( $\gamma, \gamma'$ ) Reactions

R. Moreh, A. Wolf O. Shahal and J. Tenenbaum

A comparison is made between the E1 and M1 transition strengths from bound levels populated by ( $\gamma, \gamma'$ ) reaction with the same data from unbound levels obtained via the ( $n, \gamma$ ) reaction. It is shown that there is a clear increase in the M1 strength nuclei near closed shells. The E2/M1 ratios were found to be of about the same magnitude as the Weisskopf estimate, while the M2/E1 were enhanced by a factor of  $10^3$ .

Total Radiative Width of Bound Nuclear Levels  
Excited by the  $(\gamma, \gamma')$  Reaction

R. Moreh, A. Wolf, O. Shahal and J. Tenenbaum

The total radiative widths of bound nuclear levels, at an excitation energy around 7 MeV, as function of  $A$  is presented. These widths were measured by employing self absorption, temperature variation of the scattering cross section and absolute cross section measurements. By comparing the present results with the widths of unbound levels from  $(n, \gamma)$  work, it is shown that the radiative widths are continuous across the  $(\gamma, n)$  threshold for these nuclei.

Properties of Nuclear Levels Photoexcited by Neutron  
Capture  $\gamma$  Rays of Ti and Cu

A. Wolf, R. Moreh and O. Shahal

Neutron capture  $\gamma$  rays of Ti and Cu have been used to photoexcite nuclear levels in the 5-8 MeV region. Total and partial radiative widths of several levels in various isotopes were determined using nuclear self absorption, temperature variation, and absolute scattering cross section measurements. The total radiative widths were found to be of the same magnitude as those of unbound levels obtained in neutron resonances, after applying a correction to allow for the different excitation energies. The parities of some resonance levels were measured using a Compton polarimeter. Angular distribution measurements of the scattered radiation were carried out for fixing the spins of the resonance levels and for the determination of quadrupole admixtures in elastic and inelastic transitions. The E2 widths were found to be of the same magnitude as those obtained in  $(n, \gamma)$  experiments.

Properties of Nuclear Levels Excited by Neutron Capture  $\gamma$  Rays of Cobalt

J. Tenenbaum, R. Moreh and A. Nof

Neutron capture  $\gamma$  rays of cobalt have been used to photoexcite nuclear levels in the 5-8 MeV region. The decay properties of the 7491-keV level in  $^{55}\text{Mn}$  and the 6877-keV level in  $^{142}\text{Nd}$  were studied in detail. Total and partial radiative widths of nuclear levels in several isotopes were determined using nuclear self absorption, temperature variation, and absolute scattering cross section measurements. The total radiative widths were found to be of the same magnitude as those of unbound levels populated in neutron resonances. The spins and parities of some resonance levels were determined by carrying out angular distribution and polarization measurements respectively.

Study of the Energy Levels of  $^{100}\text{Mo}$  Using Nuclear Photoexcitation

R. Moreh, A. Wolf, O. Shahal, J. Tenenbaum and A. Nof

Elastic and inelastic scattering of monochromatic photons was used for studying nuclear energy levels in  $^{100}\text{Mo}$ ; the photons were produced by thermal neutron capture in titanium, copper and vanadium. The decay of the resonances at 7637-, 6517-, and 6418-keV was studied in detail. The angular distribution of some elastic and inelastic lines were measured and the following spin determinations were made: (keV,  $J^\pi$ ): 535,  $2^+$ ; 694,  $0^+$ ; 1065,  $2^+$ ; 1462,  $2^+$ ; 2035,  $0^+$ ; 2940,  $2^+$ ; 5187,  $1^-$ ; 6418,  $1^-$ ; 6517,  $1^-$ ; and 7637,  $1^-$ . The parities of the last three levels were directly determined using a Compton polarimeter. Total radiative widths were measured and the following results were obtained:  $\Gamma(6418) = 50 \pm 35$  meV,  $\Gamma(6517) = 180 \pm 100$  meV and  $\Gamma(7637) = 140 \pm 40$  meV. The M2/E1 mixing ratios for two primary transitions were obtained.

Reported also by Israel AEC.

THEORETICAL NUCLEAR PHYSICS

Complex Hamiltonian and Three Alpha Resonances

Y. Avishai

A new method of treating few body resonances exactly as bound states is suggested. Applied to a system of three alpha particles, we have found a  $1^-$  resonance whose position and width are in good agreement with experiment.

First  $0^+$  Excited of  $^{16}\text{O}$  in the  $\alpha$ -Particle Model of Light Nuclei

Y. Avishai

The pole approximation that Narodetskii introduced into the theory of four-particle scattering is here applied to  $^{16}\text{O}$ , which is assumed to be composed of four structureless  $\alpha$  particles. The binding energy of the excited  $0^+$  state of  $^{16}\text{O}$  was calculated by using an Irving variational wave functions for the ground state of  $^{12}\text{C}$  and taking both Yukawa and exponential  $\alpha\alpha$  potentials. In the light of earlier theoretical results on  $^{12}\text{C}$ , comparing the present results with experiment suggests that at least for calculation of the bound states, the  $\alpha$ -particle model of  $^{16}\text{O}$  is reasonable.

Effect of the  $T=1$  Pairing Correlations on the Nuclear Deformation of Some Even-Mass-Number Sn Isotopes

J. Bar-Touv and G.L. Struble

The Hartree-Fock-Bogoliubov equations are solved for the even Sn isotopes between  $A=112$  and  $A=124$ . The hypothesis that pairing restores spherical symmetry is critically examined and the interplay of the pairing and single-particle degrees of freedom are discussed.

Relativistic Treatment of Low-Energy Nucleon-Nucleon Scattering

R.A. Bryan and A. Gersten

An improved version of the one-boson-exchange model is presented. In addition to  $\pi, \rho, \omega$  and  $X_0$ , the scalar mesons  $\sigma$  and  $\delta$  are used with their physical masses. The broad width of the  $\epsilon$  and  $\omega$  mesons is taken into account. The relativistic Blankenbecler-Sugar equation is utilized over the laboratory scattering energy range 0 to 425 MeV. A better fit to the experimental N-N data is obtained than in previous one-boson-exchange models. Reasonable values of the coupling constants are obtained, which agree qualitatively with other experiments. The fitting procedure was done including and excluding S-waves in order to test the influence of the core region. An approximate version of the above model is developed using the Schrödinger equation in place of the Blankenbecler-Sugar equation. A good fit to the experimental scattering data and the deuteron parameters is obtained with coupling constants similar to those of the relativistic model.

Zeros of the Scattering Amplitude in the Complex Angle Plane

A. Gersten

The possibility of reconstructing the scattering amplitude with the aid of the zeros in the complex  $\cos\theta$  plane of the differential cross section is considered. The reconstruction process is demonstrated in two examples. The location of the zeros of the scattering amplitude is examined for the strong absorption and optical models. It appears that there exists a correlation between the position of the zeros and the strength of the absorption.

Test for T-Violation in N-N Scattering

J. Binstock, R. Bryan, and A. Gersten

We make predictions for the angular distributions of nucleon-nucleon observables revealing T-violation, in the limit of very short-ranged T-violating mechanisms. Curves are shown for the observables  $P_A - P_B$ , and  $P_A + P_B$ , at 425 MeV for both p-p and n-p scattering.

## RESEARCH PROGRAMS

### Hebrew University

#### STUDY OF THE (d, $\alpha$ ) REACTIONS ON $^{42}\text{Ca}$ & $^{48}\text{Ca}$ & THE SPINS OF THE LOW-LYING EXCITED STATES IN $^{46}\text{K}$ .

M. Paul, A. Marinov, Ch. Drory, J. Burde, E. Navon & Sh. Mordechai

Angular distributions of  $\alpha$ -groups emitted from the  $^{48}\text{Ca}(d, \alpha)^{46}\text{K}$  and the  $^{42}\text{Ca}(d, \alpha)^{40}\text{K}$  reactions respectively have been measured. From their comparison spin values of  $2^-$  and  $(5^-)$  are proposed for the ground state of  $^{46}\text{K}$  and for its excited state at 692 keV excitation respectively.

#### THE CHARACTER OF THE 5.387- & 6.095-MeV STATES IN $^{49}\text{Ca}$ STUDIED VIA THEIR ISOBARIC ANALOG STATES IN $^{49}\text{Sc}$ .

R. Benin, A. Marinov, Ch. Drory, J. Burde & G. Engler

The elastic and inelastic scattering of protons by  $^{48}\text{Ca}$  were studied. Two resonances at  $E_p(\text{c.m.}) = 7.365$  and  $8.042$  MeV, were observed in the inelastic proton group leading to the 4.51-MeV ( $3^-$ ) state in  $^{48}\text{Ca}$ . The spins and parities and the corresponding values of  $\Gamma$ ,  $\Gamma_p$  and  $\Gamma_p'$  were determined.

#### ANGULAR DISTRIBUTION OF INELASTIC PROTONS FROM ISOBARIC ANALOG RESONANCES IN $^{131}\text{I}$ .

J. Burde, G. Engler, A. Ginsburg, A.A. Jaffe, A. Marinov & L. Birstein

Angular distributions of outgoing protons have been measured for some isobaric analog resonances in  $^{131}\text{I}$  and their spins and parities have been determined. The spin and parity of the state of 1.634 MeV in  $^{130}\text{Te}$  is found to be  $2+$ . Two  $3/2^-$  resonances decay predominantly by  $f_{7/2}$  waves to the first excited state in  $^{130}\text{Te}$ .

## STUDY OF ELASTIC AND INELASTIC SCATTERING OF PROTONS FROM $^{128}\text{Te}$ AND $^{130}\text{Te}$ AT ISOBARIC ANALOGUE RESONANCES

J. BURDE, G. ENGLER, A. GINSBURG, A. A. JAFFE, A. MARINOV and L. BIRSTEIN

Isobaric analogue states in  $^{129}\text{I}$  and  $^{131}\text{I}$  were studied by (p, p') and (p, p) scattering from  $^{128}\text{Te}$  and  $^{130}\text{Te}$  in the incident energy ranges 7.66–11.87 MeV and 7.48–12.65 MeV, respectively. The energy differences between the resonances and the orbital angular momentum transferred in their formation agree very well with the corresponding analogue states which have been previously observed by the (d, p) reaction on the same target nuclei. There is fairly good agreement between the corresponding spectroscopic factors. The Coulomb displacement energies were found to be 13.949 and 13.898 MeV for the pairs of isotopes  $^{129}\text{Te}$ – $^{129}\text{I}$  and  $^{131}\text{Te}$ – $^{131}\text{I}$ , respectively. The spins of the resonances at  $E_p^{c.m.} = 10.199$  and  $E_p^{c.m.} = 10.545$  MeV in  $^{129}\text{I}$  and those at  $E_p^{c.m.} = 10.455$  and  $E_p^{c.m.} = 10.520$  MeV in  $^{131}\text{I}$  were found to have spin and parity  $\frac{3}{2}^-$ . The angular distribution of the inelastic protons from the resonances at  $E_p^{c.m.} = 9.96$  and  $E_p^{c.m.} = 10.07$  MeV in  $^{129}\text{I}$  and at  $E_p^{c.m.} = 10.20$  MeV in  $^{131}\text{I}$  are consistent with an assignment of  $\frac{3}{2}^-$  to these levels and with a  $\frac{1}{2}^-$  assignment to the resonance at  $E_p^{c.m.} = 10.915$  MeV in  $^{131}\text{I}$ . The modes of the de-excitation of the two-phonon states and other higher states in  $^{128}\text{Te}$  and in  $^{130}\text{Te}$  were studied by observing the gamma-ray spectra and by coincidence measurements between the gamma rays and the inelastic protons at the various resonances. The states at 1498 and 1521 keV in  $^{128}\text{Te}$  were found to have spins and parities of  $4^+$  and  $2^+$ , respectively. The 1634 keV level in  $^{130}\text{Te}$  was found to have spin and parity  $2^+$ . Upper limits were placed on the ratios of the gamma-ray transitions  $I_\gamma(2_2^+ \rightarrow 0^+)/I_\gamma(2_1^+ \rightarrow 2_1^+)$  in  $^{128}\text{Te}$  and  $^{130}\text{Te}$  of 3%.

Seven odd-parity resonances in  $^{129}\text{I}$  and  $^{131}\text{I}$  are discussed in terms of the core excitation model.

## DENSITY DEPENDENT EFFECTS IN THE OPTICAL MODEL AND THE NUCLEAR MATTER RADII

E. FRIEDMAN

By adding to the reformulated optical model a density dependence of the interaction the discrepancy between the results of this model and the Coulomb displacement energies is removed. The results suggest that a neutron halo does not exist in heavy nuclei.

## COULOMB DISPLACEMENT ENERGIES AND NUCLEAR SIZES

E. FRIEDMAN and B. MANDELBAUM

The Coulomb displacement energy between isobaric analogue states is calculated as a function of the rms radius of the distribution of the excess neutrons for a known value of the rms radius of the charge distribution in the neutron analogue. The exchange term, the Coulomb spin-orbit term and the Thomas-Ehrman shift are included and effects of configuration mixing are studied. It is concluded that if the rms radius of the charge distribution and the Coulomb displacement energies are known, the rms radius of the excess neutrons can be extracted to an accuracy of better than  $\pm 0.1$  fm.

## ELASTIC AND INELASTIC PROTON SCATTERING FROM $^{40}\text{Ca}$ AND TWO-PARTICLE, ONE-HOLE STATES IN $^{41}\text{Sc}$

A. Marinov, Ch. Drory, E. Navon, J. Burde, and G. Engler

The elastic and inelastic scattering of protons by  $^{40}\text{Ca}$  were studied at bombarding energies from 4.8 to 6.2 MeV. 60 resonances were identified. The spins of most of them and their partial widths for decay to the ground state and to the first four excited states in  $^{40}\text{Ca}$  were determined. Levels in  $^{41}\text{Sc}$  having configurations with a large two-particle, one-hole component were identified and compared with similar levels in  $^{41}\text{Ca}$ .

## ISOBARIC ANALOGUE STATES OF RUTHENIUM ISOTOPES

E. FRIEDMAN, B. MANDELBAUM, J. ZIONI, A. A. JAFFE, A. MARINOV,  
A. GINZBURG and Z. FLITZUR

Isobaric analogue states were observed as resonances in the excitation functions for the (p, n) reaction on  $^{100,101,102}\text{Ru}$  and in the elastic scattering of protons from  $^{96,98,100,102,104}\text{Ru}$ . The results were compared to known level structure of  $^{96,100,102}\text{Ru}$  and to results of (d, p) experiments on  $^{96,102,104}\text{Ru}$ . The analogue resonances of the ground states were identified in all cases and Coulomb displacement energies were deduced. Some strong resonances with  $l_p = 0, 2$  corresponding to excited states were also observed. Total and partial proton widths were calculated for the strongest resonances.

## THE CHARACTER OF EXCITED STATES IN $^{41}\text{Sc}$ STUDIED BY ELASTIC AND INELASTIC PROTON SCATTERING FROM $^{40}\text{Ca}$

A. MARINOV<sup>1</sup>, Ch. DRORY, E. NAVON, J. BURDE and G. ENGLER<sup>2\*</sup>

Excitation functions of elastic and inelastic proton scattering leading to the ground state and to the  $0^+$  (3.35 MeV),  $3^-$  (3.74 MeV) and  $2^+$  (3.91 MeV) excited states of  $^{40}\text{Ca}$  were measured at  $90^\circ$ ,  $125^\circ$  and  $160^\circ$  at bombarding energies from 4.8 to 6.2 MeV. Sixty resonances were identified. Angular distributions of the inelastically scattered protons were measured at bombarding energies corresponding to most of the resonances observed in the excitation curves. The spins of the corresponding levels in  $^{41}\text{Sc}$  and their partial widths for decay to the ground state and to the three excited states in  $^{40}\text{Ca}$  were determined in most of the cases. In a few cases de-excitation to the  $5^-$  state at 4.49 MeV excitation in  $^{40}\text{Ca}$  was also observed. Levels in  $^{41}\text{Sc}$  having configurations with large two-particle one-hole component were identified and compared with similar levels in  $^{41}\text{Ca}$  and with theoretical predictions.

**Properties of  $^{96,98}\text{Rh}$  from the  $^{96,98}\text{Ru}(p,n)$  reaction.** J. Ashkenazi, E. Friedman, D. Nir, J. Zioni (Hebrew Univ., Jerusalem, Israel). *Nucl. Phys. A (Netherlands)*, vol. A158, no. 1, p. 146-54 (7 Dec. 1970). The threshold energies for the  $^{96}\text{Ru}(p,n)^{96}\text{Rh}$  and  $^{98}\text{Ru}(p,n)^{98}\text{Rh}$  reactions were measured as  $7.30 \pm 0.01$  and  $5.90 \pm 0.01$  MeV respectively, yielding for the mass excess of the Rh isotopes the values of  $-79.622 \pm 0.011$  MeV ( $^{96}\text{Rh}$ ) and  $-83.16 \pm 0.011$  MeV ( $^{98}\text{Rh}$ ). By observing delayed  $\gamma$  rays following the  $\beta^+$  decay of the produced Rh isotopes, two half lives of  $1.55 \pm 0.15$  min and  $9.25 \pm 0.10$  min were found in the activity of  $^{96}\text{Rh}$  and a half life of  $9.05 \pm 0.30$  min was found for the  $^{98}\text{Rh}$ . The above results together with Hauser-Feshbach analyses of the (p,n) excitation functions suggest the value  $3^-$  for the spins and parities of  $^{96,98}\text{Rh}$ . (13 refs.)

**An investigation of proton-rich nuclei and other products from the bombardment of  $^{24}\text{Mg}$ ,  $^{28}\text{Si}$  and  $^{32}\text{S}$  by  $^{16}\text{O}$  ions.** J. Zioni, A. A. Jaffe, E. Friedman, N. Haik, R. Scheetman, D. Nir (Hebrew Univ., Jerusalem, Israel). *Nucl. Phys. A (Netherlands)*, vol. A181, no. 2, p. 465-76 (21 Feb. 1972). The  $\beta^-$  and  $\gamma$  ray spectra have been studied resulting from the bombardment of  $^{24}\text{Mg}$ ,  $^{28}\text{Si}$  and  $^{32}\text{S}$  with continuous and chopped beams of  $^{16}\text{O}$  ions in the energy range of 22-33 MeV. Compound nucleus formation is found to predominate in the reactions. Proton-rich nuclei are observed via the ( $^{16}\text{O}, 2n$ ) reaction in each case. In particular the mass excess of the previously unobserved nucleus  $^{46}\text{Cr}$  is found to be  $-29.46 \pm 0.03$  MeV; its half life is  $0.26 \pm 0.06$  s. The systematics of the Coulomb displacement energies of the mass triplets up to  $A = 46$  are discussed. (18 refs.)

**A comparison of spectroscopic factors from  $^{93}\text{Mo}(d,t)^{93}\text{Mo}$  and  $^{93}\text{Mo}(p,p')^{93}\text{Mo}$  experiments.** E. Abramson, G. Engler, Z. Vager (Weizmann Inst. Sci., Rehovot, Israel), N. Cue, I. Plessner, G. F. Wheeler. *Phys. Lett. B (Netherlands)*, vol. 28B, no. 2, p. 70-2 (24 Jan. 1972). Spectroscopic factors from the  $^{93}\text{Mo}(d,t)^{93}\text{Mo}$  reaction have been compared with partial decay strengths obtained from the  $^{93}\text{Mo}(p,p')^{93}\text{Mo}$  reaction proceeding through the  $5/2^+$  g.s. analogue resonance. The results of the comparison support the treatment of the compound enhancement applied in the analysis of the  $^{93}\text{Mo}(p,p')^{93}\text{Mo}$  reaction. (6 refs.)

PROGRESS REPORT ON NUCLEAR DATA ACTIVITIES IN KOREA

Mann Cho  
Liaison Officer of INDC .

Compiled by Jung-Do Kim  
Reactor Physics Lab.  
Korea Atomic Energy Research Institute

N.

(1) OBSERVATION OF A NEW UNCLEAR REACTION - ( $2\gamma, n$ ) REACTION

S. K. Nah

Ulsan Institute of Technology

The abstract on this subject was written in the Transactions of the Korean Physical Society, Spring Meeting, Seoul National University, April 27-28, 1973.

The ( $2\gamma, n$ ) reaction, which no one has ever made, was observed using the monoenergetic and very intense thermal-neutron-capture gamma rays. At incident gamma-ray energies less than the threshold energies for the photoneutron reactions in  $\text{Cu}^{63}$ , the single-step reaction processes, ( $\gamma, n$ ), in  $\text{Cu}^{63}$  were evidently forbidden but two-step reaction processes, ( $2\gamma, n$ ), could possibly occur through intermediate states of well-defined energies and life-times. The spectra of the positron annihilation radiation following the photodisintegration processes were measured with two NaI(Tl) crystals in coincidence. Appreciable cross sections of  $5.32 \pm 0.51$ ,  $2.59 \pm 0.31$ ,  $1.31 \pm 0.13$ , and  $2.85 \pm 0.25$  microbarns were obtained at energies of 6.072, 6.753, 7.724, and 8.997 MeV, respectively. First three excited levels were found with good agreement with known values. (1)

However, the excited level at 8.997 Mev was known as new. Several different experiments were performed to ensure these observed spectra were not due to  $(n, 2n)$  reaction in  $\text{Cu}^{63}$ . Analytic expressions for the mechanism of a two-step reaction process,  $(2\gamma, n)$ , were derived using a distorted-wave theory. The measured cross sections agreed in magnitude with those predicted by this theory. It is suggested that the  $(2\gamma, n)$  reaction, and the analysis given here, promise to be a useful tool for the study of higher excited states.

(1) H. Verheul, Nuclear Data Sheets, B2(35) 1967.

National Academy of Science, National Research  
Council (U.S. Government Printing Office).

(2) CALCULATION OF THE RESONANCE INTEGRAL FOR U-233 USING  
ADLER-ADLER MULTILEVEL FORMALISM

Chang Yul Chi and Chang Hyo Kim

Seoul National University

Mann Cho and Kun Joong Yoo

Korea Atomic Energy Research Institute

In this study we expressed the capture and the fission cross sections of U-233 covering the resolved resonance energy region below 60 eV in terms of Adler-Adler multilevel formula. We first confirmed that Adler-Adler representations for the reaction cross sections are quite satisfactory, demonstrating the good agreements between the experimental cross

sections and the theoretical ones. We then calculated an integral resonance absorption, the infinite dilution resonance integral of U-233, for the purpose of determining the temperature effect on the resonance absorption by this element. We also compared this calculations with the experiments, finding again good agreements between calculations and experiments.

Recently de Saussure and Perez developed a method which can transform a set of multilevel resonance parameters into an equivalent set of single-level pseudoparameters and a smooth background. Using this method, we have obtained the single level pseudoparameters of U-233. In this calculation we intended that these parameters would be useful for those reactor codes which are not suitable for multilevel parameters.

\* A paper on this study will be submitted to the Journal of the Korean Nuclear Society soon.

(3) AN ANALYSIS OF INELASTIC NEUTRON SCATTERING BY LIQUID METHANE

Chang Hyun Chung and Won Kee Shin

Department of Nuclear Engineering, Seoul National University

Jin Soo Kim

Korea Atomic Energy Research Institute

The paper on this subject was published in the Journal of the Korean Nuclear Society Volume 5, Number 4, p.265, December 1973 with an abstract as follows.

The incoherent neutron scattering cross section of molecular liquids is analyzed using a damping function model for correlation functions of molecular translations and rotations. The present approach is different from recent works in that the scattering function is evaluated directly, not through the intermediate scattering function. The damping function is determined from a simple relation between its long-wavelength limit and the generalized frequency distribution function, and translation-rotation couplings are assumed to be neglected. A physical model is used for the translational motions of center-of-mass of a molecule, including properly its short-time and long-time behaviors. A simple model for the rotational motions is suggested which relates the damping function to the Fourier transform of the dipole correlation function, or equivalently, the infrared vibrational absorption spectrum. Theoretical absolute scattering intensities are computed for liquid methane and shown to be in satisfactory agreement with both thermal and cold neutron measurements.

(4) THE PHOTOPROTON FROM  $^{181}\text{Ta}(e, e'p)$  REACTION

B. N. Sung

Seoul National University

The abstract on this subject was written in the Transactions of the Korean Physical Society, Spring Meeting, Seoul National University, April 27-28, 1973.

The photoproton energy distribution from  $(e, e'p)$  reaction and  $(e, e'p)$  cross sections on  $^{181}\text{Ta}$  have been measured with the bombarding energies 18.0, 19.0, 19.5, 20.0, 20.5, 21.0, 21.5 and 22.0 Mev at  $\theta=90^\circ$  by using the electron linear accelerator and a broad range magnetic spectrometer with 100 solid state detectors. Two large proton groups in the proton energy distributions are found at  $E_p = 9.2$  Mev and  $E_p=11.5$  Mev in the cases of  $E_e > 20.0$  Mev. The cross section shows a strong resonance at 20.0 Mev which is expected as T coherent state. The two main proton groups are resulted through this resonance. The modified Nilsson level scheme explained well these proton groups.

(5) REACTOR NEUTRON ACTIVATION ANALYSIS BY A SINGLE COMPARATOR METHOD

Chul Lee

Korea Atomic Energy Research Institute

The paper on this subject was published in the Journal of the Korean Nuclear Society Volume 5, Number 2, p.137, June, 1973 with an abstract as follows.

A method of activation analysis, based on the irradiation and counting of an iron wire which contains manganese impurity as the single comparator, has been elaborated by critical evaluation of nuclear data involved in activation and activity measurement. The variation of effective cross section is investigated as a function of the spectral index and other parameters such as a measure of the proportion of epithermal neutrons in the reactor spectrum. The errors induced by shifts in the neutron spectrum in the irradiation positions are discussed. The known amount of each element is irradiated simultaneously together with the single comparator, and the obtained values are compared with the known amount of each element. The results show that in general the random errors are not greater than those obtained by using the conventional relative method, but the systematic errors were up to about 20%.

This method is applied to the determinations of fourteen rare earth elements in monazite as well as other seven elements in the standard kale powder. The satisfactory reproducibility of the present method makes possible the determination of the elements with an accuracy attainable with the conventional relative method.

(6) SIMULTANEOUS DETERMINATION OF MERCURY, BROMINE, ARSENIC AND CADMIUM IN BIOLOGICAL MATERIALS BY NEUTRON ACTIVATION ANALYSIS\*

Chul Lee, Nak Bae Kim and Euy Byung Park  
Korea Atomic Energy Research Institute

The paper on this subject was published in the Journal of the Korean Nuclear Society Volume 5, Number 4, p.279, December, 1973 with an abstract as follows.

A method for the simultaneous determination of mercury, bromine, arsenic and cadmium in biological samples is described. Following neutron activation and a simple distillation of volatile compounds, mercury and bromine were determined by gamma-ray spectrometry. Arsenic and cadmium were further separated by cation exchange separation and determined similarly. Determination limits for mercury, bromine, arsenic and cadmium were  $0.001 \mu\text{g}$ ,  $0.003 \mu\text{g}$ ,  $0.001 \mu\text{g}$  and  $0.02 \mu\text{g}$ , respectively. The method has been applied to the determination of mercury, bromine, arsenic and cadmium in rice and fish samples. Analysis of a standard kale powder yielded the values of  $0.046 \mu\text{g/g}$  for mercury,  $24.5 \mu\text{g/g}$  for bromine  $0.17 \mu\text{g/g}$  for arsenic and  $0.50 \mu\text{g/g}$  for cadmium.

\* This work was supported in part by IAEA under contract number 1136/RB.

(7) A STUDY OF FAST LI-FRAGMENTS FROM 28 GeV PROTON INTERACTION IN NUCLEAR EMULSION

Seung Ai Shin

Department of Physics, Ewha Womans University

The paper on this subject was published in the New Physics (Korean Physical Society) Volume 13, Number 2, p.45, June, 1973 (in Korean) with an abstract as follows.

It was found that majority of the Li-fragments were emitted by nuclear evaporation process, but that also there was a small number of fast Li-fragments ( $> 60$  MeV) not explained by this process. In the present paper, these fast ones which were emitted in the stars (due to Ag or Br) and induced by 28 GeV protons, are described. The angular distribution and energy spectra of those fragments were determined and analyzed.

It seems that the fast Li-fragments are not be produced by the evaporation process or by the direct collision processes by the primary. It is probable that they may be ejected when the nucleons and pions-sets in flight during the cascade phase of the disintegration collide with the groups of nucleons. Consequently there is the possibility of the presence of nucleon clusters in the nuclear periphery.

(8) THE DECAY OF  $^{110m}\text{Ag}$ : GAMMA-RAY INTENSITY STANDARDI-  
ZATION AND A SEARCH FOR WEAK TRANSITIONS

H. K. Chung and S. W. Cho

Korea Atomic Energy Research Institute

H. C. Kim

Department of Physics, Sungkyunkwan University

The paper on this subject was published in the Journal of the Korean Physical Society, Vol. 6, No. 1, P.1, March, 1973. with an abstract as follows.

The relative intensities of the gamma-ray transitions from the decay of  $^{110m}\text{Ag}$  have been carefully re-determined by using a true coaxial Ge(Li) detector with active volume of 20 cc. The values obtained for relative intensities are listed in the following in parentheses:  $446.790 \pm 0.020$  (3.72 $\pm$  0.11),  $620.305 \pm 0.015$  (3.00 $\pm$  0.09),  $657.720 \pm 0.010$  (1.00),  $677.590 \pm 0.015$  (11.39 $\pm$  0.57),  $686.965 \pm 0.020$  (6.86 $\pm$  0.41),  $706.650 \pm 0.020$  (16.85 $\pm$  0.39),  $744.245 \pm 0.020$  (4.42 $\pm$  0.19),  $763.930 \pm 0.020$  (23.38 $\pm$  0.67),  $817.995 \pm 0.015$  (7.73 $\pm$  0.25),  $884.655 \pm 0.015$  (79.53 $\pm$  1.83),  $937.445 \pm 0.020$  (37.46 $\pm$  0.83),  $1384.230 \pm 0.020$  (26.91 $\pm$  0.38),  $1475.710 \pm 0.015$  (4.40 $\pm$  0.10),  $1504.955 \pm 0.020$  (14.50 $\pm$  0.31),  $1562.235 \pm 0.020$  (1.33 $\pm$  0.04). Apart from these well-known transitions, additional gamma-rays with weak intensities were observed at  $626.22 \pm 0.20$ ,  $995.628 \pm 0.050$  and  $1334.808 \pm 0.050$  KeV and their relative intensities were evaluated as  $0.18 \pm 0.04$ ,  $0.19 \pm 0.03$  and  $0.20 \pm 0.03$  respectively. Our measured results on a search for weak transitions well agree with one

of the two data sets (transition energies at 133.97, 566.0, 667.2, 753.0, 785.0 and 1443.0 keV in Data 1; transition energies at 626.22, 997.13 and 1334.16 keV in Data 2) previously reported and suggest that the observed weak gamma-rays are not attributable to the decay of  $^{108m}\text{Ag}$ .

(9) AN IMPROVED PROTON RECOIL TELESCOPE DETECTOR FOR FAST NEUTRON SPECTROSCOPY

Moon Kyu Chung and Hee Dong Kang  
Korea Atomic Energy Research Institute  
Tong Seo Park  
Kyung pook National University

The paper on this subject was published in the Journal of the Korean Nuclear Society Volume 5, Number 3, p. 191, September, 1973 with an abstract as follows.

For fast neutron spectroscopy in MeV region, a recoil proton telescope detector was designed and constructed so as to increase in detection efficiency without appreciable deterioration in energy resolution by adopting a special type of recoil proton radiator which is a combination of a ring-shaped vertical radiator and a cone-shaped horizontal radiator at a certain geometry. A neutron stopper was built in the detector system to minimize the background due to direct exposure of the Si(Li) detectors to primary incident

neutrons. The detection efficiency and the energy resolution calculated at various neutron energies and geometries are given and these characteristics of the detector system were tested by 14.1 MeV neutrons. As the calculation predicted, the relative detection efficiency in case of the combined radiator system is almost 2.2 times of that for a single, ring-shaped vertical radiator system. The calculated energy resolution is 3.7% FWHM, whereas the measured resolution was 3.9% which means resolution broadening of approximately 30% was resulted by introducing a combined radiator system into the telescope. Increase in background less than 40% was also observed.

(10) APPLICATION OF A SINGLE FLAT CRYSTAL DIFFRACTION SPECTROMETER TO THE DECAY SCHEME STUDY OF  $^{110m}\text{Ag}$

M. K. Chung and S. W. Cho

Korea Atomic Energy Research Institute

The abstract on this subject was written in the Transactions of the Korean Physical Society, Spring Meeting, Seoul National University, April 27-28, 1973.

To search for the unreported weak gamma-ray transitions in the decay of  $^{110m}\text{Ag}$ , a single flat crystal diffraction spectrometer in combination with the large volume coaxial Ge(Li) detector was constructed and applied to the

verifying of the existence of small photo peaks which are usually hidden in the intense Compton background.

Apart from 15 well-known transitions, our measurements indicate the existence of additional gamma-rays with weak intensities at 626.22, 995, 628 and 1334.808 keV. By careful study of the spectra of  $^{110\text{m}}\text{Ag}$  sample sources with different cooling times, these weak transitions are proved to be from the decay of  $^{110\text{m}}\text{Ag}$  and are not to be attributed to the decay of  $^{108\text{m}}\text{Ag}$ .

(11) THE STUDY ON THE GAMMA-RAY TRANSITIONS FOLLOWING THE DECAY OF  $\text{In}^{116\text{m}}$

M. K. Chung and S. W. Cho  
Korea Atomic Energy Research Institute  
C. W. Nam  
Seoul National University

The abstract on this subject was written in the Transactions of the Korean Physical Society, Fall Meeting, Ulsan Institute of Technology, October 26-27, 1973.

The decay of  $\text{In}^{116\text{m}}$  to  $\text{Sn}^{116}$  has been studied. Both singles and  $\gamma - \gamma$  coincidence techniques were employed with the use of Ge(Li) detector. The energies and the relative intensities of all the known transitions were observed. Besides the known transitions, the unreported gamma-rays with weak intensities were observed. Two of them are

new transitions with energies of 277.799 keV and 688.664 keV which feed from 2390.82 keV(4+) level and 2800.83 keV (4+) level to 2111.93 keV(2nd 2+) level respectively. In connection with the two other gamma-rays observed at 2226.522 keV and 303.297 keV, the possible existence of an unobserved level at 2226.522 keV(2+) will also be discussed.

(12) A STUDY OF SHIELDING IN SLABS USING THE BEAM OF CP-5 REACTOR

Suk Yun Kim

Department of Applied Physics, Inha University

The paper on this subject was published in the New Physics (Korean Physical Society) Vol. 13, No. 1, P. 6, March 1973 (in Korean) with an abstract as follows.

Reactor shielding can only be evaluated through direct measurement and extensive numerical calculation. In this paper, some results of numerical calculation (flux and heat generation of fast, thermal neutron and gamma-ray) are presented. The calculations are based on the data obtained in the slab shielding experiment using the beams in the ANL Lid Tank, Shielding Facility of CP-5 Reactor.

(13) A STUDY OF THE DOSIMETRY OF SCATTERED GAMMA-RAYS  
FROM A COLLIMATING LEAD CASTLE\*

Jae Shik Jun

Korea Atomic Energy Research Institute

The paper on this subject was published in the Journal of the Korean Physical Society, Vol. 6, No. 1, P. 13, March, 1973 with an abstract as follows.

Collimated gamma-ray beams from Cs-137 and Co-60 sources contained in a lead castle are commonly used for calibration of various health physics instruments. Such beams, however, carry not only primary radiations, but also include scattered components from the collimating lead castle. To determine the energy, relative amount, and exposure rate of the scattered radiations, a scintillation spectrometer of a  $1\frac{3}{4}$ " dia. X2" long NaI(Tl) well-type crystal (well size;  $\frac{2}{3}$ " dia. X $1\frac{1}{2}$ " long) was used with a 100 channel pulse height analyzer.

For the calculations of the exposure rate due to scattered photons, a simple spectrum-dose conversion method was applied instead of correcting the spectrum by response matrix. Prior to the conversion procedure, the value of the conversion operator,  $G(E)$ , was calculated as a function of photon energy, using the values of photofraction and interaction ratio determined for the scintillator used in this study. The results show that the relative contribution of the scattered photons to total exposure rate is - 2.25% regardless of the distance

from the source to the detecting position and that the scattered photons contributing to the collimated beams consist mainly of backscattered photons of an energy given by  $E_b = E_0 / (1 + 2E_0 / 0.51)$ .

- \* Part of this experiment was carried out at Laboratorio di Dosimetria e Standardizzazione, Centro Studi Nucleari della Casaccia, Rome, Italy during the period of 1966 to 1967 under the auspices of an IAEA Fellowship.

(14) ASYMMETRICAL ANALYSIS OF REACTOR LEAKAGE GAMMA-RAYS BY MEANS OF SCINTILLATION SPECTROMETRY

Jae Shik Jun

Korea Atomic Energy Research Institute

The paper on this subject was published in the Journal of the Korean Nuclear Society Volume 5, Number 4, P. 291. December, 1973. with an abstract as follows.

EXPOSURE RATES due to leakage gamma-rays from operating reactor KARA MARK II and III were measured in a horizontal plane by means of scintillation spectrometry using a 3" X 3" cylindrical NaI(Tl) detector associated with a 400 channel pulse height analyzer under varied conditions of reactor operation.

In determining exposure rate due to the leakage gamma-

rays at each point of measurement, Moriuchi's spectrum-exposure rate conversion theory was applied instead of using conventional response matrix method which necessitates very complicated procedures to convert a spectrum into exposure rate.

The results show that a basic pattern of "typical" spectrum of the reactor leakage gamma-rays is neither affected by thermal output of the reactor, nor influenced by overall attenuation in radiation intensity. It was indicated that the attenuation of the leakage gamma-rays in air in terms of exposure rate as a whole follows an exponential law, and the total exposure rate due to the leakage gamma-rays at a certain point is nearly proportional to thermal output of the reactor. The complexity in spectrum measured for a movable core reactor, TRIGA Mark III, was analyzed through spectrum resolution, and proper judgement of the leakage gamma-rays in a complex spectrum was discussed.

(15) GAMMA-RAY DOSIMETRY WITH THIN PLASTIC FILM

Young Soo Yoo and Seung Gy Ro  
Korea Atomic Energy Research Institute

The paper on this subject was published in the Journal of the Korean Nuclear Society Volume 5, Number 3, P. 233, September, 1973 with an abstract as follows.

Thirty two different kinds of domestic plastic films for use in measuring high gamma-ray dose have been collected and their dosimetric characteristics investigated with the help of a Co-60 gamma radiation source.

Among them a rigid polyvinyl chloride (PVC) film of 0.05mm in thickness which is manufactured by Lucky Chemical Co., Korea, seem to be the most suitable one for this purpose. The relation between optical density at 3100Å and radiation exposure in this PVC film was linear in the range of  $0.6 \times 10^6 R$  to  $1.3 \times 10^7 R$ , and also the film showed a good reproducibility within 9% under the standard experimental condition. The effect of absorbed dose, oxygen content of surrounding atmosphere and irradiation temperature have also been studied for this film. It appeared to have a good property in the dosimetric point of view.

(16) MEASUREMENT OF NEUTRON ENERGY SPECTRUM FROM AN  $^{241}\text{Am-F}$  NEUTRON SOURCE USING BONNER SPHERE NEUTRON SPECTROMETER

Seung Gy Ro and Jae Shik Jun  
Korea Atomic Energy Research Institute

The abstract on this subject was written in the Transactions of the Korean Physical Society, Spring Meeting, Seoul National University, April 27-28, 1973.

The neutron energy spectrum from an  $^{241}\text{Am-F}$  laboratory neutron source with the dimension of 4.85cm high by 2.24cm in diameter has been measured using a Bonner sphere neutron spectrometer which is a  $^6\text{LiI(Eu)}$  thermal neutron detector coupled with various polyethylene spheres of 2, 3, 5, 8, 10, and 12 in. in diameter.

Assuming that the entire spectrum consists of the Maxwellian thermal, uncollided and slowing-down components and that the former two components are invariable while the latter one is of the  $1/E^\alpha$  form with a spectral parameter  $\alpha$  which is variable, the relative intensities of three spectrum components were determined with three different sizes of polyethylene spheres. A determination of the parameter  $\alpha$  can be simply made from the ratio of counting rates in two different spheres. However, the value obtained from five independent determinations of  $\alpha$  with six spheres, which is agreeable with each other within the experimental error and consequently will be more rigorous compared to that obtained from the above two spheres, was finally taken in this study and is about 1.2. The result for the spectrum measurement is presented in the graphical form.

(17) DETERMINATION OF THE ALPHA PARTICLE TRACK REGISTRATING EFFICIENCY OF POSI-FILM

Seung Gy Ro and Jae Shik Jun  
Korea Atomic Energy Research Institute

The abstract on this subject was written in the Transactions of the Korean Physical Society, Fall Meeting, Ulsan Institute of Technology, October 26-27, 1973.

Photographic posi-film which is commercially available has been found to be a possible alpha particle detector in the course of looking for a suitable material to be applied to the neutron dosimetry, and its track registration efficiency for alpha particles has been determined. In order to determine the efficiency, the posi-film foil has been determined. In order to determine the efficiency, the posi-film foil has been irradiated to alpha particles emitted from a thin  $^{241}\text{Am}$  source entering the detector foil perpendicular to the surface. The irradiated foil has been etched in a  $1.3 \text{ g/cm}^3$  NaOH solution for 1 hour at about  $60^\circ\text{C}$ , and the diameter of the etch-pits was measured under an optical microscope. Therefrom, the efficiency was calculated on the basis of Fleischer's and Tuyn's theories. The result seems to be  $(78.8 \pm 4.7)\%$ , and to be agreed well with the value of  $(75.8 \pm 2.5)\%$  obtained by measuring the critical angle for the track registration.

(18) PROTECTIVE EFFECT OF ACETYLBENZOYLACONINE AGAINST  
GAMMA-RADIATION

Philip S. Moon

Korea Atomic Energy Research Institute

The paper on this subject was published in the Journal of the Korean Nuclear Society Volume 5, Number 2, P. 83, June, 1973 with an abstract as follows.

The protective effects of acetylbenzoylaconine, 2-aminoethylisothiuronium bromide hydrobromide,  $\beta$ -mercaptoethylamine HCL, and L-thiazolidine-4-carboxylic acid were studied on the white male mice, aged 5-6 weeks. The toxicity test of acetylbenzoylaconine revealed that the LD<sub>50</sub> was 2.5mg/kg of body weight. After the administration of test substances, mice were irradiated with whole body dose of 800 rad by the Co-60 source. Observing the number of surviving mice for 30 days, the survival coefficients for the test groups were calculated and with these the protective coefficients against radiation injury, PCR, were also calculated. The PCR values are 2.24, 2.95, 2.78, and 1.23 for acetylbenzoylaconine, 2-aminoethylisothiuronium bromide hydrobromide,  $\beta$ -mercaptoethylamine HCL, and L-thiazolidine-4-carboxylic acid respectively. These values reveal that the acetylbenzoylaconine has protective potency against radiation injury on white male mice.

(19) PENUMBRA EFFECT ON INTEGRAL ABSORBED DOSE IN Co-60  
TELEETHERAPY

Philip S. Moon

Korea Atomic Energy Research Institute

The paper on this subject was published in the Journal of the Korean Nuclear Society Volume 5, Number 2, P. 87, June, 1973 with an abstract as follows.

Due to the Co-60 source size, the penumbra in Co-60 teletherapy poses a serious problem, even if the extended collimators are used. Here an empirical formula for the calculation of integral absorbed dose in the penumbra region was derived. Through a numerical calculation, the penumbra effect on integral absorbed dose was investigated. The longer the source-to-skin distance, the larger the integral absorbed dose of penumbra region, and the larger the source diameter, the larger the integral absorbed dose of penumbra region. It was also found that in some case the integral absorbed dose in penumbra region becomes several times larger than the integral absorbed dose of treatment region itself if the source-to-skin distance becomes greater. Therefore, one must consider the penumbra effect in Co-60 teletherapy.



ANNUAL PROGRESS REPORT OF NUCLEAR PHYSICS DIVISION  
PAKISTAN INSTITUTE OF NUCLEAR SCIENCE & TECHNOLOGY  
P.O. NILORE, RAWALPINDI.

The nuclear research activities at PINSTECH are centred around a 5 MW swimming pool type of Research Reactor and a Neutron Generator of Texas Nuclear Corporation design. The main activities are summarised below:-

1. Total Neutron Cross-section Measurements.

A technique has been developed to measure total neutron cross-section for neutron energies from 1.7 MeV to 14.7 MeV using a neutron generator. Primary neutrons of energy 14.7 MeV from the neutron generator are elastically scattered from a plastic scintillator and the scattered neutrons, after transmission through the sample, are detected by a liquid scintillator. The change in neutron energy is obtained by changing the angle of scattering of the neutron beam. Time of flight technique and pulse shape discrimination are used for suppressing the background. Total neutron cross-sections have been measured for  $^{12}\text{C}$ ,  $^{27}\text{Al}$  and  $^{238}\text{U}$  at 12 different energies between 1.7 and 14.3 MeV. The energy resolution varies between 100 and 150 keV. This work has been published in Nuc. Inst. & Meth. 115, (1974) 345. Similar measurements are now being made on enriched tellurium isotopes  $^{128}\text{Te}$  and  $^{130}\text{Te}$ .

2. Neutron Induced Reactions.

Experiments are in progress to measure, at 14 MeV neutron energy, the differential cross-sections for  $(n, \alpha)$  reactions and the angular distributions of outgoing alpha particles. Previous measurements made on the  $^{58}\text{Ni}(n, \alpha)^{55}\text{Fe}$  reaction using emulsion plates were reported in Nuc. Phys. A202 (1973) 123. Work is now in progress on the  $^{28}\text{Si}(n, \alpha)^{25}\text{Mg}$  reaction using solid state detectors.

### 3. Thermal Neutron Capture in even A Neodymium isotopes.

The radiative capture of thermal neutrons in even A neodymium isotopes is being investigated with a view to study the behaviour of nuclei in the region of transition from spherical to deformed nuclear shapes. The gamma ray spectra from the capture of thermal neutrons in enriched  $^{142}\text{Nd}$  and  $^{144}\text{Nd}$  targets were measured in an external target geometry using a Ge(Li)-NaI(Tl) pair/anti-Compton spectrometer. In each case the gamma rays originating from the isotope of interest were identified by comparing the spectrum with that obtained with a natural neodymium target. The data on  $^{142}\text{Nd}(n, \gamma)^{143}\text{Nd}$  reaction has also been supplemented with  $\gamma$ - $\gamma$  coincidence measurements using two Ge(Li) detectors (The  $\gamma$ - $\gamma$  coincidence measurements were made at Kernforschungszentrum Karlsruhe). Preliminary decay schemes of  $^{143}\text{Nd}$  and  $^{145}\text{Nd}$  formulated on the basis of these measurements consist of fourteen previously unreported levels in the case of  $^{143}\text{Nd}$  and three such levels in the case of  $^{145}\text{Nd}$ . The Q values for the reactions  $^{142}\text{Nd}(n, \gamma)^{143}\text{Nd}$  and  $^{144}\text{Nd}(n, \gamma)^{145}\text{Nd}$  have been estimated as  $6122.7 \pm 0.5$  keV and  $5755.3 \pm 0.7$  keV, respectively. Further work on the decay schemes of  $^{143}\text{Nd}$  and  $^{145}\text{Nd}$  is in progress. Measurements are also being made for determining the spectra of gamma rays from thermal neutron capture in  $^{146}\text{Nd}$ .

### 4. Precise Energies of Gamma Rays from $^{15}\text{N}$ .

Prominent gamma rays from the reaction  $^{14}\text{N}(n, \gamma)^{15}\text{N}$  are commonly used for energy calibration in the (n,  $\gamma$ ) experiments. The energies of these gamma rays have been determined with improved precision on the basis of a precise knowledge of the binding energy of last neutron in  $^{15}\text{N}$  derived from mass spectrometric data. The work is being processed for publication in Nuclear Instruments & Methods.

### 5. Study of spontaneously Fissioning Heavy Elements.

This programme is directed towards the study of the properties of neutron rich fission fragments as well as the fission properties of spontaneously fissioning heavy elements. The experiment consists of a correlated three parameter study in which the two fission fragments are detected by a pair of surface barrier detectors and the gamma rays emitted by one of the fragments are detected by means of a high resolution (700 eV at 122 keV) Ge(Li) detector. The pulse heights from the three detectors for each triple coincidence are recorded event by event on a magnetic tape. Measurements have been completed for a  $^{252}\text{Cf}$  source and the data are being analysed on an IBM 360/44 computer. Similar measurements are now planned using a  $^{248}\text{Cm}$  source.

### 6. Neutron Diffraction Studies.

A triple axis spectrometer is being used for neutron diffraction and inelastic neutron scattering studies. Recently completed work consists of a measurement of the Debye Waller coefficient of KCl (to be published in Acta Crystallographica-A), and the determination of the unit cell dimensions of cellulose I (to be published in the Journal of Polymer Science, Physics Section). Experiments, now in progress, are aimed at a study of the phonon dispersion curves in a mixed alkali halide crystal  $\text{K}_{0.5}\text{Rb}_{0.5}\text{I}$ .



PROGRESS REPORT ON NUCLEAR  
DATA RESEARCH IN POLAND  
/ MAY 1973 - APRIL 1974 /

GATHERED BY  
A. MARCINKOWSKI

Editor's Note

This progress report on nuclear data from Poland /May 1973 - April 1974/ contains only information on research, which is closely related to the activities of the International Data Committee of the International Atomic Energy Agency in the field of neutron physics. It does not include any information about other works or research as for example in the field of charged particles, nuclear physics or the use of neutrons for solid state physics studies.

The individual reports are not intended to be complete or formal, and must not be quoted in publications without the permission of the authors.

Uwagi edytorów

Report ten zawiera głównie informacje w zakresie fizyki neutronowej przeprowadzonej /maj 1973 - kwiecień 1974/ i związanych z działalnością Komitetu Danych Jądrowych Międzynarodowej Agencji Energii Atomowej.

Pominęto wyniki badań w innych dziedzinach fizyki jądrowej, w tym również badań prowadzonych przy użyciu cząstek naładowanych oraz w zakresie fizyki cząstek elementarnych przy użyciu neutronów.

Poszczególne prace zawierają wstępne odwołania do wyników badań nie wyczerpujące poruszonych tematów i te powinny być cytowane bez uzyskania zgody autorów.

### Замечания от редакции

Сборник этот содержит сообщения о проведенных в Польше в период от мая 1973 до апреля 1974 исследованиях в области нейтронной физики, связанных с деятельностью Комитета по Ядерным Данным Международного Агентства Атомной Энергии.

В данных не включены результаты исследований с помощью заряженных частиц а также с области применения нейтронов в физике твердого тела. Доклады эти не являются полными и не рекомендуются ссылаться на них без согласия авторов.

CONTENTS

1. Differential Cross Sections for the  $(n, \alpha)$  Reactions Induced by 12 and 18 MeV Neutrons in Some Rare-Earth Nuclei
2. Differential Cross Sections of  $^{90}\text{Zr}(n, \alpha)$  Reaction at 14.1 MeV
3. Cross Sections for Fast Neutron Induced Reactions on  $^{85}\text{Rb}$ ,  $^{190}\text{Os}$  and  $^{192}\text{Os}$  Nuclei
4. Recent Studies on Polar Emission

DIFFERENTIAL CROSS SECTIONS FOR THE  $(n, d)$  REACTIONS  
INDUCED BY 14 AND 18 MeV NEUTRONS IN SOME RARE-EARTH  
NUCLEI

B. Głowacka, M. Jaskół, W. Oskiewicz, J. Pukiewicz,  
L. Szabo.

Institute of Nuclear Research, Dept. of Nuclear Reactions  
Warsaw

and

Institute of Experimental Physics, University of Warsaw

The absolute differential cross sections for the  $^{147}\text{Sm}/n, d/^{144}\text{Nd}$ ,  $^{151}\text{Eu}/n, d/^{148}\text{Pm}$ ,  $^{153}\text{Eu}/n, d/^{150}\text{Pm}$ ,  $^{161}\text{Dy}/n, d/^{158}\text{Gd}$  reactions at  $E_n = 14\text{ MeV}$  and  $^{153}\text{Sm}/n, d/^{150}\text{Pm}$ ,  $^{159}\text{Tb}/n, d/^{156}\text{Eu}$ ,  $^{163}\text{Dy}/n, d/^{160}\text{Gd}$ ,  $^{169}\text{Tm}/n, d/^{166}\text{Ho}$  reactions at  $E_n = 18\text{ MeV}$  have been measured by direct registration of alpha particles. The experimental arrangement used in the measurements is described in our earlier work [1]. The neutrons were obtained from the  $^3\text{H}/d, n/^4\text{He}$  reaction with deuterons accelerated in the 3 MeV Van de Graaff accelerator. The neutron flux was measured by counting the recoil protons from a thin polyethylene foil. Recoil protons were registered by a CsI(Tl) scintillator followed by photomultiplier and standard electronics. The absolute calibration of the monitor was performed by measuring of the 847 keV  $\gamma$ -transition in  $^{56}\text{Fe}$  produced in the  $^{56}\text{Fe}/n, p/^{56}\text{Mn}$  reaction with successive  $\beta$ -decay of  $^{56}\text{Mn}$ . The cross section for the  $^{56}\text{Fe}/n, p/^{56}\text{Mn}$  reaction was taken as 110 mb and 57 mb for neutron energies equal to 14 and 18 MeV respectively [2].

The investigated targets were made of oxides and deposited on the thick carbon backings by means of sputter



Table 1

Differential cross sections for  $^{147}\text{Sm}(n,\alpha)^{144}\text{Nd}$  reaction at 14.05 MeV

$E_{\alpha}/\text{MeV}/$	$\text{mb} \times \text{sr}^{-1} \text{MeV}^{-1}$	$E_{\alpha}/\text{MeV}/$	$\text{mb} \times \text{sr}^{-1} \text{MeV}^{-1}$
15.92	$116 \pm 66$	20.29	$326 \pm 31$
16.12	$75 \pm 63$	20.49	$263 \pm 30$
16.32	$149 \pm 58$	20.69	$215 \pm 29$
16.51	$123 \pm 56$	20.88	$168 \pm 25$
16.71	$130 \pm 52$	21.08	$113 \pm 21$
16.91	$119 \pm 57$		
17.11	$262 \pm 48$	21.28	$107 \pm 19$
		21.48	$89 \pm 18$
17.31	$186 \pm 46$	21.68	$102 \pm 15$
17.51	$173 \pm 43$	21.87	$124 \pm 20$
17.71	$161 \pm 41$	22.07	$103 \pm 13$
17.90	$144 \pm 38$	22.27	$110 \pm 17$
18.10	$173 \pm 41$	22.47	$79 \pm 15$
18.30	$152 \pm 37$	22.67	$79 \pm 15$
18.50	$247 \pm 39$	22.87	$46 \pm 11$
18.70	$238 \pm 35$	23.06	$36 \pm 10$
18.90	$247 \pm 37$		
19.09	$284 \pm 36$	23.26	$30 \pm 9$
		23.46	$44 \pm 11$
19.29	$260 \pm 33$	23.66	$66 \pm 14$
19.49	$237 \pm 32$	23.86	$85 \pm 15$
19.69	$274 \pm 32$	24.06	$45 \pm 11$
19.89	$363 \pm 34$	24.26	$15 \pm 7$
20.09	$303 \pm 32$	24.45	$5 \pm 4$

Cross section integrated in the 15.92-24.45 MeV range is equal to  $1.361 \pm 0.046 \text{ mb} \times \text{sr}^{-1}$ .

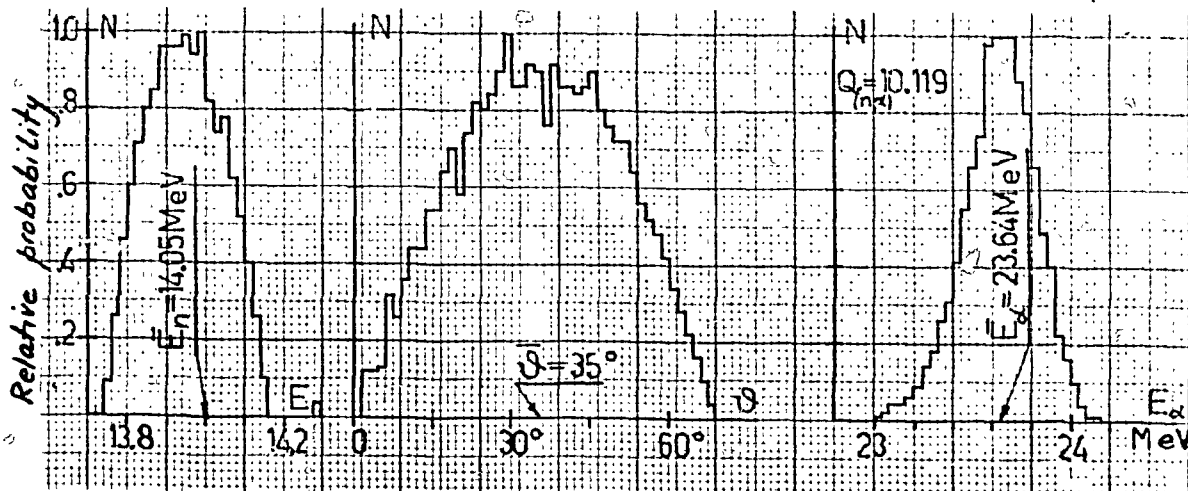


Table 2

Differential cross sections for  $^{151}\text{Eu}/n, \alpha/^{140}\text{Pr}$  reaction at 14.19 MeV

$E_{\alpha}/\text{MeV}/$	$\mu\text{b} \times \text{sr}^{-1} \text{MeV}^{-1}$	$E_{\alpha}/\text{MeV}/$	$\mu\text{b} \times \text{sr}^{-1} \text{MeV}^{-1}$
15.48	52±47	19.05	165±19
15.68	161±44	19.25	179±18
15.88	113±41		
15.98	45±33	19.44	164±17
16.28	85±36	19.64	198±17
16.47	92±34	19.84	195±17
16.67	101±31	20.04	176±16
16.87	158±30	20.24	193±16
17.07	166±29	20.43	138±14
17.27	132±25	20.63	114±13
		20.83	141±13
17.46	116±25	21.03	129±12
17.66	144±24	21.23	121±12
17.86	109±23		
18.06	140±23	21.42	146±13
18.26	161±21	21.62	122±12
18.45	162±21	21.82	91±10
18.65	171±20	22.02	32±7
18.85	179±19	22.22	0±5

Cross section integrated in the 15.48-22.22 MeV range is equal to  $0.928 \pm 0.029 \text{ mb} \times \text{sr}^{-1}$ .

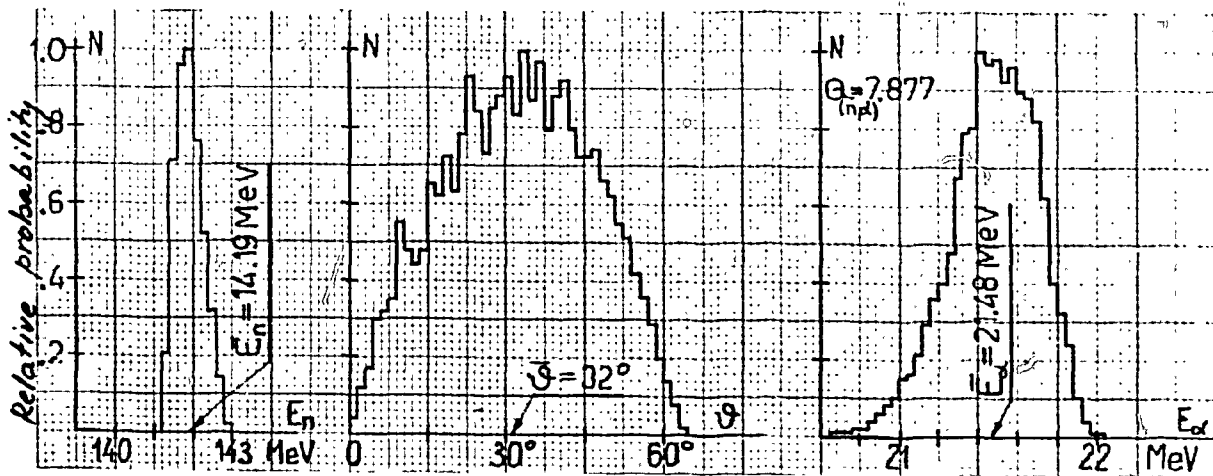


Diagram showing the dependence of the ratio  $\frac{d\sigma}{d\Omega} / \frac{d\sigma}{d\Omega}(\theta=0)$  on the angle  $\theta$  for  $E_n = 14.12$  MeV.

$\theta$ (deg)	$\frac{d\sigma}{d\Omega} / \frac{d\sigma}{d\Omega}(\theta=0)$	$\frac{d\sigma}{d\Omega} / \frac{d\sigma}{d\Omega}(\theta=0)$
0	1.0 ± 0.1	1.0 ± 0.1
10	1.0 ± 0.1	1.0 ± 0.1
20	1.0 ± 0.1	1.0 ± 0.1
30	1.0 ± 0.1	1.0 ± 0.1
40	1.0 ± 0.1	1.0 ± 0.1
50	1.0 ± 0.1	1.0 ± 0.1
60	1.0 ± 0.1	1.0 ± 0.1
70	1.0 ± 0.1	1.0 ± 0.1
80	1.0 ± 0.1	1.0 ± 0.1
90	1.0 ± 0.1	1.0 ± 0.1
100	1.0 ± 0.1	1.0 ± 0.1
110	1.0 ± 0.1	1.0 ± 0.1
120	1.0 ± 0.1	1.0 ± 0.1
130	1.0 ± 0.1	1.0 ± 0.1
140	1.0 ± 0.1	1.0 ± 0.1
150	1.0 ± 0.1	1.0 ± 0.1
160	1.0 ± 0.1	1.0 ± 0.1
170	1.0 ± 0.1	1.0 ± 0.1
180	1.0 ± 0.1	1.0 ± 0.1
190	1.0 ± 0.1	1.0 ± 0.1
200	1.0 ± 0.1	1.0 ± 0.1
210	1.0 ± 0.1	1.0 ± 0.1
220	1.0 ± 0.1	1.0 ± 0.1
230	1.0 ± 0.1	1.0 ± 0.1
240	1.0 ± 0.1	1.0 ± 0.1
250	1.0 ± 0.1	1.0 ± 0.1
260	1.0 ± 0.1	1.0 ± 0.1
270	1.0 ± 0.1	1.0 ± 0.1
280	1.0 ± 0.1	1.0 ± 0.1
290	1.0 ± 0.1	1.0 ± 0.1
300	1.0 ± 0.1	1.0 ± 0.1
310	1.0 ± 0.1	1.0 ± 0.1
320	1.0 ± 0.1	1.0 ± 0.1
330	1.0 ± 0.1	1.0 ± 0.1
340	1.0 ± 0.1	1.0 ± 0.1
350	1.0 ± 0.1	1.0 ± 0.1
360	1.0 ± 0.1	1.0 ± 0.1

Diagram showing the dependence of the ratio  $\frac{d\sigma}{d\Omega} / \frac{d\sigma}{d\Omega}(\theta=0)$  on the angle  $\theta$  for  $E_n = 19.52$  MeV.

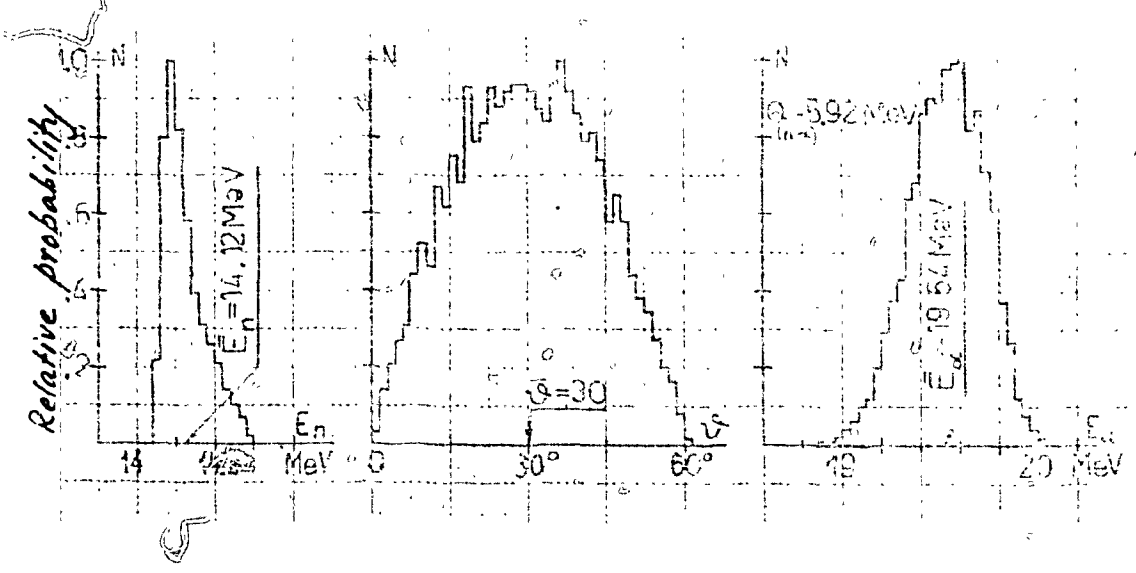




Table 5

Differential cross sections for  $^{153}\text{Eu}/n, \alpha / ^{150}\text{Eu}$  reaction  
at 18.17 MeV

$E_{\alpha}/\text{MeV}/$	$\mu\text{b} \times \text{sr}^{-1} \text{MeV}^{-1}$	$E_{\alpha}/\text{MeV}/$	$\mu\text{b} \times \text{sr}^{-1} \text{MeV}^{-1}$
18.84	$137 \pm 56$	22.03	$64 \pm 25$
19.04	$137 \pm 48$	22.23	$71 \pm 23$
19.24	$112 \pm 45$	22.43	$94 \pm 21$
19.44	$158 \pm 42$	22.63	$84 \pm 20$
19.64	$111 \pm 39$	22.83	$56 \pm 19$
19.84	$89 \pm 37$	23.03	$95 \pm 20$
20.04	$110 \pm 35$	23.23	$80 \pm 18$
20.24	$132 \pm 33$	23.43	$107 \pm 18$
20.44	$145 \pm 32$	23.63	$96 \pm 18$
20.64	$66 \pm 30$	23.83	$51 \pm 15$
20.84	$75 \pm 30$	24.03	$63 \pm 15$
21.04	$115 \pm 28$	24.23	$35 \pm 13$
21.23	$21 \pm 28$	24.43	$13 \pm 12$
21.43	$72 \pm 27$	24.63	$0 \pm 10$
21.63	$104 \pm 26$	24.83	$4 \pm 7$
21.83	$123 \pm 24$		

Cross section integrated in the 18.84-24.83 MeV range  
is equal to  $0.526 \pm 0.032 \text{ mb} \times \text{sr}^{-1}$ .

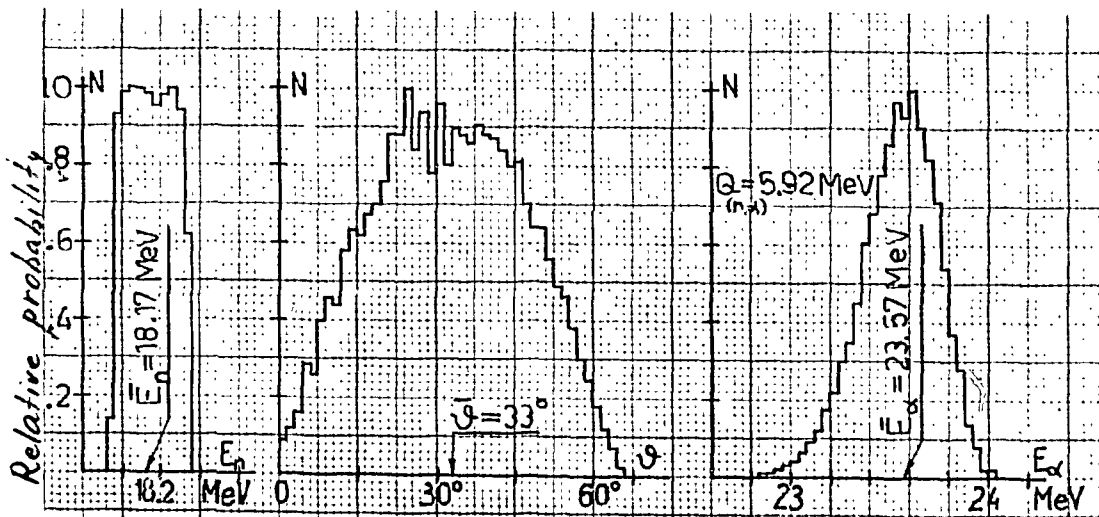


Table 6

Differential cross sections for  $^{159}\text{Tb}/n, \alpha/^{156}\text{Eu}$  reaction  
at 18.17 MeV

$E_{\alpha}/\text{MeV}/$	$\mu\text{b} \times \text{sr}^{-1} \text{MeV}^{-1}$	$E_{\alpha}/\text{MeV}/$	$\mu\text{b} \times \text{sr}^{-1} \text{MeV}^{-1}$
18.85	203±48	22.22	94±21
19.04	149±45	22.42	103±21
19.24	101±43	22.62	84±20
19.44	155±41	22.82	86±18
19.64	238±39	23.02	61±17
19.84	152±37	23.21	103±18
20.04	122±36	23.41	69±16
20.24	175±33	23.61	54±15
20.43	164±33	23.81	12±14
20.63	102±31	24.01	10±13
20.83	84±29	24.21	4±12
21.03	84±28	24.41	26±12
21.23	76±27	24.61	16±11
21.43	106±26	24.80	0±9
21.63	111±25	25.00	0±9
21.82	79±24	25.20	11±9
22.02	83±23		

Cross section integrated in the 18.85-25.20 MeV range is equal to  $0.586 \pm 0.031 \text{ mb} \times \text{sr}^{-1}$ .

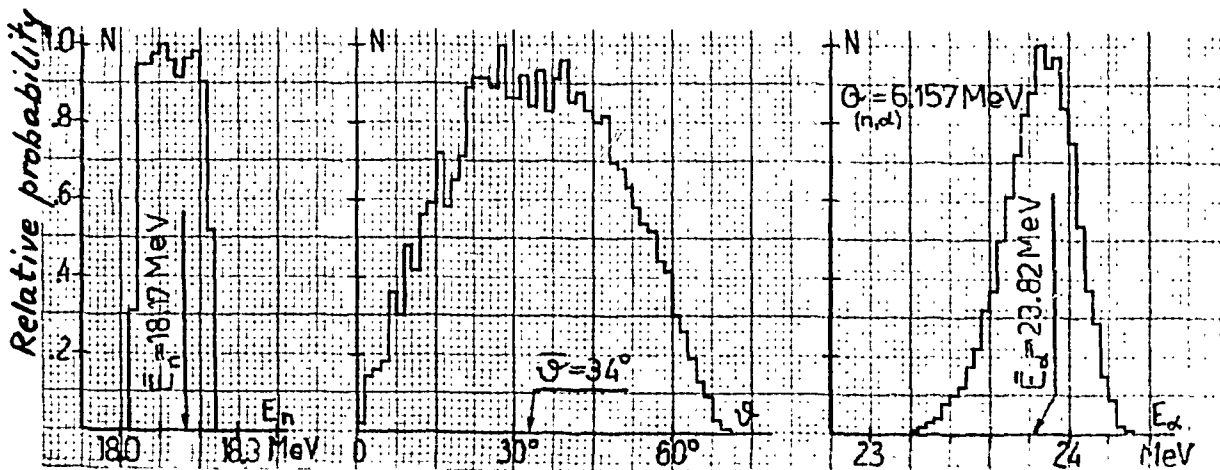
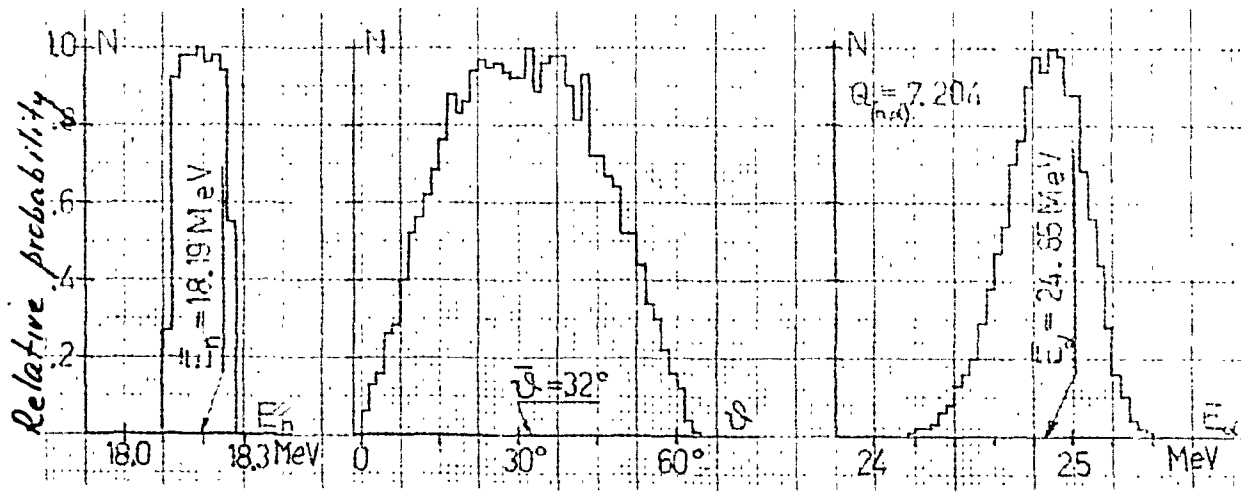


Table 7

cross section  $\sigma$  in barns for  $^{103}\text{Rh}(n, \alpha)^{101}\text{Ru}$  reaction  
 at  $18.19 \text{ MeV}$

$E_n$ (MeV)	$\mu_b \times 10^{-1} \text{ barn}^{-1}$	$E_n$ (MeV)	$\mu_b \times 10^{-1} \text{ barn}^{-1}$
18.00	100 ± 56	23.47	80 ± 24
19.00	84 ± 51	23.67	111 ± 33
19.20	160 ± 43	23.77	12 ± 21
19.40	151 ± 46	23.96	15 ± 11
19.60	145 ± 43	23.26	12 ± 10
19.80	136 ± 41	23.46	12 ± 11
20.00	127 ± 37	23.55	12 ± 11
20.20	161 ± 36	23.76	61 ± 15
20.40	145 ± 36	24.06	32 ± 16
20.60	133 ± 34	24.26	12 ± 13
20.80	147 ± 33	24.45	40 ± 13
21.00	40 ± 30	24.75	27 ± 11
21.20	130 ± 30	24.95	20 ± 11
21.40	127 ± 29	25.05	10 ± 10
21.60	131 ± 27	25.25	7 ± 9
21.80	11 ± 17	25.45	0 ± 9
22.00	100 ± 29	25.65	15 ± 8
22.20	130 ± 24		

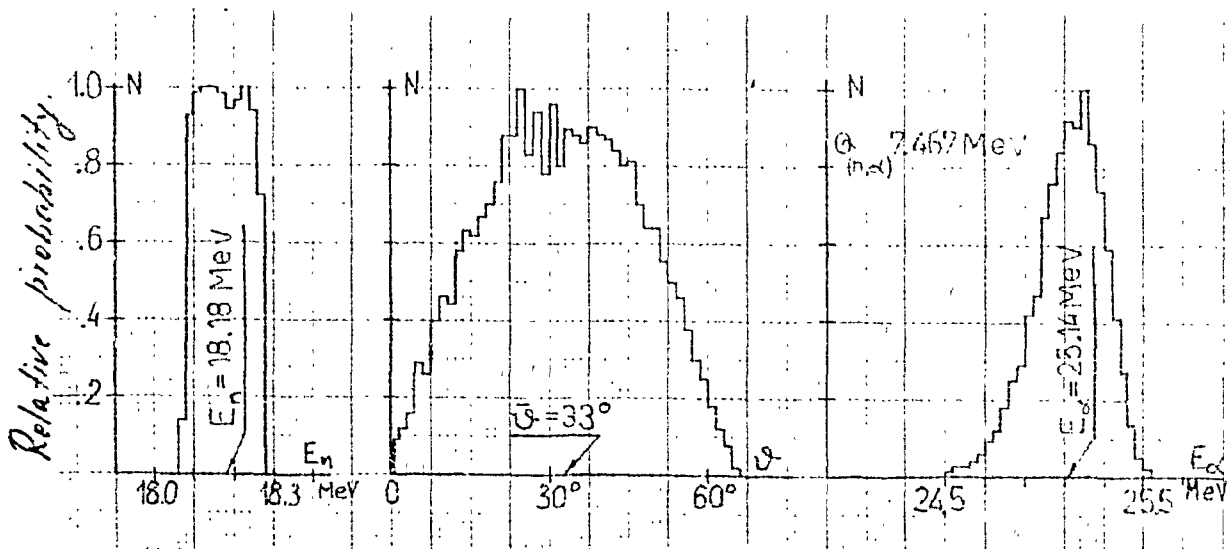
Cross section integrated in the 23.40-25.65 MeV range is equal to  $0.581 \pm 0.035 \text{ barn}^{-1}$ .



Differential cross section for  $^{16}\text{O}(\alpha, n)^{19}\text{F}$  at  $\theta = 33^\circ$

$E_\alpha$ (MeV)	$\sigma$ ( $\text{mb} \cdot \text{sr}^{-1}$ )	$E_n$ (MeV)	$\sigma$ ( $\text{mb} \cdot \text{sr}^{-1}$ )
18.38	$110 \pm 36$	23.7	$11 \pm 11$
19.38	$110 \pm 35$	23.7	$10 \pm 11$
19.38	$110 \pm 31$	23.7	$10 \pm 11$
19.38	$110 \pm 31$	23.7	$10 \pm 11$
19.38	$110 \pm 30$	23.7	$10 \pm 11$
19.38	$110 \pm 31$	23.7	$10 \pm 11$
19.38	$110 \pm 31$	23.7	$10 \pm 11$
19.38	$110 \pm 31$	23.7	$10 \pm 11$
20.38	$100 \pm 25$	24.2	$11 \pm 11$
20.38	$100 \pm 24$	24.4	$11 \pm 11$
20.38	$100 \pm 23$	24.6	$11 \pm 11$
21.38	$100 \pm 23$	24.8	$11 \pm 11$
21.38	$100 \pm 22$	25.0	$11 \pm 11$
21.38	$100 \pm 21$	25.2	$11 \pm 11$
21.38	$100 \pm 20$	25.4	$11 \pm 11$
21.38	$100 \pm 19$	25.6	$11 \pm 11$
21.38	$100 \pm 18$	25.8	$11 \pm 11$
21.38	$100 \pm 17$	26.0	$11 \pm 11$
21.38	$100 \pm 17$	26.2	$11 \pm 11$

Cross section integrated in the 18.86-26.21 MeV  $\alpha$  range is equal to  $0.534 \pm 0.025 \text{ mb} \cdot \text{sr}^{-1}$ .



DIFFERENTIAL CROSS-SECTION OF  $^{10}\text{B}(n, \alpha)^{7}\text{Li}$  REACTION AT  
14.1 MeV

B. Gurevich, R. Ruzel, W. Gurev, I.M. Partic, etc.,  
A. Andrievskii and P. Zupanski

Institute of Nuclear Research, Dept. of Nuclear Reaction,  
Warsaw

A telescope system of two gas proportional counters followed by a silicon surface barrier detector has been used for the study of the  $^{10}\text{B}(n, \alpha)^{7}\text{Li}$  reaction induced by fast neutrons.

Neutrons were obtained from the  $^3\text{H}(d, n)^4\text{He}$  reaction. Neutron flux was monitored by counting the  $\beta$ -radiation from thin polyethylene foil in a Cd/Pb scintillator. The absolute calibration of monitor efficiency was performed by activation method using the  $^{20}\text{Po}(n, p)^{19}\text{Mn}$  reaction.

A Monte Carlo simulation technique was used to determine the solid angle and the energy and angular resolution of the experimental system.

The investigated target was evaporated on a tantalum backing and placed in an iron holder. Its position inside the counter telescope could thus be changed with help of a magnet.

The background was measured replacing the investigated target by its tantalum backing.

During experimental runs data were stored



CROSS SECTION FOR FAST NEUTRON INDUCED REACTIONS

<sup>85</sup>Rb, <sup>130</sup>Cs AND <sup>137</sup>Cs ISOTOPES

W. Augustyniak, J. Bielicki, I. Borkowski, J. Kowalski

Institute of Nuclear Research, Central Institute of Physics, Warsaw

Samples of natural high purity Rb, Cs and Bi were irradiated with neutrons from the <sup>235</sup>U/1.07 reactor. The identification of reaction products in the samples was carried out by means of alpha-ray spectroscopy.

The neutron energy in the range 13.0-17.5 MeV was selected by suitable choice of the moderator thickness. The reaction final products were identified by their characteristic gamma-ray transitions. The gamma-ray activities were measured with a Ge(Li) detector. The relative detector efficiency of the Ge(Li) detector in the gamma-ray energy range from 50 keV to 2 MeV was determined using the known intensity relations of gamma-rays from <sup>226</sup>Ra and <sup>137</sup>Cs sources 1,2/.

In the case of indium samples the 4.4 h-305 keV and the 35.4 h-550 keV gamma-ray activities were measured, and the populations of the final nuclei of the <sup>115</sup>In(n,α) reactions were extracted, respectively. In Cadmium the cascade of 617, 503 and 361 keV gamma-rays, which decay with a half-life 9.9 min, was followed. The measurements were referred to the activities induced in the monitoring reactions: <sup>56</sup>Fe/n,p/<sup>56</sup>Mn 3/ for reactions in <sup>85</sup>Rb and <sup>64</sup>Zn/n,2n/<sup>63</sup>Zn 4/ for reactions in Cs isotopes.

Results of our measurements are presented in Table 1. The curves shown could be attributed to errors, comparison of detection efficiency and amount of the released nuclei. The decay characteristics of the possible nuclei listed in the present data analysis are those of Lederer et al. (5).

List of references.

1. Nuclear Data Table A-1, 3 1-2, October 1970.
2. P. Alexander and F. Boehm, Nucl. Phys. 49 /1963/ 103.
3. IRL 225 Supplement 32, p. 30-64-2.
4. D.C. Bentley and J.P. Butler, Can. J. Phys. 42 /1964/ 1030.
5. C.E. Lederer, J.M. Hollander and I. Perlman, Table of Isotopes, Wiley Sons, New York.

Table 1

$E_n \pm \Delta E_n$ MeV	$\sigma_{(n,p)} / \sigma_{(n,d)}$ $\sigma \pm \Delta\sigma$ mb	$\sigma_{(n,d)}$ $\sigma \pm \Delta\sigma$ mb
$13.0 \pm 0.1$	$4.0 \pm 0.7$	$2.1 \pm 0.1$
$13.3 \pm 0.1$	$4.1 \pm 0.9$	$3.1 \pm 0.1$
$14.5 \pm 0.1$	$3.7 \pm 0.5$	$3.3 \pm 0.5$
$15.0 \pm 0.2$	$1.2 \pm 1.0$	$3.3 \pm 0.3$
$15.5 \pm 0.2$	$4.3 \pm 0.5$	$2.6 \pm 0.2$

$E_n \pm \Delta E_n$ MeV	$\sigma_{(n,p)}$ $\sigma \pm \Delta\sigma$ mb	$E_n \pm \Delta E_n$ MeV	$\sigma_{(n,\alpha)}$ $\sigma \pm \Delta\sigma$ mb
$13.0 \pm 0.1$	$12.3 \pm 1.4$	$16.6 \pm 0.1$	$19.1 \pm 1.0$
$13.3 \pm 0.1$	$11.7 \pm 1.3$	$17.3 \pm 0.1$	$40.0 \pm 7.0$
$13.7 \pm 0.1$	$14.9 \pm 2.3$	$17.8 \pm 0.1$	$61.3 \pm 7.1$
$14.5 \pm 0.1$	$13.0 \pm 1.8$		
$15.1 \pm 0.2$	$13.4 \pm 1.7$		
$15.4 \pm 0.2$	$12.3 \pm 1.9$		
$16.0 \pm 0.2$	$10.7 \pm 1.3$		

\*) The  $(n,3n)$  reaction cross sections were obtained assuming a constant value of the  $(n,n')$  reaction cross section on  $^{190}\text{Os}$  in the neutron energy range 16.6 - 17.8 MeV.

RECENT STUDIES ON POLAR EMISSION +/

E. Piasecki, M. Dakowski and A. Kordyas

Institute of Nuclear Research, Dept. IA

05-400, Świerk near Warsaw, Poland

Revised Abstract

The intensities and spectra of the polarly emitted protons, deuterons, tritons and  ${}^6\text{He}$  particles have been investigated in the slow neutron fission of  ${}^{235}\text{U}$ . The intensities of these particles relative to the alpha particle polar emission are  $21.5 \pm 1.5$ ,  $2.75 \pm 0.5$  and  $7.3 \pm 0.9$  per cent and the mean kinetic energies are equal to  $10 \pm 0.5$ ,  $11 \pm 0.5$  and  $13 \pm 0.5$  MeV, respectively. Not one polar  ${}^6\text{He}$  event was detected per 1600 polar alphas. These results are compared with the theoretical predictions based on the evaporation hypothesis of the polar emission. The phenomenon can partly be explained using this hypothesis, but some puzzling disagreements with theory have been observed.

---

+/ This work has been carried out under the International Atomic Energy Agency Contract No. 1126/RC.

The angular and energy distributions of alpha particles emitted during fission suggest that the time and place of emission is somewhere in the vicinity of the scission point. However, recent measurements have proved [1-4] that at a certain proportion  $\alpha$ -particles are flying along the fission axis, which is difficult to interpret assuming the usual tripartition mechanism. Calculations of the classical trajectories have shown that alpha particles emitted from the neck (or more generally - from the inner part of the two-fragment system) would be deflected off the fission axis due to the fragment Coulomb forces. For these particles shadow cones would exist, centered along the fission axis, on the outer sides of the system.

The experimental facts regarding this phenomenon, which is referred to as "polar emission", are briefly as follows: its intensity determined on the basis of angular distribution [2] is of about 2% of the total tripartition rate, thus it occurs once per 25 thousands of fissions; emission along the light fragment trajectory is over 3 times as frequent as that in the opposite direction, the mean energy of  $\alpha$ -particles being about 23 MeV; the mean masses of fragments are in this process similar to the ones observed in binary fission,

but the mean kinetic energy of the fragments flying in the direction of the alphas is diminished by about 12 MeV (as measured for the light fragments). We performed extensive calculations [2,5] trying to verify the hypothesis that the polar emission is the result of the in-flight evaporation from the excited fission fragments. We are able to explain quantitatively the mean masses of fission fragments in this process, the energy spectra of alphas emitted in both directions as well as the intensity of emission in the heavy fragment flight direction without applying parameter fitting. The observed large anisotropy of polar alpha particles emission in the fragment reference system and the intensity of emission from the light fragments are difficult to interpret. This intensity appeared to be about 12 times greater than that calculated.

It was possible to explain the latter fact by taking into account the deformation of light fragments, however, this explanation was uncertain because of the approximation used as well as of the sensitivity of the results to the parameter uncertainties.

Basing on the evaporation hypothesis it was possible to predict [2,5] the intensity and spectra of particles other than alphas. To verify these predictions we performed an experiment in which we searched for the

polar protons, deuterons, tritons and  ${}^6\text{He}$ .

The experimental set-up was briefly as follows: the  ${}^{235}\text{U}$  target was irradiated in the reactor neutron beam, the polar particles were identified and their intensities and spectra were measured using a solid state telescope and the two-parameter analyser in E- $\Delta$ E configuration gated by fission fragments. Geometry of experiment is shown in Fig. 1. Here the preliminary results are reported.

As regards the  ${}^6\text{He}$  particles, our calculations [2,5] indicate that these particles would be practically absent in the shadow cones, the predicted intensity being of the order of  $10^{-3}$  per cent of the polar alphas, and this can be compared with the 1 per cent relative intensity in normal tripartition. During our measurements we registered 1600 polar alphas and not a single polar  ${}^6\text{He}$  event, which at least does not contradict our prediction. The calculated results for p,d,t are somewhat shifted towards higher energies as compared with the experimental spectra (Fig. 2). These differences go beyond experimental errors, what was already observed in  $\alpha$ -polar emission. In the latter case the agreement was improved when the fact of fragment deformation was taken into account. The comparison of the predicted and measured intensities of polar particles in the fission

of  $^{236}\text{U}$  is shown in Fig. 3. It may be seen that the evaporation model accounts quite well without any parameter fitting for the relative intensities of polar emission of the particles examined, but all the theoretical results are too low by a factor of about four. The reason of this is not yet clear. In the case of alpha particles only a part of the discrepancy can be accounted for by the uncertainties of the model parameters. Most of it is connected with the emission from the light fragments, and we have linked it with their deformation. In the present experiment we did not differentiate between the fragments. However, according to our calculations, the inclusion of deformation into the evaporation model results in a substantial improvement of agreement with experiment for the alpha particles but not for protons, deuterons or tritons.

The main conclusions of this work are as follows:

1. There exists not only the alpha but also the proton, deuteron and triton polar emission. In fact, the proton polar emission intensity is of a magnitude comparable to the intensity of the normal proton tripartition.
2. Some of the predictions based on the evaporation hypothesis agree remarkably well with the experimental results, and this could hardly be purely

accidental. On the other hand the results of this experiment can be considered as an indication that either the approximation used when accounting for the deformation is in this case not applicable or the nature of polar emission is more puzzling than we have expected.

#### References

- 1 Piasecki, E., Dakowski, M., Krogulski, T., Tys, J. and Chwaszczewska, J., Phys. Lett., 33B /1970/ 568
- 2 Piasecki, E. and Błocki, J., Nucl. Phys. A128 /1973/ 381
- 3 Nadkarni, D.M., Kataria, S.K., Kapoor, S.S. and Rama Rao, P.N., Nucl. Phys. A196 /1972/ 209
- 4 Rajagopalan, M. and Thomas, T.D., Phys. Rev. C5 /1972/ 1402
5. Piasecki, E. and Błocki, J., Acta Phys. Pol. in press .

Figure captions

Fig. 1. Geometry of the experiment.  $\phi$  is the diameter.

Fig. 2. Calculated and measured spectra of polar particles.

Fig. 3. Comparison of the measured and calculated intensities of polar particles. Note that for alpha particles the disagreement is observed only for light (L) fragments.

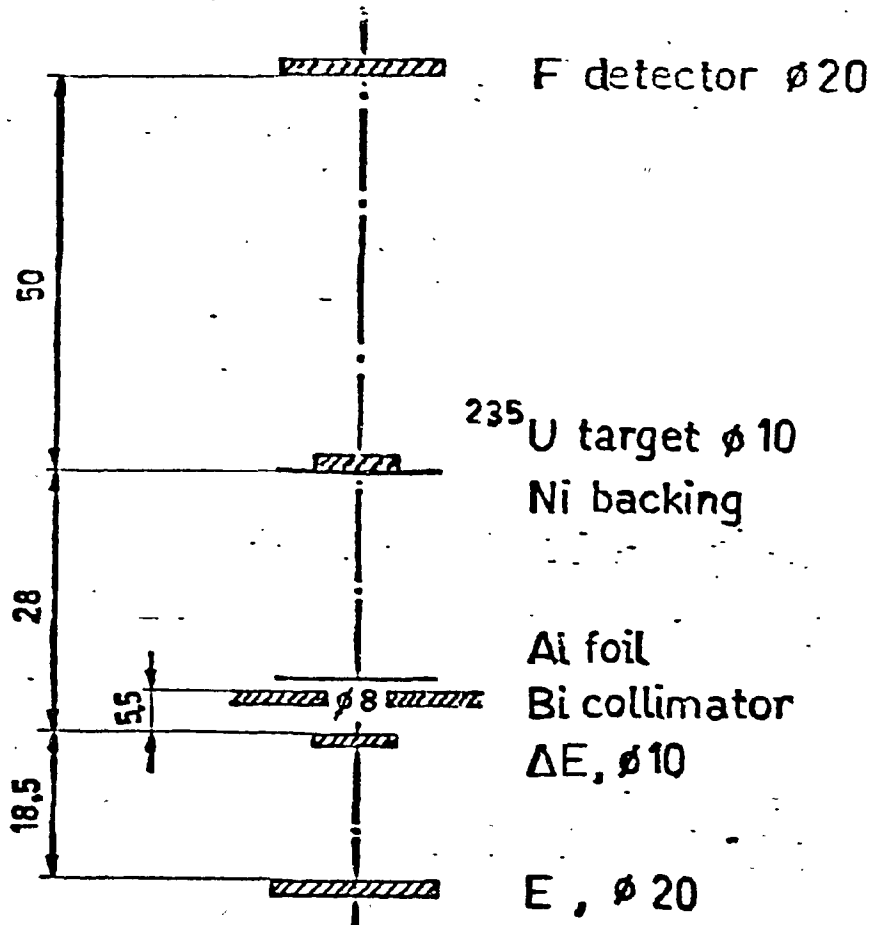


Fig 1

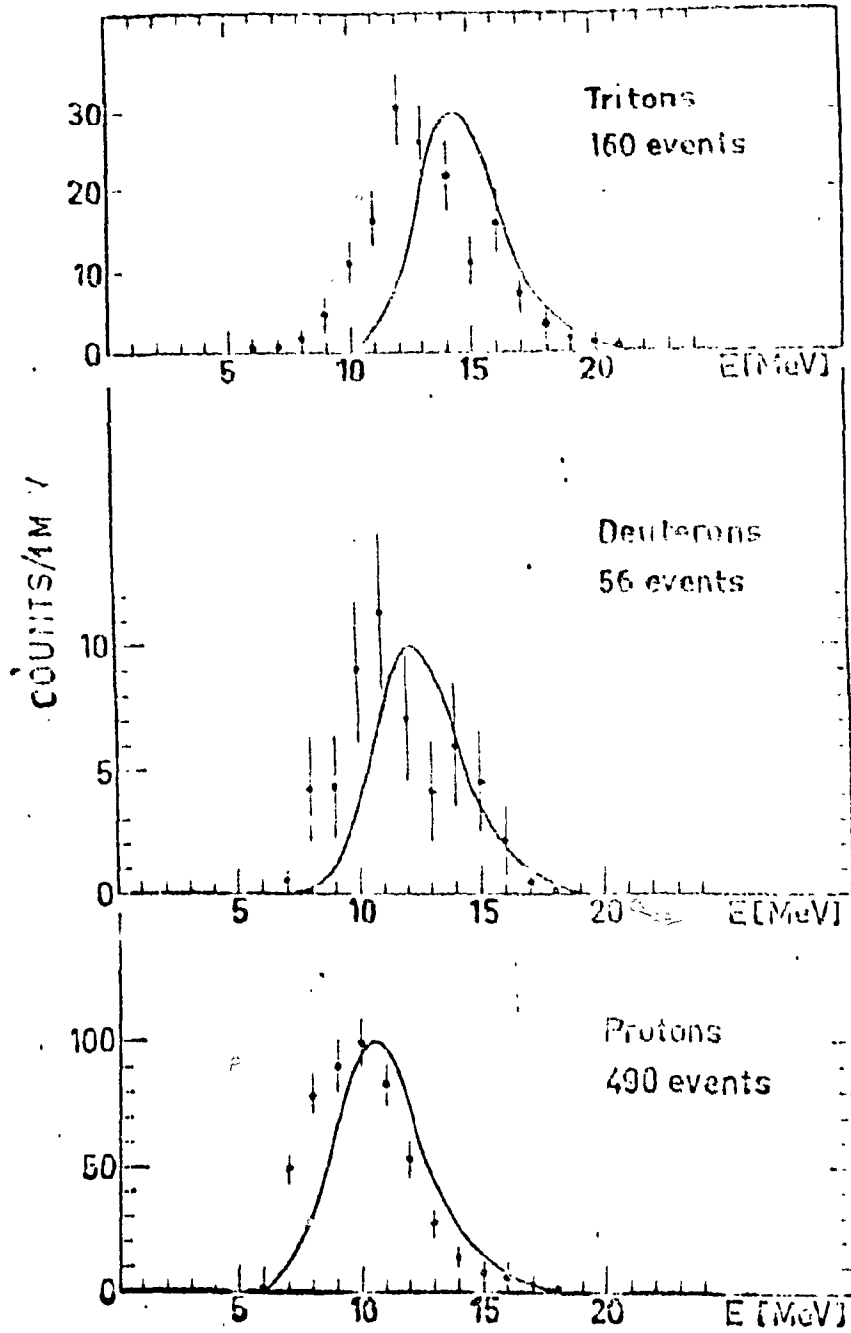


Fig. 2

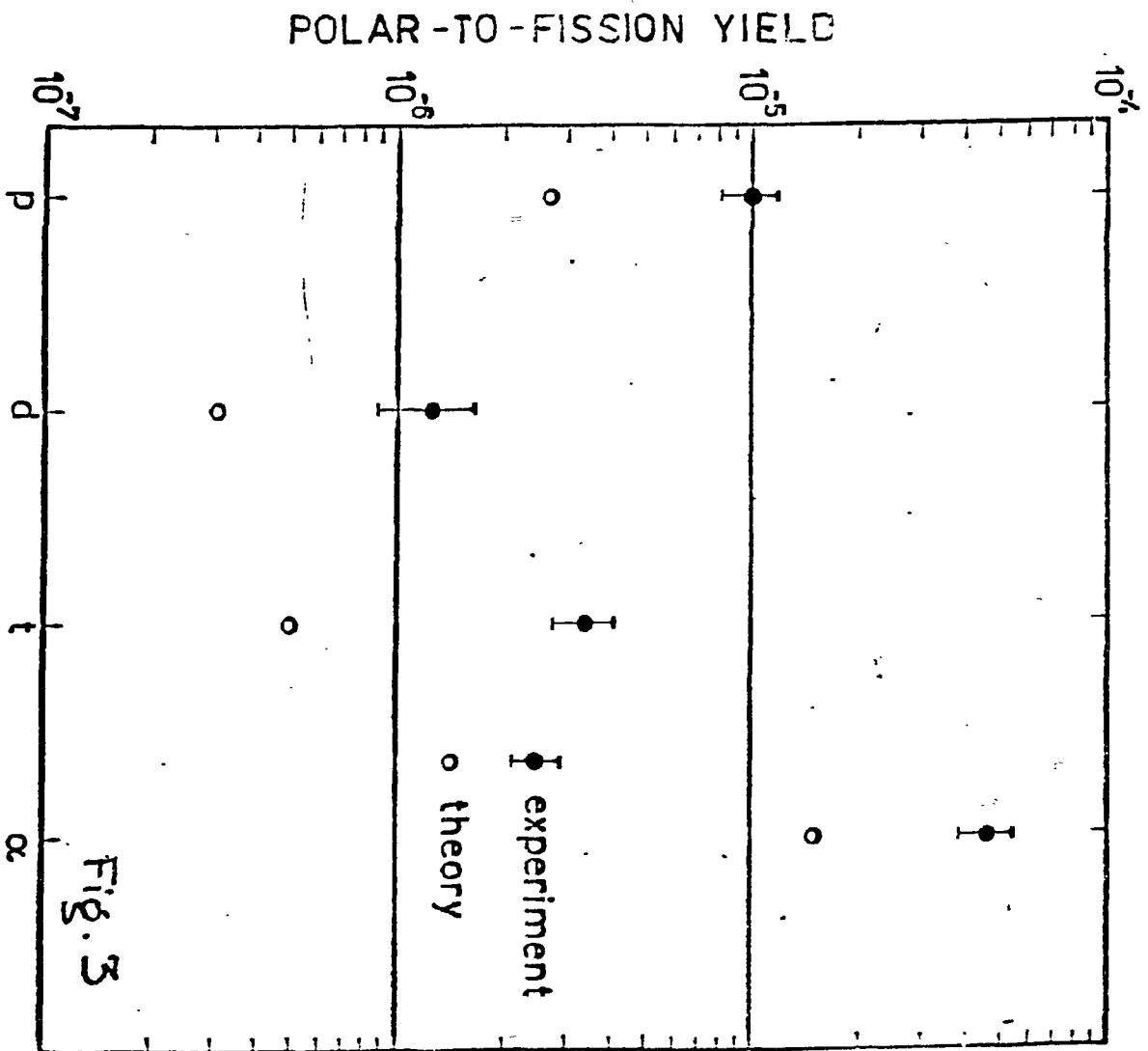
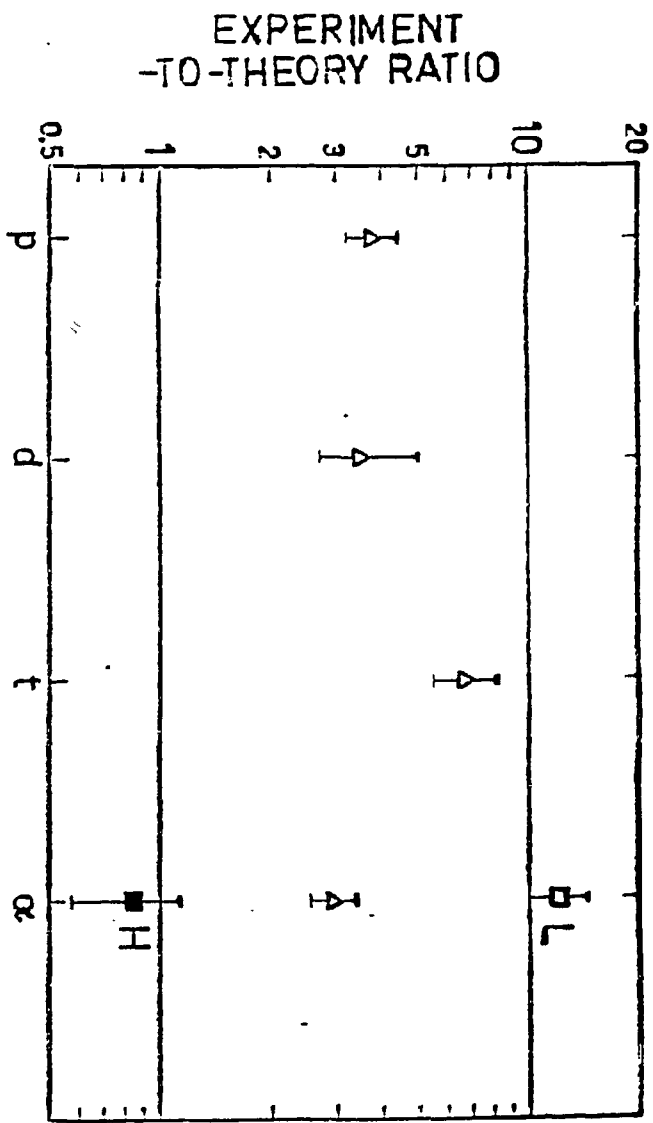


Fig. 3

STATE COMMITTEE FOR NUCLEAR ENERGY

PROGRESS REPORT  
ON NUCLEAR DATA IN ROMANIA  
during the year 1973

Compiled by  
S. RAPEANU

BUCHAREST, 1974

## Introduction

The Progress Report on Nuclear Data Activities in Romania covers the work done during the year of 1973 as follows:

- A short review on nuclear data activities in the Institute for Atomic Physics concerning: facilities, experiments, carrying on, compilation and evaluation activities, as well as the activity regarding the forming of a library with evaluated microscopic nuclear data;

- A short review on nuclear data activities in the Institute for Nuclear Technology, concerning: facilities, evaluations and the activities regarding the computing of the multigroup constants;

- Individual reports concerning certain results for nuclear data in the field of thermal and fast neutrons, both the Institute for Atomic Physics and the Institute for Nuclear Technology.

The individual reports are not intended to be complete or formal. Consequently, they must not be quoted, abstracted or reproduced without the permission of the authors.

A.Short Review on Nuclear Data Activities in the Institute for Atomic Physics - P.O.Box 35, Bucharest, Romania.

The theoretical and experimental researches on nuclear data in Romania develop according to the National Nuclear Programme, in agreement with our necessities and at the same time according to the Wrenda request of data.

The improve of experimental methods, the acquisition of more accurate nuclear data, the covering of the experimental gaps in literature, are only a few of the ideas which form the basis of our research.

The greatest part of these activities in Romania are carried out in the Institute for Atomic Physics and in the Institute for Nuclear Technology, as well as in other Institutes in Romania.

The main facilities for the experimental research in this field and for the data processing are the following:

- the VVR-S nuclear reactor operating with 10% enriched U, and using water as a moderator. Its present power is of 3.5 MW, and has a thermal flux of  $2 \cdot 10^{13}$  n/cm<sup>2</sup>sec. (These characteristics will be improved in the next future by employing certain new fuel cans).

The most important research equipment available at the reactor consists in neutron crystal and time-of-flight spectrometers, neutron monochromators, diffractometers and neutron polarizers,

- a U-120 type cyclotron accelerating charged particles at different energies (from 3 to 13 MeV for protons, 6-13 MeV for deuterons and 12-20 MeV for  $\alpha$ -particles).

- the Van-de-Graaff electrostatic accelerator of the Tandem type, model FN-15 (USA), accelerating protons at an energy of 4-15 MeV, producing a beam of a 5 mm diameter and 4-8  $\mu$ A intensity.

- 3 betatrons, having a maximum accelerating energy of 8.15 and 25 MeV.

- a linear accelerator for electrons of a 2.2-3.1 MeV energy.

- several other neutron generators (both native and imported) and a  $\gamma$  source of cobalt-60 having a 10,000 Curie activity.

- two subcritical assemblies, one of them with enriched U-graphite and the other with natural U-water and a zero power reactor with enriched U-light water.

- different types of lasers (with Helium-Neon,  $\text{CO}_2$ , ionized argon or Cd vapours).

- two "on-line" computers for various experimental facilities of the PDP-8/1 and PDP-15/20 types.

- an electronic computer of the IBM-370/135 type, having  a memory of 192 K bytes, with working capacity on a virtual memory of 512 K bytes, and equipped with various peripherals (line-printer, disk, magnetic tapes and card-readers).

According to the annual research programme, a number of scientists have performed fundamental research activities by means of these facilities which have been of a particular interest as well as in other various economic fields such as: medicine, biology, industry, agriculture, etc.

A brief description of these activities in the Institute for Atomic Physics (I.A.P.) and in the Institute for Nuclear Technology (I.N.T.) is further presented:

Using the VVR-S nuclear reactor, a number of various scattering experiments and determinations of the scattering laws for thermal neutrons, on various liquids at low temperatures, as well as on metals (in solid and liquid states) and

alloys, by crystal and time-of-flight spectrometry techniques have been carried on.

In order to assure best working conditions at the I.A.P. cyclotron, six independent beams have been provided, so that certain permanent experimental facilities susceptible of a continuous improvement in the future, could be connected.

The following temperature measurements have been carried out in this direction: density and cross section measurements for the  $(p,n)$  and  $(\alpha,n)$  reactions for a number of nuclei specified in CINDA ( $^{156,157}\text{Tb}$ ,  $^{51}\text{V}$ ,  $^{56,57}\text{Fe}$ ,  $^{116,117,118,119}\text{Sn}$ ,  $^{115}\text{In}$ , etc.).

New fissionable isomers have been pointed out and their parameters have been also specified (excitation energies, spins, Coulombian barrier).

The codes library (coupled channels, DWBA, optical model, Hauser-Feshbach, special function subroutines, etc.) necessary in nuclear data processing, has been definitely set-up.

Quite a number of research activities have been initiated concerning the use of the I.A.P. cyclotron in simulating certain phenomena developing in fast reactor and in the study of the mechanical and electrical property variations of some alloys used in reactor construction.

Starting from 1974, the activity concerning the neutron nuclear data acquisition will develop on a larger scale alongside the development of the I.A.P. cyclotron. The elastic and inelastic angular distribution measurements of the 4-14 MeV neutrons on nuclei around Cd will be mainly considered in this view.

As far as the I.A.P. cyclotron is also concerned, the ion implantation technique will be developed as well, to be

used in the study and acquisition of certain special property materials.

Another application of the nuclear techniques will be represented by the "charged particle activation analysis (including also channeling)". It will be mainly used in analyzing the nuclear materials, their structure as well as their purity.

The research activities at work by now, will be further on developed taking also into consideration the CINDA suggestions.

As far as the non-neutron nuclear data acquisition is concerned, its volume and accuracy will obviously raise. This is possible, due to the commissioning of the I.A.P. 15 MeV tandem, last year.

A larger number of angular distributions for the following reactions will be thus obtained:  $(p, p')$ ,  $(\alpha, \alpha)$ ,  $(d, \alpha)$ ,  $({}^3\text{He}, \alpha)$ ,  $(p, \alpha)$ , etc. The life-times, electric and magnetic multipole momenta and some other parameters connected with the solid body properties will be further measured.

One important groups of research, with three betatrons of I.A.P., are related firstly with photonuclear reactions and photofission and secondly with measurement of other nuclear data (the betatron of 30 MeV).

The collective treatment of the photonuclear giant resonance has been successfully extended to take into account the dynamic deformation of the nuclear surface. This is accomplished by considering the coupling between the high energy dipole oscillations and the low-energy quadrupole surface vibrations.

The systematics of the giant electric dipole resonance, which characterizes the absorption of electromagnetic radiation

by nuclei in the energy range from about 10 to 30 MeV, is of great interest today especially in order to verify the theoretical predictions.

Applying the bremsstrahlung radiation in the study of photonuclear reactions, we have followed a systematic investigation of the structure of  $(\gamma, n)$  and  $(\gamma, \Sigma n)$  reaction cross section in order to test some nuclear models and to define the nature of the giant resonance phenomenon.

Research concerning the bremsstrahlung beam dosimetry, the shape of the beam and the processing of the experimental data has created the possibility for measuring the cross section curves for photonuclear reactions on light, medium, and heavy weight elements.

The results obtained in the Electron Accelerators Laboratory in the field of photonuclear reactions, proved that the electron accelerators represent a very efficient and suitable tool for studying the fine structure in the cross section for photonuclear reactions, due to their excellent energy resolution and stability. These results stimulated us to start a programme for calculating the inverse reaction cross sections using the experimental data already available.

For a nucleus having a ground state population of  $N-1$  neutrons, the  $(n, \gamma)$  capture reaction will give rise to an excited nucleus of  $N$  neutron population. The same nucleus can be obtained through excitation of a nucleus with  $N$  population by absorption of a gamma ray.

The use of photoneutron reaction cross sections for the evaluation of inverse reaction cross section  $(n, \gamma)$  comes out to fulfil one of the most promising applications of electron

accelerators. The  $(n, \gamma)$  cross section evaluation is based on the compound nucleus statistical model.

The main <sup>evaluation</sup> activity consists in forming a national library of evaluated microscopic nuclear data. The DANEM adjusted shape for data storage represents an adjustment of the ENDF/B system to our present possibilities and needs at the same time. The code system necessary for library use, has been also worked out (storage, retrieval, checking, fitting codes and plots). At present, the library contains evaluated data received from INDC-IAEA (the KEDAK data, some other data from UKNDL and ENDF/B).

During the year 1973 the compilation and evaluation of nuclear data has been developed both in the I.A.P. and abroad by our scientists in order to have a permanent up to date library of nuclear data for various internal users.

An important activity of compilation is being carried on at the "Joint Institute for Nuclear Research" - Dubna (S.U.) by the Romanian, Russian and Finnish specialists regarding "Compilation of the cross sections producing strange particles in interactions  $(\pi^+, p)$  EI - 7,380"; the reactions are ordered according to the incident particle masses, charges and momenta. At the same time, attention will be also paid to other reactions such as:  $(K^+, p)$ ;  $(K^-, p)$  and  $(pp)$ , in the future.

Actually, a Collaboration of the University of Bucharest, Dubna (JINR) and the Helsinki University (the BUDHE Collaboration) is collecting the data on cross-sections of strange particle production. In Dubna, one uses the facilities of the Laboratory of Computing Technique and Automation (the Computers BESM-6 for plotting on CALCOMP and the CDC-6200 for Tables).

In parallel was began an analysis of the compiled data

for the observation of regularities of the strange particle production. In a first compilation, was studied the systematics of multiplicity distributions of the  $K_S^0$ -meson and  $\Lambda$ -hyperon produced in high energy collisions and compared these data with the data for non-strange particle production "On multiplicity systematics of  $\pi^0$ ,  $K_S^0$  and  $\Lambda$  produced in high energy collisions". Also, was started the study of the dependence of the cross-sections for the strange particle production in respect with the center of mass energy in the framework of different theoretical models.

With the view of stimulating the activity of nuclear data, the lectures of the international school of "Nuclear Data for Reactors and Reactor Physics" hold in Bucharest in 1972 are printed in a book which we hope to be useful for young scientists.

As a measure of the attention which is paid to nuclear data compilation and evaluation in our country, I would like to mention the fact that during the last years a number of scientists from Romania have each spent a few months in various work centres, doing compilation and evaluation works.

In addition, for a more efficient coordination of nuclear data activities in our country (needs, measurements, compilations, evaluations), the Romanian Nuclear Data Committee was founded.

I would like to thank the specialists which accepted our scientists and offered them optimal conditions for their work.

I would also like to express my thanks to IAEA, and particularly to the Nuclear Data Section for the permanent and efficient help and cooperation in this field, and the hope that in the future they will be developed in the same way.

1. National libraries for evaluated nuclear data by

A.I.Bădescu S., N.Deciu, D.Gheorghe, N.Mateescu, S.Mateescu, S.Râpeanu - The paper shows a comparison of structures of different national libraries for evaluated nuclear data ENDF/B (USA), KEDAK (FRG), UKNDL (United Kingdom), and namely, concerning the following characteristics:

- The contents of the libraries;
- The rules for storage and classification of information;
- The identification of registered data;
- The processing of stored data;
- The physical support for the storage of information;

There are shown two different modes of storage standard (MAT, MF, MT, MR) and ALTERNATE (MF, MAT, MT). Finally there is a brief description of Romanian evaluated nuclear data library of the Institute for Atomic Physics, Bucharest.

After this comparative study it was decided to adopt the ENDF/B library's format, but slightly modified.

2. Physical data which are to be stored in evaluated microscopic nuclear data library DANEM - by A.I. Bădescu-S, S.Mateescu,

D.Gheorghe, N.Deciu - I.A.P. - C.P.Box-35, Bucharest. In this paper there are described the types of physical data which will be stored in the DANEM-I library and the specific modes for representation in this library. There are presented also the six basic files of the DANEM-I library. The first file is the first part of each evaluated data set for a named material and contains the general description of data and one dictionary, which adds all the files, the section types contained in each file and the number of records. File 1, contains only one

section with the possibilities for the entrance of other sections with data about the efficiency of fission products, number of neutrons per fission, decay chain, for a done nucleus, etc. The general description is given by Hollerith characters. After that, there are given technical informations about the structure of the card, in BCD type reading format, and about the content of the dictionary. File 2 contains the data about resonance parameters and has only one section. The neutron cross-sections are continued in file 3 which is divided in parts according with the cross section types and energies. The files 4 and 5 contain data for angular distributions of secondary neutrons  $(n, n)$ ,  $(n, n')$ , and energy distributions probability  $p(E \rightarrow E')$  and file 6 contains data about the scattering law of thermal neutrons.

3. The structure of evaluated microscopic nuclear data library - DANEM - by A.I. Bădescu S., S. Mateescu, D. Gheorghe, N. Deciu. - The necessities of design and researches in the field of nuclear reactors have requested during 1971-73, the achievement at I.A.P. of the first library for evaluated microscopic nuclear data, of our country the library DANEM-I. It is presented the storage system of the data according with the physical system or the "material" (nucleus, natural element, molecule or standard mixture), the corresponding data for one material being stored in files on the basis of the physical category (cross sections, resonance parameters). Each file is composed of a few sections each one containing data about a named type of reaction, neutron-material such as  $(n, n)$ ,  $(n, n')$ ,  $(n, \alpha)$ ,  $(n, 2n)$ . The data of the DANEM-I library have also digital indicators which show the position in the library, reaction type, the type of information and the material. In the next sections of the paper, the struc-

ture of the library, is shown in detail, namely, the identifiers, the measurement units, the type of interactions neutron-material, and the data which are interesting for reactors.

4. The set of programs to manipulate the evaluated microscopic nuclear data stored in computerized library DANEM-I - by S.Mateescu, A.I.Bădescu S., N.Deciu - There are described the programs which follow:

INDA - for the entrance of the evaluated nuclear data in the computer memory from the cards.

REZONANT - for the entrance of the evaluated resonance parameters from the cards. The entered data are stored on tapes.

REDA 1/A and REDA 2/B - are programs for the retrieval of evaluated nuclear data and resonance parameters - from a magnetic tape.

GRIM - is a program for the plotting of the evaluated nuclear data stored in DANEM-I library.

CORA 1/A - is a program for checking the data and for changing data on the magnetic tapes. In this paper there are presented the flow chart of the programs, and the indicators of the programs are presented in detail. There are shown also, the general forms of records and different files.

5. Optical model calculations for Cu 63 and Cu 65 in the energy range 1-15 MeV- by N.Iliescu, V.Benzi\*, E.Menapace\*, M.Motta\*- The optical model calculations have been considered starting from 1MeV for the following reactions: Total, elastic and differential elastic, nonelastic, and inelastic for the resolved levels,

---

\* - Centro di Calcolo (CNEN) - Bologna (Italy)

using a code for Optical Model. The main problem in the use of the optical potential is the determination of a proper trend for the complex potential in concordance with a satisfactory fit for the experimental data and a physical consistency for the behaviour for the real and imaginary parts of the potential vs. energy. We adopted the following energy dependence of the depths of the real and imaginary parts of the potential:

$$E \leq 4 \text{ MeV}, V = 54.96 - 4.14E + 0.877E^2 - 0.077E^3 \text{ (MeV)}$$

(E in MeV in lab.system)

$$E > 4 \text{ MeV} \quad V = 48.798 - 0.3306E \text{ (MeV)}$$

(E in MeV)

$$1 \text{ MeV} \leq E \leq 4 \text{ MeV} \quad W = -1.399 + 8.733E - 2.599E^2 + 0.267E^3$$

$$E \geq 4 \text{ MeV} \quad W = 9 \text{ MeV}$$

For the Cu isotopes it seems reasonable to assume a spherical symmetric potential adopted in our calculations with the Wood-Saxon form and a derivative surface absorption term. The following values have been adopted for the parameters:

$$\text{Spin orbit potential term } V_{so} = 6 \text{ MeV}$$

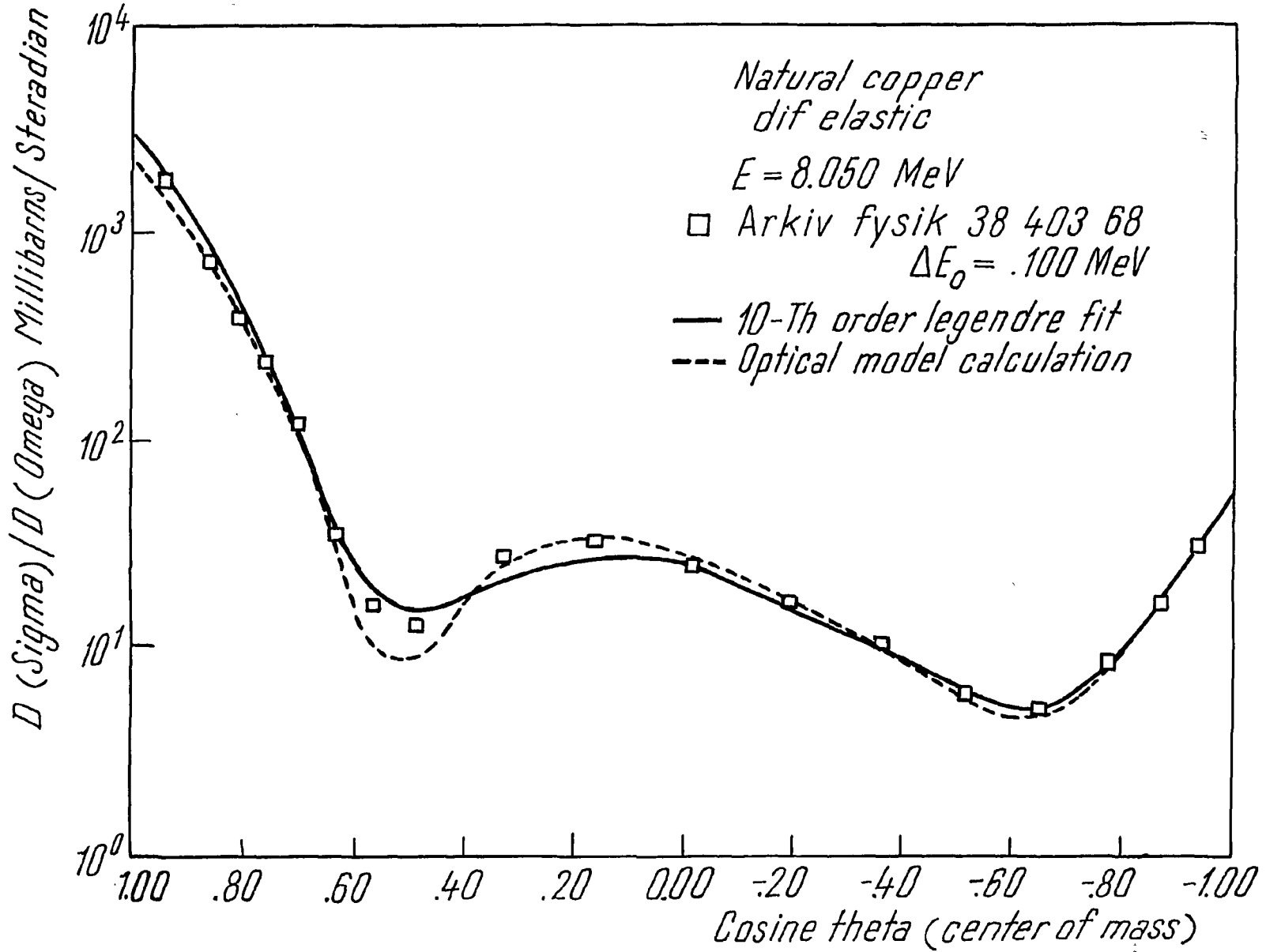
$$\text{Real potential radius } r_a = 1.25 F$$

$$\text{Imaginary potential radius } r_b = 1.25 F$$

$$\text{Real potential diffuseness } a = 0.68 F$$

$$\text{Imaginary potential diffuseness } b = 0.48 F$$

The elastic cross section can be calculated as a sum of the shape and compound parts. Differential elastic cross sections have been calculated in the following energy points for comparison with the experimental values: (MeV units): 1.016, 1.483, 2.032, 2.510, 3.047, 3.545, 4.063, 4.632, 5.079, 6.186, 7.161, 8.177, 14.729, 15.237. The non elastic cross section has been obtained by difference between the total cross section and the elas-



tic one. Inelastic cross sections for all the resolved levels of the two isotopes have been calculated by using the same spherical optical potential.

6. The evaluation of neutronic nuclear data for Berillyum by - N.Iliescu, N.Mateescu, S.Mateescu, E.Bădescu - In the programme of the nuclear data laboratory is included an evaluation of neutronic data for Berillyum, their writing in the ENDF/B format, their processing for engendering of the group constants in a number of groups corresponding to the needs of users. The compilation of data was made following the CINDA and the data provided by IAEA. In the range of resolved resonances was used a programme based on the single-level Breit-Wigner approximation. The experimental resonance parameters were obtained by the improvement of existing data in literature. This programme engenderes the cross section in a mesh of 40 points. In the range of thermal and fast neutrons the evaluation and the comparison with the theoretical models are in course.

7. The  $^{27}\text{Al}(n, \alpha)^{24}\text{Na}$  Cross Section - Evaluation of Experimental Data\* by G.Vasiliu - Investigating most of the existing experimental literature on  $^{27}\text{Al}(n, \alpha)^{24}\text{Na}$  reaction, through 1973, have been done an evaluation of the cross sections for this reaction from threshold 20 MeV, using the up-to date standards for renormalization using and experimental data selected according to the energy resolution and cross-section accuracy. The recommended curve was obtained by utilizing iterative graphics and

\* Work done during visit to the National Neutron Cross Section Center - Brookhaven National Laboratory, USA March-April 1974.

cubic spline fitting of data using a least square fitting criteria. A maximum value of 128.13 mb was obtained for the cross section at 13.52 MeV. With the evaluated curve, the microscopic integral cross section of  $^{27}\text{Al}(n,\alpha)^{24}\text{Na}$  reaction averaged in  $^{235}\text{U}$  thermal spectrum, was computed, on the basis of the simple fission spectrum formula. The value which was found is 0.732 mb for a spectrum "temperature" of 1.305 MeV in good agreement with the evaluated values of experimental integral data.

8. Fast neutron interaction with the  $\text{Be}^9$  nucleus, by V. Corcalciuc\*, B. Holmqvist\*\*, G.A. Prokopets\*\* and M. Wiedling\*\*\* -  
Regarding the interaction between neutrons and the  $\text{Be}^9$  nucleus there exist a few measurements of neutron elastic angular distributions but the experimental information on neutron inelastic ( $Q = - 2.43$  MeV) and  $(n,2n)$  reaction is rather poor. The aim of this work was to measure elastic and inelastic scattering from  $\text{Be}^9$  and also to study the continuum spectrum due to the  $(n,2n)$  processes in that nucleus. The measurements were carried out at 3.52, 4.20, 5.57, 6.08 and 7.01 MeV incident neutron energies using the T ( $p,n$ ) and D ( $d,n$ ) reactions as neutron sources. Angular distribution measurements of elastic and inelastic neutron scattering were performed in the angular range  $20^\circ$  to  $160^\circ$  in steps of  $10^\circ$ . Measurements were also made at 2.98 and 7.60 MeV incident energies at  $30^\circ$  and  $90^\circ$  in order to study the continuum spectrum. The spectra were recorded with standard time - of - flight technique together with a

---

\* On leave from Institute for Atomic Physics, Bucharest, Romania.

\*\* On leave from Kiev State University, Kiev, URSS

\*\*\* Neutron Physics Lab., Studsvik, Sweden

neutron detector with gamma discrimination properties. The flight path was 300 cm. The total energy spread was  $\pm 100$  keV. The neutron elastic angular distributions were analysed in terms of a standard spherical optical potential. The contribution due to compound contributions were calculated using the Hauser - Feshbach formalism. The elastic and inelastic angular distributions were calculated also using a optical model with collective effects. Also DWBA calculations were used taking the deformation of  $Be^9$  nucleus, into account.

9. A study of the  $(n, 2n \text{ gamma})$  reaction in the energy interval 16-20 MeV - by G.A.Prokopets\*, V.Corcalciuc\*\*, B.Holmqvist\*\*\* - The  $(n, 2n)$  and  $(n, n')$  reactions are very interesting to study since they are the dominating ones for medium weight nuclei when the incident neutron energy is in the interval from about 12 MeV to 23 MeV. Because of experimental difficulties the data available in this energy interval are very scarce. In our experiments the energy dependence of the cross sections for the production of discrete gamma-ray lines have been measured in the neutron energy interval from 16 MeV to 22 MeV for the elements F, Fe, Co. For this purpose samples (diameter 8.5 cm, height 10 cm) were irradiated with 2 ns bursts of neutrons produced by the  $T(d, n) He^3$  reaction. The gamma rays following  $(n, 2n)$  processes were observed with a well shielded 100 cm<sup>3</sup> Ge (Li) detector. Neutrons were separated from gamma rays by time of flight technique. The gamma ray interval of interest in the measurements was from 0.2 MeV to 3.0 MeV. The primary neutron flux

\* On leave from Kiev State University, Kiev, URSS

\*\* On leave from Institute for Atomic Physics, Bucharest Romania

\*\*\* Neutron Physics Lab., Studsvik, Sweden.

was monitored with a  $BF_3$ -long counter as well as with a time of flight monitor. Contributions of gamma-rays from neutron inelastic scattering of  $D(d,n)$  neutrons were connected for by making a separate scattering experiment with such a neutron source using the time-of-flight monitor for normalization purposes. The background was observed with a plexiglass sample. The cross sections were related to the known cross section of  $^{63}Cu (n,2n)$   $^{62}Cu$  reaction taken from the evaluation of Nakasima (1). (1) Nakasima R. and Kikucki K. The  $^{63}Cu (n,2n)$   $^{62}Cu$  excitation function and the knock-out process in nuclear reactions. Progr. Theoret. Phys. (Kyoto) 14 (1955) p. 126.

10. Neutron elastic scattering at forward angles - by V. Corcalciuc\*, D. Holmqvist\*\* and T. Wiedling\*\* - The general trend of neutron elastic angular distributions observed in the MeV range is that they are strongly peaked at forward scattering angles. At a constant neutron energy this effect also increases with the mass number. However, the angular distributions are usually only measured for angles larger than  $20^\circ$  or  $30^\circ$  neglecting the important forward scattering range where a considerable part of the total elastic cross section is to be found. The purpose of the present experiment was therefore to measure neutron elastic scattering from elements of different mass number at angles between  $10^\circ$  to  $40^\circ$  and in steps of  $2.5^\circ$ . The measurements have been made with the standard time-of-flight spectrometer. The angular spread introduced by the finite dimensions

\* On leave from Institute for Atomic Physics, Bucharest, Romania

\*\* Neutron Physics Lab., Studsvik, Sweden

of the target - scatterer - detector system was  $1.5^{\circ}$ . The forward angle differential cross sections were measured for Fe, Co, Ni, Pb and Bi (natural abundances). A standard spherical optical model analyses is done using a spin orbit term and with Saxon-Woods and derivative Saxon-Woods form factors for the real and imaginary potential parts.

11. Neutron Measurements for  $^3\text{He}$  Induced Reactions - by A. Alevra, A.Chevarier\*, N.Chevarier\*, R.Dumitrescu, I.R.Lucas, M. T.Magda, M.E.Nistor - Energy and angular distributions of neutrons resulting in  $^3\text{He}$  induced reactions were measured at incident energy of 25.6 MeV. Selfsupporting isotopical enriched targets of  $^{57}\text{Fe}$ ,  $^{61}\text{Ni}$ ,  $^{62}\text{Ni}$  and  $^{63}\text{Cu}$  were used. An angular range between  $23^{\circ}$  and  $145^{\circ}$  was covered. A time-of-flight spectrometer was used during measurements. The efficiency of the spectrometer was calculated by an analytical method proposed by Kurz<sup>1)</sup> and a Monte Carlo method<sup>2)</sup>. The energy spectra were fitted with the aid of a PDP-8 computer in order to transform the spectra from the time-of-flight to the energy scale and then from the laboratory system to the center-of-mass system.

REFERENCES: 1) R.J.Kurz - UCRL-11339\* (1964)

2) M.Chemarin, L.Feuvois, M.Gouanere, G.Nicolai &

J.L.Vidal - LYCEN 6877 (1968)

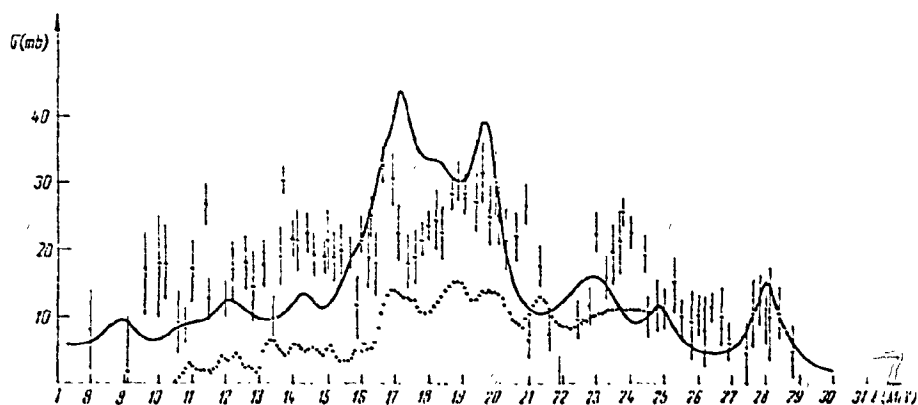
12. The Effective Cross Section of  $^{19}\text{F}(\gamma, xn)$  Reaction - by D.Catană, G.Baciu, C.Ilicscu, V.I.R.Niculescu, - The  $^{19}\text{F}(\bar{\gamma}, xn)$  reaction cross section has been measured with 100 keV bin in the range from threshold up-to 25 MeV. The analysis of the yield

---

\* IPN - Lyon, France

curve is based on the least structure solution using thick target forward direction bremsstrahlung spectrum. The our experimental data are compared with the total  $F 1$  photoabsorption cross section computed treating  $^{19}F$  as deformed nucleus<sup>1)</sup> taking into account the Nilsson level scheme, and with the total photoabsorption cross section measured by Dolbilkin et al.<sup>2)</sup>.

REFERENCES: 1) D.Catană, G.Baciu, C.Iliescu, V.I.R.Niculescu - Z. für Physik 261, 125 (1973) 2) B.S.Dolbilkin, V.A.Zapevalov, V.S.Korin, L.E.Lazareva, F.A.Nicolaev - Izv. Akad. Nauk U.S.S.R Seria Phys. XXX, 349 (1966)



Theoretical  $F 1$  photoabsorption cross section for  $^{19}F$  (full line). Experimental photoabsorption cross section from ref. 2) (points with errors). Cross section of  $^{19}F(\gamma, xn)$  reaction (point line).

13. The Delayed on Prompt Neutron Ration from  $^{238}U(\gamma, \delta, xn)$  -  
by G.Baciu, D.Catană, V.I.R.Niculescu -

- Source Bremsstrahlung generated to the betatron  
Bremsstrahlung target Ta  
Detector  $E^{10}F_3$  counters embedded in paraffin  
Target Natural  $U_2O_3$

Maximal bremsstrahlung energy (MeV)	$\frac{Nd}{Np}$	$\Delta\left(\frac{Nd}{Np}\right)$
6,0	$1.62 \cdot 10^{-2}$	$\pm 0.02 \quad 10^{-2}$
6,5	$1.01 \cdot 10^{-2}$	
7,0	$0.68 \cdot 10^{-2}$	
7,5	$0.34 \cdot 10^{-2}$	
8,0	$0.15 \cdot 10^{-2}$	$\pm 0.05 \quad 10^{-2}$
8,5	$8,63 \cdot 10^{-3}$	
9,0	$7.40 \cdot 10^{-3}$	
9,5	$7.12 \cdot 10^{-3}$	
10,0	$6.35 \cdot 10^{-3}$	$\pm 0.08 \quad 10^{-3}$
10,5	$5.06 \cdot 10^{-3}$	
11,0	$3.65 \cdot 10^{-3}$	
11,5	$3.78 \cdot 10^{-3}$	
12,0	$3.84 \cdot 10^{-3}$	$\pm 0.09 \quad 10^{-3}$
12,5	$3.61 \cdot 10^{-3}$	$\pm 0.09 \quad 10^{-3}$

14. Delayed Gamma Rays Emitted in Natural Uranium Photofission with Betatron Bremsstrahlung - by V.Gălăţeanu, M.Grecescu, G.Baciu - The final purpose of this investigation is the determination of absolute yields for the production of delayed gamma rays emitted after Uranium photofission with a bremsstrahlung beam. The necessity for these nuclear data was emphasized by T. A.Byer in the Draft Working Paper for IWGNSRD on Non-Neutron Data Needs for Safeguards Development Purposes at a IAEA meeting in 1972. Up to the present, the experimental procedure and

the data processing method were established. The preliminary results are summarized in table 1, which contains a list of the most prominent gamma rays observed in a natural uranium sample bombarded with a 16 MeV bremsstrahlung beam from a betatron. The isotopic assignment is based on accurate energy and half-life measurements.

T a b l e 1

Isotope	$E_{\gamma}$ (keV)	$T_{1/2}$
1	2	3
$^{76}\text{As}$	559.5	26 h
$^{78}\text{Ge}$	277	88 m
$^{78}\text{As}$	614	91 m
$^{84}\text{Se}$	408	3.3 m
$^{84}\text{Br}$	882	32 m
$^{88}\text{Kr}$	2392	2.8 h
$^{88}\text{Rb}$	1836	18 m
$^{89}\text{Kr}$	221	3.2 m
	586	
$^{89}\text{Rb}$	1032	15 m
	1248	
$^{92}\text{Sr}$	1384	2.7 h
$^{94}\text{Y}$	918	19 m
$^{101}\text{Mo}$	191	15 m
	591	

1	2	3
	1012	
$^{101}\text{Tc}$	307	14 m
$^{104}\text{Tc}$	358	18 m
$^{132}\text{Te}$	228	78 h
$^{132}\text{I}$	668	2.3 h
	772.5	
$^{133}\text{Sb}$	700	2.7 m
	979	
	1097	
$^{133\text{m}}\text{Te}$	913	55 m
$^{133}\text{Te}$	312	12.5 m
	408	
$^{133}\text{I}$	530	21 h
$^{134}\text{Te}$	211	43 m
	278	
	767	
$^{134}\text{I}$	847	53 m
	884	
$^{135}\text{I}$	1132	6.7 h
	1260	
$^{135\text{m}}\text{Xe}$	526.4	16 m
$^{135}\text{Xe}$	250	9.2 h
$^{137}\text{Xe}$	455	4 m
$^{138}\text{Xe}$	258	14 m

	434	
$^{138}\text{Cs}$	463	32 m
	1010	
	1436	
$^{141}\text{Ba}$	277	18 m
	304	
	344	
$^{142}\text{Ba}$	255	11 m
$^{142}\text{La}$	641	92 m
$^{143}\text{Ce}$	293	33 h

15. Tables of Gamma Rays Emitted by Radionuclides Produced through Photonuclear Reactions\* - by V.Gălăţeanu, M.Grecescu - This compilation of nuclear spectroscopy data has been prepared as an auxiliary for the interpretation of results in photoactivation analysis. Most recent data obtained by high-resolution gamma-ray spectroscopy with  $\text{Ge}(\text{Li})$  detectors were used. The tables include data concerning the disintegration of radionuclides with half-lives between 5 seconds and 1 year produced by  $(\gamma, n)$  reactions on all stable isotopes with a relative abundance greater than 1% and by  $(\gamma, p)$  reactions on elements with  $Z \leq 39$ . The gamma rays are listed in ascending order of the energies; half-lives intensities in photons per 100 disintegrations and other useful information are also included. The tables are

\* Published in Journ. Radioanal. Chem. 10 (1972) 315

of great help in solving two major problems in photoactivation analysis practice: isotopic assignment of gamma rays and determination of possible interferences. The tables can be employed also in activation analysis with fast neutrons based on the  $(n,2n)$  reaction.

16. The Influence of the Betatron Target Geometry on the Evaluation of Some Non-Neutronic Nuclear Data - by D.Catană, V.I.R.Niculescu, G.Baciu - The uses of bremsstrahlung in the study of photonuclear reactions lead to experimental results which represent integral values weighted by the bremsstrahlung spectrum, generally called the reaction yield  $V(E_0)$ . The reaction yield is defined as:

$$V(E_0) = ct \frac{\int_{E_{th}}^{E_0} \sigma(E) P(E, E_0) dE}{\int_0^{E_0} P(E, E_0) dE} \quad (1)$$

The present research was orientated towards the investigation of changes in the measured yield values  $V(E_0)$  as a function of different forms of the target producing the bremsstrahlung and of various geometrical conditions of irradiation. It has been experimentally established that the value of  $V(E_0)$  could vary drastically (up to 50%) for the same target material but in different geometrical forms. The conclusion derived from this investigation has allowed to define the optimum target form for a betatron, as well as the irradiation geometry of the probes under study. Consequently, the comparison of experimental data can be made only if the effective thickness of the target and the irradiation geometry are defined and stated. The present results are necessary for the evaluation of some non-neutronic nuclear data.

B. Short Review on Nuclear Data Activities in the Institute for Nuclear Technology - P.O.Box 35, Bucharest, Romania

In keeping with its activity displayed the Institute for Nuclear Technology takes a particular interest in setting-up some fundamental neutronic nuclear data libraries, by means of which one could generate multigroup microscopic section sets quite necessary in nuclear calculations for the fast and thermal reactor designs.

There are two main directions as regards nuclear data in the I.N.T.:

- Computing of multigroup neutron constants
- Experimental techniques for adjusting the group-constants.

The available facilities helping in solving problems connected with nuclear data consist of:

- The IBM-370/135 computer, belonging to I.A.P. displaying a memory of 142 K bytes with magnetic tapes and disks
- Experimental device to generate standard fast neutron reactor spectra

1. Computing the multigroup neutronic constants

As far as calculations of multigroup constants are concerned, our preoccupations start with fundamental microscopic data tapes that have already been formed.

New efforts have been directed towards the elaboration of some calculating codes to generate multigroup microscopic cross-sections displaying a variable group structure in keeping with the user's requirements.

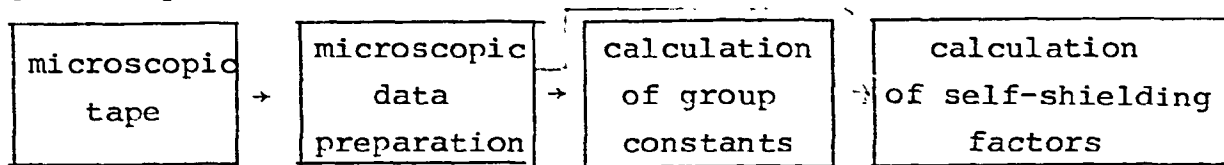
Data processing of multigroup microscopic section sets newly generated or already existent are also taken special care. The computing codes of multigroup cross-sections for homogenous or heterogenous cells are also included using the concept of self-shielding factors of resonances.

## 2. Experimental techniques for adjustments of group-constants

Using a simple facility for generating fast neutrons spectra and by means of the correlation method, they try to improve the multigroup cross-sections for fissile, fertile, structure and cooling elements.

1. NERO - as a calculus code of macroscopic cross-sections homogenized for heavy water moderated reactors - by I.Cristian, B.Cârstoiu, A.Bădescu, St.Boeriu, D.Cepraga - The cell code NERO calculates macroscopic cross-sections homogenized in a four-group scheme. In this view, the code takes the services of a Westcott type data library. The code library includes the necessary data for 30 isotopes. These data are the following:
  - the scattering cross-section weighted on a Maxwell spectrum ( $t = 20^{\circ}\text{C}$ );
  - the elastic and inelastic scattering microscopic cross-sections
  - fission cross-sections at 2200 m/s
  - the  $g(T)$  and  $S(T)$  Westcott factors
  - the lower cutting energy for the resonance integral of each isotop
  - microscopic cross-sections for calctulating the fast fission bonus.

2. Computation program for generation of group constants for fast reactors - by V.Cuculeanu, D.Gheorghe\* - At present, we have a KEDAK microscopic data tape and a few ENDF-B tape elements we obtained through the mediation of I.A.E.A. For multi-group cross-section generation, in collaboration with the I.A.P. nuclear data laboratory, a complex program for generation of fast neutron group-constants is being drawn up. The program diagram is presented bellow



The spectrum follows the ABBN scheme, namely  $\phi(E) = \phi_0(E)/\Sigma_t(E)$ .  $\phi_0(E)$  is supposed to be a Fermi spectrum except the groups corresponding to high energies in which case it is considered as a fission spectrum. The group structure proves to be variable, at the user's disposal. The inelastic scattering matrix is calculated by employing the evaporation model and that of the discrete levels. The code calculates dilutions for 6 types of reactions and the self-shielding factors of the resonances for 5 temperatures.

3. Computing program for the processing of multigroup microscopic nuclear data for fast reactors - by V.Cuculeanu, D.Mocioiu, E.Druță, D.Constantinescu - The PRESEC code has been elaborated for processing the ABBN multigroup nuclear data sets. Using the hyperbolic interpolation among the self-shielding factors for the tabled dilutions, the code calculates the self-shielded macroscopic cross sections for any composition of a

---

\* Institute for Atomic Physics

fast reactor. In calculating the mean neutron number per fission, a spectrum calculated in the fundamental mode with a material parameter indicated by user is also used. Optionally, it can read the fission spectrum or calculate a composition dependent fission spectrum. Alongside the macroscopic sections, the program supplies microscopic self-shielded cross-sections used in calculating the reaction rates.

4. Transmission method application for nuclear data (multi-group cross sections) testing and evaluation by I.Gârlea, P.I-lie, Al.Thurzo, L.Moisin - In view of testing and evaluating group cross-sections within an energy range of 10 KeV-3 MeV, a facility generating standard spectra for fast neutrons has been built. The very simple geometry (one-dimensional) and its small number of component parts result in an accurate computation of the spectra inside the device employing a calculation transport code. The neutron spectrum can be measured by differential methods (proton recoil, spectrometers with  $Li^6$ ,  $He^3$ ) and integral methods (fission chambers and activation detectors). If the neutron spectrum in the presence of the elements to be studied is known, the group cross-sections can be tested and improved. The data for reaching an agreement between calculation and experiment are being adjusted by a correlation method proposed by Gandino and Salvatores (1973).



REPUBLIC OF SOUTH AFRICA

PROGRESS REPORT TO THE INDC

1973

Compiled by D. Reitmann

1. PHYSICS DIVISION, ATOMIC ENERGY BOARD, PELINDABA, TRANSVAAL

The major facilities used for neutron physics research are the 20 MW research reactor, Safari I, and a pulsed 3 MV van de Graaff accelerator, equipped with terminal bunching and a CDC-1700 on-line computer.

1.1 Neutron capture reactions

C. Hofmeyr

A curved wave guide for subthermal neutrons was installed at the reactor and produced neutron fluxes comparable to those from the tangential beam tube but an improvement in the cadmium ratio by a factor four. A data link to the on-line computer was installed in order to carry out multiparameter experiments. Angular correlation experiments were done on  $^{71}\text{Ge}$  and  $^{59}\text{Ni}$ . In the former case good agreement was obtained with results from the  $^{71}\text{Ga}(p,n)^{71}\text{Ge}$  reaction studied at the van de Graaff accelerator (section 1.3).

1.2 Scattering of fast neutrons

E. Barnard, J.A.M. de Villiers, J.G. Malan, D. Reitmann and P. van der Merwe

The investigation of fast neutron interactions with caesium was completed. Measurements include total cross sections as well as elastic and inelastic scattering cross sections. Results were compared with optical model and Hauser-Feshbach calculations. The results of a

similar study on titanium carried out jointly with a group from Argonne National Laboratory, were published as a laboratory report<sup>1)</sup>. Some preliminary measurements were done on inelastic scattering of fast neutrons from  $^{103}\text{Rh}$ , in an attempt to resolve some of the existing uncertainties in its activation cross section.

1) Argonne National Laboratory report ANL/NDM-3 (1973).

### 1.3 (p,n) reactions

J.G. Malan, P. van der Merwe, E. Barnard and J.A.M. de Villiers

The study of the  $^{49}\text{Ti}(p,n\gamma)^{49}\text{V}$  reaction was completed and the results have been published<sup>1)</sup>. The experimental work on the  $^{73}\text{Ge}(p,n)^{73}\text{As}$  reaction by means of neutron time-of-flight and gamma-ray spectroscopy, was completed. High resolution gamma spectroscopy and multiparameter  $\gamma$ - $\gamma$  coincidence measurements yielded information on the level scheme of  $^{71}\text{Ge}$  as excited in the  $^{71}\text{Ga}(p,n)^{71}\text{Ge}$  reaction. Energy levels up to 1300 keV were established to within 0.2 keV and two unknown levels were found. The results of the latter two experiments were reported at the Munich conference.

1) Nucl. Phys. A195 (1972) 596

## 2. SOUTHERN UNIVERSITIES NUCLEAR INSTITUTE, FAURE, CAPE PROVINCE

The research program was based on a 5,5 MeV pulsed van de Graaff accelerator and covered a variety of topics in basic and applied nuclear physics, the most relevant of which are listed below:

### 2.1 Neutron induced reactions

#### 2.1.1 The inelastic scattering of neutrons by $^{232}\text{Th}$

W.R. McMurray, I.J. van Heerden and R.J. van Reenen (SUNI);  
E. Barnard and P. van der Merwe (AEB)

The investigation of the details of the  $^{232}\text{Th}$  level structure was continued by means of the measurement of inelastic neutron and of gamma production cross sections. As  $^{232}\text{Th}$  is an important fissile material, these cross sections are of some importance. Available measurements of inelastic scattering cross sections are virtually

non-existent except for the lowest levels<sup>1)</sup>.

Absolute cross sections have now been determined for all the levels up to 1100 keV. The measurements for these results were obtained using the time-of-flight system on the van de Graaff accelerator at the AEB, Pretoria. Analysis of the data used a line stripping procedure based on a detailed knowledge of the level scheme<sup>2,3)</sup>. The present measurements cover the neutron energy range from 900 to 1250 keV. It is intended to extend the range of measurements down to  $E_n = 200$  keV and increase the statistical significance of the present data. Work has begun on the Hauser-Feshbach analysis of the inelastic neutron scattering cross sections using the ABACUS and NEARREX codes on the Stellenbosch IBM 360 computer.

To obtain precise data on the gamma production cross sections, the  $(n, n'\gamma)$  reaction has been re-measured over the energy range 750 to 2100 keV. These will be directly compared with the neutron inelastic scattering cross sections. Due to low energy inter-band transitions, EO decays, and internal conversion of the gamma rays, the relevant gamma yields can be lower than expected from the inelastic neutron cross sections. This work has been partially analysed using the SAMPO spectrum analysis program. It should also be possible to extend the level scheme deduced from earlier studies using the  $(n, n'\gamma)$  reaction.

- 1) A.B. Smith, P.R. 126 (1962) 718
- 2) W.R. McMurray and I.J. van Heerden, Z. Physik 253 (1972) 289
- 3) F.K. McGowan, Oak Ridge Report CONF-720669 (1972)

#### 2.1.2 The collective band structure of $^{238}\text{U}$

W.R. McMurray

This work is a part of a continuing effort to determine the details of the level scheme of  $^{238}\text{U}$  and its collective band structure. The relevant experimental studies have been correlated to derive a level scheme which is consistent with all the evidence. In previous work, detailed (but different) collective bands were assigned by Diamond and Stephens<sup>1)</sup> using Coulomb excitation and by Herrmann et al<sup>2)</sup> using the radioactive decay of  $^{238}\text{Pa}$ . Additional levels, however, were observed

using the  $(n, n'\gamma)$  reaction<sup>3,4)</sup> so that neither of the previously proposed collective schemes could have been in all respects complete or correct. Additional evidence was provided from  $^{238}\text{U}(d, d)$  measurements<sup>5)</sup>. On the basis of the accumulated evidence, levels at 45, 148, 307, 680, 732, 827, 927, 931, 950, 966, 997, 1037, (1046), 1060, 1106, 1128 and 1168 keV are proposed. The  $^{238}\text{U}(d, d)$  measurements<sup>5)</sup> found levels corresponding to  $2^+$  members of the  $\beta$  and  $\gamma$  bands at 1033 and 1055 keV and observed a  $3^-$  octupole level at 1164 keV as well as another strongly excited level at 993 keV with octupole characteristics. These levels correspond to our levels at 1037, 1060 and 1168 and 997 keV respectively.

The spin assignments proposed are also compatible with the observed gamma decay branching from these levels to states in the ground state rotational band. A possible exception is the uncertain 1045.9 keV level. This level is tentatively assigned  $J^\pi = 4^-$  because such a weakly excited state is expected in this energy region. Higher spin states found by Diamond and Stephens<sup>1)</sup> are not significantly excited by means of inelastic neutron scattering.

The evidence from different sources, as well as the requirements of the proposed band structure, indicates the existence of several overlapping levels which even the gamma measurements<sup>4)</sup> could not resolve. For example, it must be assumed that the  $0^+$  level at 997 keV, firmly assigned using Coulomb excitation, must overlap with a  $3^-$  level in an octupole band. This would explain the observed decays from the 997 keV level(s) to  $2^+$  and  $4^+$  states in the ground state band. It would also fit the observation in  $^{238}\text{U}(d, d)$  scattering<sup>5)</sup> that the "993 keV" level has octupole character and is much too strong to correspond to a  $0^+$  level.

It is similarly deduced that there are other overlapping levels at 1060 and possibly 1168 keV excitation.

As a check on this level scheme, a Hauser-Feshbach analysis was undertaken to compare with previously measured neutron inelastic scattering cross sections<sup>6)</sup>. The comparison is sufficiently good to provide some confirmations of the level scheme proposed.

The Hauser-Feshbach computations were kindly undertaken by D. Wilmore (AERE, Harwell) using his own program. The computation

incorporated line width fluctuation corrections and also took account of unassigned levels above 1300 keV excitation by using a level continuum, the strength of which could be adjusted to fit the integrated inelastic scattering cross section at higher energies<sup>7)</sup>. The optical model parameters were obtained from the fit to the elastic scattering cross sections for neutrons on  $^{238}\text{U}$ . The calculated H-F inelastic cross sections for the well known ground state band also give a reasonable fit to the experimental data. An additional correction was introduced to correct for the fission channel.

- 1) R.M. Diamond and F.S. Stephens, Arkiv för Fysik 31 (1966) 221
- 2) G. Herrmann et al., Int Conf. on properties of nuclei far from the region of  $\beta$ -stability, Vol. II, p.985, Cern (1970)
- 3) W.R. McMurray and I.J. van Heerden, Z. Physik 253 (1972) 289
- 4) W.P. Poenitz, Argonne App. Phys. Ann. Report, p. 24 (1969-70)
- 5) A.T.G. Ferguson and B. Elbek, private communication
- 6) E. Barnard et al., Nucl. Phys. 80 (1966) 46
- 7) B.H. Armitage et al., Conf. on Nucl. Struct. Study with Neutrons, Budapest (1972).

### 2.1.3 The level structure of $^{115}\text{In}$ from $(n, n'\gamma)$ measurements

I.J. van Heerden and W.R. McMurray

Although the nucleus  $^{115}\text{In}$  has been the subject of many investigations, various uncertainties still remain. The ground and first excited states form an isomeric pair with assigned spins of  $9/2^+$  and  $1/2^-$ , and are interpreted in terms of the  $1g_{9/2}^{-1}$  and  $2p_{1/2}^{-1}$  proton-hole configurations coupled to vibrations of the  $^{116}\text{Sn}$  core. The  $3/2^-$  level at 597 keV is part of the multiplet obtained from coupling a  $2^+$  excitation of the even core to the  $p_{1/2}$  hole state.

Recent investigations of the  $\beta$ -decay of  $^{115}\text{Cd}$  by Bäcklin et al<sup>1)</sup> have observed states at 828 and 864 keV in  $^{115}\text{In}$  to which they have assigned spins of  $3/2^+$  and  $(1/2^+$  or  $3/2^+)$  respectively. On the basis of the enhanced E2 strength between these levels, it was suggested that these levels formed the beginning of a  $K = 1/2$  rotational band. McDonald et al<sup>2)</sup> have attempted to identify some of the higher states reached by Coulomb excitation as members of this rotational band.

Recently the collective states of  $^{115}\text{In}$  have been studied by Coulomb excitation<sup>3)</sup> with  $^{16}\text{O}$  and  $^{12}\text{C}$  ions and by inelastic scattering of 12 MeV deuterons. Strong coupling of the  $g_{9/2}$  proton hole for the vibrational states of  $^{116}\text{Sn}$ , produced results in good agreement with the experimental levels and other measured parameters of these levels. No support for the existence of a rotational band could be found.

The present study was performed to possibly reveal further members of the proposed rotational band. The  $(n, n'\gamma)$  reaction is not so selective regarding the mode of excitation of a particular level, and might therefore present the possibility of observing deformed states in a nucleus with a spherical ground state.

Gamma rays from levels in  $^{115}\text{In}$  were observed following inelastic neutron scattering at several neutron energies up to 2,5 MeV. A consistent level scheme was deduced taking into account the  $\gamma$ -ray threshold energies, and the shapes of the excitation curves. The observed  $\gamma$ -ray yields have been determined using the SAMPO programme and corrected for incident neutron flux, gamma attenuation in the scatterer, detection efficiency and for the effect of the time-gate used to depress neutron induced  $\gamma$ -rays in the Ge(Li) detector. Inelastic neutron scattering cross sections as a function of neutron energy are at present being compared with Hauser-Feshbach calculations, corrected for level width fluctuations, using the NEARREX programme.

As a start, optical model parameters obtained from neutron elastic scattering<sup>4)</sup> were used, and it was found that these did not give best fits to the excitation curves of levels with known  $J^\pi$  as at 933,6 ( $7/2^+$ ), 941,2 keV ( $5/2^+$ ), 1448,4 keV ( $9/2^+$ ) and 1462,4 keV ( $7/2^+$ ). The parameters are therefore being adjusted and the values which, up to now, have given the best fits are:

$V_0 = 48,9$  MeV (Saxon-Woods form),  $W_0 = 5,8$  MeV (surface derivative form),  $V_{S_0} = 8,00$  MeV,  $a = 0,66$  fm,  $b = 0,48$  fm and  $R = 1,25 A^{1/3}$  fm. Good fits are obtained for the levels mentioned above. Eventually it

should be possible to obtain values of  $J^{\pi}$  for most of the observed levels.

- 1) Backlin, A., Fogelberg, B. and Malmskog, S.G.: Nucl. Phys. A96 (1967) 539
- 2) McDonald, J., Porter, D. and Stewart, D.T.: Nucl. Phys. A104 (1967) 177
- 3) Dietrich, F.S., Herskind, B., Naumann, R.A., Stokstad, R.D. and Walker, G.E.: Nucl. Phys. A155 (1970) 209
- 4) Holmqvist, B. and Wiedling, T.: AE-430 (1971).

#### 2.1.4 The level structure of $^{75}\text{As}$

W.R. McMurray, P.J. Celliers and R. Saayman

Comparison of theoretical level schemes for  $^{75}\text{As}$  with experiment had previously been limited by the paucity of experimental data. The present work has now provided a detailed level and decay scheme for  $^{75}\text{As}$  up to an excitation of 1872 keV. The results have been submitted for publication.

The present work has used the  $(n, n'\gamma)$  and  $(n, n')$  reactions involving both gamma detection and neutron detection to derive neutron inelastic cross sections and gamma decay information. Together with a Hauser-Feshbach analysis of the measured cross sections, this has enabled spin and parity assignments to be made for most of the deduced levels.

A theoretical explanation for the structure of the odd-A isotopes in the mass region of  $^{75}\text{As}$  is presently only feasible in terms of a phenomenological model in which the odd-A nucleus is treated as a single particle coupled to the neighbouring even-even core nucleus. The negative parity states can be associated with combinations of a single proton in a 1f or 2p shell with excited states of a  $^{74}\text{Ge}$  core. In the Coriolis coupling calculations of Scholtz and Malik<sup>1)</sup> the unpaired proton is in a Nilsson deformed orbit coupled by a Coriolis force to the rotational motion of the even-even core. Intermediate coupling calculations have been made which assume an even-even vibrating core with dipole and quadrupole interactions with the quasiparticle-proton. Both models confirm the presence of levels with spins as assigned experimentally.

Several positive parity states in  $^{75}\text{As}$  have been positively identified using the  $^{74}\text{Ge}(^3\text{He},d)^{75}\text{As}$  reaction<sup>2)</sup>. Such states could arise from the coupling of an even-even core with a proton in the 1g, 2d or 3s shells. The comparison between theoretical calculations and experiment favours the rotational description of the core even though a vibrational character is expected for nuclei in this mass region.

- 1) W. Scholtz and F.B. Malik, Phys. Rev. 176 (1968) 1355
- 2) R.R. Betts et al., Phys. Rev. Lett. 26 (1971) 1576

#### 2.1.5 Scattering Studies in $^{16}\text{O}$

S. Wynchank, F.D. Brooks, S.M. Perez and I.J. van Heerden

It is possible that an optical potential can describe scattering and reactions with the  $^{16}\text{O}$  nucleus. In order to obtain optical model parameters for this description of neutron elastic scattering and other reactions on  $^{16}\text{O}$  preliminary measurements of elastic scattering cross sections using a water sample with incident neutrons produced by the  $\text{D}(d,n)$  reaction have been initiated. Using open geometry and a shadow bar, scattered neutron detection was not possible, but after introducing the large SUNI neutron detector shielding enclosure, a great improvement was observed. It is intended next to employ a variety of neutron energies and a liquid oxygen scattering sample. The required dewar has been ordered.

#### 2.1.6 Three nucleon experiments at neutron energies in the range 7-22 MeV

The nuclear three-body problem has become highly topical with both theorists and experimentalists. For example the application of Faddeev methods to the exact solution of this problem has stimulated theoretical calculations on topics such as the properties of the bound states ( $^3\text{H}$  and  $^3\text{He}$ ), nucleon-deuteron scattering and deuteron-breakup. Calculations have been made using different forms for the nucleon-nucleon potential. The choice between one potential form or another must depend ultimately on comparisons with experimental data. The experimental data available at present on neutron-deuteron scattering and on neutron-induced deuteron breakup are very limited. The work reported here was undertaken with a view to providing further experimental data on these topics.

#### 2.1.6.1 Polarization in neutron-deuteron scattering

M. Steinbock, F.D. Brooks and I.J. van Heerden

A scintillation polarimeter based on a deuterated anthracene crystal is being used to study the polarization in n-d scattering<sup>1)</sup>. The light collection properties and hence also the energy resolution of the system have been greatly improved by mounting the crystal on a light pipe. Some preliminary polarization data were obtained at 7,9 MeV. The incident neutron beam for this measurement was obtained from the  $^9\text{Be}(\alpha, n)$  reaction and was 60% polarized. The trend of our data is consistent with the values reported by Taylor<sup>2)</sup> and confirm the angular dependence reported by these authors.

Measurements have also been made using 10 MeV neutrons from the  $^{14}\text{N}(d, n)$  reaction and 16 and 22 MeV neutrons from the  $\text{T}(d, n)$  reaction. In the former case the incident neutron beam was parallel to an axis of symmetry of the crystal while in the latter case the crystal was aligned for maximum dispersion across the plane of pulse height (L) versus PSD (S). The LS spectra are complicated at high neutron energies by the presence of an additional 'proton ridge' arising from deuteron breakup. However, by taking advantage of the good proton-deuteron separation at the symmetry orientation the proton contribution can be estimated accurately. The asymmetry in n-d scattering can then be determined from the deuteron ridge in the normal way. The data obtained at 10, 16 and 22 MeV are now being analysed.

- 1) M. Steinbock et al., Item 2.1.7., SUNI Annual Research Report, SUNI-23 (1972)
- 2) C.J. Taylor et al., Phys. Rev. C1 (1970) 803

#### 2.1.6.2 The n-d breakup cross section between 8 and 22 MeV

G. Pauletta and F.D. Brooks

The n-d breakup cross section has been measured at eleven energies between 8 and 22 MeV by integrating the energy distributions of breakup protons in a deuterated scintillator<sup>1,2)</sup>. The breakup protons were separated from the recoil deuterons by pulse shape discrimination.

Recent calculations of the n-d breakup cross section<sup>3-7)</sup> based on the Faddeev<sup>8)</sup> formalism have shown sensitivity to the details of the

potentials used. The cross sections measured in the present work are somewhat larger than other measurements<sup>9-12)</sup> and calculations<sup>3,4)</sup>. It is concluded that these measurements favour calculations using local potentials<sup>2)</sup>.

- 1) G. Pauletta and F.D. Brooks, Item 2.1.8, SUNI Annual Research Report SUNI-23 (1972)
- 2) G. Pauletta, Ph.D. thesis submitted to the University of Cape Town (1973)
- 3) I.M. Sloan, Nucl. Phys. A168 (1971) 211
- 4) W.M. Kloet and J.A. Tjon, Proc. Conf. on Few Nucleon Problems in the Nuclear Interaction, ed. I. Haus et al. (North-Holland Pub. Co.), p. 380
- 5) W.M. Kloet and J.A. Tjon, Nucl. Phys. A120 (1973) 380
- 6) P. Doleschall, Private communication
- 7) S.C. Pieper, Private communication
- 8) L. Faddeev, Soviet Physics "Doklady", 7 (1963) 600
- 9) M. Holmberg et al., Nucl. Phys. A129 (1969) 327
- 10) H.C. Catron et al., Phys. Rev. 123 (1961) 218
- 11) E.R. Graves and J.D. Seagrave, NCSAC 38 (1971) 116
- 12) R.F. Carlson et al., Los Alamos Conf. (1972).

2.1.7 Direct excitation of the analogue dipole state in  $^{28}\text{Al}$   
K. Bharuth-Ram, S.M. Perez, F.D. Brooks, W.R. McMurray  
and S. Wynchank

This work forms part of a study of the excitation of analogue dipole states in  $(n,p)$  reactions. The project was motivated by the work of Clement and Perez<sup>1)</sup> who have developed a collective theory which shows that the excitation of analogue dipole states in  $(p,n)$  and  $(n,p)$  reactions proceeds via a direct reaction mechanism. The long-term aim of the project is to search for isospin splitting of the giant dipole resonance in neutron-rich nuclei. The  $(n,p)$  reaction selects the  $T = T_0 + 1$  component of the analogue dipole state ( $T_0 =$  ground state isospin of target) hence a comparison of data obtained from this reaction with that obtained from other reactions which are not subject to this selection rule may provide evidence of the splitting of this state.

The initial work reported here was on the  $^{28}\text{Si}(n,p)^{26}\text{Al}$  reaction (for which  $T_0 = 0$ ) and was aimed at testing certain aspects of the theory as outlined in the previous SUNI report<sup>2)</sup>. The target for the reaction was a 264 micron thick, totally-depleted, Si surface barrier detector. Neutrons of energy 22 MeV were obtained from the  $T(d,n)$  reaction. The detection system was designed to identify protons, deuterons and alpha-particles resulting from neutron-induced reactions and to measure their energies. To do this two energy parameters and time-of-flight were stored on buffer tape (using the ND/PDP15 system) and were analysed in detail afterwards. The angular distributions for two energy-regions of the proton spectra (viz. 7-8 MeV and 8,5- 9,5 MeV) are characteristic of a direct reaction process.

Work is now in hand to reduce the relative cross sections to absolute values. For this purpose we use the alpha spectrum from  $^{28}\text{Si}(n,\alpha)$  reactions detected (as singles) in the target detector as a neutron flux monitor. The results will be compared with the theory of Clement and Perez.

The next stage of the investigation, namely the study of  $(n,p)$  reactions on some neutron-rich targets, has also been started. Preliminary studies have been made of the  $^{127}\text{I}(n,p)$  reaction using a similar experimental arrangement but with a CsI scintillation crystal replacing the Si surface barrier detector.

- 1) C.F. Clement and S.M. Perez, Nucl. Phys. A165 (1971) 569
- 2) Item 2.1.9, SUNI Annual Research Report.

2.1.8 A high resolution measurement of the neutron total cross section of iron from 24 keV to 1000 keV

N.J. Pattenden, I.T. Belcher, I.M. Blair, P.H. Bowen, G.C. Cox and P.E. Dolley (AERE) and W.R. McMurray (SUNI)

A neutron time-of-flight spectrometer was developed to measure neutron total cross sections using the 160 MeV synchrocyclotron at AERE, Harwell. A pulsed 140 MeV proton beam was deflected vertically on to an internal tungsten target with a repetition rate of about 800 Hz. The evaporation-spectrum neutrons passed through 2 cm of water moderator contained in a tantalum box fixed to the target to boost the yield of

low energy neutrons. A  $^6\text{Li}$ -loaded glass neutron detector was developed<sup>1)</sup> and used with a digital-time-analyser coupled by a CAMAC interface to a DDP 516 Honeywell computer. The neutron detector viewed the target from the backward direction along a 100 meter flight path. Details of the system have been published.

Total cross sections for  $^{56}\text{Fe}$  were measured<sup>2)</sup> for a sample of thickness 0,2546 Fe atom/barn. Many of the narrow p-wave resonances now observed had not previously been reported. Together with neutron capture cross section data, this would enable the first extensive series of p-wave resonance  $\Gamma_\gamma$  values to be determined. A computer-based tabulation of these results has been sent to "The Centre, ENEA de Compilation de Données Neutroniques, B.P. 9, 91-Gif-sur-Yvette, France".

- 1) W.R. McMurray, N.J. Pattenden and G.S. Valail,
  - (a) AERE Report R-7396 (1973)
  - (b) Nucl. Instr. and Meth. (accepted for publication)
- 2) N.J. Pattenden et al., AERE, Report R-7425 (1973)

## 2.2 (p,n) Reactions

Studies of (p,n) and (p,n $\gamma$ ) reactions have proved to be successful in determining the level structure of many nuclei in the mass region  $A = 45$  to  $65$ . In many cases the reaction Q-values are well suited to the available 5,5 MeV proton energy, allowing the excitation of the interesting lower energy levels. The mentioned mass region is of interest insofar as a number of nuclear models are applicable so that acquired experimental data becomes immediately useful in evaluating the success of the various models.

### 2.2.1 Properties of excited levels in $^{65}\text{Zn}$

I.J. van Heerden, R.J. van Reenen and J.V. Pilcher

The  $^{65}\text{Cu}(p,n)^{65}\text{Zn}$  reaction has been investigated with incident proton energies between 2,5 MeV and 5,0 MeV. A series of time-gated gamma-ray spectra were recorded at systematically increased proton energies and a detection angle of  $55^\circ$ . These measurements were used in determining the level scheme of  $^{65}\text{Zn}$  for excitation energies up to 2 MeV. The assignment of energy levels to the level scheme was facilitated by measuring coincidence spectra with the neutron groups observed

in fast coincidence with associated gamma-rays. Time-of-flight measurements with a 3m flight path provided positive identification of the neutron groups.

Angular distribution measurements were obtained for incident proton energies of 3,4 MeV, 3,8 MeV and 4,2 MeV and analysis of this data is at present being carried out.

A preliminary measurement, in which neutron t.o.f. spectra and the associated gamma-ray spectra were recorded simultaneously in multi-parameter mode under software control of a PDP 15/20 computer, was attempted to evaluate the feasibility of employing this type of measurement routinely in  $(p, n\gamma)$  studies. First results seem to indicate that a low counting rate detracts from the obvious advantages that this method offers for establishing level schemes in a single measurement.

#### 2.2.2 The $^{49}\text{Ti}(p, n\gamma)^{49}\text{V}$ and $^{50}\text{V}(p, n\gamma)^{50}\text{Cr}$ reactions

I.J. van Heerden, R.J. van Reenen, J.V. Pilcher and W.R. McMurray

The properties of excited levels in  $^{49}\text{V}$  have been studied by means of the  $^{49}\text{Ti}(p, n\gamma)$  reaction ( $Q = 1,38$  MeV) for incident proton energies between 2,4 and 4,5 MeV. This work has been undertaken in order to extend to higher excitation energies the recently published results of Malan et al<sup>1)</sup>. Gamma-ray spectra were recorded at a detection angle of  $55^\circ$  and angular distribution measurements were started at a proton energy of 3,5 MeV.

Although Raman et al<sup>2)</sup> have published the results of a fairly extensive investigation of the levels of  $^{50}\text{Cr}$ , an attempt is being made to solve the reported ambiguities in the decay scheme by studying this nucleus through the  $^{50}\text{V}(p, n\gamma)^{50}\text{Cr}$  reaction. The successful application of the multi-parameter method of measurement (mentioned in Item 2.2.1 above) should readily clear up many of the uncertainties in the decay scheme. The first measurements include gamma-ray spectra recorded with a target of  $\text{V}_2\text{O}_5$  (enriched to 36% in  $^{50}\text{V}$ ) in the range  $E_p = 2,5$  MeV to 4,6 MeV in order to determine the excitation of the lower lying energy levels. Positive identification of decay gamma-radiation from  $^{50}\text{Cr}$  was facilitated by the measurement of comparative gamma-ray spectra resulting from the bombardment of a natural  $\text{V}_2\text{O}_5$  target.

1) J.G. Malan, E. Barnard, J.A.M. de Villiers, J.W. Tepel and P. van der Merwe. Nucl. Phys. A195 (1972) 596

2) S. Raman, R.L. Auble, W.T. Milner, J.B. Ball, F.K. McGowan, P.H. Stelson and R.L. Robinson. Nucl. Phys. A184 (1972) 138.

4. NUCLEAR PHYSICS RESEARCH UNIT, UNIVERSITY OF THE WITWATERSRAND,  
JOHANNESBURG

Application of activation analysis in the Nuclear Physics Research Unit relating to science and industry has involved both neutrons and charged particle activation studies.

Neutron activation research, done in collaboration with the National Institute for Metallurgy (NIM) has been applied to an extensive range of Geological specimens as well as to specific studies of diamonds and biological specimens. Both thermal and epithermal (reactor) neutron and fast (generator) neutron sources have been used.

The recent acquisition of a Tandem van de Graaff accelerator has led to the initiation of charged particle activation studies which, in the first instance has been related to the determination of trace elements specifically B and N, in diamonds. Nuclear back-scattering and reactions are being used at lower bombarding energies to investigate surface and bulk impurities in diamonds.

Reports and reprints related to relevant work already completed are listed below:

Publications by members of the Activation Analysis Research Group (NPRU)  
during 1973/74

1. "Clinopyroxene - Ilmenite Xenolith from Kimberlites" J.J. Gurney, H.W. Fesq and E.J.D. Kable. A volume in Lesotho Kimberlites edited by P.H. Nixon, p. 238-253, 1973
2. "Use of Discriminant Analysis for Classification of Strata in Sedimentary Successions." S.E. Rasmussen and D.M. Hawkins. Math. Geology 5, No. 2, 1973
3. "The Accurate Determination of Oxygen in Geological Materials" D.M. Bibby and J.P.F. Sellschop. J. Radioanal. Chem. 20 (1974) 677.
4. "Some Aspects of the Geochemistry of Kimberlites from the Premier Mine, Tv1." H.W. Fesq, E.J.D. Kable and J.J. Gurney. Proceedings of Kimberlites Conference, Cape Town (1973)
5. "A Comparative Trace Element Study of Diamonds from Premier, Finsch and Jagersfontein Mines". H.W. Fesq, D.M. Bibby, C.S. Erasmus, E.J.D. Kable and J.P.F. Sellschop. Proceedings of Kimberlites Conference, Cape Town (1973)
6. "The Significance of the Inter-Element Relationship of Some Refractory Elements" in Proceedings of Kimberlites Conference, Cape Town (1973)

7. "The Determination of Oxygen and Silicon in Diamond by 14 MeV Neutron Activation Analysis". D.M. Bibby and J.P.F. Sellschop. J. Radioanal. Chem. (In Press)
8. "Studies of Ion Channelling and Surface Impurities in Diamond". J.P.F. Sellschop and W.M. Gibson, Diamond Research, (1973) 32
9. "Determination of Impurities in Diamond by Nuclear Methods" J.P.F. Sellschop. Paper presented at the Diamond Conference, Reading, 1973
10. "Neutron Activation Analysis in Geological Problems". J.P.F. Sellschop. Paper presented at the Nuclear Activation Analysis Conference, Cambridge, 1973
11. "Characteristics of Sedimentary Strata using Trace Element Patterns". S.E. Rasmussen, H.W. Fesq, J.P.F. Sellschop and D.W. Hawkins. 12th Annual International Symposium on Computer Applications in the Mineral Industry (1974)
12. "Multivariate Techniques for the Classification of Granites". J.I.W. Watterson and D.M. Hawkins. 12th Annual International Symposium on Computer Applications in the Mineral Industry, 1974
13. "Sea Floor Basalt Alteration : Some Chemical and Sr Isotopic Effects" S.R. Hart, (Dept. of Terrestrial Magnetism Carnegie Institution of Washington and A.J. Erlank and E.J.D. Kable. Submitted to "Contributions to Mineralogy and Petrology". 1973

#### NIM Reports

1. The Activation Analysis of Samples for Molybdenum and other elements Watterson. August 1969. No. A.276
2. The Determination by Neutron Activation and Tracer Techniques, of the losses of Iridium during the Fire-Assay Procedure for the Platinum-Group Metals. Watterson, Robert and van Wyk. Sept. 1970. No. 1048
3. Distribution of Trace and Minor Elements in Durban Roodepoort Deep Rock Samples. Sellschop, Rasmussen and Fesq.No. C87/69
4. The Instrumental Neutron-Activation Analysis of Samples Taken at Different Levels of the E.R.P.M. Mine. Uken and Erasmus. Sep. 1970 No. 1013
5. The Recovery of Noble Metals for Analysis. A Radiotracer Investigation of Losses. Palmer and Watterson. Jan. 1971. No. 1185
6. Neutron Generator Shielding Watterson, Uken, Knight, Faure, Steele. No. C32/63A

7. The Application of Neutron Activation Analysis for Sorting Witwatersrand Gold Bearing Ores. Uken, Watterson, Knight and Steele. No. C32/63/E
8. Clinopyroxene - Ilmenite Xenoliths from Kimberlites. Fesq and Kable. April, 1973
9. Determination of Lanthanum and Cerium in Carbonatites from the Barberton Area by Neutron Activation Analysis. Oosthuizen, Uken. No. 974
10. Determination of some of the Major Constituents of ores and Minerals by Fast Neutron Activation Analysis. Watterson, Faure, Steele. No. 236
11. The Determination of the Platinum-Group Metals and Gold in Ore Samples. Watterson, Steele, Robert, Dixon, Fowler, Mallett and Pohlandt. No. 526
12. The Use of  $^{252}\text{Cf}$  Fission Neutron Sources. Watterson. No. 445
13. Kimberlite Heavy Minerals Dissolution. Loo. No. C45/71
14. A Magnetic-Tape Oriented System for Data Reduction in Neutron Activation Analysis. Watterson, J. & L., Rasmussen. No. 1476
15. Simultaneous Radiometric Determination of Uranium and Thorium in Ores. E. Uken, J. Watterson, A. Knight. No. L. 10/65
16. Simultaneous Determination by Instrumental Thermal Neutron Activation Analysis of some selected Trace Elements likely to be present in Lunar Material. Erasmus and Uken. No. 889
17. Reactor - Neutron Flux Monitoring using Cobalt/Aluminium Wire. S.E. Rasmussen, December, 1972
18. The Research Reactor "SAFARI I" as a Neutron Source for Activation Analysis. J.I.W. Watterson, September, 1973
19. Fast Neutron Activation Analysis for the Determination of Oxygen in Rock Samples. Bibby. No. 1503
20. Neutron Activation Analysis of Samples from the Kimberley Reef Conglomerate. Rasmussen and Fesq. September, 1973. No. 1563.
21. Standardisation of neutron flux monitoring procedures, S.E. Rasmussen Technical Memorandum NIM (1972)
22. Reduction of counting errors using sample rotator. N. Hulse, Technical Memorandum (1972). 051/74
23. Reactor-neutron flux monitoring using cobalt/aluminium wire. S.E. Rasmussen NIM Memorandum (1972).